ANALYSIS OF STRUCTURAL MODELING FOR RECYCLED ASPHALT PAVEMENT USED AS A BASE LAYER

A Dissertation
Submitted to the Graduate Faculty
of the
North Dakota State University
of Agriculture and Applied Science

By

Ehab Magdy Salah Noureldin

In Partial Fulfillment of the Requirements
for the Degree of
DOCTOR OF PHILOSOPHY

Major Department:
Civil and Environmental Engineering

September 2015

Fargo, North Dakota

North Dakota State University

Graduate School

Title

ANALYSIS OF STRUCTURAL MODELING FOR RECYCLED ASPHALT PAVEMENT USED AS A BASE LAYER

By

Ehab Magdy Salah Noureldin

The Supervisory Committee certifies that this ***disquisition*** complies with North Dakota State University's regulations and meets the accepted standards for the degree of

DOCTOR OF PHILOSOPHY

SUPERVISORY COMMITTEE:

Dr. Magdy Abdelrahman
Chair

Dr. Dinesh Katti

Dr. Ying Huang

Dr. Yarong Yang

Approved:

11/19/2015
Date

Dr. Dinesh Katti
Department Chair

ABSTRACT

Reusing RAP in the base layer became a common practice in the last decade. However, some crucial issues must be resolved to succeed in using RAP satisfying the standard specifications as a base layer. The most important unknown factor is the mechanistic behavior of RAP. This question may be satisfied by understanding the role of RAP in terms of whether it just behaves as a black rock or has a stabilizing effect with traditional aggregates used for base layer.

The first stage of this study is modeling the structural behavior of RAP via prediction M_R. This stage then comprises comparing the predicted results to actual measured data under several field conditions. The second stage focuses on the modeling behavior of PD. This stage takes in consideration two sets of data, the first is for the measured PD data calculated from M_R test. While another traditional set of measured data for PD from repeated tri-axial loading (RTL) test either single or multi-stage is collected for the same RAP sources used in the first stage. The third stage concerns on M_R-PD relationship. It indicates the typical relationship for the M_R-PD behavior that can be understood for the RAP in base layer. The fourth and last stage is essential to investigate the Poisson's ratio of RAP blends and its effectiveness on both parameters M_R and PD. This ratio is measured during un-confined compression test. Two main testing conditions: various water and RAP contents are taken in consideration during this measurement for different RAP/Aggregate sources.

This study proves that both prediction models used in the MEPDG for prediction of both parameters M_R and PD are totally significant for RAP/Aggregate blends used for pavement base layer. The prediction is at the highest accuracy at water content levels close to OMC%, MDD and with 50% to 75% RAP content. In addition, it is proved that Poisson's ratio is an effective parameter on both M_R and PD parameters especially with variation of water content. This

conclusion recommends to take in consideration Poisson's ratio as an effective parameter in M_R and PD prediction models used in MEPDG software.

ACKNOWLEDGEMENTS

First, I wish to thank my main advisor Dr. Magdy Abdelrahman for his guidance and academic support during my study. Also, I would like to thank my committee members: Dr. Dinesh Katti, Dr. Ying Huang from Civil and Environmental Engineering Department, and Dr. Yarong Yang from Statistics Department for their help and patience during my study. I would like to acknowledge Dr. Mohammed Attia for his measured data collected during his Ph.D work at NDSU and used here in the modeling part of this study. An additional acknowledgement to my previous committee members: Dr. Frank Yazdani from Civil and Environmental Engineering Department and Dr. Vlodymyr Melnykov from Statistics Department in the beginning of my study.

Furthermore, I would like to thank the Minnesota Department of Transportation (MN/DOT) for supplying the needed materials used in this research. Also, I would like to thank the Civil and Environmental Engineering Department at NDSU, and National Science Foundation (NSF) for financial support during this research. Additional thanks to Mechanical Engineering Department at NDSU for renting the load cells needed to complete the experimental stage of this research. Special thanks to Rob Sailor in Mechanical Engineering department for helping in this issue.

Finally, thanks for all the team research members in CEE materials lab: Mohyeldin Ragab, Anthony Waldenmaier and Amir Ghavibazoo, who helped the author during his work to complete this research. Special thanks to my close friends: Ahmed El Fatih and his wife Nesreen El Doliefy, Amr Salem and Ahmed El Ghazaly, who supported me here during my life in US. I would like to extend my gratitude to all my close family members and old friends in Egypt who kept caring and supporting during my Ph.D progress.

DEDICATION

Thanks for God’s support and blessings during my whole life and studying here in US, which without it I cannot achieve my goal.

I dedicate this work to my dear father for his help and guidance during my whole personal and career life.

Additional dedication to my dear mother and sister for their deep concern and caring.

Finally, a special dedication to my beloved home country Egypt, hoping a brilliant future to achieve its goals.

TABLE OF CONTENTS

LIST OF TABLES

LIST OF FIGURES

LIST OF ABBREVIATIONS

AASHTO…….. American Association of State Highway and Transportation Officials

AC……..... Asphalt Concrete

ASTM……..... American Society of Testing and Materials

CBR…… California Bearing Ratio

FDR……..... Full Depth Reclamation

FWD……... Falling Weight Deflectometer

F-T……. Freeze-Thaw cycles

HMA…….. Hot Mix Asphalt

MEPDG…….. Mechanistic-Empirical Pavement Design Guide

MDD…….. Maximum Dry Density

MN/DOT……..... Minnesota Department of Transportation

M_R…….. Resilient Modulus

NCHRP…….. National Cooperative Highway Research Program

OMC……... Optimum Moisture Content

PD…….. Permanent deformation

RAP…… Recycled Asphalt Pavement

RLT…… Repeated Load Tri-axial test

TH…….. Trunk Highway

WC……. Water Content

LIST OF APPENDIX TABLES

LIST OF APPENDIX FIGURES

CHAPTER 1. INTRODUCTION

1.1. General Overview

Nowadays the worldwide paving industry is facing tremendous problems due to the severe shortage of suitable aggregates in general and/or the high cost of virgin aggregates used in different pavement layers. Therefore, utilizing the recycled asphalt pavement (RAP) concept to construct an adequate granular base course layer is an excellent alternative especially in cases where lack of suitable aggregates exists. The Federal Highway Administration (FHWA) reported in 2007 that about 100 million tons of RAP are produced each year during pavement rehabilitation activities (M. Attia, Abdelrahman, Alam, Section, & Department, 2009), which presents a major solid waste concern, and consequently several environmental pollution and hazards. RAP has already become one of the most widely used recycled materials in the United States now. Nationally, the use of RAP in new pavement layers is expected to be doubled by 2014, compared to its recorded annual usage of 60 million tons in 2009 (Zahid Hossain, 2012).

RAP is collected when asphalt pavements are removed for reconstruction, resurfacing, or to obtain access to buried utilities. Rehabilitation projects of old asphalt pavements produce a huge amount of RAP. FHWA reported that at least 13 state agencies (Arizona, Illinois, Louisiana, Maine, Nebraska, New Hampshire, North Dakota, Oregon, Rhode Island, South Dakota, Texas, Virginia, and Wisconsin) had used RAP as an aggregate in the base layer (M. I. E.-S. Attia, 2010). Many mechanical tests are currently used to investigate the strength parameters of the base layer, such as the resilient modulus (M_R) and/or repeated loading tri-axial (RLT) for measuring the permanent deformation (PD). It is recommended to measure both parameters M_R and PD by the mechanistic empirical pavement design guide (MEPDG) for the granular unbound base layer. A

prediction model for each is available in the MEPDG software if testing is not possible (Guide, 2008).

These tests were performed on RAP and/or RAP/Aggregate blends to compare its performance with traditionally granular aggregates used for base layer. In general, it was found that using RAP alone in the base layer did not achieve the standard specifications required for this layer. Contrary, when RAP was mixed with various qualities granular aggregates especially at 50/50 percentage, the RAP behavior in the blend became similar to that of the unbound granular aggregates (M. I. E.-S. Attia, 2010). Accordingly, RAP/Aggregate blend well achieved the required specifications for base layer in several previous studies covering this research area. However, there is a need to investigate the structural modeling parameters for RAP/Aggregate blends used as a base layer.

1.2. Problem Statement

Using RAP in the base layer is facing many challenges nowadays. One of the most important ones is the uncertainty concerning structural behavior of RAP in the base layer and whether it behaves just as a black rock or has a stabilization effect on traditional aggregates used as a base layer. Modeling the structural behavior of RAP blends, especially the resilient modulus, can solve this key question of RAP behavior in base layer. Many parameters should be taken into consideration in resilient modulus behavior modeling, such as different testing conditions, RAP components, permanent deformation and Poisson's ratio of base layer. Firstly, the need is apparent to investigate previous constitutive models in terms of assessing the prediction of structural capacity of base layer. This assessment would yield significant conclusions in terms of goodness to fit of these models for RAP behavior under different testing conditions, such as moisture contents, densities, freeze-thaw cycles and percentages of RAP in blends.

In addition, the permanent deformation (PD) is important to be investigated with respect to describing the structural modeling behavior of RAP as a base layer. Previous studies on PD for RAP blends in base layer construction had contradictive results. Some studies proved that PD increased with higher RAP contents and others were vice versa. The M_R results were more directly proportional with percentage of RAP in the blend. On the other hand, PD contradictive values resulted in not being able to determine the optimum percentage of RAP that can be used in the base layer. Therefore, there is a need for a further study on PD modeling behavior of RAP/Aggregate blends and its relation to M_R modeling of the base layer under different testing conditions. Also, it is essential to take into consideration the PD as an effective parameter on the structural modeling of RAP as a base layer expressed by the resilient modulus M_R.

Finally, the Poisson's ratio was not considered in previous studies as an important parameter affecting the structural capacity for granular base layer, especially when measured during the resilient modulus test. Usually, Poisson's ratio was estimated during all methods of pavement design including the MEPDG. However, effect of Poisson's ratio on both M_R and PD modeling behavior for RAP blends is essential to be studied to investigate its effectiveness on the structural capacity of base layer. This stage of study is needed to confirm the difference in behavior of RAP blends from granular aggregates, especially under variation of water content.

1.3. Research Objectives

Results of literature survey, yielded that the effectiveness of aged RAP components characteristics would be minimal on the measured M_R and PD values. Also, no environmental hazards are expected from using RAP in the granular base layer blends. Therefore, there is no need to investigate both factors in this study. Main objectives of this research are concluded in the following points:

- Comparing RAP/Aggregate blends to granular aggregate through constitutive prediction models of the main effective parameters (M_R and PD) previously used for granular base layer.
- Investigating the structural modeling behavior of RAP/Aggregate base layer blends by prediction of M_R and PD.
- Investigating the relation between permeant deformation and resilient modulus for different RAP blends as a base Layer.
- Determine the effectiveness of Poisson's ratio on measured M_R and PD values for RAP base layer blends.
- Reassessing the prediction models of M_R and PD to assess the need for additional parameters to be taken in consideration.

1.4. Thesis Organization

This thesis is divided into 8 chapters as follows:

Chapter 1: Introduction

It explains the problem statement, main objectives and organization of this research.

Chapter 2: Literature Review

This chapter presents the previous work related to using of RAP in pavement construction generally and base layer specifically, and its effect on the surrounding environment. Also, it focuses on the main design parameters and the previous prediction models used for unbound base layer.

Chapter 3: Methodology and Experimental Work

This chapter describes the main tasks that achieve the research objectives. In addition, it presents testing procedures and materials tested to collect the data analyzed in this research.

Chapter 4: Resilient Modulus Modeling

This chapter concerns the adequacy of several previous resilient modulus prediction models used for unbound granular base layer on RAP/aggregate blends at different testing conditions.

Chapter 5: Permanent Deformation Modeling

This chapter focuses on the rutting MEPDG model used in permanent deformation prediction for unbound granular base layer on RAP/aggregate blends at different testing conditions.

Chapter 6: Correlation of Resilient Modulus and Permanent Deformation

This chapter explains the correlation between both parameters M_R and PD for RAP/aggregate blends under the most expected field conditions that could happen for base layer.

Chapter 7: Poisson's Ratio Measurement

This chapter describes the relation between Poisson's ratio and ultimate compressive strength values for RAP/aggregate blends and its effectiveness on the main design parameters of the base layer.

Chapter 8: Conclusions and Recommendations

This chapter presents summary of the research results, conclusions and recommended future work.

CHAPTER 2. LITERATURE REVIEW

2.1. Background on RAP

Three most common asphalt pavement removal processes are milling, full-depth reclamation (FDR) and asphalt plant waste. In first process, the top pavement surface only is removed using a milling machine, which can remove up to a 2 in. thickness in a single pass. FDR involves ripping and breaking the pavement using a rhino horn on a bulldozer and/or pneumatic pavement breakers. This process removes both the top old pavement surface and the underlying base or sub-base layers. Asphalt plant waste is generated as all asphalt plant operations accumulates some waste during plant start-up, transition between mixes, and clean-out. When these accumulated materials are properly crushed and screened, the RAP consists of high-quality, well-graded aggregates coated by asphalt. After collecting the RAP, material characterization is performed with respect to aggregate gradation and asphalt content.

In the early 1970's pavement recycling became of interest as a result of severe price inflation in the oil market due to decrease supplies from the oil producing and exporting countries (OPEC) caused from 1973 war in the Middle East. FHWA initiated a project to demonstrate the technical viability of asphalt recycling as a rehabilitation technique. This effort resulted in materials, mix design and construction guidelines for implementing an asphalt recycling project. States and paving contractors began making extensive use of RAP and over the years a number of applications were developed including: addition to hot-mix asphalt (HMA); aggregate in cold-mix asphalt; granular or stabilized base and sub-base course; fill or embankment material. In 2000, FHWA reported that in the United States 33 million metric tons RAP were used in highway construction applications out of 41 million metric tons RAP produced amounting to some 80%

reuse (P. J. Cosentino, Kalajian, Dikova, Patel, & Sandin, 2008). Lately, FHWA reported that presently all 50 states are using RAP (P. J. Cosentino et al., 2008).

As large quantities of RAP are produced during highway maintenance and construction, some can be used in new HMA, while the surplus RAP is still frequently available. If this material could be reused on site as a sub-base or base material, it would reduce the environmental impact, reduce the waste stream, and reduce the materials transportation costs associated with road maintenance and construction. There are an estimated 90 million tons of RAP milled yearly with 80% to 90% being reused in roadway repaving, translating into 18 million tons of RAP being available for other uses (P. Cosentino et al., 2003). Using RAP as recycle material was developed through a combination of environmental, economic and technological factors. Recycling eliminates the disposal and the concurrent hauling and transportation costs, provides a source of readily available aggregate as a substitute for limited natural resources, and finally takes advantage of the technological advancements brought about by inexpensive material processing techniques.

The clear conclusion from the expansion test results was that RAP materials have much lower tendencies to expand or swell when compared to the high expansion potentials of especially the virgin steel slag aggregates (Deniz, Tutumluer, & Popovics, 2009). As it is well known, RAP has both elastic and viscous properties. An elastic material can be modeled as a spring. For a spring, the deformation is proportional to the applied force. A viscous material can be modeled as a dashpot. For the dashpots, force is proportional to velocity (stress is proportional to rate of strain).

2.2. RAP Used in HMA

One recurring question regarding RAP is whether it acts like a “black rock”. If RAP acts like a black rock, the aged binder will not combine to any appreciable extent with the virgin binder added and will not change the total binder properties (R. McDaniel & Anderson, 2001). To remedy

the situation of using RAP in HMA layer, the Federal Highway Administration's Superpave mixtures expert task group used past experience to develop interim guidelines for the use of RAP in the Superpave method. These guidelines reflect the fact that the effect of aged binder from RAP on the performance properties of the virgin binder depends upon the level of RAP in the HMA. When the level is low, the effect is minimal, and the RAP is likened to a "black rock" that influences the mix volumetric and performance through its aggregate gradation and properties. As the level of RAP in the HMA increases, the black rock analogy breaks down as the aged binder blends with the virgin material in sufficient quantity to significantly affect its performance properties (R. McDaniel & Anderson, 2001).

During the construction and service life of the roadway from which the RAP was obtained, the asphalt binder in the roadway became aged or hardened by reacting with oxygen in the air. If a high percentage of RAP is used in HMA (greater than 15 to 30 percent), the RAP binder will have to be considered when choosing the virgin asphalt grade added. Because of variability concerns, some states limit the amount of RAP that can be included in new mixtures. Some states allow the use of higher percentages of RAP, if the material is milled off the same project where the new mix will be placed. Nevertheless, if RAP is used from a stockpile that includes material from several projects, smaller RAP content may be used.

RAP materials are not as likely to segregate as aggregates because the asphalt binder in RAP helps keep coarse and fine aggregate bound together (R. S. McDaniel, Soleymani, Anderson, Turner, & Peterson, 2000). The moisture-holding capability of RAP is negligible, because there is little minus No. 200 fraction, and most RAP aggregates are coated with asphalt (Puppala, Saride, & Williammee, 2011). The effect of introducing RAP into the binder course mix was evaluated through a series of laboratory tests including the Marshall test, the indirect tensile stiffness

modulus test, the indirect tensile fatigue test and the water sensitivity test. The laboratory tests have shown that the introduction of RAP to the binder course mix resulted in an improvement in all mechanical properties. In particular, it was found that the mix containing up to 30% RAP, displayed improved fatigue resistance relative to the control mix manufactured from virgin materials (Tabaković, Gibney, McNally, & Gilchrist, 2010).

The description of the process of extracting, recovering and testing the RAP aged binder properties when needed, shows that for low RAP contents (<15%) it is not necessary to do this testing because there is not enough of the old, hardened RAP binder present to change the total binder properties. However, at higher RAP contents (>25%), the RAP aged binder will have a noticeable effect, and it must be accounted for by using a softer grade of binder. For intermediate ranges of RAP (15-25%), the virgin binder grade can simply be dropped one grade. For higher percentages of RAP, there is a need to extract and recover the RAP binder and determine its properties. These results provide compelling evidence that RAP does not act like a black rock. It seems unreasonable to suggest that total blending of the RAP binder and virgin binder ever occurs, but partial blending apparently occurs to a significant extent. The findings also support the concept of a tiered approach to RAP usage because the effects of the RAP binder are negligible at low RAP contents (R. S. McDaniel et al., 2000).

These findings mean that in general, conventional equipment and testing protocols can be used with RAP binders. The tiered approach allows for the use of up to 15 to 30 percent RAP without extensive testing. Higher RAP contents can also be used when additional testing is conducted. The significance of these results is that the concept of using a softer virgin binder with higher RAP contents is supported. A tiered approach to the use of RAP is found to be appropriate. The advantage of this tiered approach is that relatively low levels of RAP can be used without

extensive testing of the RAP binder. If the use of higher RAP contents is desirable, conventional Superpave binder tests can be used to determine how much RAP can be added or which virgin binder to use (R. McDaniel & Anderson, 2001).

2.3. RAP Aging Characteristics

Asphalt for pavement construction is called asphalt cement. Asphalt cement is often added to aggregate to make asphalt concrete or asphalt mix for construction of flexible asphalt pavements for highways and parking lots. When these asphalt pavements are removed from a road surface, the by-product is commonly called reclaimed asphalt pavement (RAP). RAP mostly consists of ground up old asphalt pavement that stayed for its lifetime until it completely distressed. As asphalt ages and is exposed to various waste elements, it tends to harden and become brittle. As a result the viscosity of the asphalt cement increases and elasticity decreases (Huesemann, Hausmann, & Fortman, 2005).

Asphalt binder originally consists largely of hydrocarbons, along with other molecules and molecular structures. These molecules generally consist of carbon, hydrogen, sulfur, oxygen and nitrogen, as well as a traceable amount of metals (Bennert & Dongré, 2010). To understand the asphalt chemistry and its components especially for aged binder as the case in using RAP, many tests are recommended for the extracted asphalt binder collected from RAP.

The role of the aged binder in the RAP was studied before in several researches especially in the case of reusing RAP in HMA mixtures as mentioned before. As it is important to understand the blending probability of the aged asphalt binder in RAP with the virgin asphalt added to restore its original properties. One of the main issues to determine appropriate levels of RAP in asphalt mixtures was that it assumes an ideal condition that the RAP aged asphalt binder fully blends with the virgin asphalt binder added. However, different researches had shown that this is not most

likely the case and may be less than originally assumed (Bennert & Dongré, 2010). Many researchers proved that the mechanical blending with the virgin asphalt added to the RAP in HMA mixtures interact only with a small portion of the RAP asphalt binder (Bennert & Dongré, 2010). This result agree partially with the assumption that RAP will behave just as a black rock if it is used in HMA mixes especially if the RAP content is below 15% (R. S. McDaniel & Shah, 2003).

However, the extraction and recovery process for collecting the aged binder with PG grading tests indicated that the asphalt binder did not stiffen linearly with increasing RAP content in HMA mixtures (Bennert & Dongré, 2010). That means that the aged binder has indirect relation with the stiffness and has partially blending effect with the virgin asphalt added. Therefore, it is important to study the role of the aged binder in RAP if it is used as a base layer especially that it is usually used in higher contents (50% or more) than HMA layer (25% or less). Most probably there will be an effect of aged binder on stiffness parameters of base layers with the variation of different field conditions, such as moisture content, density, fine contents, etc.

The definition of asphalt aging refers to a series of changes in asphalt concrete such as evaporation, oxidation, polymerization, and changes of the internal structure of asphalt. In the aging process of asphalt, the asphalt binder is exposed to the temperature, water and oxygen in the air which causes the aromatics, resins and asphaltenes partially oxidize to produce dehydrogenation of water (Zhang & Sun, 2012). Then, the remaining parts of heavy oil component of active groups will polymerize or shrink and produce higher molecular weight substances (Zhang & Sun, 2012). And, during this process, it was seen that its softening point will increase, and its penetration will lower, the insoluble heptane's will increase, and its mobility is also greatly reduced (Zhang & Sun, 2012).

The Abson method was used frequently to recover asphalt binder from RAP, but several studies have warned that it may cause excessive hardening of the extracted binder. This excessive oxidative hardening of the recovered binder is partly due to chemical and physical hardening processes which the asphalt binder experiences during the removal process of the solvent (Zahid Hossain, 2012). Therefore, it is recommended to use the rotary evaporator instead. This practice is intended to recover asphalt from a solvent using the rotary evaporator to ensure that changes in the asphalt properties during the recovery process are minimized.

Gel permeation chromatography (GPC), also known as size exclusion chromatography (SEC), is used to separate the molecules of a solution into its various sizes, yielding a clear depiction of the molecular weight distribution within the medium. Jennings et al. (Jennings et al., 1980) found that, based on a primitive asphalt rating system, the worse the asphalt pavement was with respect to damage, the higher the number of large molecules (LMS) present in the asphalt. The concept of large molecular size (LMS) increase with respect to the stiffening of asphalt binder due to oxidation and aging is a popular one.

Fourier transform infrared spectroscopy (FTIR) is a method of determining chemical functional groups within a medium. Chemical functional groups are groups of atoms responsible for different reactions within a compound. Bowers et al. (Bowers, Huang, Shu, & Miller, 2014) explore the blending efficiency of RAP within asphalt paving mixtures by considering GPC and FTIR to investigate each layer collected from the stage extraction of asphalt and determine the binder blending that occurs in HMA mixtures on the basis of the molecular and chemical characteristics defined by the aging processes.

As stated in this research by Bowers et al. (Bowers et al., 2014), it was found that the carbonyl and sulfoxide functional group’s increased with aging time. However, the sulfoxide

group decreased after 507 hours of aging. An increase in the carbonyl is characteristic of an increase in the oxidation, or aging of the asphalt binder. The carbonyl component found in the aged binder is well known to be sensitive to moisture level variation. This issue may be very important factor in analysis of mechanical testing results for RAP blends used as a base layer. Based on the comparison between GPC and FTIR in the previous study, the FTIR yielded a higher differentiation in ratio than the GPC. This leads to the belief that the FTIR may be more effective for determining asphalt aging properties in a layered system such as the stage extraction. On the other hand, GPC is considered as a gradation test for asphalt components while the FTIR is used to measure the percentage of the molecular compounds present in the aged binder such as carbonyl. Therefore, both tests are important to investigate the aged asphalt characteristics.

2.4. RAP Used in Base Layer

The old asphalt pavement is often recycled and processed in the same place to produce a granular pavement base. Hot in-place and cold in-place are the two methods of in-place recycling of asphalt pavement. Sometimes this recycling is performed by adding some additives, for example, cement or foamed asphalt to produce a stabilized base layer (M. Attia et al., 2009).

Many State Departments of Transportation allow the use of recycled asphalt pavement (RAP) to be blended with mineral aggregates to produce a composite base course material. An increased percentage of RAP in base course materials could offer potential economic and environmental benefits. However, as more RAP material is incorporated into the base course material, concerns are being raised by the agencies, such as the impact of a high percentage RAP on pavement, appropriate compaction requirements, and drainage characteristics, all of which may affect the overall long-term performance of both flexible and rigid pavement structures (Wen & Wu, 2011).

Base and sub-base layers are often the load-bearing layers of the pavement whereas subgrade is the underlying ground where the excavation stops and construction begins. Main functions of base layer in flexible pavements can be summarized as follows:

- Distribution of the wheel load over larger surface area by building up relatively thick layer to protect the subgrade layer underneath.
- Provide support and stability to the top surface asphalt concrete (AC) layers.
- Provide drainage of water from pavement layers especially during thawing periods in cold climates.
- Gives additional protection against frost action if necessary during cold climates.
- Improving structural support or resistance to deformation by reducing the thickness. This may be more desirable and economic by stabilizing the base course with asphalt or cement, or to reinforce it with geo-synthetics.

Materials for base and sub-base layers are selected such that they provide maximum drainage, stiffness, and strength. Material strength helps in prevention of rutting for the top asphalt layer as base layer is responsible for carrying traffic loads on traditional flexible pavement as shown in Figure 2.1. Drainage is important because increased water content decreases material strength and thus pavement failure. In cold climate, increased water content in the base and sub-base layers can also lead to pavement heaving and fracturing. Water retention characteristics and hydraulic conductivity are surrogates for drainage characteristics whereas resilient modulus is a surrogate of material stiffness and rutting. And cohesion and friction angle are surrogates for material shear strength (Kang, Gupta, Ranaivoson, Siekmeier, & Roberson, 2011).

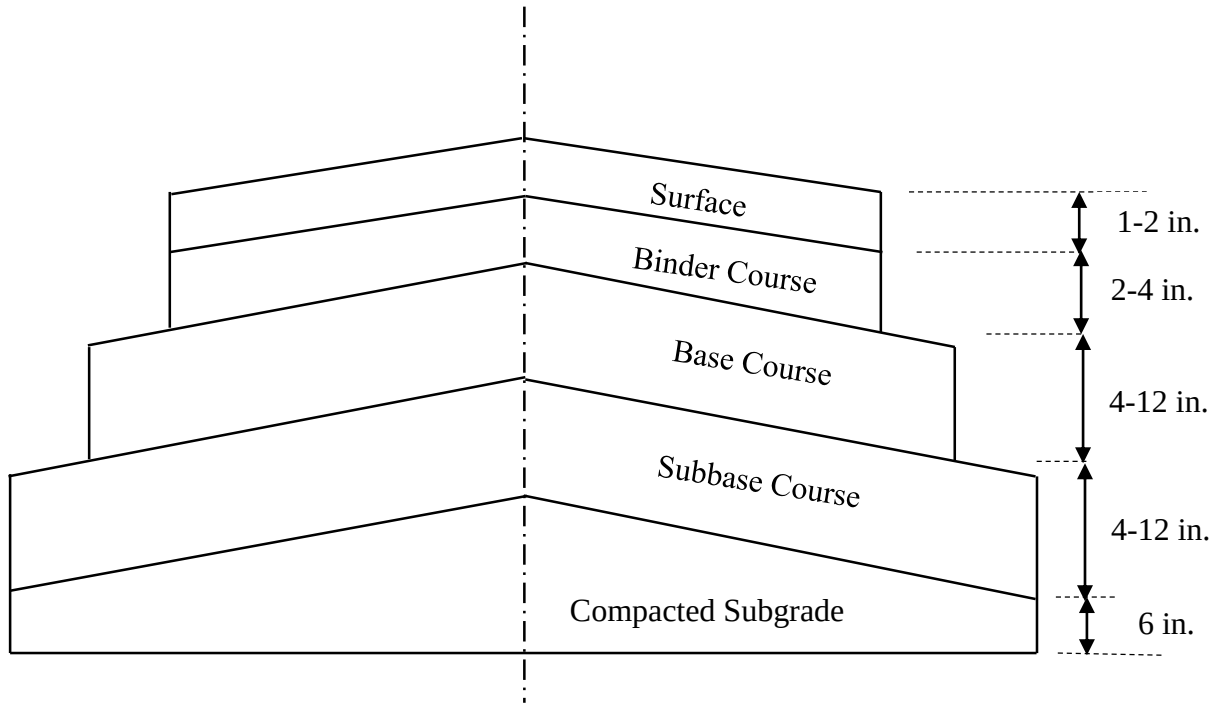

Figure 2.1. Conventional Flexible Pavement Design (Huang, 1993)

Reclaimed asphalt pavement (RAP) can be used as granular base or sub-base material in virtually all pavement types, including paved and unpaved roadways, parking areas, bicycle paths, gravel road rehabilitation, shoulders, residential driveways, trench backfill, engineered fill, pipe bedding, and culvert backfill. RAP that has been properly processed and in most cases blended with conventional aggregates has demonstrated satisfactory performance as granular road base for more than 20 years and is now considered standard practice in many areas.

At least 13 state agencies (Arizona, Illinois, Louisiana, Maine, Nebraska, New Hampshire, North Dakota, Oregon, Rhode Island, South Dakota, Texas, Virginia, and Wisconsin) have used RAP as aggregate in base course. In addition at least four state agencies (Alaska, New York, Ohio, and Utah) have used RAP as unbound aggregate in sub-base, and at least two states (California and Vermont) have experience with RAP use in stabilized base course.

In addition to the states listed above, it has also been reported that RAP has been used as a base course additive in Idaho and New Mexico. Some of the positive features of RAP aggregates that have been properly incorporated into granular base applications include adequate bearing capacity, good drainage characteristics, and very good durability. However, non-properly processed RAP or blended to design specification requirements may result in poor pavement performance (Chesner, Collins, & MacKay, 1997).

The most common RAP applications as base materials are mixed RAP and granular aggregate blends, full-depth reclamation and cold in-place recycling. Researchers described initial trials of RAP as a base layer as satisfactory but recommended further research in two main areas: (i) the structural capacity of RAP-aggregate blends considering fundamental engineering properties and (ii) the possibility of using RAP at higher content. Strain is an important structural factor for base material in fatigue analysis. The base layer is designed specially to resist fatigue cracking (Alam, Abdelrahman, & Schram, 2010). Finding innovative ways to incorporate RAP into highway base course applications will provide both environmental and economic benefits by allowing in situ recycling of material for projects such as widening or shoulder addition. RAP is a well-drained granular material which is already on site. However, 100% RAP has low bearing strength and creeps under load.

Two main problems limit the reuse of RAP in a roadway base course; relatively low strength and tendency to creep under a constant stress. In general, adding RAP to lime-rock blends for example increased the soaked retained strength and improved permeability compared to 100% lime-rock. Also, the FHWA found that properly processed RAP and in most cases blended with conventional aggregates has demonstrated satisfactory performance as granular road base for more than 30 years. However, most reclaimed asphalt pavement materials, when used as a total

substitute for natural aggregates in base applications, do not often meet the minimum stiffness property requirements set by AASHTO (Puppala, Hoyos, & Potturi, 2011).

To use RAP as a base layer, different engineering properties need to be investigated. Gradation is a very important material property for a pavement base layer because it influences the base stability. In an aggregate plus RAP blend, the gradation also depends on the characteristics of the virgin aggregate. It was found that the addition of RAP to the virgin materials resulted in an increase in the amount of particles passing the upper sieves, and a decrease in the percentage of particles passing the lower sieves. A final report of Florida DOT (P. J. Cosentino et al., 2012) collects a group of several researches that concludes the effect of different RAP/Aggregate blends on different physical and mechanical properties.

Generally, it was found that the resilient modulus increases with adding RAP to base layer, however CBR decreases which is another measure of stiffness but under static load. While the results coming from compaction curves gave lower optimum moisture content and maximum dry densities for RAP/Aggregate blends. Permeability results were contradictory as Mac George et al. (MacGregor, Highter, & DeGroot, 1999) declared no change and Bennert & Maher et al. (Bennert & Maher, 2005) declared it decreased while Taha et al. (Taha, Ali, Basma, & Al-Turk, 1999) declared it increased.

It is well known that granular pavement layers show a nonlinear and time-dependent elastic-plastic response under traffic loading. To deal with this nonlinearity and to differentiate from the traditional elasticity theories, the resilient response of granular materials is usually defined by resilient modulus (M_R) and Poisson's ratio. Previous investigations, from the early studies reported that stress level is the factor that has the most significant impact on resilient properties of granular materials (Lekarp, Isacsson, & Dawson, 2000a). Compared to the resilient

modulus, very few studies have aimed at characterizing Poisson's ratio. Determination of Poisson's ratio requires very accurate measurement of radial strain, which in practice has proved to be much more difficult than measuring axial strain. Therefore, it is common to assume a constant value, for instance, 0.35, for the resilient Poisson's ratio of granular materials (Lekarp et al., 2000a). However, there is a need to measure Poisson's ratio at various testing conditions to investigate the relation between both parameters M_R and Poisson's ratio.

Several researchers (Garg & Thompson, 1996; Jeon, Steven, & Harvey, 2009; Kim & Labuz, 2007; MacGregor et al., 1999) have investigated permanent deformation for RAP under cyclic loading when compared to several typical base layers but they got different results. While RAP had higher M_R so it should have lower permanent deformation, which was found in (M. I. E.-S. Attia, 2010; Bennert & Maher, 2005; MacGregor et al., 1999; Papp, Maher, Bennert, & Gucunski, 1998). Through this literature review, a full project was found in Illinois which consisted of the construction of the pavement base and then the observation of the performance of the roadway. In 1993, the Lincoln Avenue of Urbana, Illinois, was constructed with RAP base. The overall structural response and the field performance were monitored; in the conclusion the author mentioned that RAP can be successfully used as a conventional flexible pavement base material (Garg & Thompson, 1996).

2.5. Environmental Impacts of Using RAP

Recycling of RAP has both environmental and economic benefits. Environmentally, recycling of RAP saves natural resources and landfill space. Economically, recycling of RAP saves the asphalt facility owner money. In comparison, there are two different types of environmental concerns related to leaching of pollutants from RAP. The first is the leachate produced when rainfall infiltrates the RAP stockpiles. The second environmental concern is the use of RAP as fill

material, either in a beneficial reuse option such as construction of pavement layer or simply as mono-fill disposal. RAP used as fill material could potentially leach off contaminants when rainfall infiltrates the waste in an unsaturated condition. In some instances, the RAP material could be placed below the water table in a saturated condition. In both situations, the leachate produced could potentially be contaminated with trace amounts of hazardous chemicals, namely organic compounds or heavy metals.

Clean fill is defined as "any solid waste virtually inert, not a pollution threat to ground water or surface waters, not a fire hazard, and is likely to retain its physical and chemical structure under expected conditions of disposal or use". Many states have already determined that asphalt road waste should classified as clean fill. Under most current waste management policies, the evaluation of leaching risk is performed by determining the concentration of a pollutant that would occur in the groundwater after leaching from a waste, and comparing that concentration to the applicable groundwater guidance concentration. The researchers concluded that reclaimed asphalt pavement (RAP) should give no concern if used as a clean fill material. There were two studies concerned with RAP in general as a fill material as follows:

2.5.1. RAP leaching characteristics (Townsend, 1998)

This study investigated the leaching characteristics of RAP in thorough laboratory investigation program. The results lead to the conclusion that RAP poses minimal risk to groundwater because of pollutant leaching under normal land disposal or beneficial reuse. It is observed that there was a loss of asphalt content over time. However, the research indicates that old asphalt pavement is not a hazardous waste and does not leach chemicals greater than typical groundwater standards.

One limitation to using RAP as fill material stems from the unknown risks of pollutants leaching from the waste to the environment. Data regarding the composition of leachate from RAP is limited. It has been suggested that chemical compounds, such as polycyclic aromatic hydrocarbons (PAH's) and heavy metals, might be present in RAP and therefore leach from RAP. A series of leaching tests were performed at both batch-scale and in leaching columns.

This study focused on leachable pollutants and did not attempt to characterize the total concentration of pollutants in the RAP. The primary chemicals investigated were volatile organic compounds (VOC's), polycyclic aromatic hydrocarbons (PAH's), and heavy metals. The results of the toxicity characteristic leaching procedure (TCLP) tests performed indicated that the RAP tested was not a hazardous waste.

Volatile organic compounds (VOC's) were not expected to be a major concern in regard to leaching from RAP. Because of their volatility, most of these compounds would tend to evaporate quickly when spilled on the roadway or be expected to leave the RAP samples in the field. Polycyclic aromatic hydrocarbons (PAH's) are a group of chemicals formed primarily during the incomplete burning of coal, oil and gas, or other organic substances. It has been reported that sources of PAH's have included vehicle exhaust, weathered material from asphalt roads, lubricating oils, gasoline, diesel fuel, and tire particles. The results indicated that there was no PAH occurrence greater than the groundwater guidance concentrations in the extracted leachate.

Heavy metals are often cited as a concern when dealing with materials from roadways. Vehicle wear, fuel emissions, and fuel leakage could all result in contamination with heavy metals. Leachate samples were analyzed on both the flame atomic absorption spectrometer and graphite furnace atomic absorption spectrometer in order to reach a detection limit below the groundwater

guidance. These results indicate that the older samples likely contained more lead because of longer exposure to vehicle traffic and emissions.

A few chemicals were observed to leach from asphalt road waste. The primary chemicals encountered were the heavy metals lead, chromium, and barium. The asphalt tested by TCLP was never found to be hazardous. Some concentrations in the TCLP leachate were greater than drinking water standards. The TCLP test is an aggressive test designed to simulate the interior of an anaerobic landfill. Other leaching tests are likely more suitable to measure actual leaching in non-landfilled environments.

The first tests were typical batch-leaching tests including the TCLP, synthetic precipitation leaching procedure (SPLP), and de-ionized water leaching procedure. The second test was a column-leaching test performed to simulate a more realistic environmental condition. Leachate samples obtained from the batch experiments and column experiments were analyzed for the same parameters. The primary chemicals investigated were volatile organic compounds (VOC's), polycyclic aromatic hydrocarbons (PAH's), and heavy metals. The total concentrations of pollutants in the RAP were not measured. Batch tests were performed on all six RAP samples.

In the leachate generated during the TCLP batch test, measurements of volatile organic compounds (VOC's), polycyclic aromatic hydrocarbons (PAH's), and heavy metals all were below detection limit (BDL) and below any applicable TCLP limits. The RAP samples evaluated were therefore not a hazardous waste. The TCLP test is a somewhat aggressive test that represents the conditions inside an anaerobic landfill. Less aggressive tests were therefore also conducted in this study (SPLP and deionized water). Previous studies regarding asphalt road waste also found trace amounts of lead in some circumstances. Since lead was encountered in greater concentrations in older samples, the source of lead was likely prolonged exposure to vehicle traffic and emissions.

Most of the previous studies regarding RAP leaching were consistent with the results found in this study. Organic compounds do not leach from typical RAP under the conditions tested. Heavy metals are sometimes encountered. The literature indicated the presence of chromium, lead, and barium. Only lead was detected in this study and was ascribed to prolonged exposure to traffic and vehicle emissions. The literature often referred to chromium resulting from slag used as aggregate. It should be noted that the aggregate used in the asphalt

As discussed previously, the batch tests were more dilute than the column test. This condition helps to explain why lead concentrations were observed in the column study but not in the batch test. In a real world situation, rainfall and other surface water runoff would ultimately dilute leachate produced from a stockpile before it reaches the groundwater table or a nearby receiving body of water. This phenomenon is commonly referred to as dilution attenuation.

Possible conditions of risk would be from RAP used as fill below the groundwater table in areas with little dilution. Lead was observed in the greatest concentrations in the oldest RAP samples. This indicated that the lead was not a result of the aggregate or asphalt cement, but rather a result of vehicle traffic and emissions. Lead was used for many years in leaded gasoline and in crankcase oil. Since vehicle accidents and accidental spills contribute to this contamination, there is a possibility that this contamination was site specific. Previous studies regarding asphalt road waste also found trace amounts of lead in some circumstances. Lead was encountered in greater concentrations in older samples, indicating that the source of lead was prolonged exposure to vehicle traffic and emissions.

Only lead was detected in this study and was attributed to prolonged exposure to traffic and vehicle emissions. The literature often referred to chromium resulting from slag used as aggregate. It should be noted that the aggregate used in the asphalt samples collected for this study

was assumed to be natural aggregate (e.g. lime rock). If other materials, especially waste materials such as slag, spent sandblast grit and ash, are used as aggregate, the results gathered here may not be applicable. It should also be noted that fresh asphalt was not tested, nor were extremes in temperatures evaluated.

2.5.2. Inorganic contaminant leaching (Kang, Gupta, Bloom, et al., 2011)

Another study was under taken to evaluate the suitability of fly ash (FA), reclaimed asphalt pavement (RAP), recycled cement material (RCM), and foundry sand (FS) mixed in with virgin aggregates as base and sub-base materials. In this research, the results on inorganic contaminants leaching from six mixtures of FA–RAP aggregates under batch and flow through conditions were reported. The concentrations of most inorganic chemicals in both batch and flow through modes from all six mixtures were either below the detection limit of the instrument or less than the EPA drinking water standard. Briefly, from other literature researches, these leaching tests showed that lead concentrations were higher than the drinking water standard for some of the RAP and RCM mixtures with aggregates. For a couple of mixtures of RAP with aggregates, cadmium concentrations in the leachate were also higher than the drinking water standards.

Maximum concentration of inorganic chemicals in the leachate from the flow through tests was generally lower than the corresponding concentration in the batch test. This is expected considering that the reaction time of water with particles in a flow through tests will be limited compared to 18 h in a batch mode, that is, likely insufficient reaction time to completely dissolve or desorb in a flow through set-up. Since flow in column tests is closer to field conditions, results from breakthrough are more realistic in terms of field applications rather than results from the leaching test in batch mode.

The results from this study showed that addition of up to 5% FA and 75% RAP in virgin aggregates will lead to some leaching of aluminum but not any substantial leaching of other inorganic chemicals to the surrounding environment. All mixtures in the batch mode and mixtures containing 15% FA in the flow through set-up showed significant leaching at least initially (<1 pore volume) of several inorganic contaminants thus suggesting that increased residence time of water in contact with the mixture may lead to higher elution of these chemicals above the EPA drinking water standards. There is slight risk that dissolved inorganic chemicals at concentrations higher than the EPA drinking water standards could laterally move to the surface water bodies if mixtures containing 15% FA are used in base and sub-base layers.

2.6. Main Design Base Layer Parameters

2.6.1. Resilient modulus (M_R)

Resilient modulus (M_R) is the main mechanistic design parameter of the base layer as it is used to characterize the elastic stiffness of the pavement materials rather than Young's modulus (Christopher, Schwartz, & Boudreau, 2006; Huang, 1993; Tutumluer & Meier, 1996). Resilient modulus is directly related to the stiffness of the base layer and is mainly associated with the fatigue behavior that happens for hot mix asphalt layer (Itani, 1990; Seed, Chan, & Lee, 1962). Achieving a proper modulus for an unbound base course is important for pavement performance. One commonly used parameter to define material stiffness is the resilient modulus (M_R) similar to Young's modulus, based on the cyclic axial loading as shown in Figure 2.2. M_R is the ratio of imposed axial (deviator) stress (σ_d) and recoverable axial strain (ε_r) after frequent number of loading cycles as shown in Equation 2.1:

$$M_R = \frac{\sigma_d}{\varepsilon_r} \quad (2.1)$$

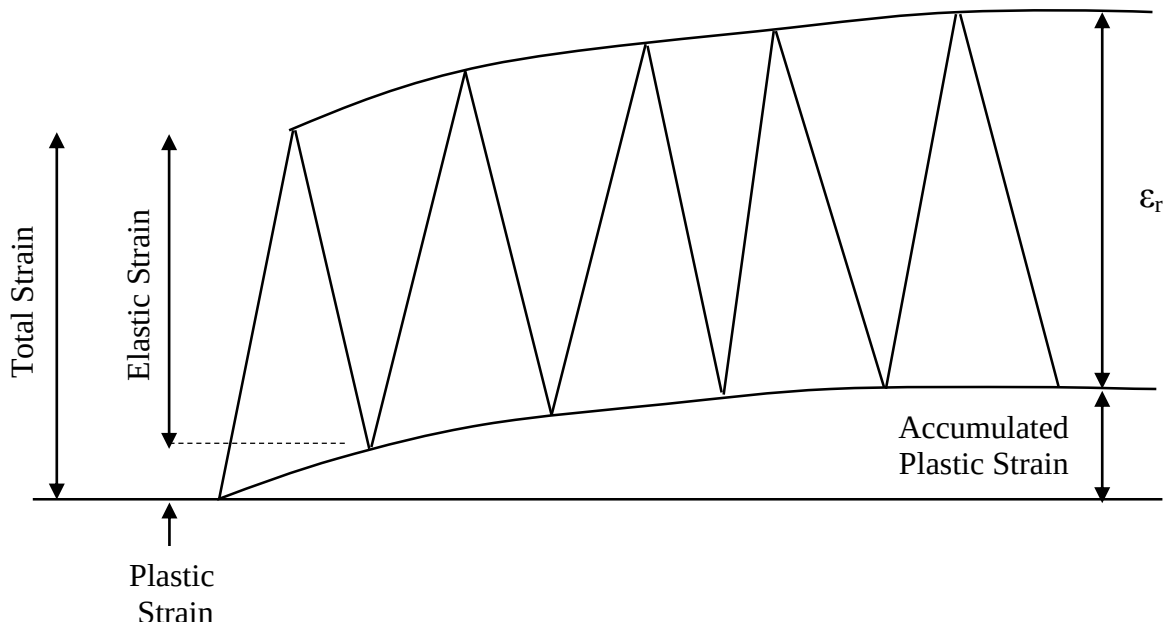

Figure 2.2. Loading Shape of M_R Testing

The resilient modulus (M_R) of unbound layers is a required property during any mechanistic or mechanistic-empirical analysis procedure for flexible pavements. The NCHRP 1-37A Guide for Mechanistic–Empirical Design of New and Rehabilitated Pavement Structures (M. Witczak, Andrei, & Houston, 2004) and the 1993 AASHTO Guide for Design of Pavement Structures (Highway & Officials, 1993) recommend the use of resilient modulus of base materials as a material property in characterizing pavements for their structural analysis and design.

The M_R test is a commonly conducted laboratory procedure to characterize the stiffness and elasticity responses of the base material (Huang, 1993). As pavements are subjected to repeated wheel loads, static testing procedures are not suitable for determining the behavior of aggregate materials subject to moving wheel load (Christopher et al., 2006; Papp et al., 1998; Tutumluer & Meier, 1996). Therefore, the M_R of base materials can be estimated from laboratory repeated load tri-axial tests. It also can be estimated from empirical correlations with soil properties or non-destructive test results.

The M_R test is conducted in the laboratory by maintaining constant confining pressure within a conventional tri-axial cell and applying a cyclic axial stress to simulate traffic loading. There are a number of methods to perform the resilient modulus testing. The most common protocols for this testing are: AASHTO T 292-91, AASHTO T 294- 92, AASHTO T-307, AASHTO T P46-94, LTPP protocol P46 (Protocol, 1996) and NCHRP 1-28A (M. W. Witczak, 2003). During the M_R test, the sample is subjected to different levels of confining pressures and deviator stresses.

The NCHRP 1-28A (M. W. Witczak, 2003) test protocol is the most updated standard for measuring M_R after all required modifications of the other previous standards. This standard for unbound granular materials, consists of 30 loading sequences, but the protocol loading involves conditioning stage, which attempts to establish steady state or resilient behavior, through the application of 1000 cycles of 30-psi deviator stresses at 15-psi confining pressure. The cycles are then repeated 100 times for 30 loading sequences with different combinations of deviator stress and confining pressure. The M_R value is calculated as the mean of the last five cycles of each sequence from the recoverable axial strain and cyclic axial stress.

The resilient modulus (M_R) of unbound granular material is affected by several factors including: the state of stress, moisture content, dry density and freeze-thaw action. Several researchers have tried to understand and model the effect of these factors on the resilient modulus of different granular materials. A limited effort was conducted to understand the effect of those factors on M_R of RAP and RAP/aggregate blends as a pavement base course layer (Mohamed Attia & Abdelrahman, 2011). From the literature survey of M_R for base layer, it was found that M_R is more dependent on confining pressure than deviator stress levels (Huang, 1993).

Several constitutive M_R models were studied for base layer, especially in case of using RAP without taking in consideration all factors mentioned before and the effective confining pressure levels at different state of stresses. The MEPDG model was found to be the best suitable prediction model for M_R (Mohamed Attia & Abdelrahman, 2011). This prediction model is called mechanistic-empirical because of the mechanistic calculation of stresses, strains, and deflections properties of a pavement structure. These properties are the fundamental pavement responses under repeated traffic loadings. The relation of these responses to field distresses and performance is determined using existing empirical relationships, widely known as transfer functions. This design process is an iterative procedure that starts with a trial design and ends when predicted distresses meet the acceptable limits based on the level of statistical reliability desired (Chehab & Daniel, 2006).

Based on the literature review, Attia et al. (M. I. E.-S. Attia, 2010) collected nine prediction models were previously used for granular base materials and, tested on RAP and RAP/aggregate blends but only under the effect of different state of stresses. A summary of the investigated models is presented in Table 2.1. The M_R for granular material was found to increase with the increase in the confining pressure, as presented in the first model (Kim & Labuz, 2007). Several researchers reported that the M_R value was dependent on the bulk stress θ (first stress invariant) applied to the sample. The K-θ model (Huang, 1993) was used to describe the resilient behavior of unbound material, as presented in the second model at Table 2.1. In reality, most soils are affected by both the confining pressure and shear stress. Uzan proposed a model which accounted for the shear stress effects (Uzan, 1985). Uzan's model is presented as the third model in Table 2.1.

Later the octahedral shear stress was used instead of deviator stress, as presented in the fourth model (M. Witczak & Uzan, 1988). The M_R was also modeled based on both the deviator

stress and confining pressure by Pezo et al. (Pezo, 1993), as presented in the fifth model. Tam and Brown (Tam & Brown, 1988) suggested modeling the M_R of granular material using the mean stress to the deviator stress ratio, as presented in the sixth model. Itani (Itani, 1990) developed a model that included bulk stress, shear stress and an additional confining pressure component, as presented in the seventh model in Table 2.1.

A modified form of Uzan's equation is used by the mechanistic-empirical pavement design guide (MEPDG) (Lekarp et al., 2000a), as presented the eights model in Table 2.1. Witczak evaluated 14 constitutive models (M. Witczak, Andrei, & Houston, 2000) in both log-log and semi-log forms for their capabilities of predicting the resilient behavior of different granular material and recommended a five-parameter model as the model that statistically has the overall goodness of fit. Witczak's model is presented the ninth model in Table 2.1. Several researchers proposed correlations of the resilient modulus with the stress state (Mohammad, Herath, Rasoulian, & Zhongjie, 2006).

The influence of stress state on unbound material stiffness has long been recognized in pavement engineering. For coarse-grained granular soils as base layer, an increase in stiffness with increasing confining stress is usually the dominant effect. In reality, most soils exhibit both effects of increasing stiffness with increasing confinement and decreasing stiffness with increasing shear (Andrei, Witczak, Schwartz, & Uzan, 2004). Witczak and Uzan (M. Witczak & Uzan, 1988) have proposed a "universal" model that combined both effects into a single Equation 2.2:

$$M_R = K_1 . P_a \left(\frac{\theta}{P_a}\right)^{K_2} \left(\frac{\sigma_d}{P_a}\right)^{K_3} \quad (2.2)$$

Where $K_1 > 0$, $K_2 \geq 0$ and $K_3 \leq 0$ and each K parameter is a multiple regression constant calculated from resilient modulus test.

Table 2.1. Resilient Modulus Predictive Models (M. I. E.-S. Attia, 2010)

Model No.	Model Name	Equation
1	Confining Pressure	$M_R = K_1 . P_a . \left(\frac{\sigma_3}{P_a}\right)^{K_2}$
2	K - Θ	$M_R = K_3 . P_a . \left(\frac{\Theta}{P_a}\right)^{K_4}$
3	Uzan (Deviator Stress)	$M_R = K_5 . P_a . \left(\frac{\Theta}{Pa}\right)^{K_6} . \left(\frac{\sigma_d}{Pa}\right)^{K_7}$
4	Uzan (Octahedral Shear Stress)	$M_R = K_8 . P_a . \left(\frac{\Theta}{P_a}\right)^{K_9} . \left(\frac{\tau_{oct}}{P_a}\right)^{K_{10}}$
5	Pezo	$M_R = K_{11} . P_a . \left(\frac{\sigma_3}{P_a}\right)^{K_{12}} . \left(\frac{\sigma_d}{P_a}\right)^{K_{13}}$
6	Tam & Brown	$M_R = K_{14} . \left(\frac{P}{\sigma_d}\right)^{K_{15}}$
7	Itani	$M_R = K_{16} . P_a . \left(\frac{\Theta}{3P_a}\right)^{K_{17}} . \left(\frac{\sigma_3}{P_a}\right)^{K_{18}} . \left(\frac{\sigma_d}{P_a}\right)^{K_{19}}$
8	MEPDG	$M_R = K_{20} . P_a . \left(\frac{\Theta}{P_a}\right)^{K_{21}} . \left(\frac{\tau_{oct}}{P_a} + 1\right)^{K_{22}}$
9	Witczak	$M_R = K_{23} . P_a . \left(\frac{\Theta - 3K_{26}}{P_a}\right)^{K_{24}} . \left(\frac{\tau_{oct}}{P_a} + K_{27}\right)^{K_{25}}$

In all the models, stress terms are normalized with respect to atmospheric pressure (P_a)

where:

σ_d = deviator stress (psi), $\sigma_d = \sigma_1 - \sigma_3$

σ_1 = axial stress (psi)

σ_2 = lateral stress (psi), $\sigma_2 = \sigma_3$

σ_3 = confining pressure (psi)

θ = bulk stress (psi) = $\sigma_1 + \sigma_2 + \sigma_3 = \sigma_d + 3\sigma_3$ (psi)

Pa = atmospheric pressure = 14.7 (psi) = 101.5 (KPa)

P = mean normal stresses = $\frac{(\sigma_1+\sigma_2+\sigma_3)}{3} = \frac{\sigma_d}{3} + \sigma_3$ (psi)

τ_{oct} = octahedral shear stress = $\frac{1}{3}\sqrt{\{(\sigma_1 - \sigma_2)^2 + (\sigma_1 - \sigma_3)^2 + (\sigma_2 - \sigma_3)^2\}}$, (psi)

K_i = multiple regression constants evaluated from the resilient modulus tests.

The modification of previous Equation 2.2 has been adopted for the new national pavement design guide being finalized in NCHRP Project 1-37A (M. Witczak et al., 2004):

$$M_R = K_1 . P_a (\frac{\theta}{P_a})^{K_2} (\frac{\tau_{oct}}{P_a} + 1)^{K_3} \quad (2.3)$$

Where the 1 in the (τ_{oct}) term is to avoid numerical problems when (τ_{oct}) approaches zero. As the model presented in Equation 2.3 shows a clear improvement for some materials and tests while for others it actually diminishes model accuracy. After some trials and errors in NCHRP 1-28A (M. W. Witczak, 2003), it was found that adding K_4 (as Equation 2.4) to the previous model increases accuracy generally but the model remains inconsistent. For some materials, it shows improvement and for some others it shows less accuracy. Because the (+1) model were not consistent in showing improvement on all tests or for all materials, it was obvious that 1 was not always the right value. Hence, in the last model as presented in Equation 2.4, a regression constant K_5 was introduced instead of (+1). As expected, the analysis showed that the model exhibits the best overall goodness-of-fit statistics (Andrei et al., 2004).

$$M_R = K_1 . P_a (\frac{\theta - 3K_4}{P_a})^{K_2} (\frac{\tau_{oct}}{P_a} + K_5)^{K_3} \quad (2.4)$$

The M_R is a primary input to any mechanistically-oriented pavement design procedure. The pavement design computer code must be adapted to support the specific predictive equation selected for M_R. Upon completion of NCHRP Project 1-28A (M. W. Witczak, 2003), no recommendation was made about the final form for the M_R model. It was obvious that the selection of the final model had to be coordinated with the pavement design method or code in which it was to be implemented. Development of the AASHTO 2002 "Guide for the Design of New and Rehabilitated Pavement Structures" was just getting under way when NCHRP Project 1-28A (M. W. Witczak, 2003) was being completed.

After a thorough review of the results of Witczak & Uzan (Andrei et al., 2004) and other studies from the literature dealing with prediction of the resilient response of unbound materials, the NCHRP Project 1-37A (M. Witczak et al., 2000) team selected the model presented in Equation (2.3) as the recommended M_R model to be implemented and used in the 2002 design guide. This model was deemed the best compromise between accuracy, ease of implementation, and computational stability (for the case of $\tau_{oct} = 0$). The model form given in Equation 2.3 was implemented successfully in the AASHTO 2002 design guide software.

2.6.2. Permanent deformation (PD)

The mechanistic pavement design requires proper understanding of the properties and performance of the materials used. Strain is carried into a material when it is loaded and this strain is divided into two parts resilient and permanent. The resilient strain part from the applied load can be recovered when the material is unloaded. The rest of the strain not recovered is the permanent capable of doing stress behavior on the material (Adu-Osei, 2000). Permanent deformation (PD) in unbound granular base and/or sub-base layers was generally assumed to be negligible. But this assumption proved to be false, because serious rutting can occur within those layers if they are not properly designed, constructed or characterized (Park, 2000). PD happens in all layers of pavement structure; top asphalt mix, base and/or sub-base layer and subgrade soil.

Therefore, PD became a key factor in the failure of the whole pavement structure as accumulation of PD in base layer causes rutting failure for the top asphalt layer (Erlingsson & Rahman, 2013). The plastic deformations of different pavement layers contribute to the surface rutting in flexible pavements. However, rutting in flexible pavements is often associated with permanent deformation of the unbound granular layer (Erlingsson & Rahman, 2013). PD has always been considered as one of the most important distresses in flexible pavements, and unbound

materials can have a major contribution in the overall amount of rutting. The typical behaviors of PD for base layer can be denoted by three different types as shown in Figure 2.3: Initial stage "A" (Shakedown theory), Secondary stage "B" (Creep phenomena), and Tertiary stage "C" (incremental failure) (Arnold, 2004; Werkmeister, 2004).

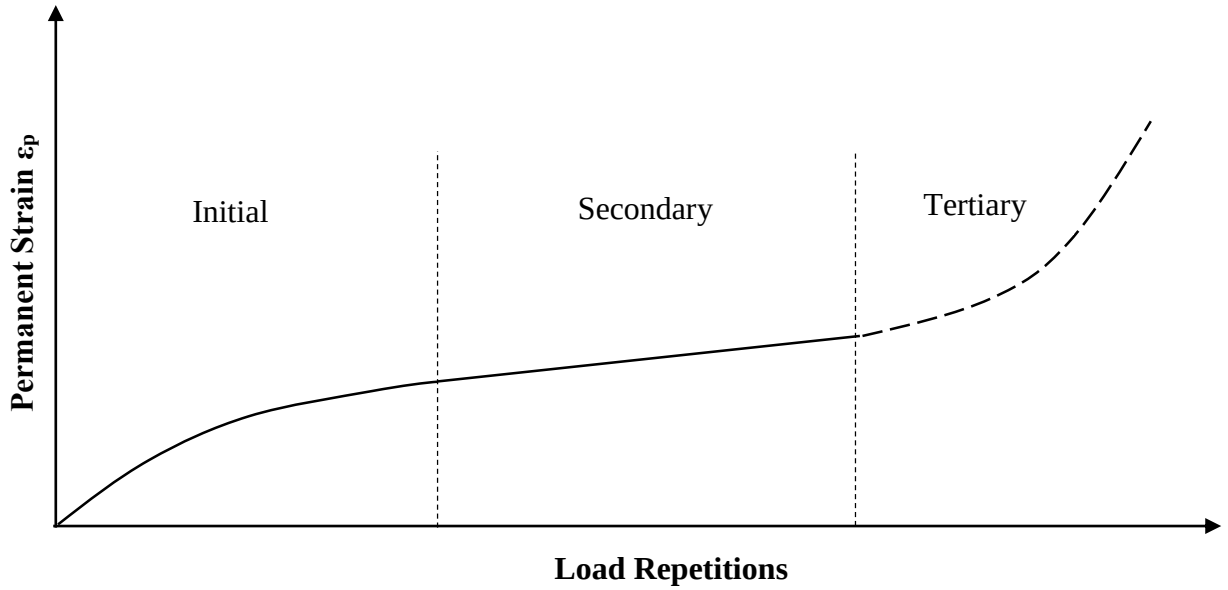

Figure 2.3. Permanent Deformation Stages (Werkmeister, 2004)

For a well-designed pavement structure, with high quality base aggregates, enough water content and compaction, the granular base behavior is expected to be of Type "A". However, the use of RAP particles within the unbound granular base typically cause the material to behave like Type "B", meaning that the permanent strain rate may never stabilize and remain either constant or increases until the material failure is reached. It was reported that the permanent deformation of the unbound layer is questionable and depends on many factors (Lekarp, Isacsson, & Dawson, 2000b; Werkmeister, 2004).

There are several important factors affecting the permanent deformation of unbound materials. Based on published results, the most important factors are the number of load repetitions, confining pressure, stress level, moisture content, density, loading time and frequency,

and stress history (Bani Hashem & Zapata, 2013). Usually in base layer, most of the stress goes into permanent strain that accumulates with repeated loading and unloading of traffic flow. It is this accumulating permanent strain in an aggregate base course that creates rutting.

The measurement of permanent deformation characteristics of unbound aggregates has received relatively less experimental attention than resilient modulus, as M_R considered the main engineering design parameter in base layer. Some notable contributions were made on the testing procedure for permanent deformation of base layer such as repeated load tri-axial (RLT) which have two types: single-stage and multi-stage of loading. This is partly because this experiment is inherently destructive and require many specimens to be tested compared to the lower stress level, essentially non-destructive, resilient strain tests (Adu-Osei, 2000). The RLT test involves imposing cyclic stresses, similar to the stress conditions in the field, on a prepared cylindrical specimen where the corresponding deformations are measured.

A multi-stage (MS) testing approach has been introduced where a number of consecutive stress paths are applied to the same specimen reducing considerably the effort needed to test the material. This approach is also more realistic since it takes into account the effect of stress history as the same specimen is subject to different stress paths of varying magnitudes. The drawback of this method, on the other hand, is the complexity of modeling the accumulation of permanent deformation compared to single-stage RLT tests (Erlingsson & Rahman, 2013). The MS testing procedure is very close to the situation of resilient modulus testing except that MS testing change the deviator stress levels without changing the confining pressure levels. The M_R testing apply 30 sequences by changing both deviator and confining stress with lower number of load repetitions (100 cycles) than MS test (5000 cycles).

Huge efforts of research on granular base layer were focused on modeling the resilient behavior of these materials. On the other hand, less research was done focusing on their permanent behavior. This because permanent deformation tests are more difficult to perform than resilient modulus tests. These permanent deformation tests are time consuming and a new sample should be prepared for each stress condition as mentioned before. Therefore, greater achievements were accomplished with the resilient behavior of granular base layer materials rather than the long-term rutting distress of granular materials (El-Badawy, 2006).

Utilizing recycled asphalt pavements (RAP) as a base layer is questionable by many state agencies and researchers. This is mainly due to the PD accumulated when using RAP. Many researchers had several contradictive results. Few studies (M. I. E.-S. Attia, 2010; Jeon et al., 2009) proved that PD decreases when increasing percentage of RAP in the base layer blend and more studies (Bennert & Maher, 2005; Garg & Thompson, 1996; Kim & Labuz, 2007) proved opposite result. However, resilient modulus (M_R) results were more significant than PD. M_R values were directly proportional to the percentage of RAP in the blend. This result yields that modeling of M_R for RAP in base layer is much an easier process than modeling PD. Modeling the PD for RAP used in base layer was not extensively studied before. Also, there are no specific models for prediction of PD for RAP base layer.

Two main design methods were used by most of the design agencies to control permanent deformation. The first is to control the vertical compressive strain on the top of the subgrade and the second is to limit the total accumulated permanent deformation on the top pavement surface based on the permanent deformation of each individual layer within the whole pavement matrix to a tolerable amount (Huang, 1993; Yoder & Witczak, 1975). The second method follows the concept taken in consideration during implementation of the mechanistic-empirical pavement

design guide (MEPDG) (Guide, 2008). This concept was based on prediction of accumulated deformation in each pavement layer through predictive models. Therefore, prediction of permanent strain for unbound granular materials is essential but it requires constitutive relationships or mathematical models.

It is well known that the two most important factors affecting the PD accumulated in the base layer, are the number of load repetitions and stress condition. Therefore, both parameters are taken in consideration in order to model the permanent deformation of granular base layer. Several models were presented in previous researches to model permanent deformation in unbound base layer and subgrade based on both field and laboratory data. Researchers found and documented the importance of the number of load cycles on PD. Therefore, the number of load cycles is a main component in all permanent deformation models.

Badawy and Lekarp et al. (El-Badawy, 2006; Lekarp et al., 2000b) had summarized the permanent deformation models established several years ago. Generally they differentiate these models as relationships describing the influence of number of load applications and relationships describing the influence of applied stresses. In addition, almost all researchers pointed that the moisture content plays a critical role in accumulation of permanent deformation for unbound materials. Until now, there is a limited number of models that take the moisture content as a primary predictor. In order to estimate the permanent deformation of unbound materials when using Level 3 analysis of MEPDG, a PD model was established as a function of the number of repetitions, the groundwater table depth and CBR of the soil (Lekarp et al., 2000b).

Finally MEPDG permanent deformation model for granular base layer takes effect of load repetitions, water content, stress levels and resilient deformation. However, the resilient modulus prediction model in MEPDG does not take the effect of permanent deformation (PD). This effect

is a very important parameter for base layer, especially for the case of using RAP as it is a questionable parameter as mentioned before. As a general trend, the increase of RAP content within granular materials increases the permanent deformation sensitivity. This may be related to the increase of bitumen coated particles associated with the increase of RAP content (Bilodeau, Doré, & Depatie, 2013).

The original model of the MEPDG was proposed by Tseng and Lytton (Tseng & Lytton, 1989) as represented in Equation 2.5 combines the influence of the number of load applications with the resilient deformation which is a function of the stress levels. This is the model used here in after with further modifications in the MEPDG.

$$\delta_a(N) = \left(\frac{\epsilon_o}{\epsilon_r}\right) e^{-(\frac{\rho}{N})^{\beta}} \epsilon_v \, h \tag{2.5}$$

Where:

- δ_a (N) = permanent deformation within a material sub-layer of thickness "h" after N repetitions.
- ϵ_r = resilient strain imposed in the laboratory test to obtain material properties ϵ_o, β and ρ.
- ϵ_v = vertical resilient strain in the layer as obtained from the primary response model.
- h = layer thickness.

Tseng and Lytton used a total of 16 permanent deformation data set presenting unbound base layer from repeated load tri-axial (RTL) data found before in literature to find ϵ_o, β and ρ values for these base materials. Multiple regression analysis for the granular base materials are used to find these material properties as follows:

$$\text{Log}(\frac{\epsilon_o}{\epsilon_r}) = 0.80978 - 0.06626\, W_C + 0.003077\, \Theta + 0.000003\, M_R \tag{2.6}$$

$$\text{Log}\,\beta = -0.919 + 0.03105\, W_C + 0.001806\, \Theta - 0.0000015 M_R \tag{2.7}$$

$$\text{Log}\,\rho = -1.78667 + 1.45062\, W_C - 0.003784\, \Theta^2 + 0.002074\, {W_C}^2 \Theta - 0.0000105 M_R \tag{2.8}$$

Where:

- M_R = resilient modulus of base layer (psi).
- W_C = water content (%).
- Θ = bulk stresses (psi).

A sensitivity study was achieved later on this model by El-Basyouny (M. M. El-Basyouny, 2004) using the same data that Tseng and Lytton used before in establishing this model. This study showed unusable trends and predictions of permanent deformation using this model. Therefore, El-Basyouny & Witczak (M. El-Basyouny, Witczak, & Kaloush, 2005) modified this model for calculation of PD for unbound granular materials. The modified model was implemented in the MEPDG software.

The final form of the modified model by El-Basyouny & Witczak for granular base layer recommended to the MEPDG and used for this study as follows:

$$\delta_a(N) = \beta_{s_1} K_1 h \epsilon_v \left(\frac{\epsilon_o}{\epsilon_r}\right) [e^{-(\frac{\rho}{N})^{\beta}}] \quad (2.9)$$

$$Log\beta = -0.61119 - 0.017638(W_C) \quad (2.10)$$

$$\rho = 10^9 \left[\frac{C_o}{(1-(10^9)^{\beta}}\right]^{\frac{1}{\beta}} \quad (2.11)$$

$$C_o = \ln\left(\frac{a_1 {M_R}^{b_1}}{a_9 {M_R}^{b_9}}\right) = \ln(0.0075) = -4.893 \quad (2.12)$$

Where:

- δ_a (N) = permanent deformation of the base layer (inches).
- N = number of load repetitions.
- ϵ_r = resilient strain (in. /in.).
- ϵ_v = primary response model (assumed to be equal to ϵ_r in this study).
- h = thickness of the layer (inches).
- ϵ_o, ρ, β = material properties.

- K_1 (granular materials) = 1.673 (natural calibration).
- βs_1 = field calibration factor = 1 (unless there are field data).
- M_R = resilient modulus of base layer (psi).
- W_C = water content (%).
- a_1, b_1, a_2, b_2 = regression constants = 0 (natural calibration).
- (ϵ_o/ϵ_r) is calculated from the previous Equation 2.6 suggested by Tseng and Lytton as no new prediction equations were instead suggested by the MEPDG software.
- The natural calibration values were taken from the manual of practice of MEPDG.

This study focuses on the rutting performance model in the MEPDG, as it is the last model established for PD of unbound base layer. Attia et. al. (M. I. E.-S. Attia, 2010) results reflected that permanent deformation of RAP can be modeled like a typical granular material. The analysis of his study focused on six different models which reflected that both the exponential function, currently used in the MEPDG, and the power model (log-log relation between number of load cycles and permanent strain) are suitable functions to be used to model the permanent deformation of RAP/aggregate blends.

2.6.3. Poisson's ratio

This ratio is an essential factor used in analytical pavement design theories based on stress-strain relationship. For base, sub-base and subgrade layers, the Poisson's ratio is affected with other parameters by several factors; elastic modulus of material, temperature, cohesion, saturation degree, coarseness and roughness of material particles. When a compressive force acts on a cylinder body, the force causes the sample to contract in the direction of the force and expand laterally. Within the elastic range of the material, the ratio of these strains is a constant for that

particular material. The ratio of the strains, ($\Delta L/L_o$) for longitudinal strain and ($\Delta R/R_o$) for lateral strain, is referred to Poisson's ratio as shown in Figure 2.4 (Maher & Bennert, 2008).

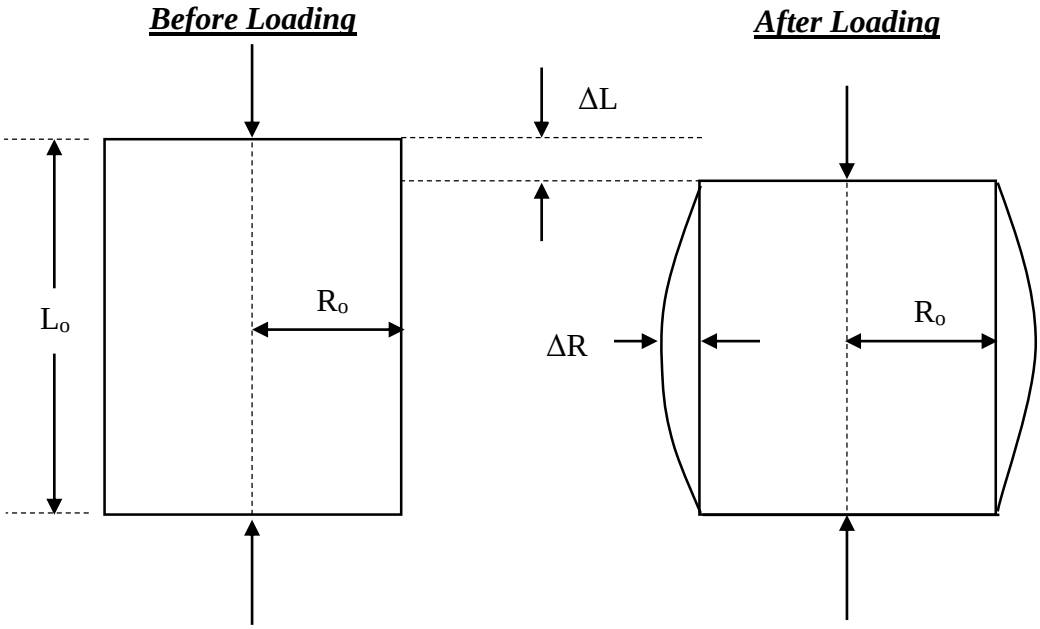

Figure 2.4. Poisson's Ratio for Cylinder during Un-Confined Compression Test

Poisson's ratio of a material is defined experimentally as the linear radial strains curves and axial strains of the material for small strains (Madjadoumbaye & Tamo, 2012). The resilient modulus and Poisson's ratio of subgrade soils in highway foundation are important parameters in design and quality control process. Currently, there are standardized procedures to evaluate the stiffness parameters of both asphalt and soil. For hot mix asphalt, AASHTO TP62 (Highway & Officials, 2011) "Dynamic Modulus of Hot Mix Asphalt" is recommended for the measurement of modulus values over a wide range of temperatures and loading frequencies. Although designed to measure the vertical strain and resultant modulus, Maher et al. (Maher & Bennert, 2008) also provides a means of determining the Poisson's ratio via the use of radial measurements. In the past, methods were developed for the evaluation of the Poisson's Ratio utilizing the indirect tensile test (IDT). However, the use of IDT-type testing at higher test temperatures, greater than 20º C,

for stiffness determination is not recommended due to excessive deformations that may occur in the vicinity of the loading platens, as well as the inappropriateness of using linear elastic theory in the diametric loading position (Tayebali, Tsai, & Monismith, 1994).

In addition, the currently used techniques include CBR (California Bearing Ratio) test, resilient modulus test, DCP (Dynamic Cone Penetrometer), and FWD (Falling Weight Deflectometer) tests. However, these techniques have certain limitations and sometimes fail to satisfy the requirement and accuracy for design purposes (Zeng & Hu, 2013). Nowadays, Poisson's ratio is estimated rather than measured directly in most soil tests especially the CBR which cannot be used in measuring Poisson's Ratio because the loading conditions in a CBR test is different compared with those happen in the field. Usually these estimated values are assumed depending on the soil type as shown in Table 2.2. As for each soil type there is a range for the linear elastic stress-strain relationship and an average value is taken to represent the midpoint of this linear relationship. This procedure will be used in this research depending on the linear elastic region measured for each sample.

The ASTM standard method C469/C469M-14 (Astm, 2014) for measuring Poisson's Ratio of concrete samples in compression test uses a rate of loading 1 mm/min in loading. However, this rate may be too high in case of using RAP because it is much weaker than concrete. In addition, this standard recommends measuring Poisson's ratio at 40% from the ultimate compressive strength of the samples to be confident that the result in the linear elastic region. For unbound materials, the MEPDG only allows the user to estimate a constant value for the Poisson's Ratio, thereby; neglecting any effect of applied stress or change in resilient modulus may have on Poisson's Ratio. However, for the case of RAP, the variation in several testing conditions have a huge effect on the structural capacity, especially permanent deformation. This effect may be

related to the relation of strength parameters M_R and PD with Poisson's ratio. This prediction was estimated from the falling weight deflectometer FWD sensitivity analysis (Maher & Bennert, 2008). As it appears that both the Poisson's Ratio of the asphalt layer and the unbound aggregates layer (base layer) have an influence on the back-calculated modulus values.

Table 2.2. Typical Values of Poisson's Ratio (Maher & Bennert, 2008)

Material	Range of Values	Typical Value
Hot Mix Asphalt	0.3 – 0.4	0.35
Portland Cement Concrete	0.15 – 0.2	0.15
Untreated Granular Materials	0.3 - 0.4	0.35
Cement Treated Granular Materials	0.1 - 0.2	0.15
Cement Treated Fine Grained Soils	0.15 – 0.35	0.25
Lime Stabilized Materials	0.10 – 0.25	0.20
Lime Fly Ash Mixtures	0.10 – 0.15	0.15
Loose Sand or Silty Sand	0.20 – 0.40	0.30
Dense Sand	0.30 - 0.45	0.35
Fine Grained Soils	0.30 -0.50	0.40
Saturated Soft Clays	0.40 – 0.50	0.45

Maher et al. (Maher & Bennert, 2008) research project encompassed the evaluation of whether or not the Poisson's Ratio can be measured using the same test procedures commonly used to obtain the modulus values for flexible pavement design (i.e. dynamic modulus test for asphalt and resilient modulus test for unbound materials). The research concluded that the Poisson's Ratio can be measured during the dynamic modulus test for asphalt mixtures but should not be measured during the resilient modulus (M_R) test for unbound materials. This is mainly because the M_R test does not typically test the material in its natural linear elastic state, where the

Poisson's Ratio concept is valid. The Poisson's Ratio parameter is only valid with testing materials within their linear elastic range. This means that, theoretically, there should be no permanent deformation accumulated during any of the loading cycles and the vertical strain should be in the low strain range (< 0.001%). Poisson's ratio is an important characteristic that enters into the pavement design process. Usually this parameter is estimated instead of measuring according to typical values for each pavement material. The flexible asphalt pavement is a three-component system consisting of stone aggregates, pores filled by air and asphalt binder. Nowadays, this system is characterized as elastic in pavement design practice which means that the ideal state for measuring Poisson's ratio at the linear elastic stress-strain relationship (Zak et al., 2014).

As mentioned before, there is almost 13 states nowadays in the field that adds RAP within base layer up to 50%, but most of researchers are trying to investigate the effects by exceeding this critical content. From this strategy, it will be more economical and beneficial to use more than 50% RAP within base layer without any defects or effectiveness on pavement lifetime. Therefore this study will focus on studying the RAP with contents varying from 50% to 100%.

CHAPTER 3. METHODOLOGY AND EXPERIMENTAL WORK

3.1. Main Research Tasks

The objectives of this study are achieved via four main tasks, as shown in the flow chart represented in Figure 3.1. The first task of the research is concerned with modeling the structural behavior of RAP in the base layer utilizing measured data collected for M_R of RAP/Aggregate blends in base layer (M. I. E.-S. Attia, 2010). This task is implemented taking into consideration several testing conditions describing the possible circumstances that may be encountered in the field for RAP in base layer. The second task concerns modeling behavior of the permanent deformation of RAP blends utilizing values measured by M_R and single & multi-stage RTL tests through MEPDG rutting model. The third stage is also essential to correlate values of M_R with permanent deformation accumulated during stages of loading of M_R tests for the same RAP blends tested in the first task under identical testing conditions, especially three water content levels.

Finally, the last task comprises measuring Poisson's ratio for the same RAP/Aggregate blends to evaluate its effectiveness on the modeling behavior of both parameters M_R and PD. Based on literature review results, this ratio cannot be measured during the M_R test. Therefore, the un-confined compression test is used to determine the respective results. This test is more suitable and practical to implement in measuring the lateral deformation without any effect of confining pressure like M_R or RTL tests.

3.1.1. M_R modeling task

The main objective of this research task is to assess the nine constitutive models previously tested by Attia et. al.(M. I. E.-S. Attia, 2010), as represented in Table 2.1, for RAP as a base layer under the effect of different actual environmental and field conditions other than the state of stresses. This objective is fulfilled in three stages as described in the flow chart represented at

Figure 3.2. The laboratory data is collected from the same previous study (M. I. E.-S. Attia, 2010) on several RAP blends used for base layer tested at different testing conditions as described in Figure 3.3 based on two replicates for each condition. The moisture-density relationship is investigated according to gyratory compacted as mentioned in kneading procedure in NCHRP 1-28A protocol.

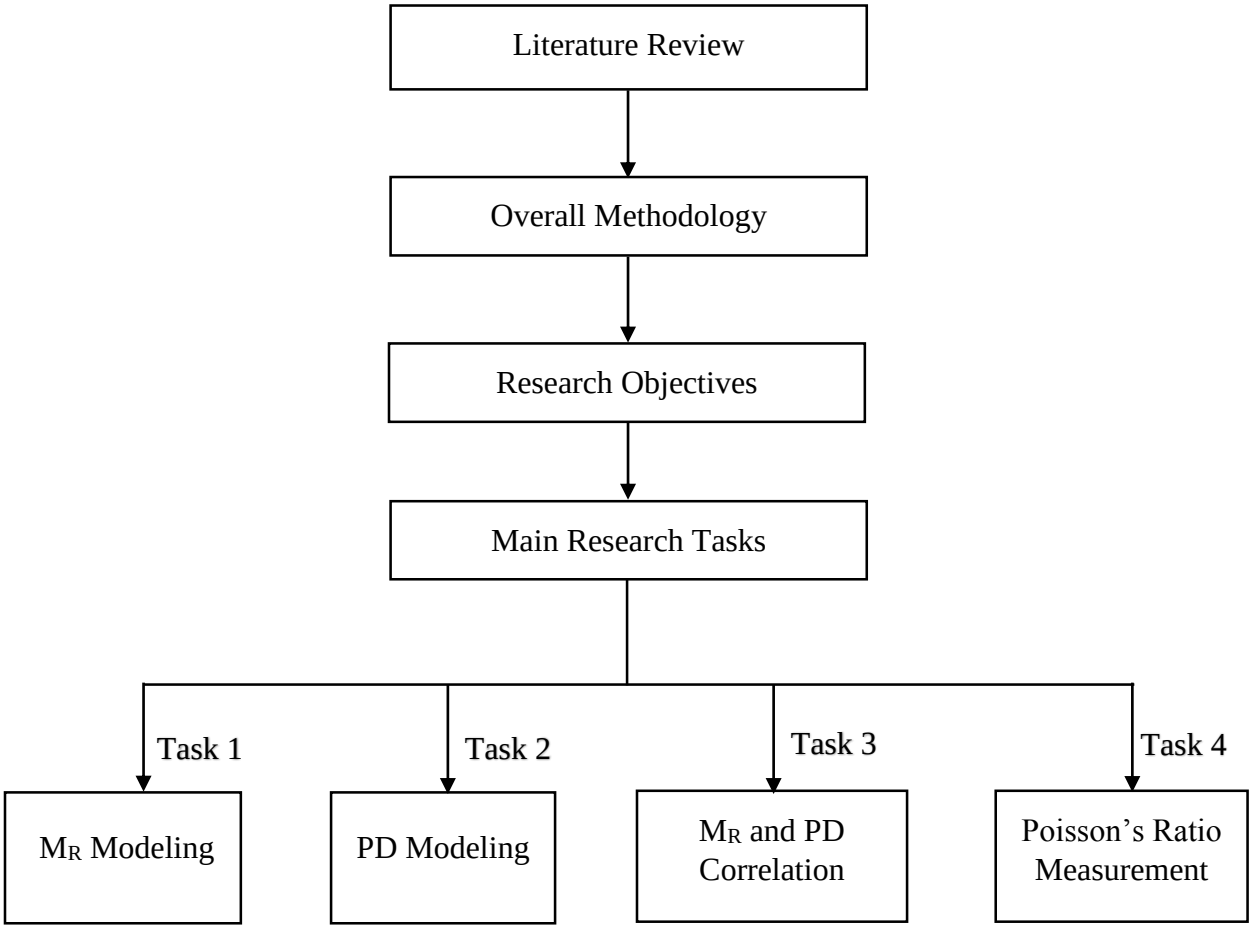

Figure 3.1. Research Hierarchy Flow Chart

The first stage aims to investigate the accuracy of these models by statistical analysis to show how they may be affected by the new conditions alone or in conjunction with various interactions at different percentages of RAP on the prediction of the resilient modulus. The second stage is tailored through a sensitivity analysis for the three best statistical models to choose the

best-fit one and its suitability in predicting the resilient modulus of RAP. This stage also assesses the adequacy of these factors in representing most of the field conditions affecting the base layer. Then, this stage is important to investigate the need for more future laboratory measurements and/or more, environmental and field conditions in predicting the resilient modulus such as leaching components or Poisson's ratio. In the third stage, a parametric analysis is achieved for the M_R-MEPDG model by using the measured M_R values under different measured testing parameters used in this model. This stage is considered to calculate each K parameter under five different levels of confining pressure (3, 6, 10, 15 and 20 psi) using the Excel solver software. Six replicates are considered for each level of confining pressure.

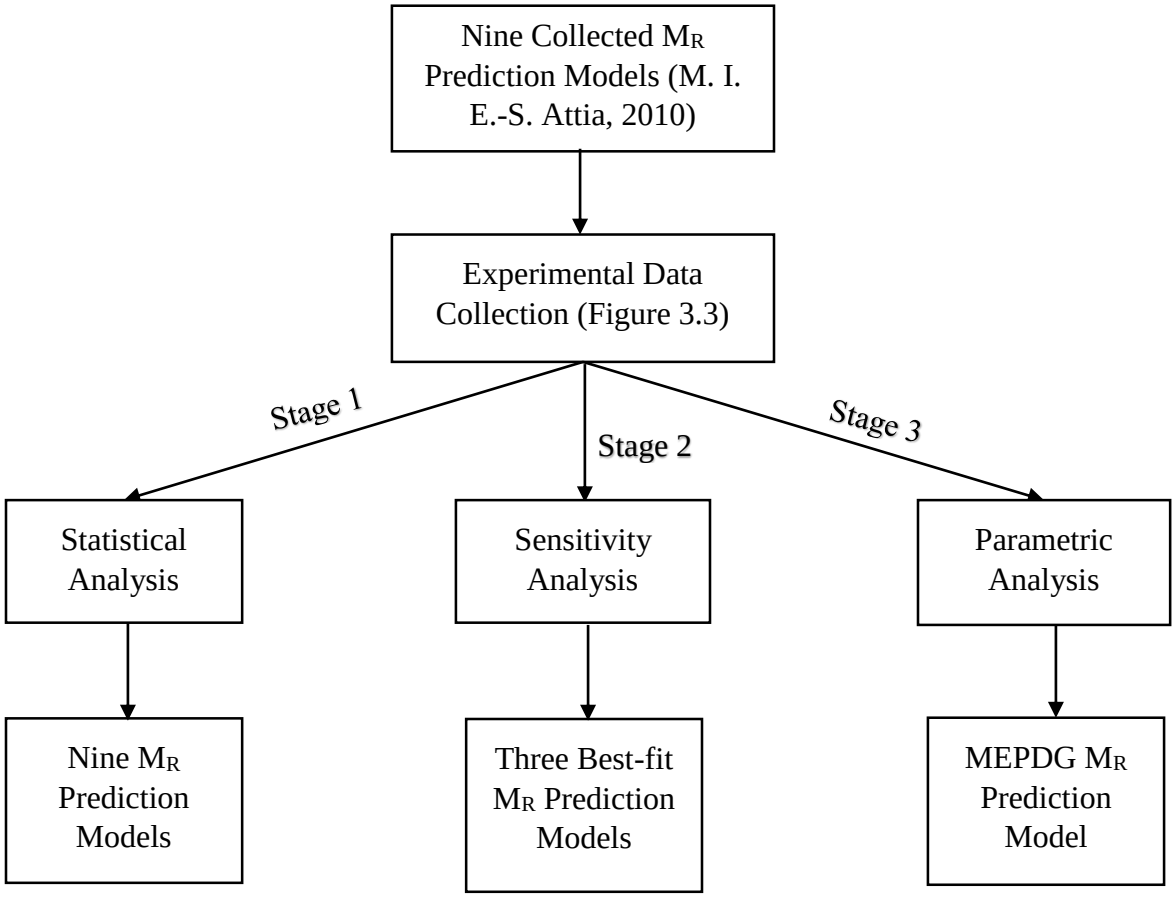

Figure 3.2. M_R Modeling Flow Chart

Each replicate is assigned a different value of deviator stress. This stage of analysis comes as a further study to the last stage, which did not take the effect of different state of stresses on K regression parameters on the same MEPDG model. This analysis cannot be conducted at different levels of deviator stress as testing sequences required by NCHRP 1-28A protocol used in M_R testing, do not group deviator stress like confining pressure levels mentioned before.

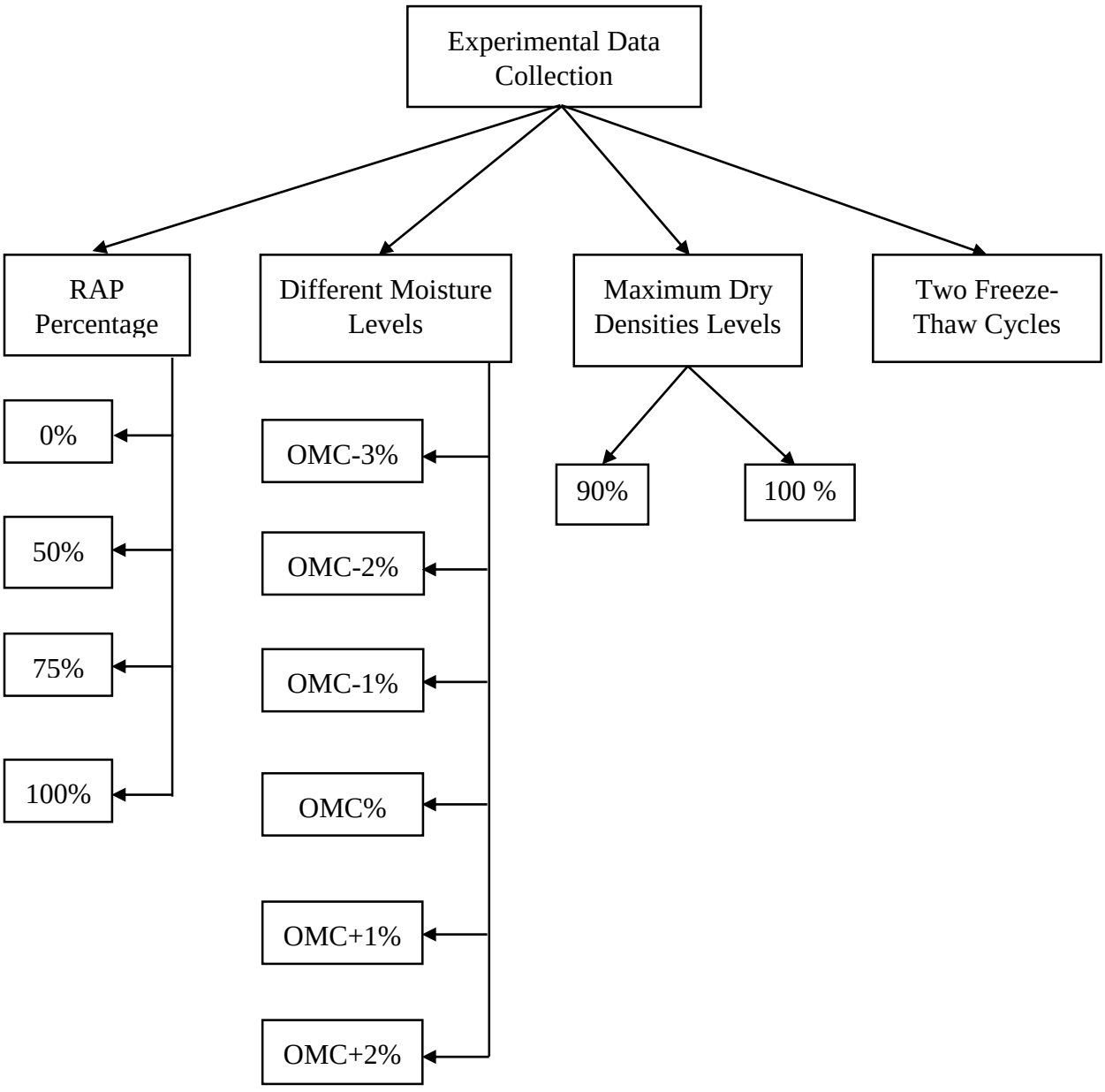

Figure 3.3. Experimental Data Collection

3.1.2. PD modeling task

The M_R modeling task yielded that the M_R-MEPDG model is the best-fit model that works for RAP base layer. Also, Attia et al.(M. I. E.-S. Attia, 2010) found that the PD-MEPDG model was the best-fit model for RAP base layer. Therefore, this task comprises investigating the ability of predicting the permanent deformation for RAP using the MEPDG rutting prediction model. This task concentrates on how the major factors (state of stresses, moisture content, load repetitions and stress history) affect permanent deformation modeling behavior of RAP and RAP/aggregate blends.

To achieve this objective, PD data collected from both resilient modulus (M_R) and repeated tri-axial (RTL) loading tests are taken into consideration. Each test is responsible on investigation one of the major factors affecting PD accumulated from using RAP. The M_R takes in consideration the stress history of different successive stages of loading, while the single-stage RTL is responsible on measuring PD after frequent number of load repetitions (20,000 or more). The multi-stage RTL is close to the trend of the M_R test than single-stage RTL test. Different stages of loading were applied with equal number of load repetitions (5000) and different deviator stress levels but with same confining pressure (3 psi).

The comparison between predicted and measured PD values using the rutting MEPDG model is achieved on three main stages, as described in Figure 3.4. In the first stage, a comparison is made between PD values measured from the M_R test to predicted PD values using PD-MEPDG prediction model on the main RAP source (TH 10). This comparison is achieved on three major testing conditions; four RAP contents (0%, 50%, 75% and 100%), three water content levels (OMC-2%, OMC% and OMC+2%) and three base layer thickness (6, 9 and 12 inches). Also, this stage focuses on the same comparison of measured and predicted PD of other four field RAP

sources. Three RAP sources (TH 19-101, TH 19-104 and TH 22) contain 50% RAP and 50% granular aggregates. The fourth RAP source (Cell 18) contains 100% RAP. This comparison of RAP sources is achieved on PD measured values collected from M_R test at the same testing conditions. The first number of each source refers to the Trunk Highway location in Minnesota State, while the other number refers to the mile location

The second stage focuses on the comparison of PD values with those measured in the single-stage RTL. This test is more reliable for measuring PD taking into consideration the effect of several load repetitions (20,000 or more). The comparison is achieved for RAP TH10 on two levels of water contents (OMC% and OMC+2%) and two contents of RAP (0% and 50%). Also, this comparison takes in consideration the effect of adding 6% fines on PD modeling for 50% RAP blend. The third stage focuses on the comparison of PD values versus those measured in the multi-stage RTL. This test is important for measuring PD taking into consideration the effect of stress history. The comparison is achieved for RAP TH 10 on three levels of water contents (OMC-2%, OMC% and OMC+2%), two contents of RAP (0% and 50%). In addition, this comparison takes in consideration the effect of adding 3.5% fines on PD modeling for 50% RAP blend.

3.1.3. M_R and PD correlation task

This study focuses on M_R-PD relationship for different sources of RAP under variable confining pressure, moisture content and RAP levels. The confining pressure is the most effective state of stresses on the structural behavior of the base layer. Firstly, this relation is important to be investigate in terms of how the PD affects M_R values under the variation of all mentioned testing conditions. Also, it shall indicate if there is a typical relation for the M_R-PD behavior that can be understood for the RAP in base layer or not. Secondly, this stage helps to decide the optimum RAP content that can be used in base layer blends. This content will result in achieving the highest M_R

values with acceptable PD percentage not causing rutting in the future. Based on this comparative analysis, a recommendation will be concluded to ascertain if the PD can be used as an effective parameter in M_R modeling or not.

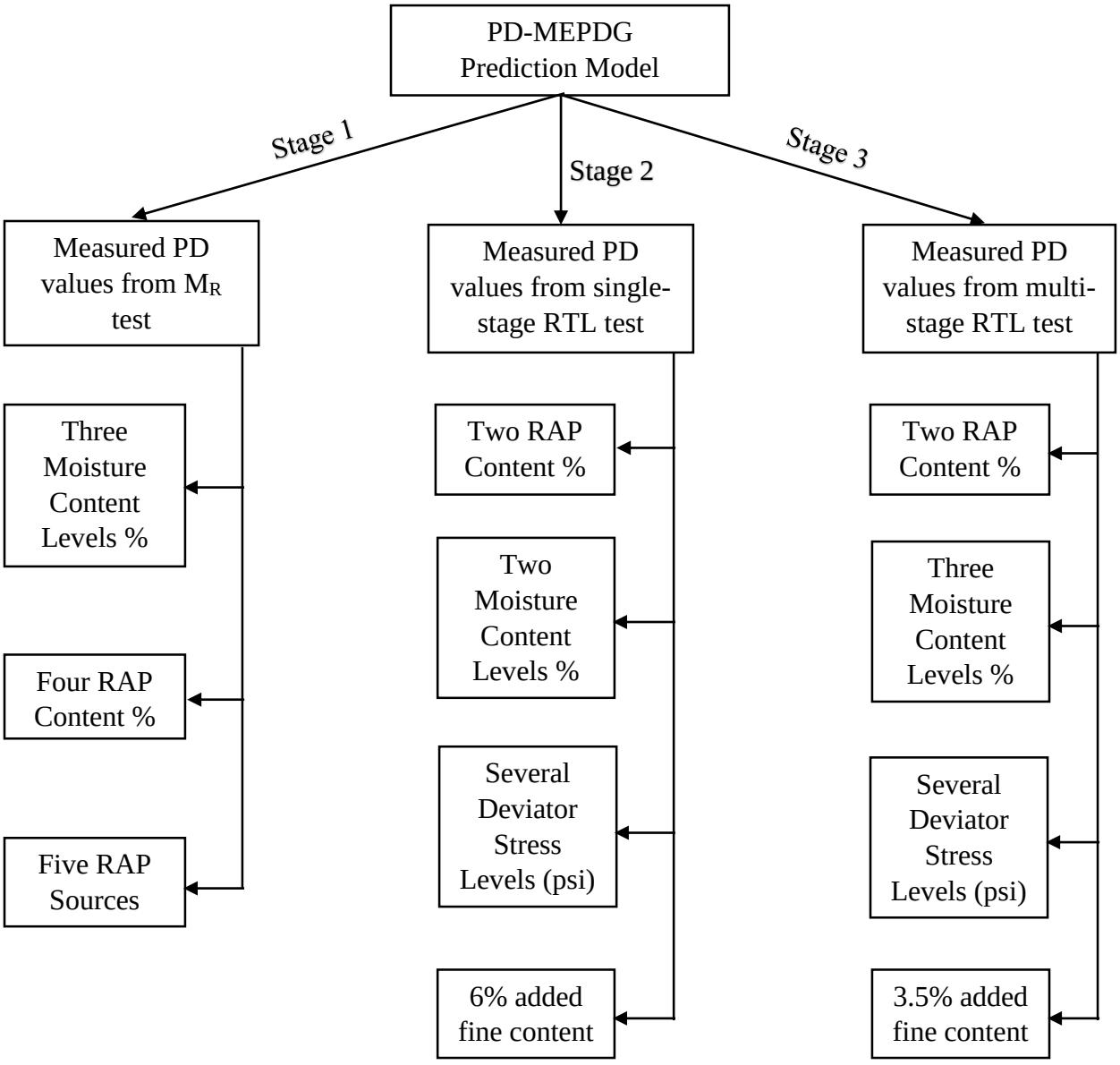

Figure 3.4. PD Modeling Flow Chart

This approach is followed in the mechanistic empirical pavement design guide (MEPDG) (Guide, 2008). As the resilient strain is used as an effective parameter in PD modeling for granular base layer, while the permanent strain is not used in M_R modeling for the same layer. Therefore,

the work performed in this task is divided into three main stages, as described in Figure 3.5. The first stage is achieved on five different RAP sources collected and tested before in previous researches. On the other hand, both second and third stages are achieved on the main RAP source (TH 10) with its blends with MN/DOT Class 5 granular aggregates.

The first stage of this study is concerned with comparing M_R and accumulated PD values from the resilient modulus determination test. The PD is calculated as a percentage of the accumulated permanent strain from the total strain for the sample tested during M_R determination. This comparison is achieved on the main source of RAP (TH 10). The comparison is achieved at three levels of water content varying from optimum moisture content (OMC %); OMC-2%, OMC% and OMC+2%. This comparison comprised different levels of confining pressure and different percentages of RAP with traditional Class 5 granular base aggregates.

The data of the other four different RAP sources are collected for this research from MN/DOT project (M. Attia et al., 2009) other than the main source (TH 10). These RAP sources are analyzed under the same testing conditions discussed before. Three out of four RAP samples (TH 19-101, TH 19-104 and TH 22) are collected from the field containing 50% RAP and 50% granular aggregates. The first number refers to the truck highway number in Minnesota and the second number refers to the mileage station in each road.

The fourth RAP source consists of 100% RAP is collected from Cell 18 (Minnesota Destination). In the second stage of the study, the comparison is achieved on PD results collected from the single-stage RTL for Class 5 and 50% RAP (TH 10 + 50% Class 5). The analysis of this stage also takes in consideration stabilizing the 50% RAP sample with 6% high plastic fines additive to reach the maximum allowable 10% fines. In the last stage of this study, M_R-PD

comparison is achieved on PD values collected from multi-stage RTL for the same samples tested before in the previous stage but with 3.5% normal fines only.

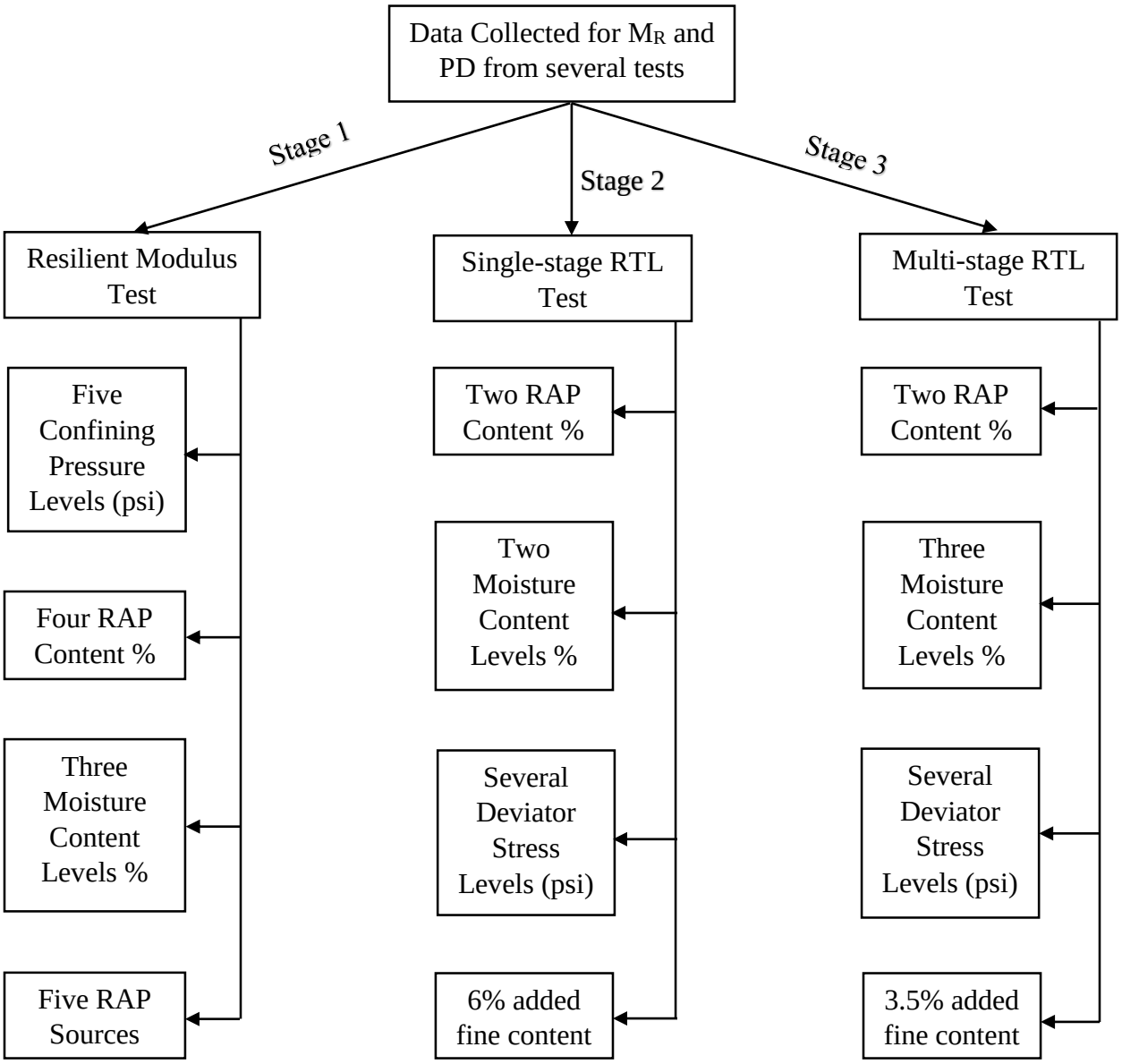

Figure 3.5. M_R and PD Correlation Flow Chart

3.1.4. Poisson's ratio task

The last task of this study is an experimental program to measure Poisson's ratio for different RAP/Aggregate blends. This program is described in the flow chart shown in Figure 3.6. Identical cylindrical samples (6-inches diameter and 12-inches height) are prepared similar to

those tested for measuring of M_R and PD. Two RAP sources (TH 10 and TH 29) are tested mixed with Class 5 granular aggregates, at three levels of moisture content (OMC-2%, OMC% and OMC+2%) and three RAP contents (0%, 50% and 100%). Three additional field RAP sources (TH 19-101, TH 19-104 and TH 22) are tested (mixed before with 50% traditional granular aggregates) to take in consideration the RAP sources variability parameter. The first number of each source refers to the Trunk Highway location in Minnesota State, while the other number refers to the mile location.

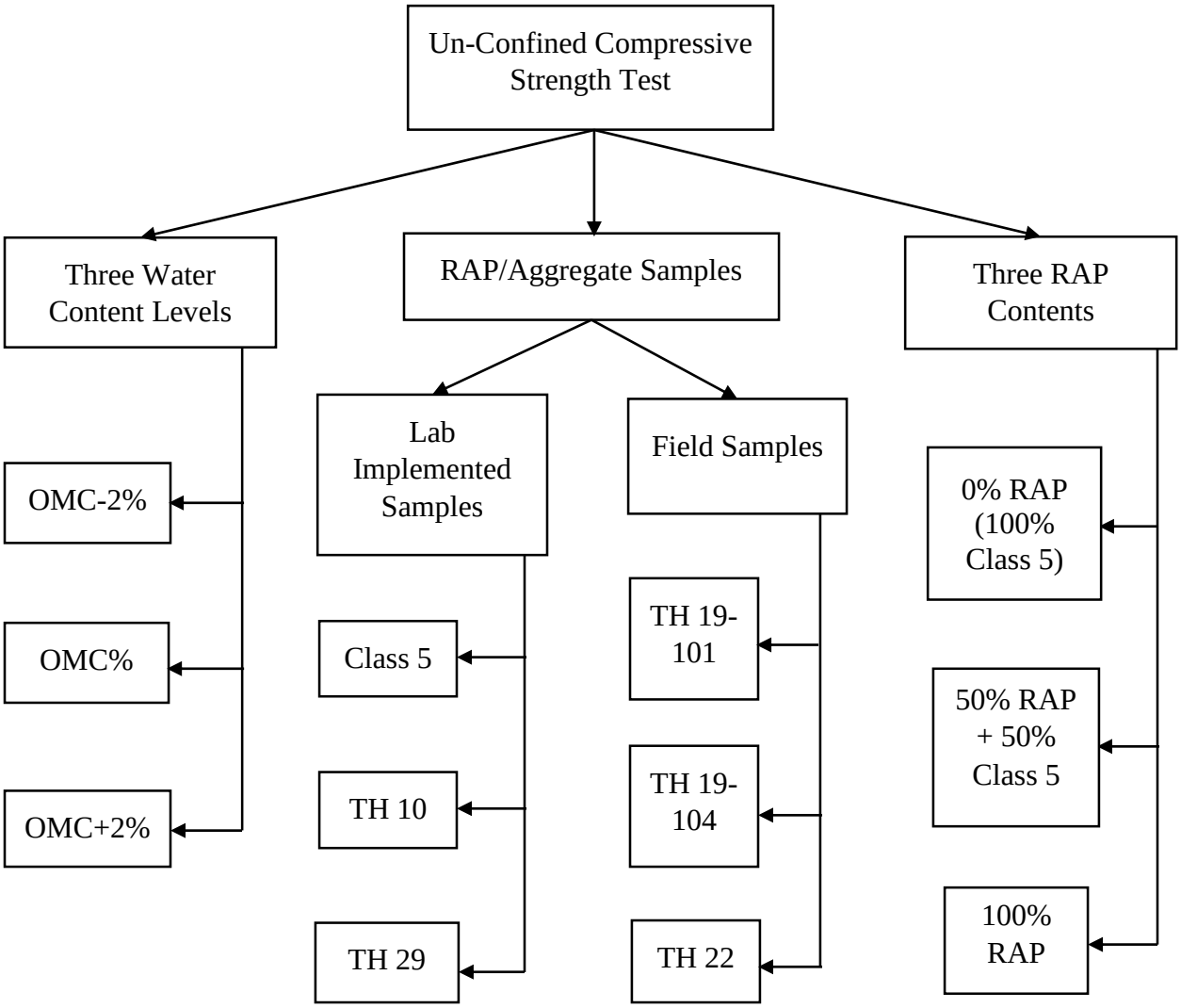

Figure 3.6. Poisson's Ratio Flow Chart

This test aims at measuring ultimate compressive strength and Poisson's ratio of these samples. Both axial and lateral strains are measured during the whole test and recorded at the linear axial stress-strain relationship to calculate the Poisson's Ratio. Two digital dial gauges simultaneously measure lateral strains, then the average of both readings is considered in calculating the Poisson's ratio.

3.2. Experimental Program

This section includes the procedures used for testing the physical and/or mechanical properties of RAP/Aggregate blends investigated in this research even for collecting the data used in the modeling section of both design parameters M_R and PD or measuring Poisson's ratio and ultimate compressive strength values.

3.2.1 Sieve analysis gradation test

Gradation is a very important material property for the pavement construction layers in general because it influences on each layer stability strength and drainage characteristics. Dry sieve analysis is done based on ASTM C 136 standard. Representative material of each sample is collected and oven dried at a temperature less than 140° F for 2 days. Then, the material of each sample is put on soil sieve shaker and the mass retained on each sieve is measured after 10 minutes of shaking. While, the material finer than 0.075 mm is determined by washing the material on 4.75 mm sieve using ASTM C 117 standard.

3.2.2. Asphalt extraction test

Asphalt content is one of the criteria that are normally considered by the highway agencies when trying to utilize RAP material. In this research, asphalt extraction is done by reflux extraction following ASTM D 2172 (Method B) standard.

3.2.3. Moisture content-dry density relationship

For RAP/aggregate blends tested for collecting M_R and PD data, the relation between the dry density and moisture content is achieved by gyratory compactor. All material greater than 12.5 mm is replaced by material passing 12.5 mm and retained on sieve no. 4 (4.75 mm) for material homogeneity. The optimum moisture content and maximum dry density are based on samples compacted by the gyratory compactor at a pressure equal to 600 Kpa, the number of gyrations equal to 50, the machine is set to conduct 30 revolutions per minute and the angle of gyration was set to 1.25 degrees. While for RAP/aggregate blends tested by un-confined compression test to collect Poisson's ratio and ultimate strength values, the relation between dry density and moisture content is achieved by modified proctor hammer using ASTM D 1557 standard to determine the optimum moisture content (OMC %) at maximum dry density level.

3.2.4. Tri-axial shear test

Shear strength is an important property for materials used as a base layer. The tri-axial shear test is achieved after the resilient modulus testing on the same sample, unless the sample failed during M_R test. The shear test is conducted in strain controlled mode, at a loading rate of 0.03 mm/sec (0.6% strain /minute) and confining pressure of 4 and 8 psi. The results are used to calculate the friction angle and cohesion for the tested materials.

3.2.5. Resilient modulus test

The resilient modulus test is achieved based on NCHRP 1-28A (M. W. Witczak, 2004) testing protocol and MN/DOT requirements. The resilient modulus is the ratio of axial cyclic deviator stress to the recoverable strain. Generally for base layer, cyclic stress of fixed magnitude for 0.1 second is applied to the specimen followed by a 0.9 second rest period, in order to determine the resilient modulus. The specimen is subjected to a confining stress provided by means of a tri-

axial pressure chamber. The sample is subject to 30 different sequences stages of loading, unless it failed early in the test. The samples are dried first at 150º F for 24 hours before adding determined water content. Gyratory compactor is used for compacting the samples into two molds 6 inches height each. Then the surface between the two molds, is scratched and the two molds are compacted with vibratory hammer in split mold. No visual lateral movement was found between the top and bottom samples in any of the tested samples. Details regarding the testing system and the calibration process can be found in Attia et al. (M. I. E.-S. Attia, 2010).

3.2.6. Permanent deformation test

For PD test, the sample is prepared exactly like the M_R sample, with one exception in the loading sequences. The effects of moisture content and fine content on PD are evaluated based on repeated load tri-axial (RTL) testing. The effect of those factors on permanent deformation (PD) of base layer containing RAP is evaluated using both single-stage and multi-stage PD testing. In the single-stage PD test, the sample is subject to cyclic loading at one level of stress up to predetermined number of cycles or failure of the sample. In this research the number of cycles is selected to be 20,000 cycles, except for limited number of samples where the number of cycles is only 10,000 cycles. The single-stage PD test has the advantage of avoiding the effect of stress history on the material. However, single stage PD test is very time consuming and it incorporates the variability of the material, sample preparation and testing.

For the multi-stage PD test, each load is applied to the sample for 5000 cycles, then the deviator stress is increased and another 5000 cycles are applied to the sample and so on until the sample failed (more than 5% strain is achieved). The advantage of the multi-stage testing is that the behavior of the material under different states of stress can be evaluated from one sample, which saves time and money. The disadvantage is the possible effect of stress history on material

response. Samples at OMC+2% showed much higher PD and fails very early in the test when subject to high levels of deviator stresses. For this reason, samples at OMC+2% are tested at lower deviator stresses. The selection of the confining pressure to be 3 psi is based on earlier work in the literature for base layer (Kim & Labuz, 2007; Song & Ooi, 2010).

3.2.7. Un-confined compression test

Each sample specimen is prepared according to NCHRP 1-28A (M. Witczak, 2003), which was the same testing procedure used before in M_R and PD determination. Gradation of each specimen is modified by replacing particles retained on sieve ¾ in. (19 mm) with particles passing the same sieve and retained on sieve No. 4 (4.75 mm). Each sample is compacted with modified proctor hammer manually on 6 layers with same modified proctor compaction energy which results in 123 blows per each layer according to Equation 3.1.

$$E = \frac{WHNn}{V} \tag{3.1}$$

Where:

- E = compaction energy equals to 56000 ibs.ft/ft^3.
- H = hammer drop equals to 18 inches (1.5 ft).
- W = weight of hammer equals to 10 ibs.
- V = volume of mold equals to 339.29 in^3 (0.1964 ft^3).
- n = number of layers equals to 6.
- N = number of blows per layer equal to 123.

After trial and error of testing several specimens varying the loading rate from 1 to 0.25 mm/min, the analyzed samples are tested by un-confined compression test at strain rate 0.25 mm/min until reaching failure. This rate is found the most suitable allowing enough time for accumulating lateral strain at the mid-height of the tested specimen. Both axial and lateral strains

are measured during the whole test period every 30 seconds and recorded at the linear elastic axial stress-strain relationship to calculate the Poisson's Ratio. Two digital dial gauges simultaneously measure lateral strains, then the average of both readings is considered in calculating the Poisson's ratio.

3.3. RAP Index Properties Data

All the data of M_R, single and multi-stage RTL testing of all RAP/aggregate blends used in this research were tested in MN/DOT previous report (M. Attia et al., 2009). While all the data of the unconfined compression test for Poisson's ratio measurement is collected in the last task of this research. Group of preliminary tests are performed prior to actual measuring M_R, PD and Poisson's ratio, such as gradation, compaction, shear parameters, etc. A list of the index properties for RAP TH 10 is given in Table 3.1, while the index properties of the other field RAP sources are given in Table 3.2.

A concern is taken in this study on the shear strength properties, therefore a tri-axial test is done by the MN/DOT project on the same RAP samples tested before for M_R. Shear strength is an important property especially if the base layer was constructed under a thin HMA layer, for this case the base will be subjected to high shear stresses. Previous research on MN-ROAD Cell 26 (Mulvaney & Worel, 2001) presents one of the full depth reclamation cases where the material had enough resilient modulus but failed due to high shear stress in the base layer that exceeded the material shear strength. The maximum deviator stress carried by all RAP samples changed between 85 to 135 psi at 8 psi confining pressure and between 70 to 110 psi at 4 psi confining pressure. Garg & Thompson reported that granular base materials carried more than 90 psi deviator stress at 15 psi confining pressure had low rutting potential in the field (Garg & Thompson, 1997).

Table 3.1. Index Properties for RAP TH 10/Class 5 Blends (M. I. E.-S. Attia, 2010)

Index Property	Material				
	Class 5	50% RAP TH 10 + 50% Class 5	75% RAP TH 10 +25% Class 5	RAP TH 10	RAP TH 10 (after extraction asphalt)
% Passing 3/8 inches Sieve	84	76	73	69	90
% Passing Sieve No.4	68	58	53	49	63
% Passing Sieve No.200	2.9	1.6	1	0.4	3.6
% Passing Washing Sieve No.200	8	5.6	4.2	2.9	9.8
Optimum Moisture Content %	6.4	5.5	5.7	5.5	6
Maximum Dry Density (Ibs/ft^3)	138.7	136.5	134.8	132.5	138.4
% Asphalt Content	NA	1.8	2.4	4	NA
ASSHTO classification	A-1-b	A-1-b	A-1-b	A-1-b	A-1-a
USCS classification	SP-SM	SP	SP	GP	SP
Cohesion, c (psi)	12	10.5	17	13	NA
Friction Angle Φ (degrees)	46	47	37	44	NA

This reflects that all evaluated materials are good candidates as a base layer at their maximum loading conditions. The friction angle varied between 37 to 52 degrees while the cohesion varied between 8 to 17 psi. Those results indicate that from the point of view of both the friction angle and cohesion, the evaluated RAP sources have shear strength parameters similar to granular materials.

Table 3.2. Index Properties for Other Tested RAP/Aggregate Blends

Index Property	Material					
	RAP TH 19-101	RAP TH 19-104	RAP TH 22	New Class 5	50% RAP TH 29 + 50% Class5	RAP TH 29
% Passing 3/4 inches Sieve	100	100	100	98	95	93
% Passing 1/2 inches Sieve	100	100	100	88	86	89
% passing 3/8 inches Sieve	91	90	84	82	77	81
% Passing Sieve No.4	78	76	59	70	60	60
% Passing Sieve No.200	1.4	2.1	1.3	0.1	0.4	0.3
% Passing Washing Sieve No.200	7.1	9.6	3.9	10.3	6.7	0.8
Optimum Moisture Content %	5.9	7	5.25	6	7	7
Maximum Dry Density (Ibs/ft^3)	122.5	125	134.8	146.5	136	128
% Asphalt Content	1.7	2	2.8	NA	NA	NA
ASSHTO classification	A-1-b	A-1-b	A-1-b	A-1-b	A-1-a	A-1-a
USCS classification	SP-SM	SP-SM	SP	SP-SM	SP-SM	SP
Cohesion, c (psi)	16.5	8	16	NA	NA	NA
Friction Angle Φ (degrees)	49	52	44	NA	NA	NA

Also as the tri-axial samples were tested before on M_R machine, this ensure that all RAP samples evaluated didn't fail by any shear distress which means that the shear stress happened to the sample didn't exceed its shear strength. There isn't so much concern on the shear strength of RAP samples tested by single or multi-stages RTL tests. As for both tests samples were tested at 3 psi confining pressure and at much lower levels of deviator stresses than the range found above at 4 psi.

CHAPTER 4. RESILIENT MODULUS MODELING

4.1. Introduction

The main objective of this research task is to assess the constitutive models previously tested for RAP as a base layer as presented in Table 2.1 under the effect of different actual environmental and field conditions other than the state of stresses. This objective is fulfilled in three stages. The first stage aims to investigate the accuracy of these models by statistical analysis to show how they may be affected by the new conditions alone or in conjunction with various interactions at different percentages of RAP on the prediction of the resilient modulus.

Then, the second stage is tailored by a sensitivity analysis for the best statistical models known from the first stage in order to choose the best-fit one and its suitability in predicting the resilient modulus of RAP. Otherwise, determine the need if any, to establish a new prediction model in the future. The study also assesses the adequacy of these factors in representing most of the field conditions affecting the base layer. Then to investigate the need for more laboratory measurements in the future to take the effect of other and/or more, environmental and field conditions in predicting the resilient modulus for the RAP mixes to be utilized in the base course layers such as the leaching contents of RAP.

From the first two stages, the MEPDG model is proved to be the most reliable and best-fit model for predicting the M_R of RAP as a base layer under different field conditions. However, it is found that there is no exact relationship between each K parameter and the studied field conditions individually. These field conditions include various water contents, decreased dry density and applied freeze-thaw cycles at different RAP concentrations. Therefore, the third parametric analysis stage is needed to assess the physical meaning of each constant in the model especially from the point of view of state of stresses representing the most influencing parameter

on M_R for base layer. In addition, this stage is important to check the model suitability for traditional base course aggregates and RAP-Aggregate mixes depending on the behavior of each constant parameter of MEPDG model at different state of stresses.

4.2. Experimental Considerations

This study is conducted on one source of RAP (RAP-TH 10 - Trunk Highway at 10 miles location) collected by the Minnesota Department of Transportation (MN/DOT) in previous researches. This decision is taken to avoid the problem of RAP variability if it collected from several sources or sites. This material is mixed with Class 5 of base aggregates with 50%, 75%, and 100% of RAP. For sample homogeneity, the maximum particle size is recommended to be less than 10% of the mold size; therefore all material greater than 12.5 mm is replaced by other materials passing the 12.5 mm sieve and retained on sieve No.4 (4.75 mm). This is the only adjustment for aggregate gradation in this stage of the research (Kim & Labuz, 2007). For this kind of RAP, the OMC% is 5.5% and MDD 2,124 kg/m^3, and for Class 5, the OMC% is 6.4% and MDD 2,223 kg/m^3 (Mohamed Attia & Abdelrahman, 2011).

The M_R test is conducted immediately after sample compaction. The target sample size is 6 inches in diameter and 12 inches in height. In addition, the sample is subjected to 1000 load cycles for pre-conditioning followed by the 30-load sequences, as specified by the NCHRP 1-28A protocol, procedure 1A. The resilient modulus test is conducted inside a tri-axial pressure chamber, capable of maintaining the required confining pressure. These results of the measured resilient modulus were produced before by the NDSU research team with the cooperation of MN/DOT which supplied the material samples. These results are used in this study to compare the measured and predicted values of M_R for the constitutive models under consideration.

The nine prediction models for M_R shown in Table 2.1, previously used for prediction of M_R for granular base course layer, are considered in this study. The comparison between measured and predicted M_R values at various percentages of RAP is taken under consideration of different factors. These factors are: water content varying from OMC-3% to OMC+2%, dry density of the sample changing from 100% to 90% of the maximum dry density (MDD) and finally the freeze-thaw (F-T) cycling, never studied before for the RAP behavior. For the purpose of freeze-thaw, the samples are subjected to two cycles of freeze-thaw prior to testing for determining the M_R values. The freezing-thawing limits are freezing samples at -12° F for 24 hours then thawing for 24 hours again at 75°F (M. I. E.-S. Attia, 2010). All these factors are compared under the effect of different percentages of RAP to the equivalent measured M_R samples at the same conditions.

4.3. Statistical Analysis

The known constitutive models for granular material are investigated for their suitability in modeling M_R behavior of RAP materials and mixtures. Each predictive model is run to predict the measured M_R values from laboratory tests conducted on RAP at different conditions and percentages. For each model, a multiple regression comparison is utilized for all state of stresses at various testing conditions and different RAP percentages together with their interactions to determine the multiple regression factors (K's constants) using the Excel Solver. Then, a linear regression comparison is made using the Minitab software for each model between the predicted and measured M_R at all tested conditions. This procedure is used to calculate all regression-related parameters, such as R^2. Each prediction model is evaluated at a different RAP percentages varying from 50% to 100% for each tested condition or interactions between these conditions.

From the comparison between the predicted and measured values of M_R, it is obvious that six models are rejected as shown in Table 4.1. Only three can be considered applicable for the

RAP behavior. These are: the Pezo, MEPDG, and Witczak models. This result is attributed to the relative closeness of the regression lines, obtained from these models, to the equity line. This implies that the best prediction of the M_R values may be obtained with these models as shown in Figures 4.1, 4.2, and 4.3. This finding is confirmed by results of the calculated R^2 as these three models yield the highest values for all the tested conditions as shown in Tables 4.2, 4.3 and 4.4.

Finally, the summary of this statistical analysis involves the nine resilient modulus (M_R) prediction models previously used for granular materials to study the effect of the RAP under some field and environmental conditions (water content, dry density, and freeze-thaw cycles) and at three different percentages of RAP (50%, 75% and 100%). The analysis in this first stage is achieved by comparing the predicted and measured M_R values under the above mentioned testing conditions.

This analysis is proceeded with calculating dimensionless multiple regression constants K parameters in each model to know their value. From these comparisons, three models are chosen as shown in Figures 4.1, 4.2 and 4.3 based on the criteria of higher R^2 and less deviation from the equity line of measured and predicted M_R values. The two following stage analysis will focus on measuring these K parameters under the variation of previous testing conditions and taking in consideration the most influential factor on M_R which is the state of stresses. Those two extra analysis stages are needed to choose the best-fit model for predicting M_R for RAP base layer under all possible field conditions.

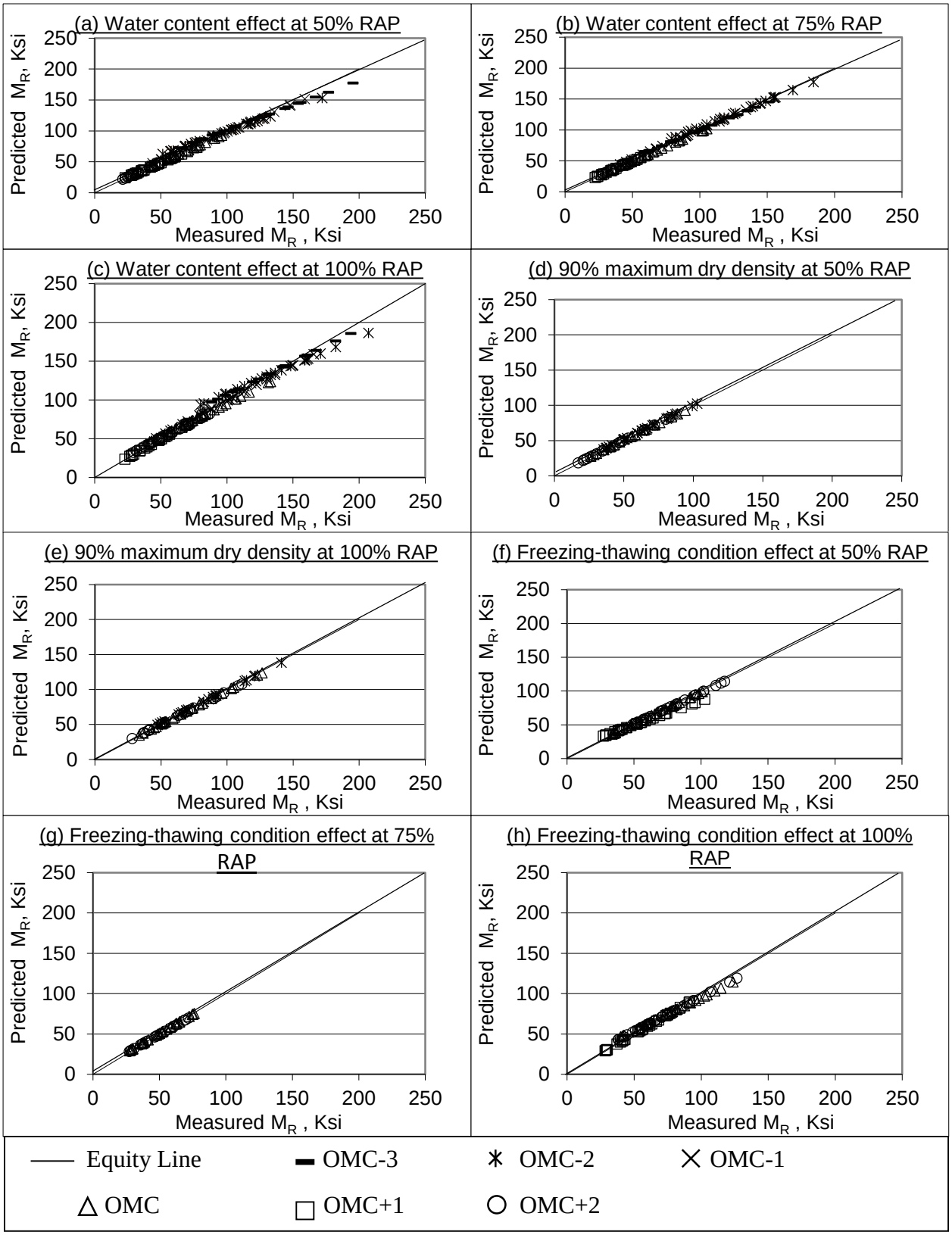

Figure 4.1. Measured versus Predicted M_R Values of Witczak Model

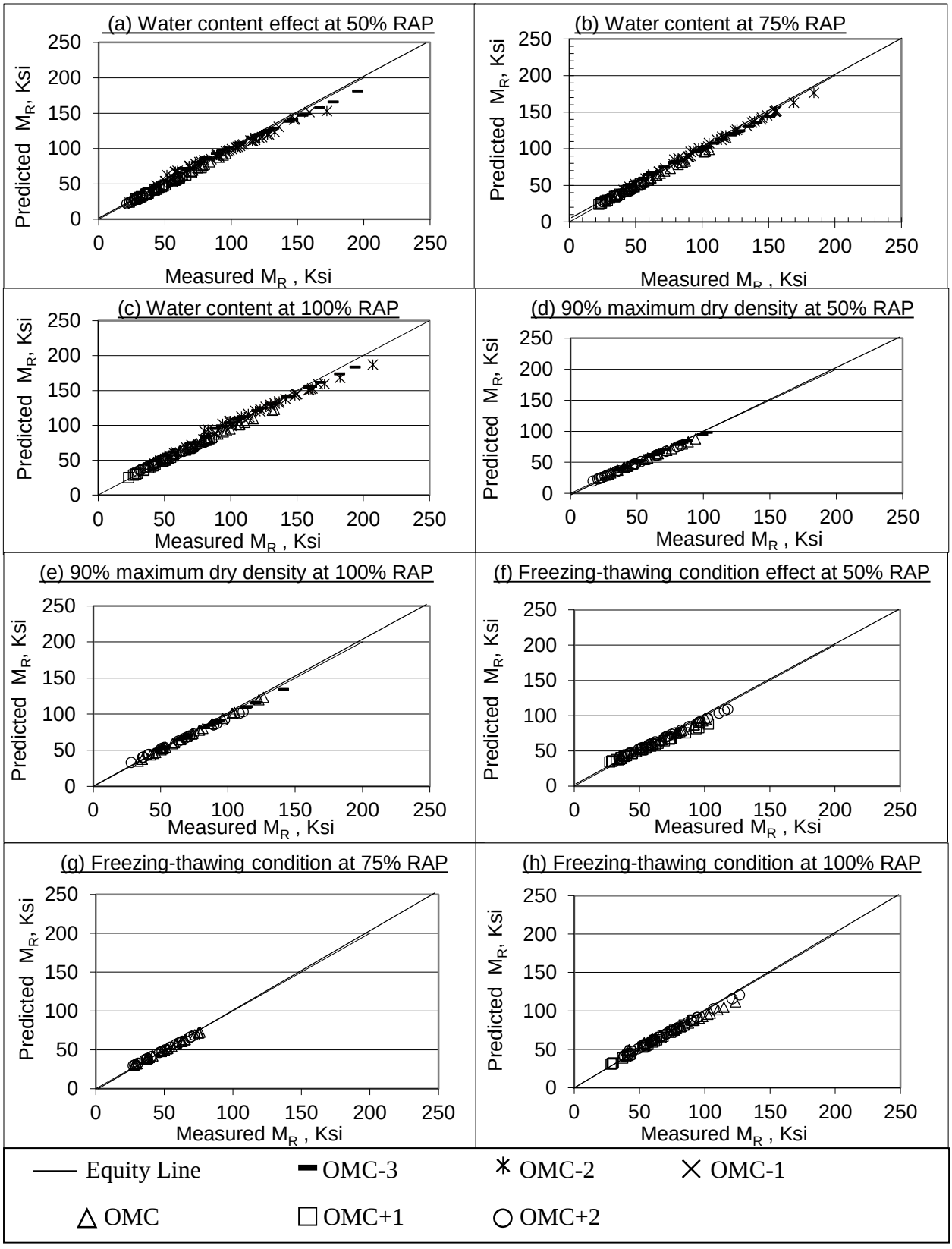

Figure 4.2. Measured versus Predicted M_R of MEPDG Model

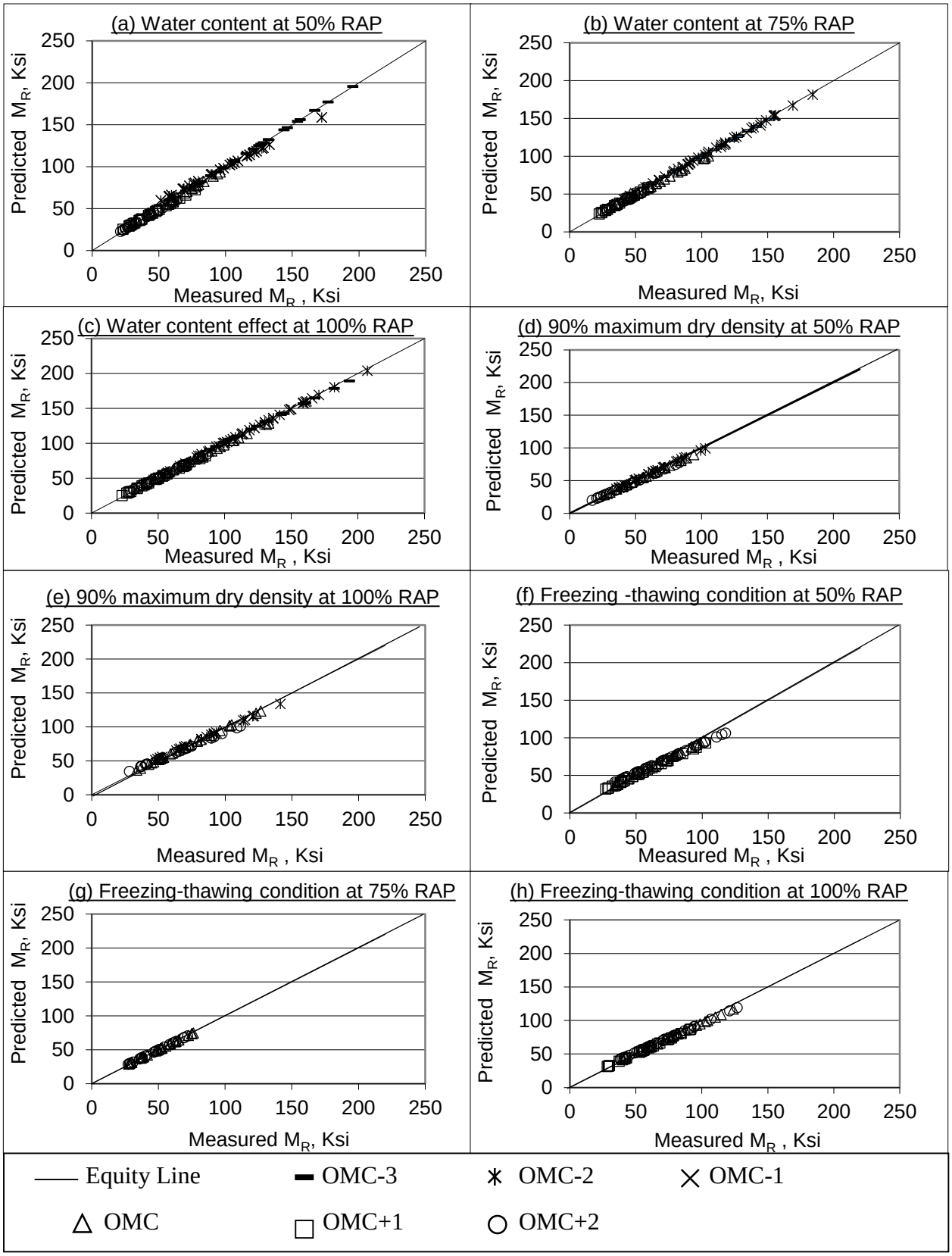

Figure 4.3. Measured versus Predicted M_R Values of Pezo Model

Table 4.1. R^2 for the Six Rejected Models

50% RAP								
W.C %	Maximum Dry Density %	F-T Condition	Conf. Pressure Model	K-Θ Model	Uzan (Deviator Stress) Model	Uzan (Octahedral Shear Stress) Model	Tam & Brown Model	Itani Model
OMC-3	100	No	0.81	0.38	0.94	0.94	0.32	0.98
OMC-2	100	No	0.84	0.55	0.72	0.72	0.01	0.86
OMC-1	100	No	0.88	0.44	0.91	0.91	0.22	0.96
OMC	100	No	0.94	0.53	0.87	0.87	0.02	0.96
OMC+1	100	No	0.88	0.48	0.82	0.82	0.02	0.92
OMC+2	100	No	0.91	0.80	0.88	0.88	0.02	0.04
OMC-2	90	No	0.85	0.37	0.88	0.88	0.17	0.95
OMC	90	No	0.85	0.43	0.86	0.86	0.17	0.70
OMC+2	90	No	0.82	0.46	0.81	0.81	0.05	0.90
OMC	100	Yes	0.96	0.70	0.90	0.90	0.003	0.96
OMC+1	100	Yes	0.86	0.55	0.85	0.85	0.006	0.80
OMC+2	100	Yes	0.77	0.33	0.66	0.66	0.05	0.90
75% RAP								
W.C %	Maximum Dry Density %	F-T Condition	Conf. Pressure Model	K-Θ Model	Uzan (Deviator Stress) Model	Uzan (Octahedral Shear Stress) Model	Tam & Brown Model	Itani Model
OMC-3	100	No	0.96	0.66	0.97	0.97	0.15	0.98
OMC-2	100	No	0.91	0.50	0.96	0.96	0.30	0.98
OMC-1	100	No	0.81	0.32	0.91	0.91	0.34	0.98
OMC	100	No	0.93	0.62	0.87	0.87	0	0.93
OMC+1	100	No	0.93	0.81	0.88	0.88	0.01	0.96
OMC+2	100	No	0.92	0.76	0.90	0.90	0.08	0.95
OMC	100	Yes	0.95	0.57	0.85	0.85	0.008	0.96
OMC+2	100	Yes	0.95	0.65	0.92	0.92	0.06	0.97
100% RAP								
W.C %	Maximum Dry Density %	F-T Condition	Conf. Pressure Model	K-Θ Model	Uzan (Deviator Stress) Model	Uzan (Octahedral Shear Stress) Model	Tam & Brown Model	Itani Model
OMC-3	100	No	0.77	0.40	0.93	0.93	0.22	0
OMC-2	100	No	0.82	0.40	0.97	0.97	0.31	0.81
OMC-1	100	No	0.76	0.29	0.91	0.91	0.30	0.27
OMC	100	No	0.86	0.40	0.86	0.86	0.04	0.37
OMC+1	100	No	0.92	0.51	0.84	0.84	0.03	0.46
OMC+2	100	No	0.94	0.66	0.89	0.89	0.03	0.63
OMC-2	90	No	0.74	0.29	0.88	0.88	0.33	0.93
OMC	90	No	0.69	0.16	0.81	0.81	0.03	0.92
OMC+2	90	No	0.65	0.24	0.71	0.71	0.21	0.91
OMC	100	Yes	0.83	0.41	0.73	0.73	0.04	0.91
OMC+1	100	Yes	0.86	0.42	0.77	0.77	0.03	0.92
OMC+2	100	Yes	0.66	0.19	0.86	0.86	0.24	0.93

Table 4.2. R^2 for Water Content (W.C) Variation on RAP Approved Models

W.C %	50 % RAP			75 % RAP			100% RAP		
	Pezo Model *(Fig. 4.3-a)*	MEPDG Model *(Fig. 4.2-a)*	Witczak Model *(Fig. 4.1-a)*	Pezo Model *(Fig. 4.3-b)*	MEPDG Model *(Fig. 4.2-b)*	Witczak Model *(Fig. 4.1-b)*	Pezo Model *(Fig. 4.3-c)*	MEPDG Model *(Fig. 4.2-c)*	Witczak Model *(Fig. 4.1-c)*
OMC-3	0.99	0.90	0.89	0.98	0.93	0.93	0.95	0.89	0.87
OMC-2	0.84	0.78	0.80	0.98	0.92	0.90	0.96	0.82	0.79
OMC-1	0.96	0.94	0.95	0.97	0.96	0.95	0.97	0.94	0.92
OMC	0.96	0.95	0.97	0.93	0.96	0.98	0.96	0.91	0.91
OMC+1	0.91	0.86	0.91	0.94	0.94	0.97	0.93	0.95	0.98
OMC+2	0.91	0.92	0.96	0.92	0.89	0.93	0.94	0.89	0.90

Table 4.3. R for 90% Maximum Dry Density (MDD) on RAP Approved Models

W.C %	50 % RAP			100% RAP		
	Pezo Model *(Fig. 4.3-d)*	MEPDG Model *(Fig. 4.2-d)*	Witczak Model *(Fig. 4.1-d)*	Pezo Model *(Fig. 4.3-e)*	MEPDG Model *(Fig. 4.2-e)*	Witczak Model *(Fig. 4.1-e)*
OMC-2	0.95	0.94	0.96	0.93	0.94	0.96
OMC	0.93	0.91	0.95	0.94	0.91	0.94
OMC+2	0.89	0.87	0.90	0.83	0.81	0.88

Table 4.4. R^2 for Freezing-Thawing (F-T) Cycles on RAP Approved Models

W.C %	50% RAP			75% RAP			100% RAP		
	Pezo Model *(Fig. 4.3-f)*	MEPDG Model *(Fig. 4.2-f)*	Witczak Model *(Fig. 4.1-f)*	Pezo Model *(Fig. 4.3-g)*	MEPDG Model *(Fig. 4.2-g)*	Witczak Model *(Fig. 4.1-g)*	Pezo Model *(Fig. 4.3-h)*	MEPDG Model *(Fig. 4.2-h)*	Witczak Model *(Fig. 4.1-h)*
OMC	0.96	0.93	0.96	0.96	0.94	0.97	0.87	0.80	0.82
OMC+1	0.88	0.82	0.80	NA	NA	NA	0.90	0.95	0.98
OMC+2	0.83	0.85	0.91	0.96	0.93	0.87	0.93	0.93	0.87

4.4. Sensitivity Analysis

A second stage is performed to assess the best-fit of the three models chosen on RAP behavior considering all the interactions taken in the study at the three different concentrations of RAP. This second stage is carried out by comparing each multiple regression constant K values of each model under the effect of tested conditions at different RAP percentages in order to understand the possible change(s), if any, of each K value with the tested conditions.

4.4.1. Witczak model parametric analysis

Based on the Witczak model equation, it is obvious that K_{23} is directly related to M_R. From Figure 4.4, K_{23} increases for 75% and 100% of RAP and it reaches its maximum value at the optimum moisture content (OMC%). Also, it hugely increases when the maximum dry density (MDD) decreases from 100% to 90% for all RAP percentages. However, K_{23} value differs completely under the effect of freeze-thaw as it decreases in general for all RAP percentages and increases after exceeding the OMC%. In general, K_{23} is usually at its highest values at 100% RAP under the effect of all tested conditions resulting in an increase in the M_R.

For K_{24}, the same K_{23} behavior is noticed under the effect of the water content as it reaches its maximum value at the OMC% for all RAP percentages. There is no general trend for K_{24} under the effect of freeze-thaw and its values are almost the same for all RAP percentages, but with different behavior for each percent. The effect of decreasing MDD increases slightly the K_{24} values. This increase continues with increasing the water content. However, the percentage of RAP does not have a remarkable significance on the K_{24} values in general under the effect of all the factors studied. The effect of K_{24} on the M_R differs according to the value under the power as M_R may increase or decrease, as shown in Witczak model equation in Table 2.1.

Concerning K_{25}, its effect on M_R is directly proportional, as the lower the K_{25} the lower is the M_R as shown in the equation in Table 2.1. Under the effect of water content, it reaches its minimum value at the OMC especially for the 75% and 100% RAP cases. There is no noticeable difference in the K_{25} under the effect of decreasing MDD level. However, it tends to show a rather linear trend with water content variations. On the other hand, the effect of freeze-thaw on K_{25} showed a significant increase for all RAP percentages without a definite behavior for water content variations. So, in general K_{25} affects negatively on M_R especially under the effects of water content and decreasing MDD. However, this negative effect is minimized with the effect of freeze-thaw.

The study does not consider the effect of the tested factors for both parameters K_{26} and K_{27}. This is attributed to the fact that, after trial and error assumptions of different values for both parameters at various percentages of RAP, it is found that at K_{26} = -5 and K_{27} = 5 yield the highest R^2 for the linear comparison between predicted and measured M_R values. Therefore, it is assumed that K_{26} = -5 and K_{27} = 5 for all interactions of tested factors at all percentages of RAP.

4.4.2. MEPDG model parameter analysis

From the equation of MEPDG model, it is clear that K_{20} is directly related to M_R. In general, as shown in Figure 4.5, K_{20} decreases with increasing the water content for all RAP percentages with slight higher values at 100% RAP. The effect of decreasing MDD decreases K_{20} slightly especially at water content less than OMC%. In addition, it has the higher values at higher percentage of RAP. Furthermore, freeze-thaw cycles negatively affect K_{20} especially at OMC-1% for all percentages of RAP. In general, K_{20} negatively affects all results of the tested conditions especially when water content exceeds OMC%. On the contrary it has a positive effect when the RAP percent increases.

For $K_{21,}$ Figure 4.5 shows that for all RAP percentages, K_{21} reaches its maximum value when the water content is much close to the OMC%. The percent of RAP does not have a large effect on K_{21} values. Also, in terms of the effect of the other two factors, 90% MDD and freeze-thaw cycles are not significant on K_{21} values. Furthermore, there is no general trend for the interaction between these factors and water content. In addition, K_{21} is almost the same for all RAP contents. So, it seems that this parameter is affected only by varying the water content. In addition, the effect of K_{21} on M_R is not clearly obvious, as it depends on the value under the power, as shown in MEPDG model equation in Table 2.1.

For K_{22} parameter, it reaches is its minimum values when water content approaches the OMC% irrespective of the percent of RAP. But, the absolute values of K_{22} slightly increases under the effect of decreasing MDD with increases at higher percent of RAP especially at lower water contents. There is no a significant effect of the freeze-thaw cycles on K_{22} for all RAP percentages. Therefore, in general the parameters of this model are affected more by the water content variation with small effect of decreasing MDD and almost no effect of freeze-thaw cycles at all RAP contents. Also, the parameters are not remarkably affected by increasing the percentage of RAP.

4.4.3. Pezo model parameter analysis

K_{11} is directly proportional to M_R. Figure 4.6 shows that K_{11} decreases at increased water content and increased percent of RAP. Both factors, 90% MDD and freeze-thaw cycles, negatively affect K_{11} with varying the water content especially for 90% MDD. Its interaction with water content is more obvious than that of the freeze-thaw cycles with water content variation. In general, all the tested factors negatively affect K_{11} values with consequently negative effects on the M_R values, as shown in Pezo model equation in Table 2.1.

For K_{12} parameter, Figure (4.6-c) indicates that it reaches its maximum values at the OMC irrespective to the percent of RAP. For both other two factors, K_{12} increases slightly especially for the interaction of 90% MDD and water content, as shown in Figure (4.6-d). Almost no significant effects may be noticed for applying freeze-thaw cycles on K_{12} parameter alone. For K_{13}, as shown in Figure (4.6-e), is affected by water content as it reaches its minimum value when water content approaches to the OMC%. Also, the percent of RAP has a little significance. Decreasing MDD slightly, decreases K_{13} also slightly with significance of the percent of RAP. Freeze-thaw cycles have almost no significance on K_{13} at all RAP percent's. Therefore, in general, parameters of this model do not show a well-defined behavior trend under the effect of the tested factors, except only that K_{11} factor is negatively affected by the tested conditions and therefore, negatively affect the M_R values.

Finally, these three models are considered the best-fit for RAP behavior under tested conditions. However, another analysis is felt needed in a second stage to confirm the results of the first one and choose the best-fit model for RAP behavior. Therefore, this second sensitivity analysis is carried out on the three models to compare each K under the effect of each condition of the tested factors. Figures 4.4, 4.5, and 4.6, show that the MEPDG model gives the best physical meanings of the obtained results when compared to the other two models. In general, the parameters of this model are highly affected by the water content variation, slightly affected when decreasing the MDD, almost not affected by freeze-thaw cycles at all RAP contents. This model's parameters are not highly affected by increasing the percentage of RAP. This model in general, gives the best prediction M_R values at 75% RAP**.**

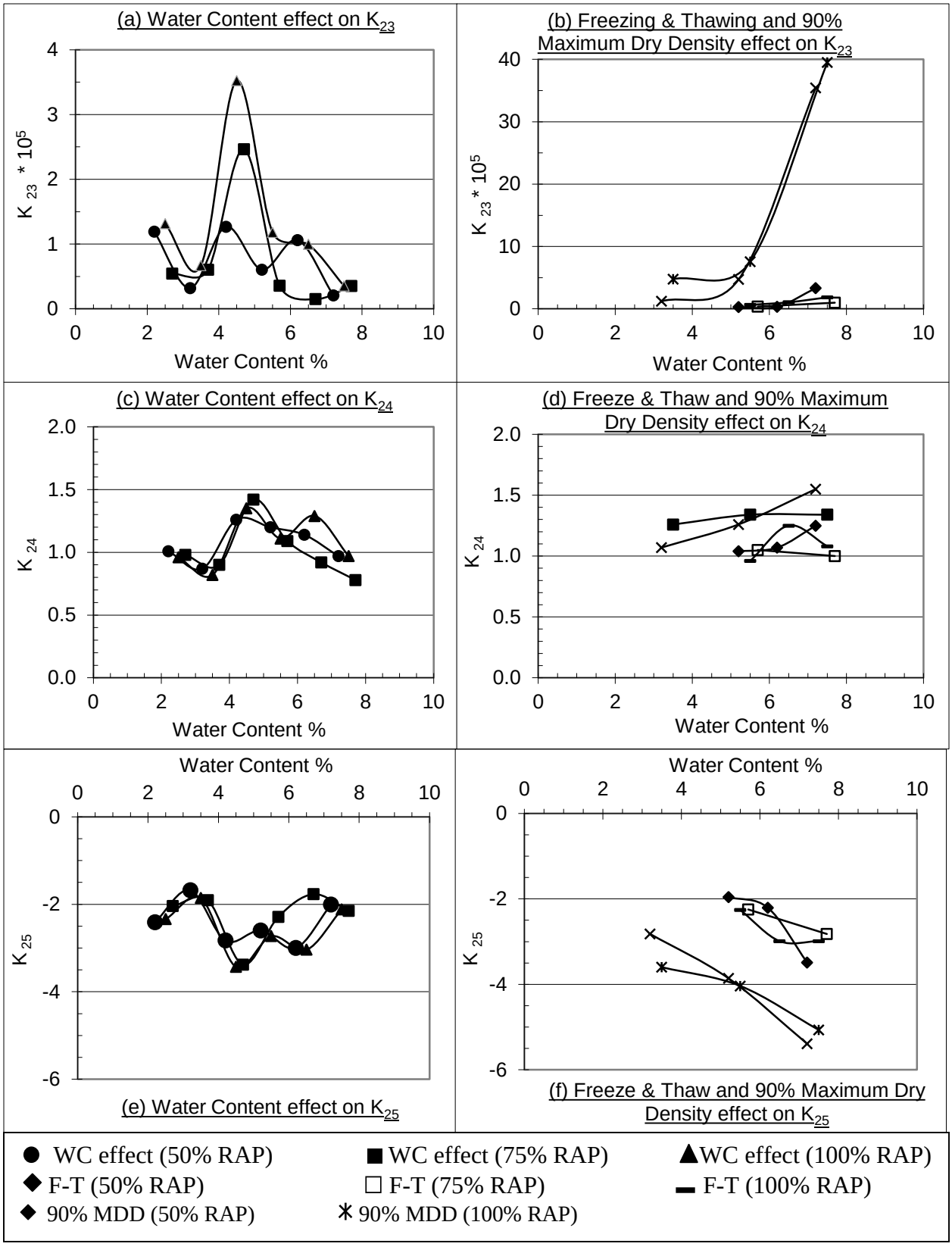

Figure 4.4. Analysis of K Parameters for Witczak Model under Tested Factors

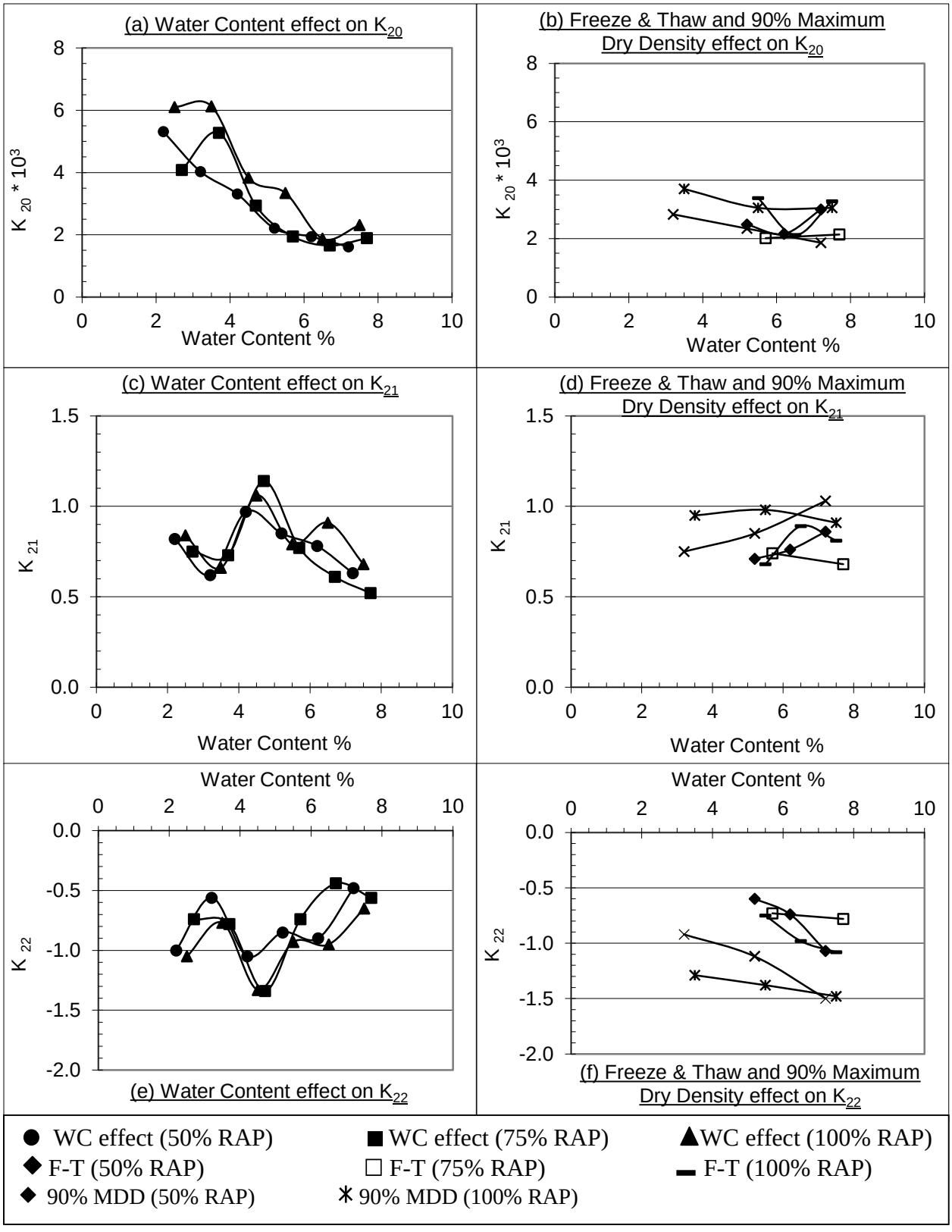

Figure 4.5. Analysis of K Parameters for MEPDG Model under Tested Factors

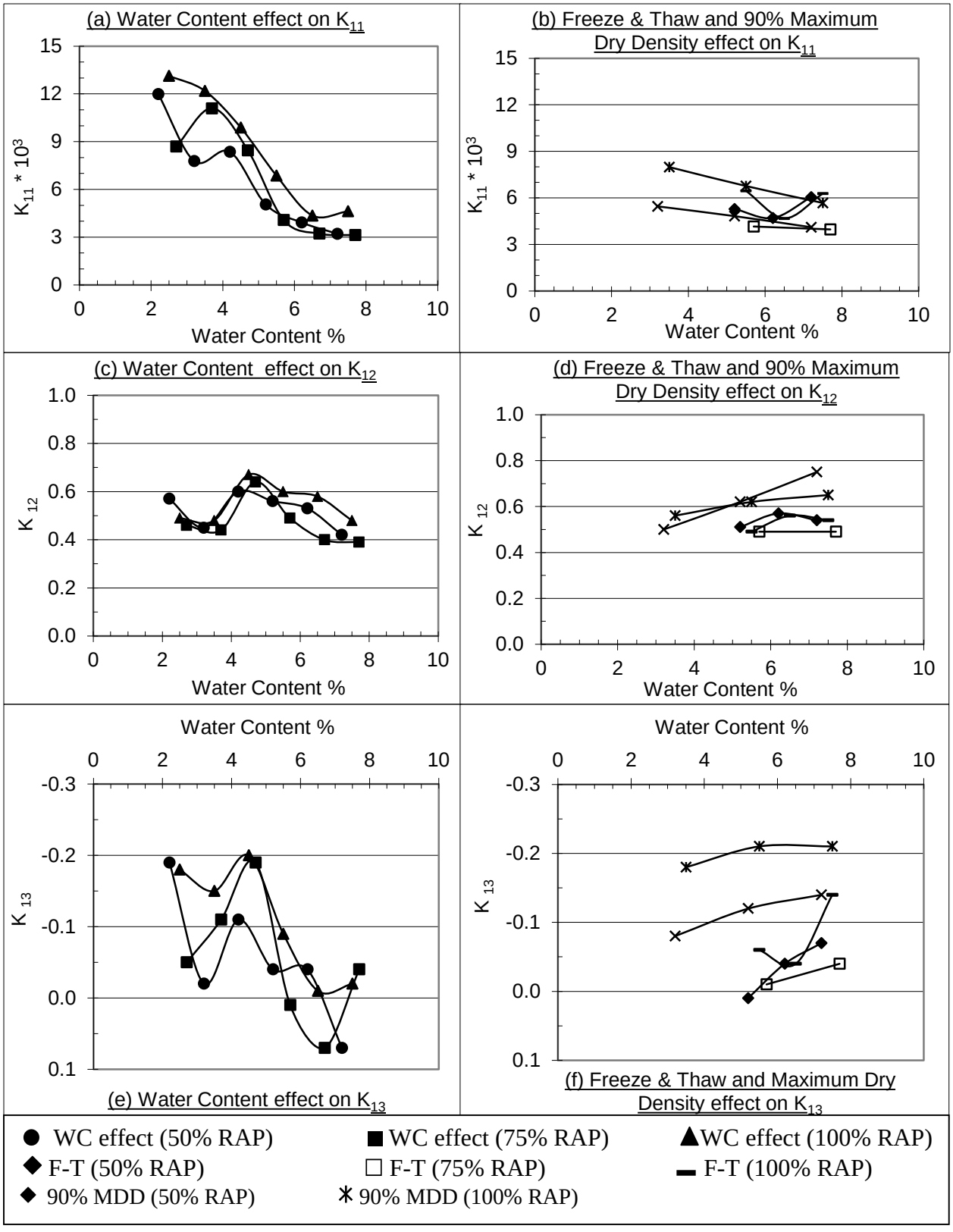

Figure 4.6. Analysis of K Parameters for Pezo Model under Tested Factors

4.5. Parametric Analysis

This third stage analysis is focused on the MEPDG model which is proved to be the best prediction model from the previous two stages. But, this analysis is focused on the different state of stresses applied during the resilient modulus test under the same testing conditions taken in consideration before. The state of stresses was proved from different researches in the literature survey to be the most important effective parameter on the M_R of the base layer. This factor is needed to be studied to be more confident for using the MEPDG model for RAP in base layer.

At first, multiple regression analysis is achieved for the MEPDG model by utilizing the measured M_R values under different measured testing parameters inside this model. This stage comprises calculating each K parameter under five different levels of confining pressure (3, 6, 10, 15 and 20 psi) using the Excel solver software. Six replicates are considered for each level of confining pressure. Each replicate is assigned a different value of deviator stress. This analysis cannot be done at different levels of deviator stress as testing sequences required by NCHRP 1-28A protocol used in M_R testing, do not group deviator stress at the grouped levels of confining pressure mentioned before. This regression is repeated under four different field conditions:

i. Percentages of RAP (0%, 50%, 75% and 100%).
ii. Six different moisture contents, ranging from OMC-3% to OMC+2% with 1% increments.
iii. Two different levels of compaction, 100% and 90% Maximum Dry Density (MDD).
iv. Two cycles of Freeze-Thaw (F-T).

$$\text{MEPDG model:} \quad M_R = K_1 . P_a \left(\frac{\theta}{P_a}\right)^{K_2} \left(\frac{\tau_{oct}}{P_a} + 1\right)^{K_3} \tag{4.1}$$

Where:

- M_R = Resilient modulus (psi)
- K_i = multiple regression constants evaluated from the resilient modulus tests.

- P_a = atmospheric pressure = 14.7 psi = 101.5 kPa.
- θ = bulk stress (psi) = $\sigma_1 + \sigma_2 + \sigma_3 = \sigma_d + 3\sigma_3$ (psi).
- σ_d = deviator stress (psi), σ_3 = confining pressure (psi).
- τ_{oct} = octahedral shear stress (psi) $= \frac{1}{3}\sqrt{\{(\sigma_1 - \sigma_2)^2 + (\sigma_1 - \sigma_3)^2 + (\sigma_2 - \sigma_3)^2\}}$.

Review of previous literature with respect to the M_R-MEPDG model showed that $K_1 > 0$ and refers to the Young's Modulus of the material. Also, $K_2 > 0$ which refers to stress stiffening and $K_3 < 0$ refers to shear softening (Andrei et al., 2004). Most of the results collected satisfy the trend concluded from literature at different confining pressure levels and various field conditions tested, which includes water content, dry density and freeze-thaw cycles at different RAP percentages in the blend. In the following sections, the analysis of each K parameter in the model at those different testing conditions is presented.

4.5.1. Analysis of K_1

The variation of this parameter is considerably high under the variation of confining pressure at different testing conditions. Therefore, the data collected for this parameter is shown on semi-log charts in Figures 4.7, 4.8 and 4.9 to represent K_1 under the variation of confining pressure factor for all testing conditions at different RAP concentrations. Firstly, confining pressure levels can be divided into three categories: low (3&6 psi), intermediate (10 psi) and high (15&20 psi). Under the variation of water content at different levels of confining pressure and different percentages of RAP (Figure 4.7), K_1 increases with increasing the percentage of RAP exceeding the original values before using RAP (0%). This relation is obvious at low confining pressure levels (3&6 psi) and most of water content levels except OMC-3%.

At intermediate confining pressure level (10 psi), K_1 decreases dramatically approaching zero on granular coarse aggregates before using RAP (0%). In case of using RAP at different water

content levels, K_1 also approaches zero except at 100% RAP and water content levels ranging from OMC-2% to OMC.

At high confining pressure levels (15&20 psi), K_1 increases dramatically at 0% RAP and the case is the same when using RAP. However, it does not exceed the original values at 0% RAP. There is an exception for this relation at low water content levels OMC-2 and OMC-3% as K_1 does not increase dramatically like the other water content levels and it decreases with increasing percentage of RAP.

For the case of decreasing MDD from 100% to 90% (Figure 4.8), at low confining pressure category, K_1 increases with increasing percentage of RAP exceeding the original values of K_1 at granular base coarse aggregates (0% RAP). At intermediate confining pressure, K_1 decreases remarkably to approach zero for all percentages of RAP. At high confining pressure levels, K_1 increases dramatically for all percentages of RAP. In general, K_1 values at 90% MDD are higher than 100% MDD in the same other testing conditions.

Finally, for the last case of freeze-thaw cycles (Figure 4.9) at low confining pressure levels, K_1 increases with increasing percentage of RAP exceeding the original K_1 values at 0% RAP. This relation is clearer at 3 psi confining pressure than 6 psi. At intermediate confining pressure, K_1 decreases approaching zero except at 100% RAP in OMC+2%. At high confining pressure category, K_1 increases dramatically except at high percentage of RAP and water content concentration. Generally, K_1 values are not affected significantly by freeze-thaw cycles at the same testing field conditions.

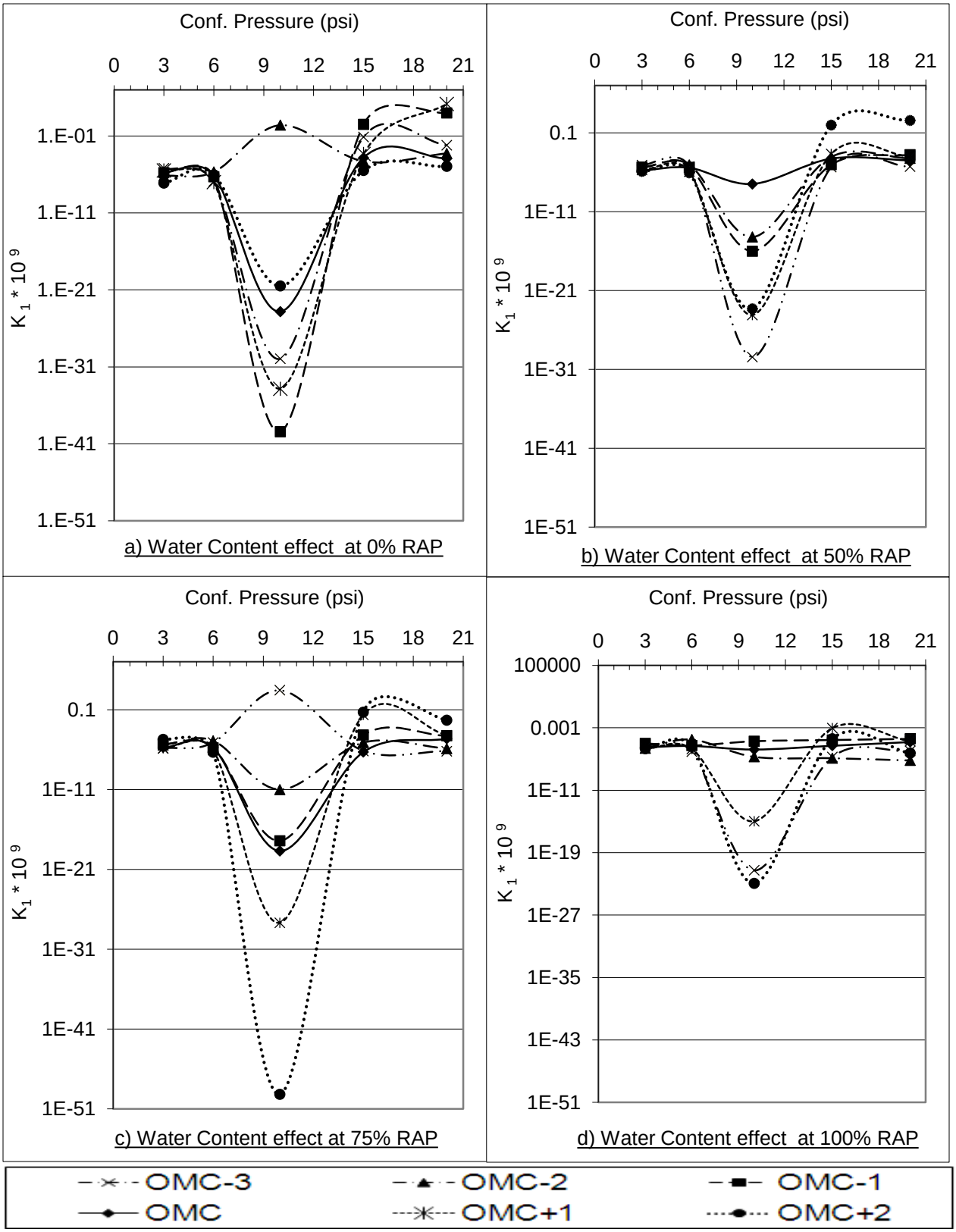

Figure 4.7. K_1 versus Water Content Variation

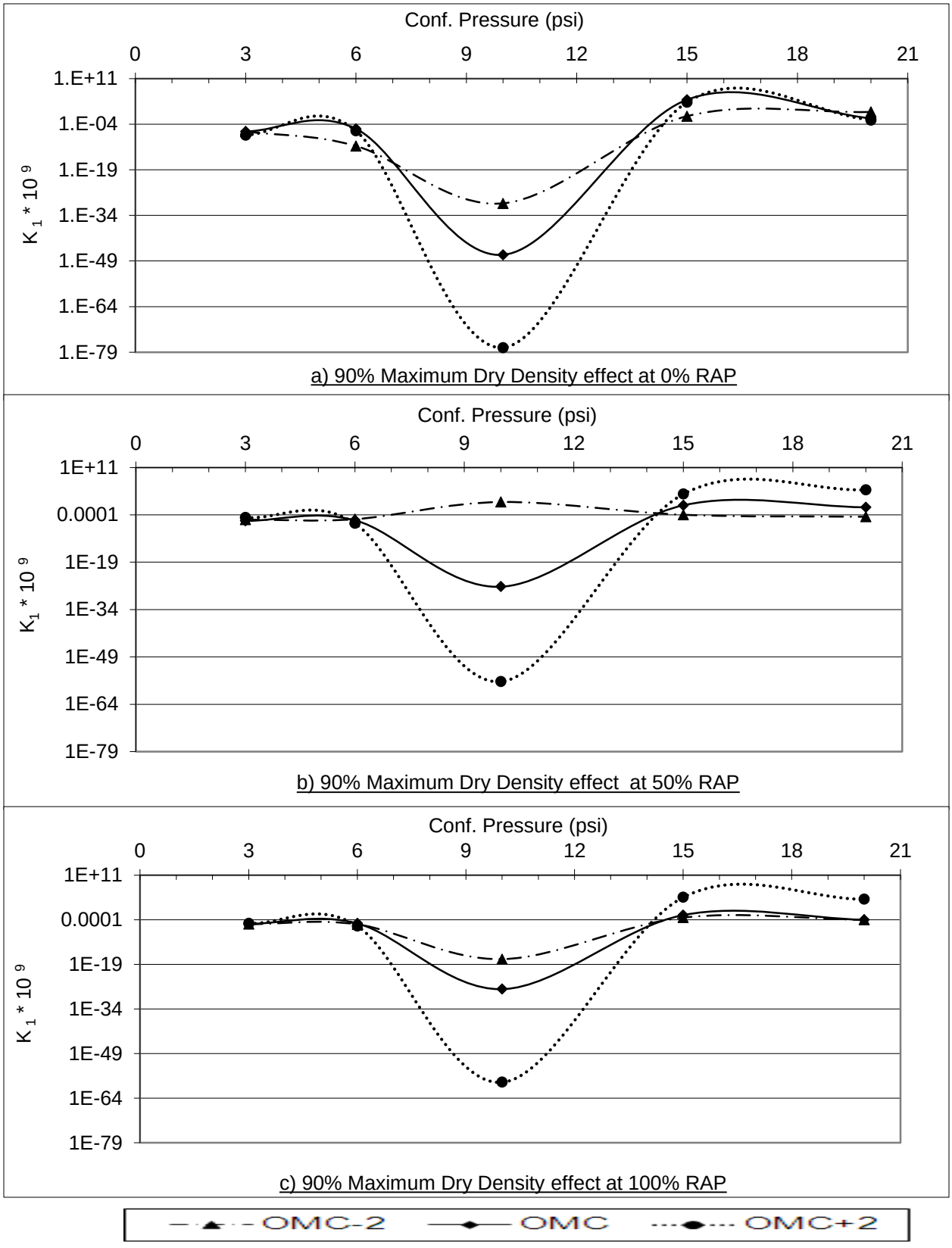

Figure 4.8. K_1 versus Maximum Dry Density Variation

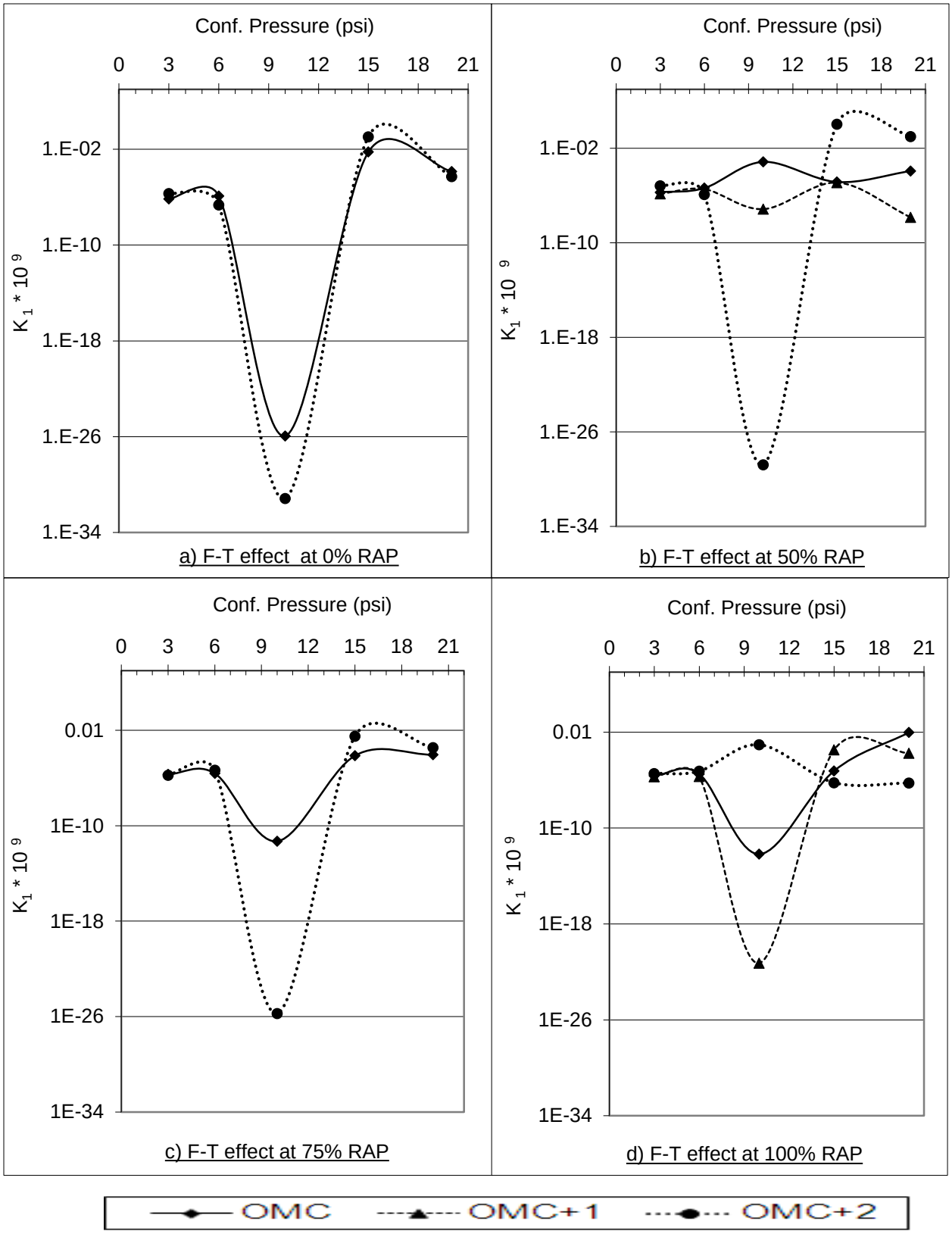

Figure 4.9. K_1 versus Freeze and Thaw Cycles

4.5.2. Analysis of K_2

It is obvious for all testing conditions that K_2 is positive at most confining pressure levels and reaches its maximum values for most of the testing conditions at confining pressure of 10 psi. Therefore, K_2 seems to be more reliable at intermediate confining pressure than others. As it is shown in Figures 4.10, 4.11 and 4.12, K_2 values are very close to zero and sometimes negative. This result satisfies those of the literature for this model and confirmed that K_2 values should be positive for base layer. This describes the behavior of stress stiffening (Andrei et al., 2004).

For water content variation (Figure 4.10), the maximum values of K_2 are usually reached when water content is far-away from the optimum moisture content (at OMC-3% and OMC+2%) especially at 50% and 100% of RAP where K_2 values at OMC are the lower than 0% and 75% of RAP. But, this relation is not the same for granular base aggregates as shown at 0% RAP (Class 5), the maximum values reached at OMC-1% and OMC+1%. The comparison between different RAP concentrations and granular base aggregates shows that the trend of K_2 seems to be very close at 75% RAP. Generally, maximum K_2 values are reached in far-away water contents than OMC% and ranged between 50 to 80 at 50% RAP, while it is in between 70 to 140 at 75% RAP and around 50 at 100% RAP. Nevertheless, for granular base aggregates, it ranges in between 75 to 100 at water contents close to OMC%.

By decreasing MDD to 90% (Figure 4.11), K_2 values increases reaching 170 for 50% and 100% RAP and 250 for 0% RAP. These optimum values are reached especially with high water content levels such as OMC+2%. However, K_2 values at OMC-2% for 50% and 100% RAP remarkably decrease and reach non-realistic negative values for K_2. This behavior is not the same for granular base aggregates (0% RAP) at high water content.

After applying freeze-thaw cycles (Figure 4.12) at different water contents, K_2 values range between 65 to 75 especially at OMC+2% for 50% and 75% RAP. However, at 100% RAP, K_2 values decrease to 55 at OMC+1%. For granular base aggregates (0% RAP), optimum K_2 values reach 80 at OMC+2% and 65 at OMC%. This is much higher than 50% and 100% RAP. Application of freeze-thaw cycles affects K_2 values positively as it increases after F-T cycles at the same water content levels for all percentages of RAP.

4.5.3. Analysis of K_3

As shown in Figures 4.13, 4.14 and 4.15 for all testing conditions, K_3 is negative at most confining pressure levels and reaches its minimum values for most of the testing conditions at a confining pressure of 10 psi. This result satisfies those shown in previous literature that K_3 values should be negative for base layer. Thus, describes the behavior of shear softening (Andrei et al., 2004). In the case of water content variation (Figure 4.13), K_3 values reach their minimum values at water content levels away from OMC% such as OMC-3% and OMC+2%. This trend is obvious at 50%, 75% and 100% of RAP. Approximately, the lowest K_3 values are around -80, -140 and -60 for cases of 50%, 75% and 100% RAP respectively. At 0% RAP, the lowest K_3 value reaches -110 at water content level of OMC-1%. By comparing both percentages 0% and 100% RAP, it seems to be that the general trend of K_3 values at 0% is much lower than 100%, which means that this model is more suitable for granular base aggregates than RAP.

For the case of decreasing MDD to 90% (Figure 4.14), K_3 values are lower than 100% MDD reaching -170 especially at OMC+2% for 50% and 100% RAP. In the case of 0% RAP, K_3values are lower than those for all percentages of RAP (50% and 100%) at the three different water contents of OMC-2%, OMC% and OMC+2%. At 0% RAP, K_3 reaches -250 in the case of OMC+2% compared to -170 at both RAP percentages 50% and 100%.

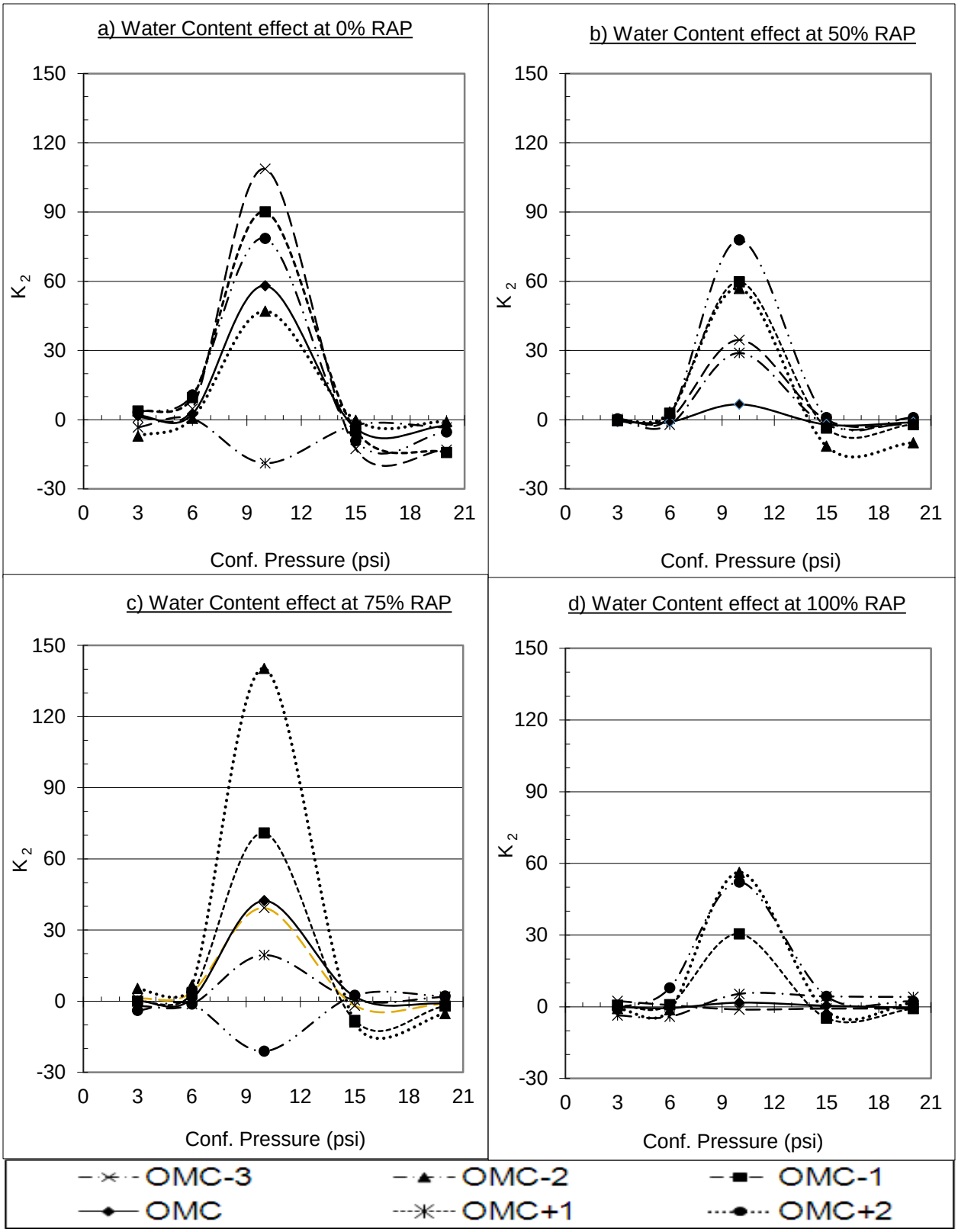

Figure 4.10. K_2 versus Water Content Variation

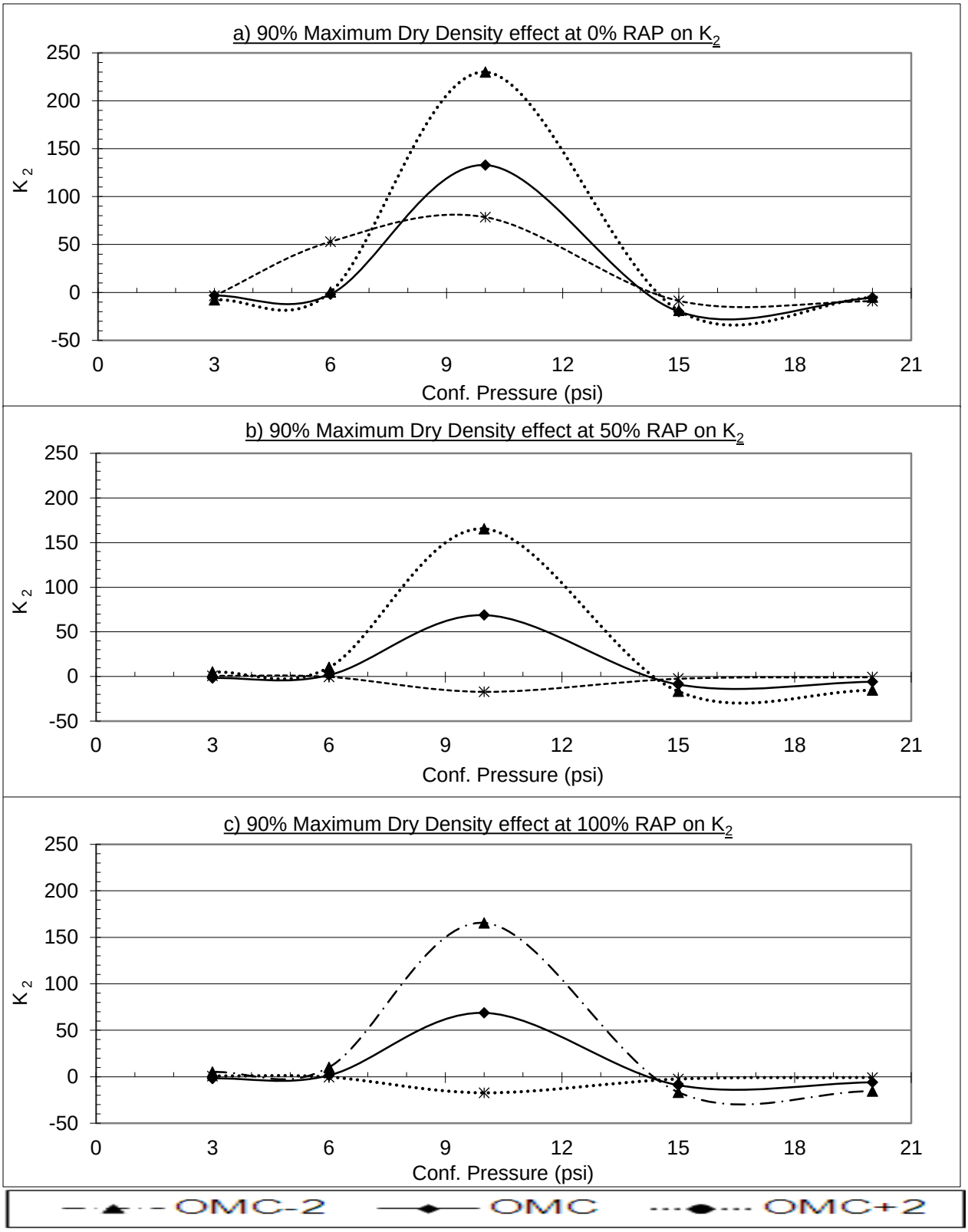

Figure 4.11. K_2 versus Maximum Dry Density Variation

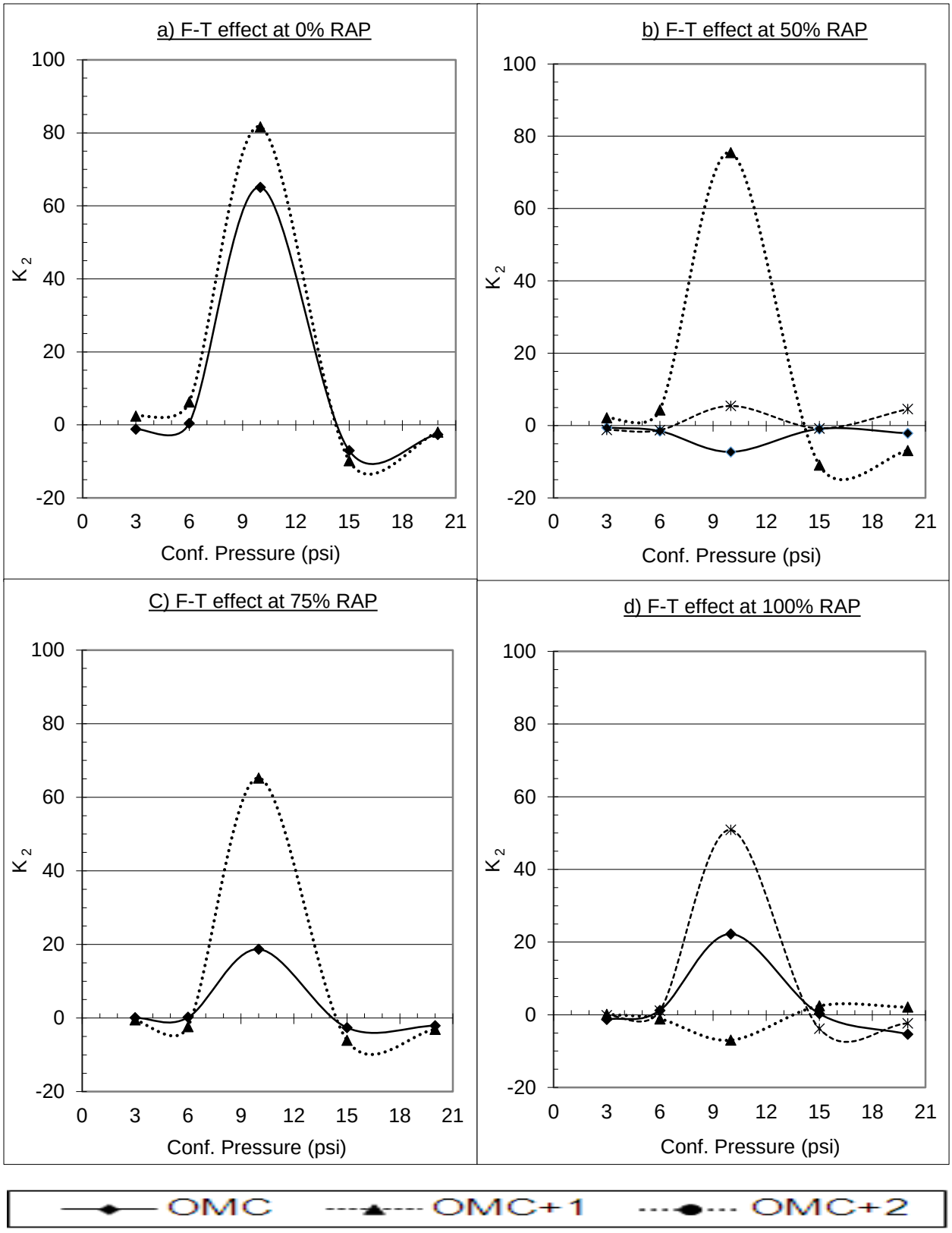

Figure 4.12. K_2 versus Freeze and Thaw Cycles

Decreasing MDD to 90% result matches with the same conclusion in the case above of water content variation.

After applying freeze-thaw cycles (Figure 4.15) at different water contents, K_3 reaches -80 at OMC+2% for 50% RAP compared to -60 at the same field conditions before F-T cycles. K_3 reaches -65 at OMC+2% for 75% RAP and reaches -50 at 100% RAP and OMC+1%. For the case of granular coarse aggregates (0% RAP), K_3 reaches -80 at OMC+2% compared to -50 at the same case before applying F-T cycles. Then, F-T cycles affect more positively on K_3 absolute values. Therefore, by comparing granular coarse aggregates (0%) and RAP (100%), traditional coarse aggregates are more suitable to the model as K_3 absolute values are higher which describes shear softening behavior for base layer better than RAP.

4.5.4. RAP-aggregate combination analysis

After the analysis of each K parameter with different confining pressure levels under various testing conditions, it is felt necessary to assess the variation of each K parameter with different RAP concentrations for all confining pressure levels studied before. In this case, testing conditions are only concerned with OMC% and 100% MDD without freeze-thaw cycles as these are the most frequent field conditions probable to happen at early life stages of pavement section. This stage of analysis is achieved to differentiate between the behaviors of each K parameter when granular base coarse aggregates or RAP are used. The following paragraph present the analyses included as shown in (Figure 4.16):

- K_1 values are low for granular base coarse aggregates and RAP concentrations (50%, 75% and 100%) at low and intermediate confining pressure levels (Figure 4.16-a). However, K_1 increases dramatically at high confining pressure levels (15 and 20 psi) especially for base coarse aggregates. It remarkably increases by increasing RAP concentration.

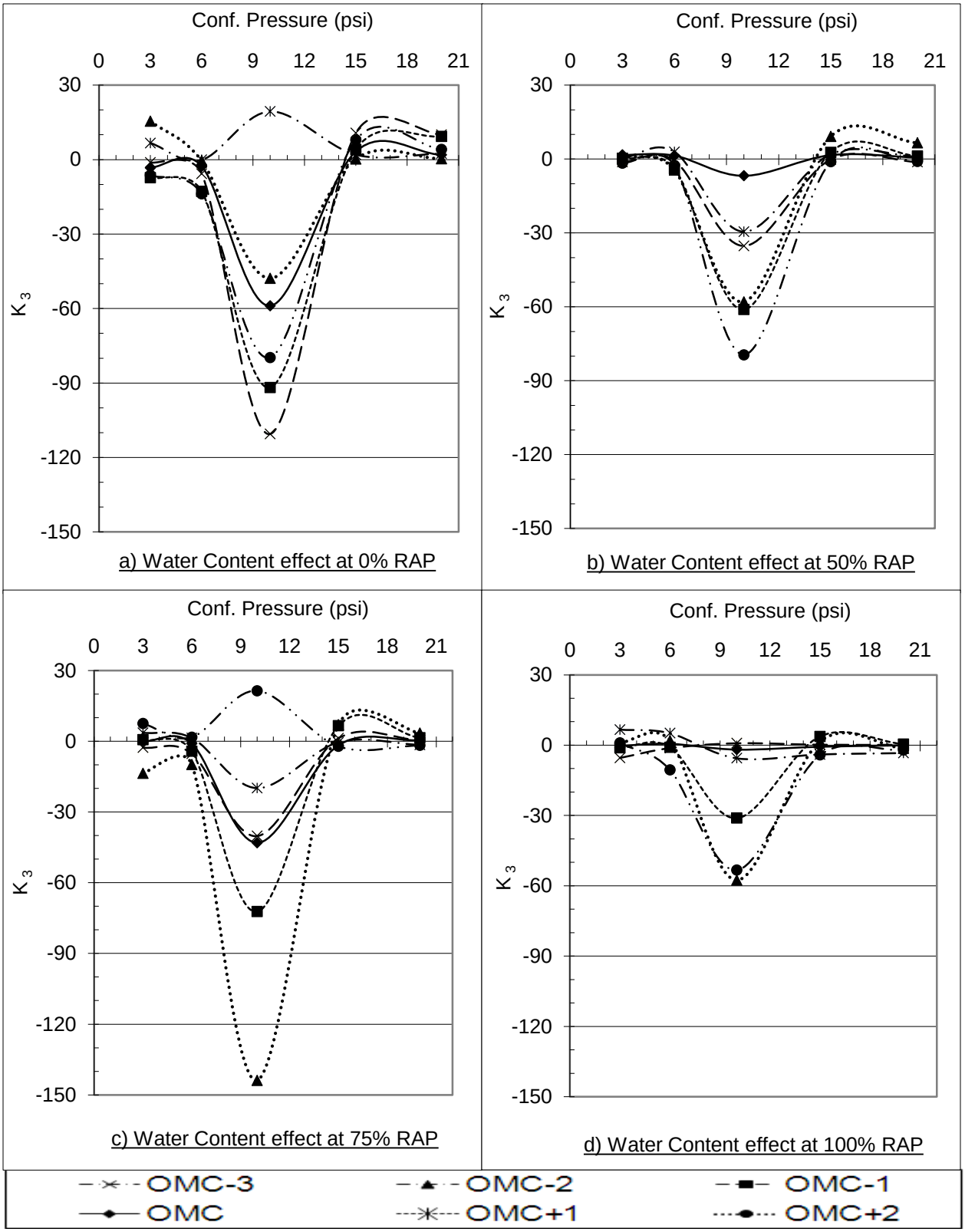

Figure 4.13. K_3 versus Water Content Variation

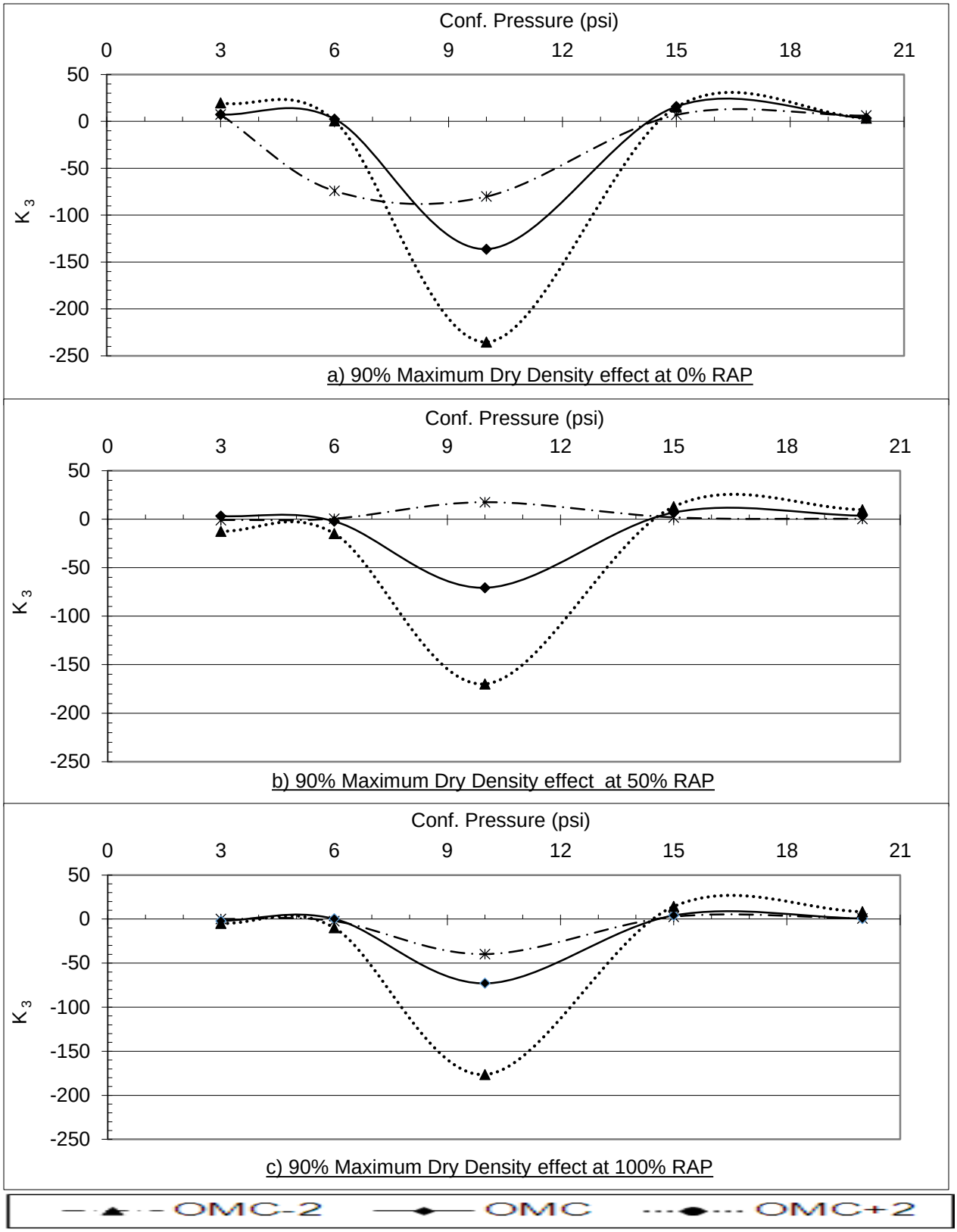

Figure 4.14. K_3 versus Maximum Dry Density Variation

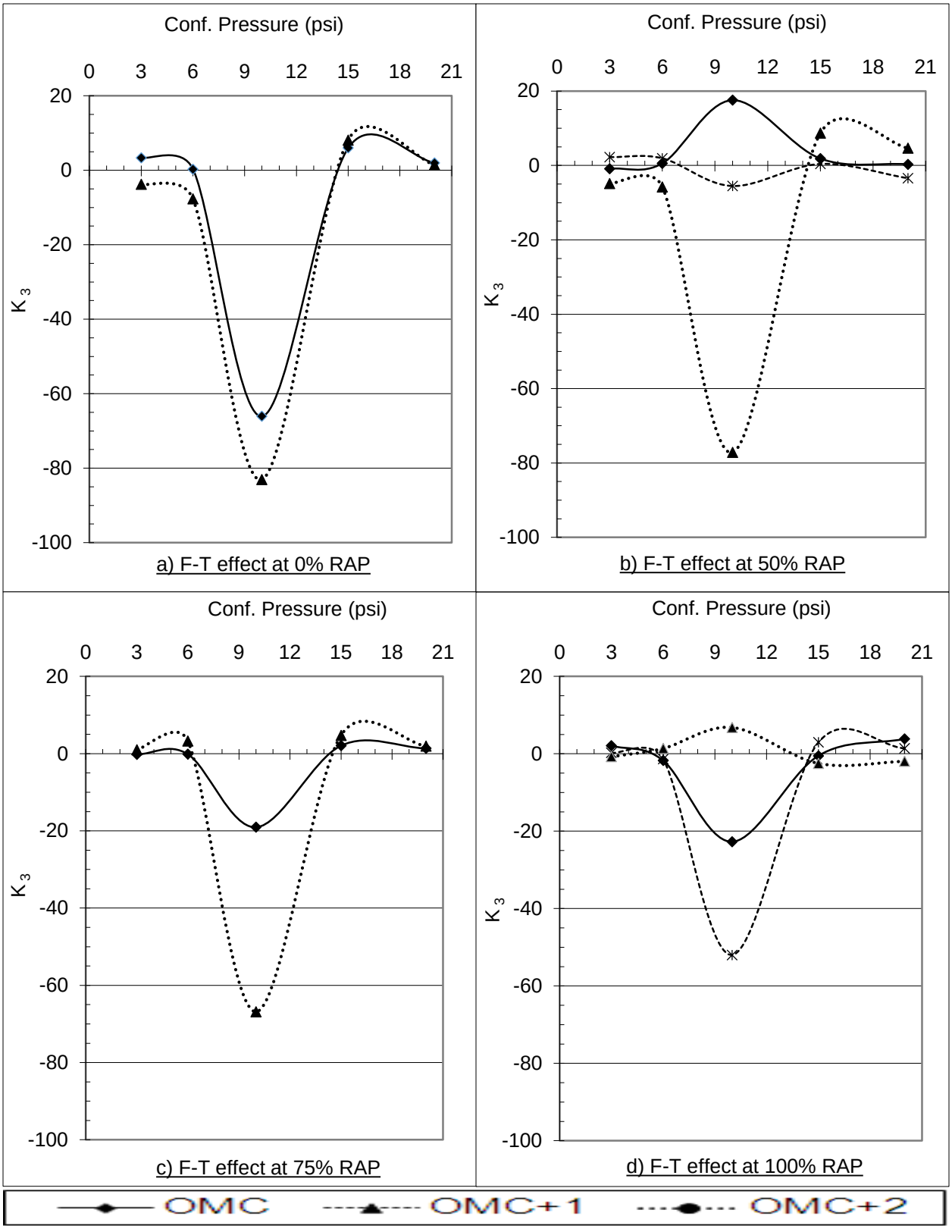

Figure 4.15. K_3 versus Freeze and Thaw Cycles

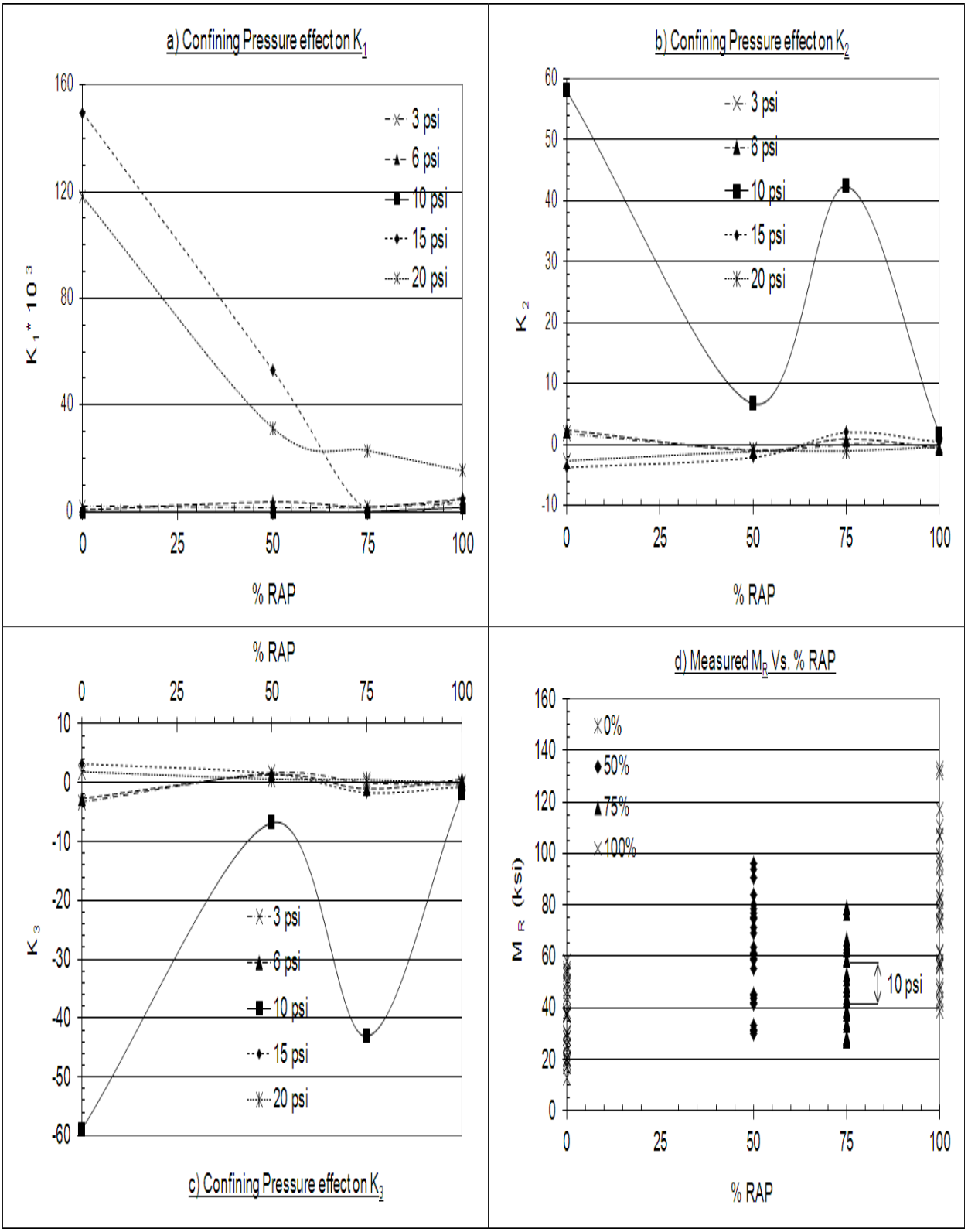

Figure 4.16. Analysis of MEPDG Model versus RAP Concentration

- K_2 values are almost zero for all RAP concentrations (Figure 4.16-b) at both low and high confining pressure levels, except for intermediate level (10 psi). It has high positive value at granular coarse aggregates (0% RAP) compared to the other percentages (50%, 75% and 100%). For 75% RAP, K_2 values' seem to be unreasonable compared to those at the other two percentages of RAP (50% and 100%).
- K_3 values are almost zero for all RAP concentrations (Figure 4.16-c) at both low and high confining pressure levels except for intermediate level (10 psi). It has high negative value at granular coarse aggregates (0% RAP) compared to those of the other percentages of RAP (50%, 75% and 100%). The 75% RAP values seem to be unreasonable compared to those of the other two percentages of RAP (50% and 100%).
- The behavior of this model seems to be approximately the same for both granular base coarse aggregates and RAP when used in base layer. On the other hand, by increasing the confining pressure levels up to 10, 15 and 20 psi, the model seems to better fit for the case of granular base coarse aggregates. In this case, the values of each K parameter are reasonable and agree more with those shown in the literature for the M_R-MEPDG model.
- To prove the variation of K_2 and K_3 at 10 psi for 75% RAP, Figure (4.16-d) shows that the general trend of the original measured M_R data for 75% RAP were lower than both percentages 50% and 100% RAP at all confining pressure levels tested. These results were much lower than expected for 75% RAP as the general trend that M_R increases when percentage of RAP increases.

4.6. M_R Modeling Task Summary

By comparing each dimensionless K regression parameter in the M_R-MEPDG prediction model versus confining pressure levels and different RAP concentrations at various testing field conditions such as water content, maximum dry density and freeze-thaw cycles, few important points are analyzed as following:

- K_1 is dramatically affected by confining pressure levels for both base course layer cases; RAP and granular coarse aggregates. However, this variation is minimized at water contents close to OMC% for the case of RAP. Generally, K_1 increases by increasing percentage of RAP at confining pressure levels below 10 psi.
- K_1 values at 90% MDD are higher than those of 100% MDD at all the other same testing conditions for RAP and granular coarse aggregates. But, they are not significantly affected by freeze-thaw cycles under the other testing conditions.
- General trend of K_2, it decreases with increasing percentage of RAP at low confining pressure levels (< 10 psi) and vice versa at high confining pressure (> 10 psi). Water content variation is an effective factor on K_2 values for the case of RAP. However, this effect diminishes when reaching the OMC%.
- K_2 values increase at 90% MDD for both cases of RAP and granular coarse aggregates. Freeze-thaw cycles do not negatively affect K_2 for both cases. Generally K_2 values decrease at 90% MDD and F-T cycles by increasing percentage of RAP in base layer.
- K_2 values at high confining pressure levels above 10 psi are below zero which contradicts with the concept of stress stiffening related to this parameter confirmed by the literature survey.

- K_3 values are affected by confining pressure variation especially at intermediate level (10 psi). Nevertheless, this variation is the least at water content levels close to OMC% when using RAP.
- K_3 value is negative at low confining pressure levels (<10 psi) and water contents close to OMC%. This finding seems to be reasonable and satisfy the concept of shear softening related to this parameter, as confirmed in the literature. K_3 values are almost the same for the two cases of with or without RAP in the base course.
- 90% MDD is an effective factor on K_3 values for both cases of granular coarse aggregates and RAP, as the absolute values increased compared to 100% MDD at the same testing conditions. However, F-T cycles are not effective on K_3 parameter for both cases of with or without RAP in base layer.
- The resilient modulus prediction by MEPDG model fits the two base course cases studied, the traditional base coarse aggregates and three different concentrations of RAP-Aggregate combination (50%, 75% and 100%) for confining pressure levels below 10 psi.
- The case of 75% RAP in the base layer has some extreme absolute values related to the trend of the other two percentages (50% and 100%). This result is found repeated in several other testing conditions.

CHAPTER 5. PERMANENT DEFORMATION MODELING

5.1. Introduction

The permeant deformation (PD) parameter is essential for evaluating the adequacy of using RAP as a base layer. To measure PD, regularly using repeated tri-axial loading test (RTL), is very time consuming and un-economic in most cases. Then, prediction of PD for RAP used as a base layer is an essential step. However, studying the significance of previous PD prediction models of granular base layer for RAP is insufficient. The M_R prediction model in MEPDG is found from previous task to be the most significant model for predicting M_R for RAP base layer.

Therefore, this study task is focusing on MEPDG rutting prediction model of granular base layer when RAP is used. From previous researches on this topic, it was found that the MEPDG model for PD was highly significant in predicting the PD values compared to repeated tri-axial loading (RTL) measured values. But, there is no sufficient research on prediction of PD from data collected from the resilient modulus test. The PD-MEPDG model takes into consideration the resilient strain calculated from the resilient modulus test. This proves that both parameters are related to each other in evaluating the base layer characteristics. Survey of several previous researches indicates that the most effective parameters on PD are load repetitions, moisture content and stress condition. However, there are other factors needed to be investigated especially for the case of using RAP in a base layer. These factors are stress history, RAP content and different RAP sources which are easier to be investigated from the resilient modulus test.

The main objective of the modeling in this research task is to develop an understanding of RAP behavior as compared to typical granular material. In addition, it concentrates on how the major factors (state of stresses, moisture content, load repetitions and stress history) affect permanent deformation modeling behavior of RAP and/or RAP/aggregate blends. Therefore, this

study comprises investigating the ability of prediction the permanent deformation for RAP used as a base layer utilizing the MEPDG rutting prediction model.

To achieve this objective, PD data collected from both resilient modulus (M_R) and repeated tri-axial (RTL) loading tests are taken into consideration. Each test is responsible on investigation one of the major factors affecting PD accumulated from using RAP. The M_R takes in consideration the stress history of different successive stages of loading, while the single-stage RTL is responsible on measuring PD after frequent number of load repetitions (20,000 or more). In addition, the multi-stage RTL is responsible for taking the effect of both stress history and different axial or deviator stresses applied for each stage of loading. To take the effect of RAP sources variability, different RAP sources are collected for this study. However, the PD data were collected from M_R test only.

5.2. PD-MEPDG Prediction Model

The final form of the modified model by El-Basyouny & Witczak (M. El-Basyouny et al., 2005) for granular base layer recommended to the MEPDG and used for this study is as follows:

$$\delta_a(N) = \beta_{s_1} K_1 h \epsilon_v \left(\frac{\epsilon_o}{\epsilon_r}\right) [e^{-(\frac{\rho}{N})^{\beta}}] \quad (5.1)$$

$$\text{Log}\beta = -0.61119 - 0.017638(W_C) \quad (5.2)$$

$$\rho = 10^9 \left[\frac{C_o}{(1-(10^9)^{\beta}}\right]^{\frac{1}{\beta}} \quad (5.3)$$

$$C_o = \ln\left(\frac{a_1 {M_R}^{b_1}}{a_9 {M_R}^{b_9}}\right) = \ln(0.0075) = -4.893 \quad (5.4)$$

$$\text{Log}(\frac{\epsilon_o}{\epsilon_r}) = 0.80978 - 0.06626\, W_C + 0.003077\, \Theta + 0.000003\, M_R \quad (5.5)$$

Where:

- δ_a (N) = permanent deformation of the base layer (inches).

- N = number of load repetitions.
- ϵ_r = resilient strain (in. /in.).
- ϵ_v = primary response model (assumed to be equal to ϵ_r in this study).
- h = thickness of the layer (inches).
- ϵ_o, ρ, β = material properties.
- K_1 (granular materials) = 1.673 (natural calibration).
- βs_1 = field calibration factor = 1 (unless there are field data).
- M_R = resilient modulus of base layer (psi).
- W_C = water content (%).
- a_1, b_1, a_2, b_2 = regression constants = 0 (natural calibration).
- The natural calibration values are taken from the manual of practice of MEPDG.

5.3. Modeling Methodology

The comparison between predicted and measured PD values using the rutting MEPDG model is achieved on three main stages as follows:

5.3.1. Stage I

In this stage, first a comparison is made between PD values measured from the M_R test to those predicted PD values using PD-MEPDG prediction model. This comparison is achieved on three major testing conditions; four RAP contents (0%, 50%, 75% and 100%), three water content levels (OMC-2%, OMC% and OMC+2%) and three base layer thickness (6, 9 and 12 inches). This comparison is made on the main RAP source TH 10 in Figures (5.1, 5.2, 5.3 and 5.4). Each point in the graph represents different stress condition.

Another comparison is made in this stage between measured and predicted PD of other four field RAP sources. Three RAP sources (TH 19-101, TH 19-104 and TH 22) contain 50% RAP

and another 50% granular aggregates. The fourth RAP source (Cell 18) contains 100% RAP. Also, the comparison of these RAP sources are achieved on PD measured values collected from M_R test at the same testing conditions.

5.3.2. Stage II

The single-stage RTL test is more reliable for measuring PD as it neglects the effect of the stress history, taking into consideration the effect of several load repetitions (20,000 or more). Therefore, this stage focuses on the comparison of predicted PD values versus those measured in the single-stage RTL. This comparison is achieved for RAP TH 10 on two levels of water contents (OMC% and OMC+2%), two contents of RAP (0% and 50%). In addition, this comparison takes in consideration the effect of adding 6% fines on PD modeling for 50% RAP blend to reach 10% fines total in the RAP/Aggregate blend. This is the maximum fine content accepted for MN/DOT Class 5 base layer specification.

5.3.3. Stage III

The multi-stage RTL test is more time consuming and un-reliable for measuring PD. But, it better reflects field conditions. This test comprises applying different sequences of deviator stresses taking into consideration the effect of fewer load repetitions compared to the single-stage test. It was found that most of the accumulated permanent happens in the first 1000 cycles (Waldenmaier, Abdelrahman, & Attia, 2013). Therefore, this stage focuses on the comparison of predicted PD values versus those measured in the multi-stage RTL after 5000 cycles only for each stage. This comparison is achieved for RAP TH 10 on three levels of water contents (OMC-2%, OMC% and OMC+2%), two contents of RAP (0% and 50%). In addition, this comparison takes in consideration the effect of adding 3.5% of high plasticity silt clay on PD modeling for 50% RAP blend.

5.4. Analysis of Results

Each stage of work in this task is analyzed separately and compared to the previous stage. So, this comparison may lead to which test data is more significant for prediction using MEPDG model. This analysis also compares different RAP sources to show if they have similar relation as the main source TH 10. It is proved from all stages of work that both measured and predicted PD values increase with the increase of the base layer thickness. Almost no change is found in the regression parameter R^2 at each thickness (6, 9 and 12 inches) for all testing conditions.

5.4.1. PD from resilient modulus test

It is obvious from Figure 5.1 of Class 5-MN/DOT granular aggregates that increasing the water content from OMC-2% to OMC+2% results in an increase in the measured PD values. The largest increase happens between OMC-2% to OMC%. However, it seems that the predicted PD values at the three water content levels are much lower than the measured values.

It is proved from literature review that this prediction model fits for the granular base aggregates layer. However, this finding was achieved on data collected from repeated tri-axial loading test. This result most probably is related to the effect of stress history and low number of repetitions of the resilient modulus test. Each point on the graph is for each water content level and only represents the PD accumulated after 100 load repetitions. This number of load repetitions is much lower compared to those obtained from the RTL test either single (20,000) or multi stage (5000 per each stage). However, it seems that the variation of both measured and predicted values have high correlation as R^2 values varied from 0.74, 0.78 and 0.87 at OMC+2%, OMC% and OMC-2% respectively.

After adding 50% RAP to the base layer blend, as shown in Figure 5.2, the measured PD values slightly decrease than those Class 5 aggregates before adding RAP (Figure 5.1). However,

the difference between the predicted and measured PD values becomes smaller at OMC-2% with high correlation (R^2 = 0.86). But, still there is a large difference for both water contents OMC% and OMC+2% with lower correlation as R^2 values are equal to 0.58 and 0.61 for OMC% and OMC+2% respectively.

For 75% RAP content as shown in Figure 5.3, the measured PD values do not significantly change from those at 50% content, as it shows a slight increase at OMC% and OMC+2% for 75% RAP. However, the difference between both measured and predicted values is still large as Class 5 and 50% RAP cases, especially at OMC% and OMC+2%. This result is also probably related to the same reason of stress history as explained above which is related to the resilient modulus test procedure. On the other hand, this relation still shows high correlation as R^2 values are 0.87, 0.85 and 0.67 for OMC-2%, OMC% and OMC+2% respectively.

For the case of 100% RAP, as shown in Figure 5.4, the measured PD values decrease significantly from 75% RAP and approach to the values of 50% RAP. In addition, the measured PD values do not change significantly after the extraction of aged binder at OMC% as shown in Figure 5.4(d). The predicted PD values are close to those measured at the OMC-2% case only. The trend of 100% RAP generally is found so similar to that of the 50% RAP. Again, high correlation is evident between the measured and predicted values as R^2 values are 0.85, 0.87, 0.55 and 0.66 for OMC-2%, OMC%, OMC+2% and extracted RAP, respectively.

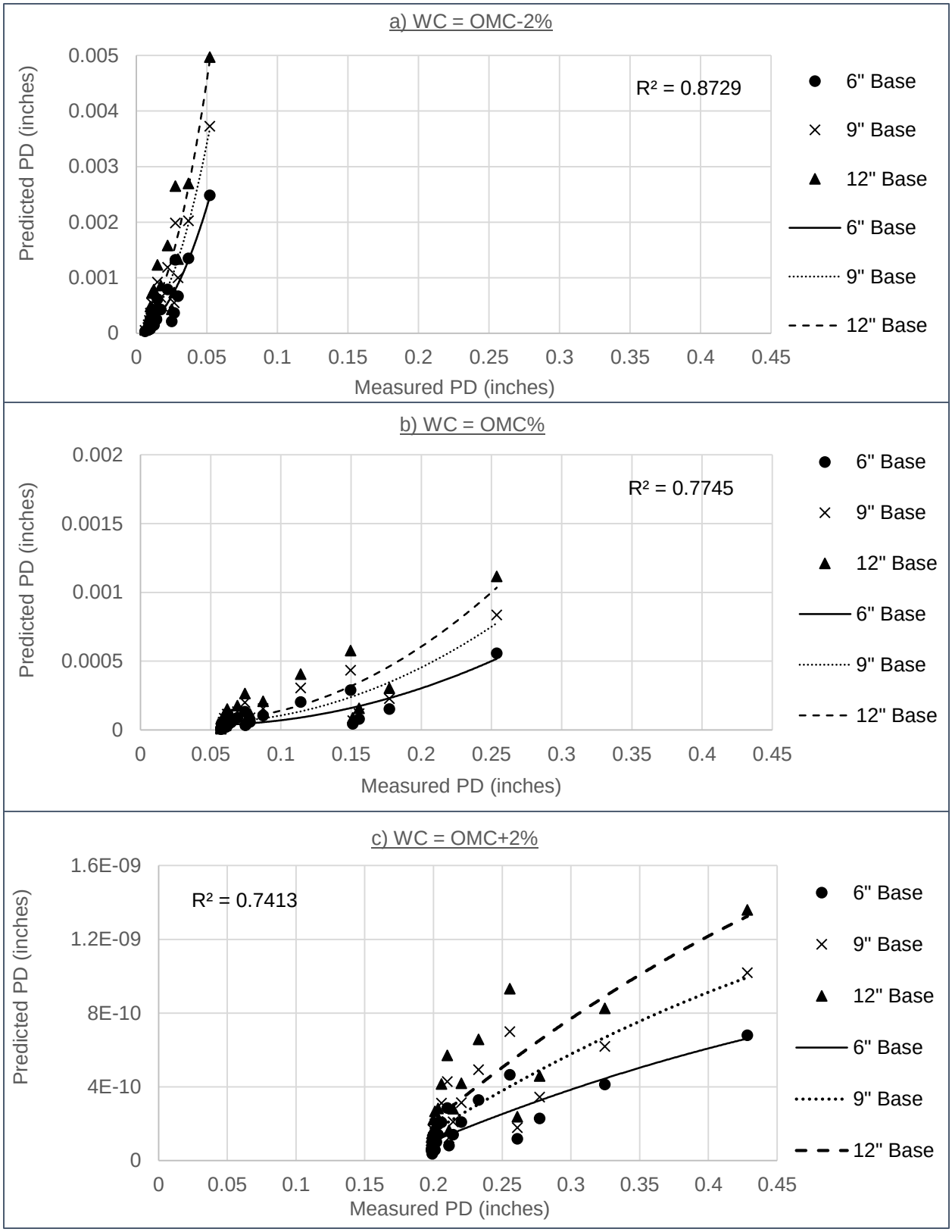

Figure 5.1. Measured versus Predicted PD for Class 5 (0% RAP)

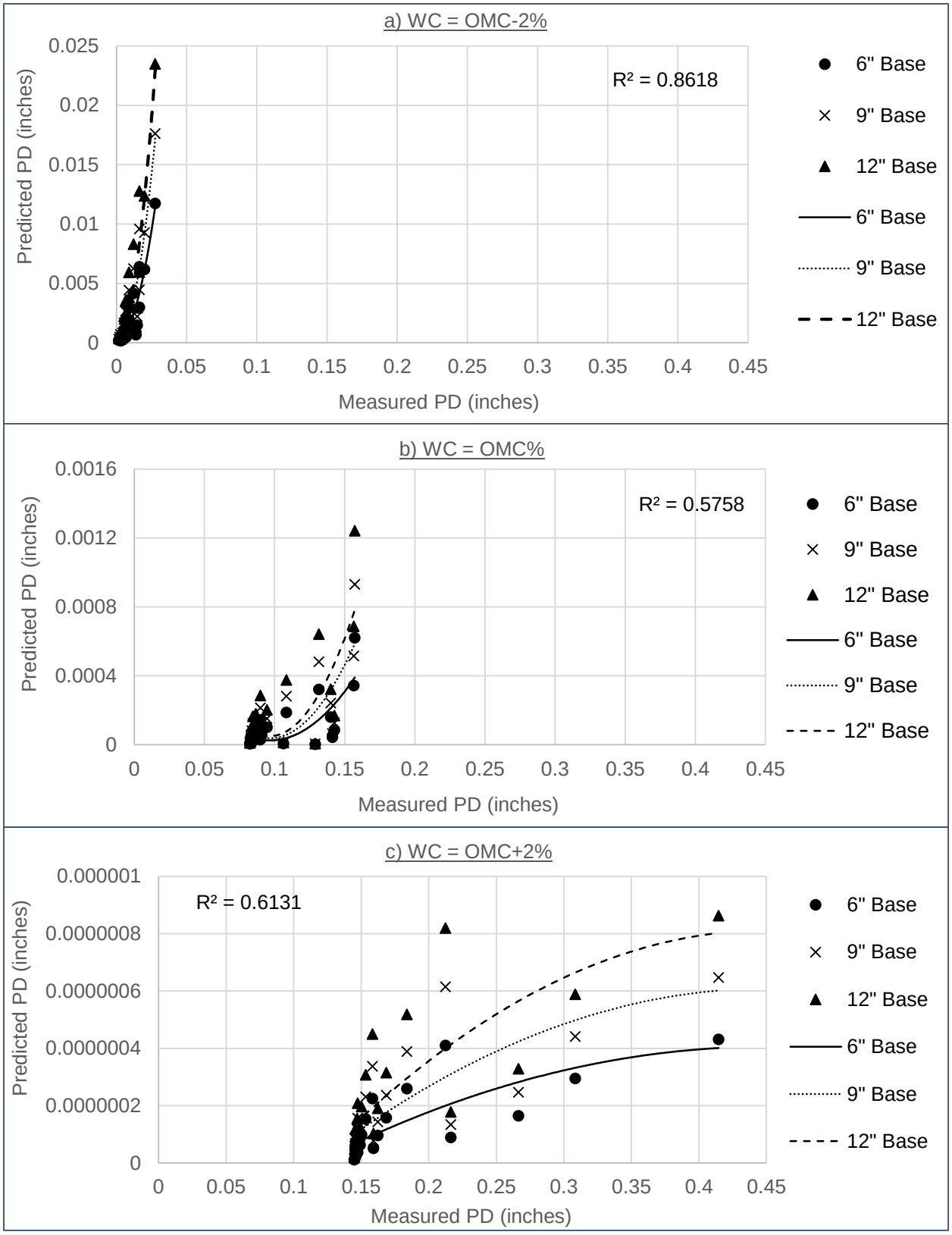

Figure 5.2. Measured versus Predicted PD for 50% RAP TH 10 + 50% Class 5

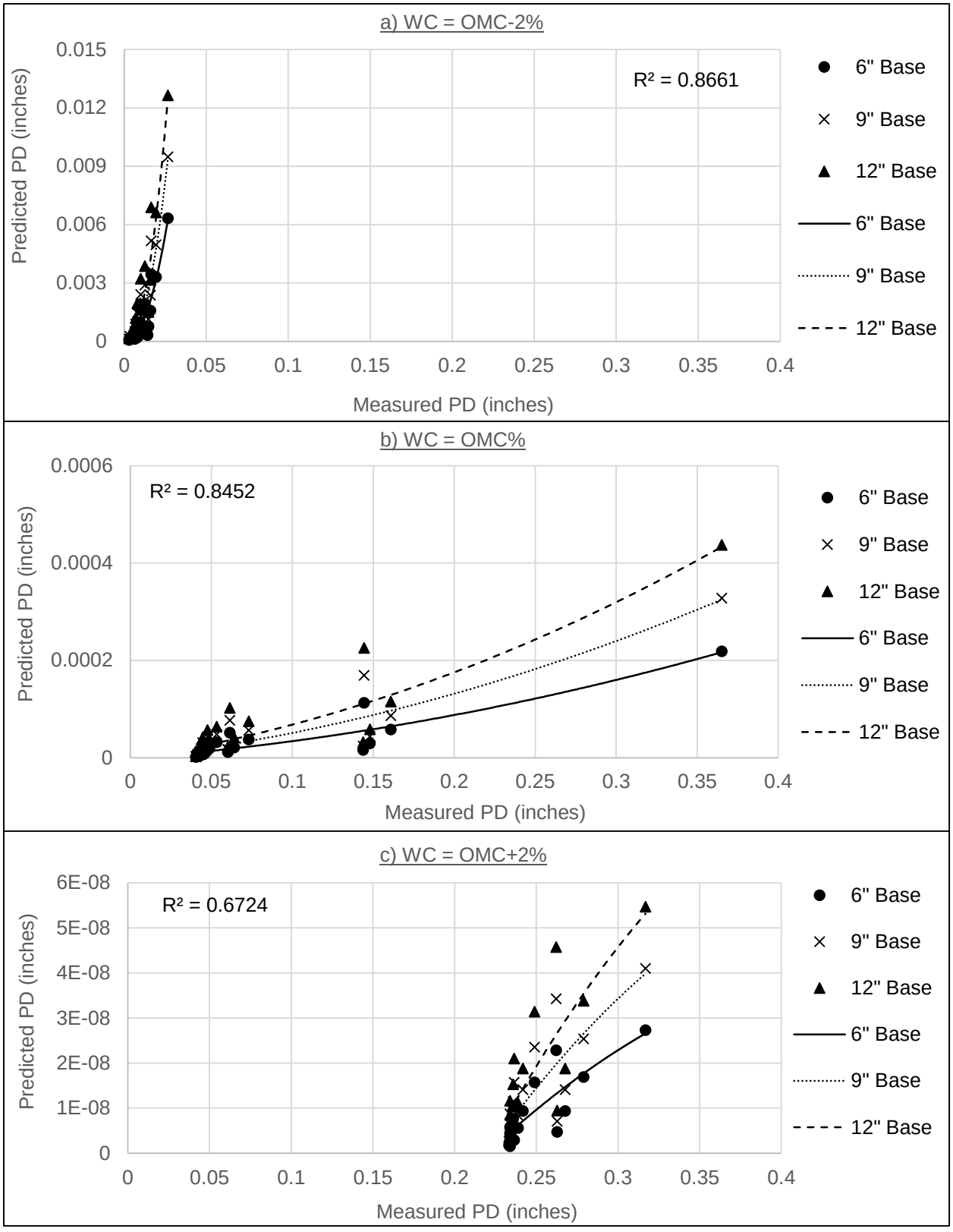

Figure 5.3. Measured versus Predicted PD for 75% RAP TH 10 + 25% Class 5

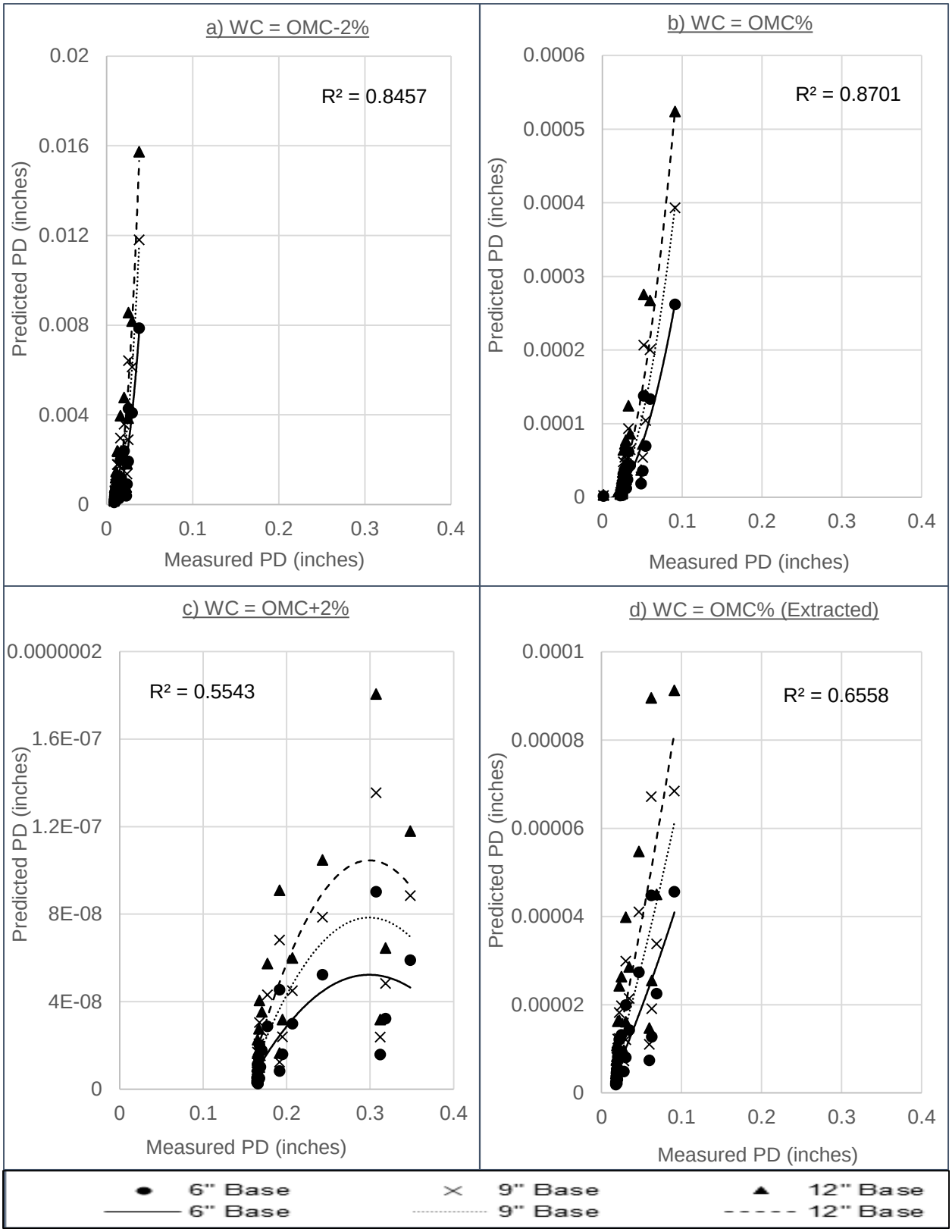

Figure 5.4. Measured versus Predicted PD for 100% RAP TH 10

Then, it can be concluded from the resilient modulus test, that the PD-MEPDG model is found highly significant in two cases only: 50% and 100% RAP at OMC-2% as predicted values are so close to those measured. However, the predicted values for the other RAP contents are significantly less than those measured at different water contents. These results are expect to be related to the stress history of resilient modulus test procedure used for collecting PD data.

To assure the results collected for the main RAP source (TH 10), other RAP sources are analyzed in this stage using the same M_R testing procedure and same testing conditions. First, the study begins with the 50% field RAP sources: TH19-101, TH 19-104 and TH 22. For RAP TH 19-101, as shown in Figure 5.5, similar relation is found as RAP TH 10 for the three studied water content levels. Still the predicted PD values are much less than measured ones. Nevertheless, the correlation trend at this case is higher as R^2 values vary between 0.75 to 0.92 for OMC+2% and OMC%, respectively. For RAP TH 19-104, as shown in Figure 5.6, the same trend is found for both RAP's TH 10 and TH 19-101. For the three water content levels, the predicted PD values are far away from the measured ones and the correlation is worse than before as R^2 values are 0.49, 0.64 and 0.55 for OMC-2%, OMC% and OMC+2%, respectively.

For RAP TH 22, as shown in Figure 5.7, the trend is almost the same as RAP TH 10. The predicted values are close to those measured at OMC-2% (Figure 5.7-a) and far away in the other two water content levels. Expectedly, this behavior is similar to TH 10 and PD measured values for both RAP's are so close to each other without a significant difference in M_R values too, especially at OMC-2%. Finally, from comparing the fourth 100% RAP source (Cell 18), as shown in Figure 5.8, the same trend exists as the other field RAP sources TH 19-101 and TH 19-104. The predicted PD values are much less than the measured ones with reasonable R^2 values of 0.54, 0.83 and 0.91 at OMC-2%, OMC% and OMC+2%, respectively.

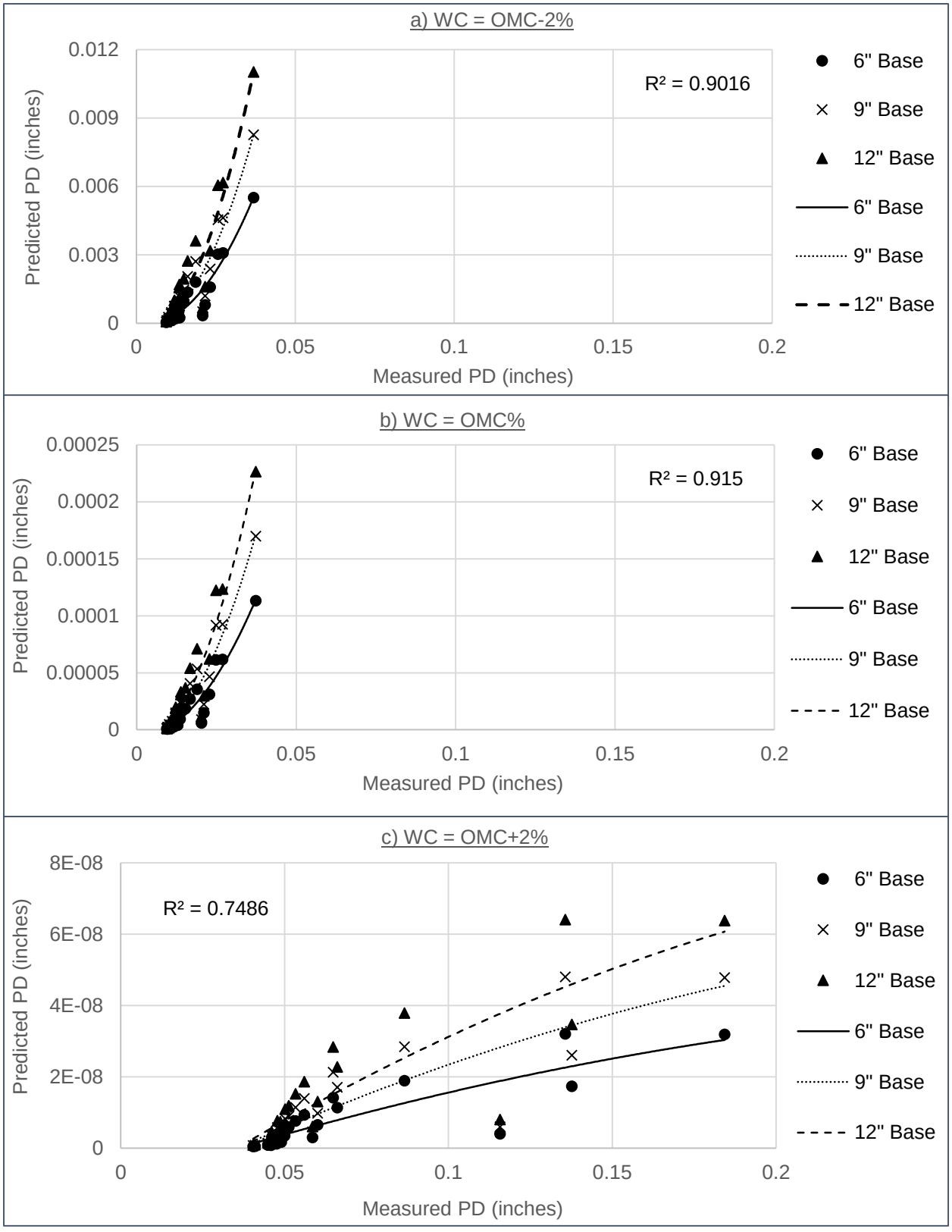

Figure 5.5. Measured versus Predicted PD for RAP TH 19-101

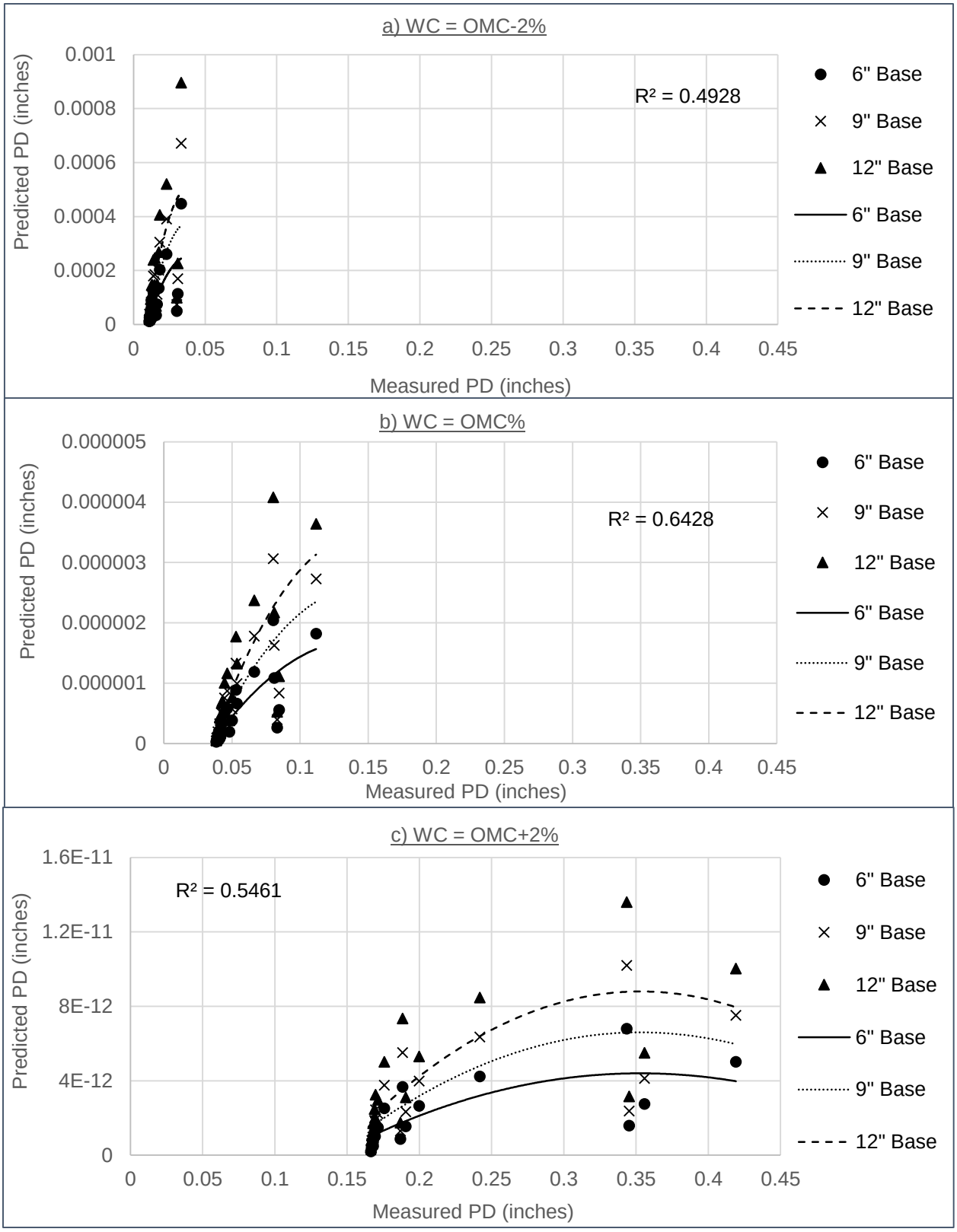

Figure 5.6. Measured versus Predicted PD for RAP TH 19-104

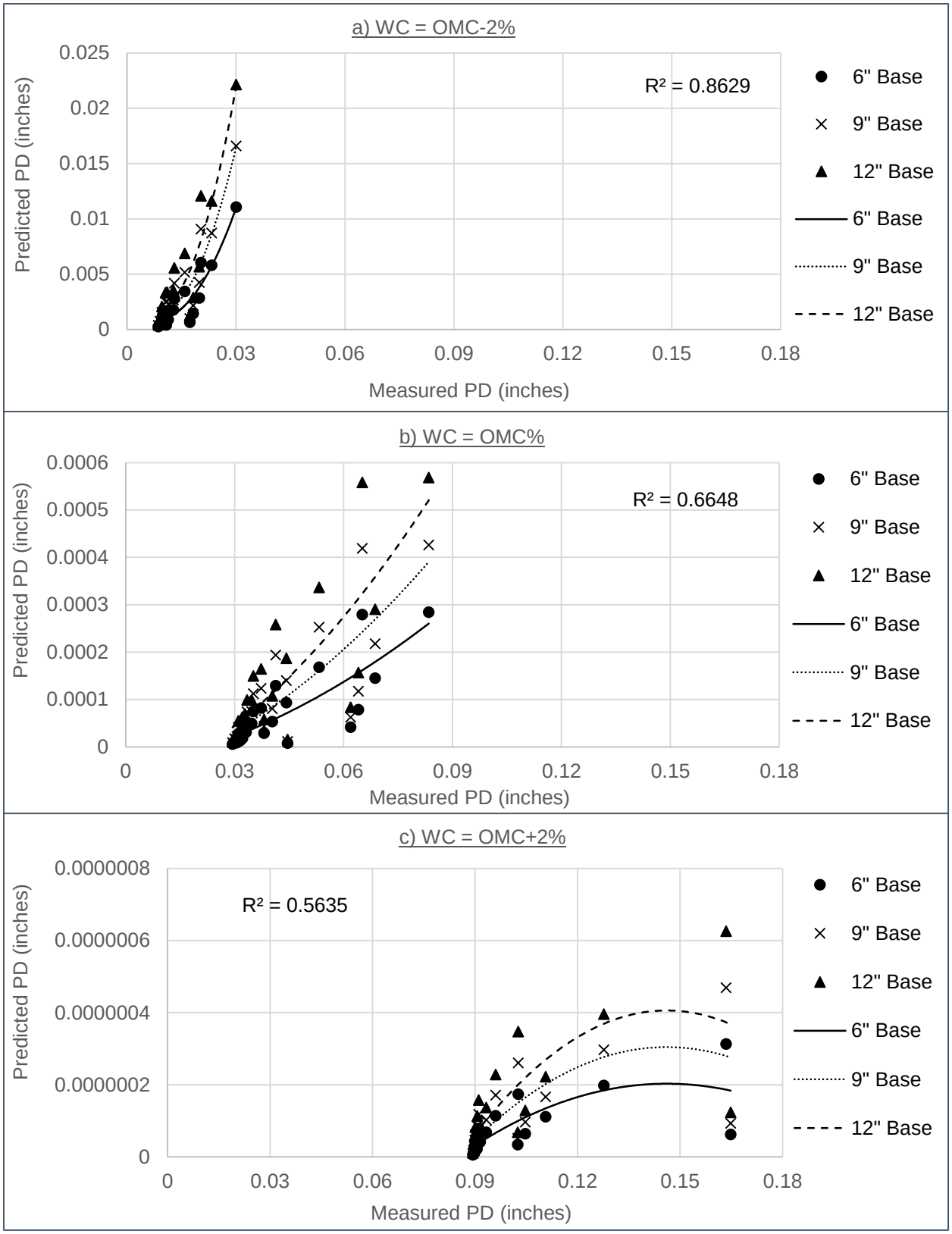

Figure 5.7. Measured versus Predicted PD for RAP TH 22

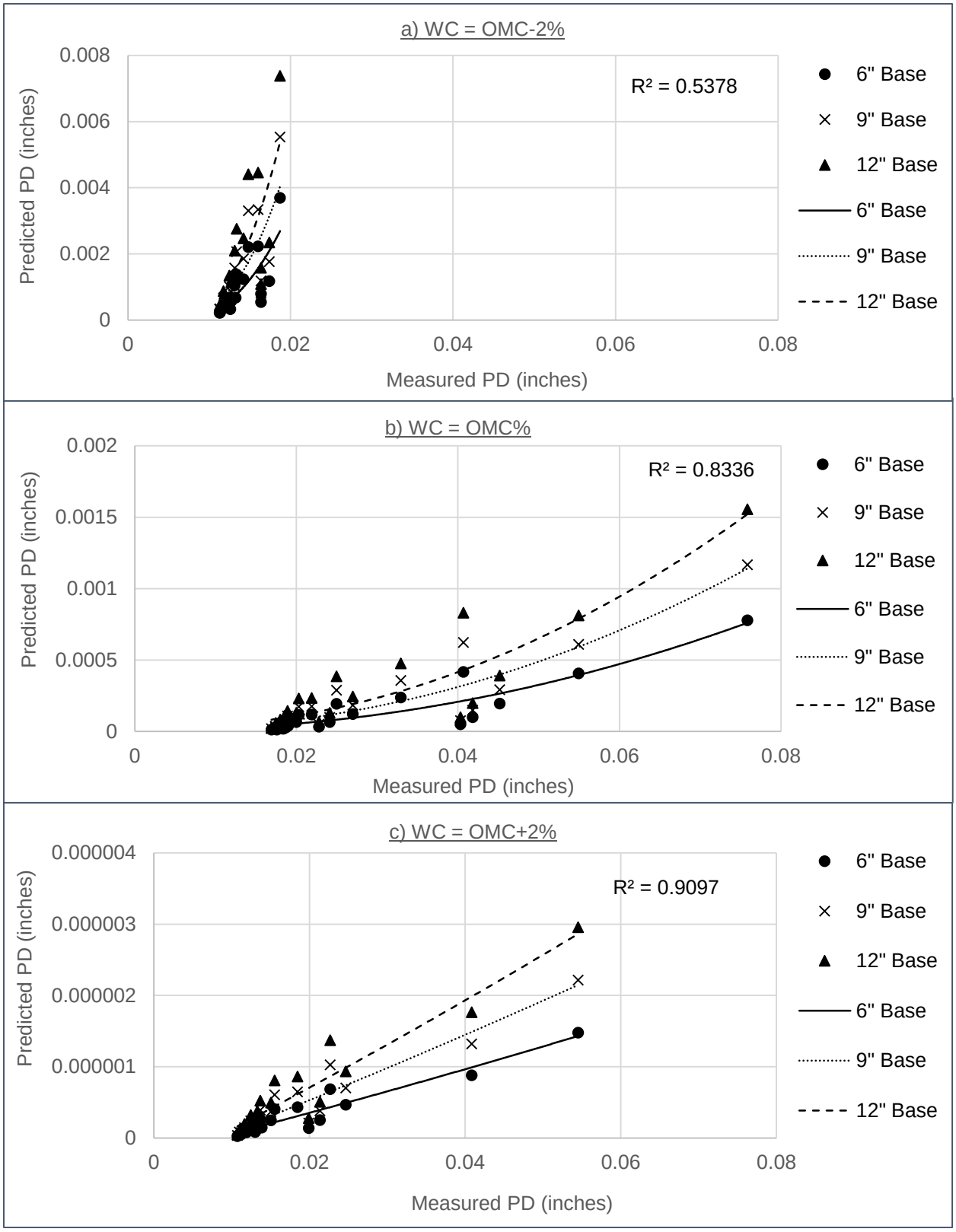

Figure 5.8. Measured versus Predicted PD for Cell 18

Therefore, all of the field RAP sources studied using the PD data collected from M_R test in this stage have the same insignificant prediction trend of RAP TH 10 with more similarity with RAP TH 22. Generally, the PD predicted values are much lower than the measured values at different testing conditions such as RAP content and water content level. This result is due to the low load repetitions (100 cycles) applied in each sequence and the effect of stress history from successive sequences of loading. Both RAP's TH 10 and TH 22, are the only sources that give a significant prediction but at OMC-2% water content only. The RAP content for both RAP sources is 50% mixed with another 50% traditional granular aggregate sources. Regression analysis from comparing predicted and measured PD values gives high correlation. However, it does not give an accurate prediction of PD as M_R test proved that it cannot be used in measuring PD during the 30 sequences of loading of the test due to the stress history.

5.4.2. Single-stage RTL test

In this stage, a single-stage repeated tri-axial loading (RTL) test procedure is followed. This test is the typical or standard technique used to measure permanent deformation for granular base layer. This test procedure can measure the PD accumulated in the sample after high number of load repetitions (20,000 or more) expected from traffic loads. The multi-stage test is another type of this RTL technique. However, the single-stage test has the advantage of not including the effect of the stress history of previous stages. Therefore, it is expected to find accurate prediction of PD values when using this model for single-stage RTL test data.

In Figure 5.9, prediction of PD is achieved on Class 5 aggregates before adding RAP. A comparison is made between measured and predicted PD. This comparison is achieved at two water content levels; OMC% & OMC+2% and two levels of deviator stress (σ_d); 17 & 24 psi for OMC% content and 12 & 17 psi for OMC+2% content. As shown in Figure (5.9-a), the PD

predicted values are very accurate and close to the measured ones. However, by increasing the deviator stress level to 24 psi (Figure 5.9-b), the accuracy becomes weaker, as the predicted values are lower than those measured. By increasing the water content level at both deviator stress levels (12 and 17 psi), the prediction accuracy is still weak. But, from the high regression parameter R^2 for all testing conditions for this Class 5 aggregates, the MEPDG model is still quietly efficient for PD prediction.

Both Figures 5.10 and 5.11, show the comparison between predicted and measured PD values for 50% RAP TH10 blends with Class 5 at OMC% and OMC+2%, respectively. At OMC% (Figure 5.10), the comparison is achieved at three deviator stress levels; 17, 24 and 37 psi. At both deviator stress levels 17 and 37 psi, the prediction accuracy is relatively high as the PD predicted values are too close to the measured ones. However, the accuracy decreased slightly for the 24 psi deviator stress level. But for this case, the predicted values are higher than the measured ones. At OMC+2% (Figure 5.11), the comparison is achieved at two deviator stress levels; 12 and 17 psi. The prediction accuracy decreases significantly especially at 17 psi. Generally, the PD prediction accuracy for the 50% RAP TH10 blend is significantly high and even better than the previous case for Class 5 aggregates tested with the same procedure single-stage RTL test.

The same comparison of 50% RAP is repeated again in Figure 5.12 but with the addition of 6% fines. This percent of fines is selected to reach 10% (maximum allowable fine content for base layer) to investigate its effectiveness on the PD accumulated. The comparison is achieved at two deviator stress levels 17 & 24 psi for OMC% and 12 & 17 psi for OMC+2%. Results indicate that addition of fines increase PD values. The prediction for these samples decrease slightly especially at OMC+2%. Generally, the prediction is under-estimating the PD values. Contrary, the predicted values are over-estimated at OMC% with the 17 psi deviator stress.

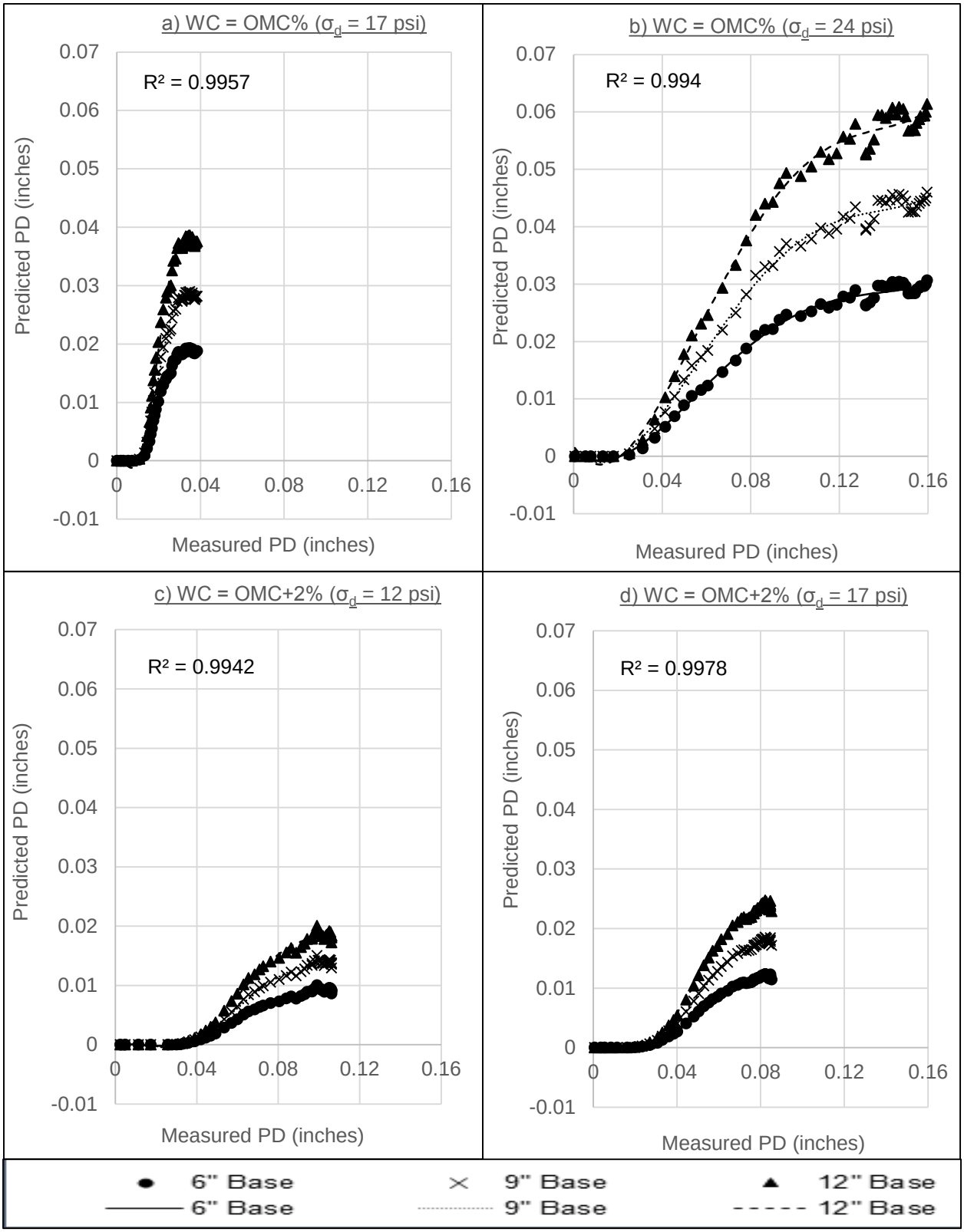

Figure 5.9. Measured versus Predicted PD of Single-stage RTL for Class 5

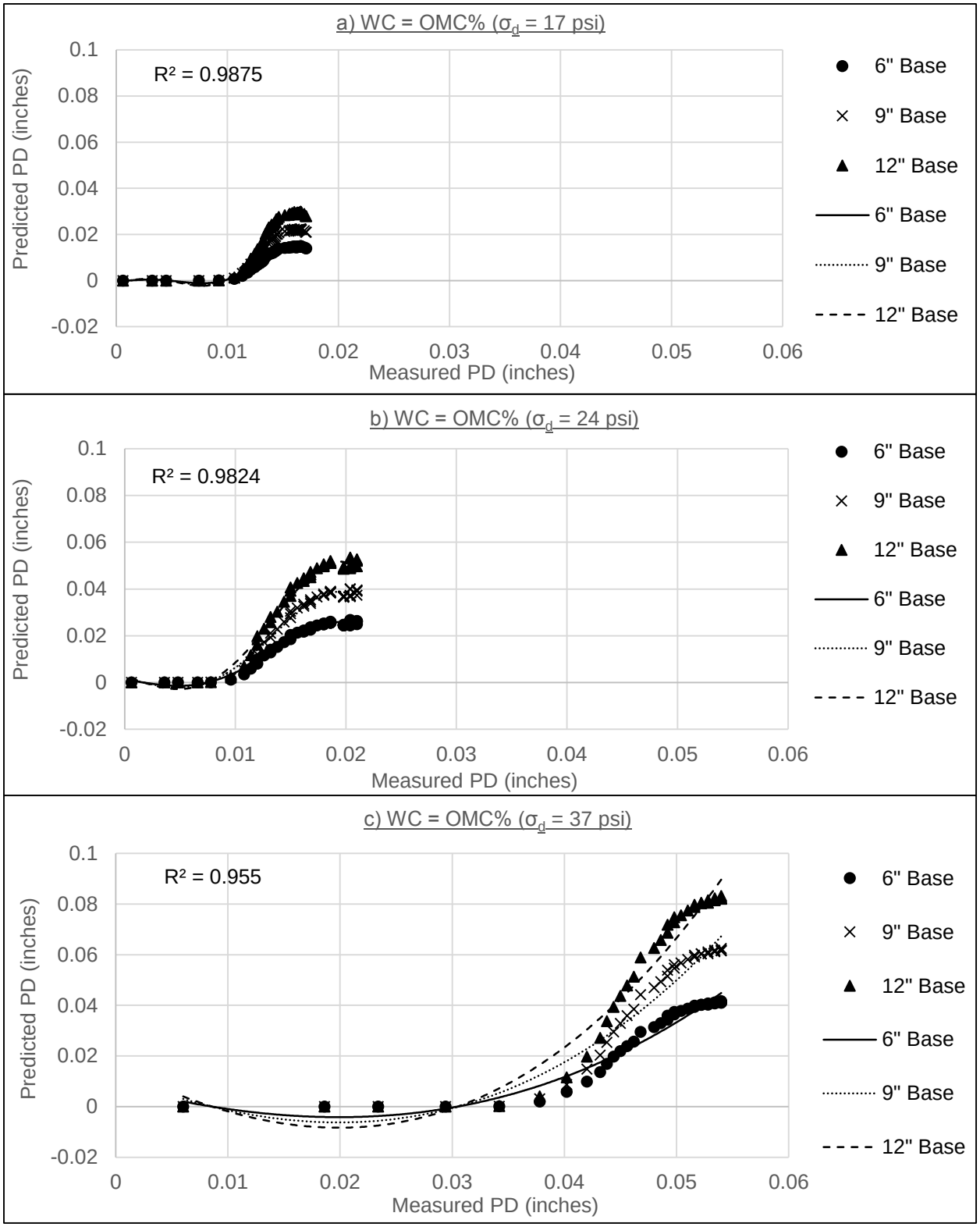

Figure 5.10. Measured versus Predicted PD of Single-stage RTL for 50% RAP TH 10 + 50% Class 5 at OMC%

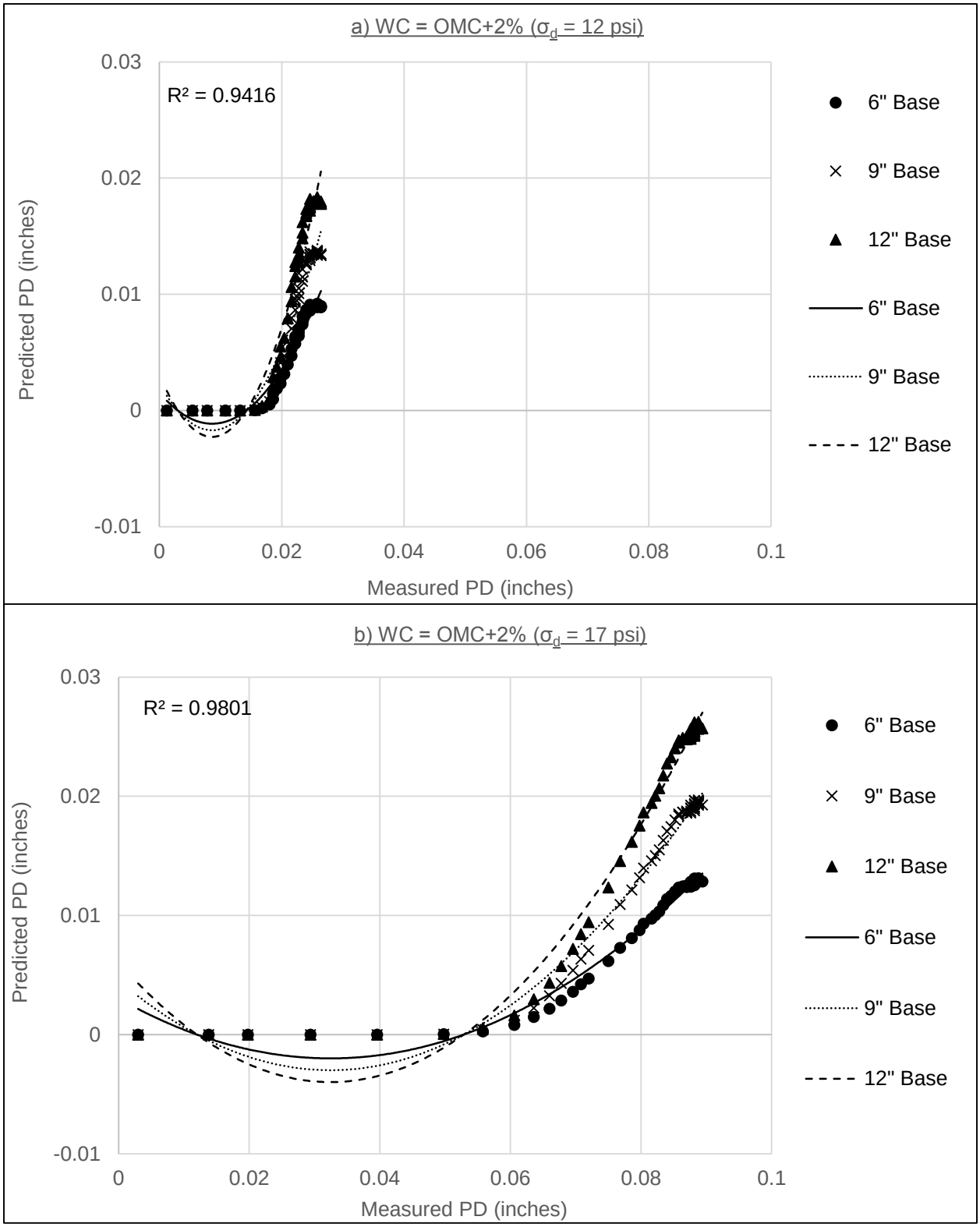

Figure 5.11. Measured versus Predicted PD of Single-stage RTL for 50% RAP TH 10 + 50% Class 5 at OMC+2%

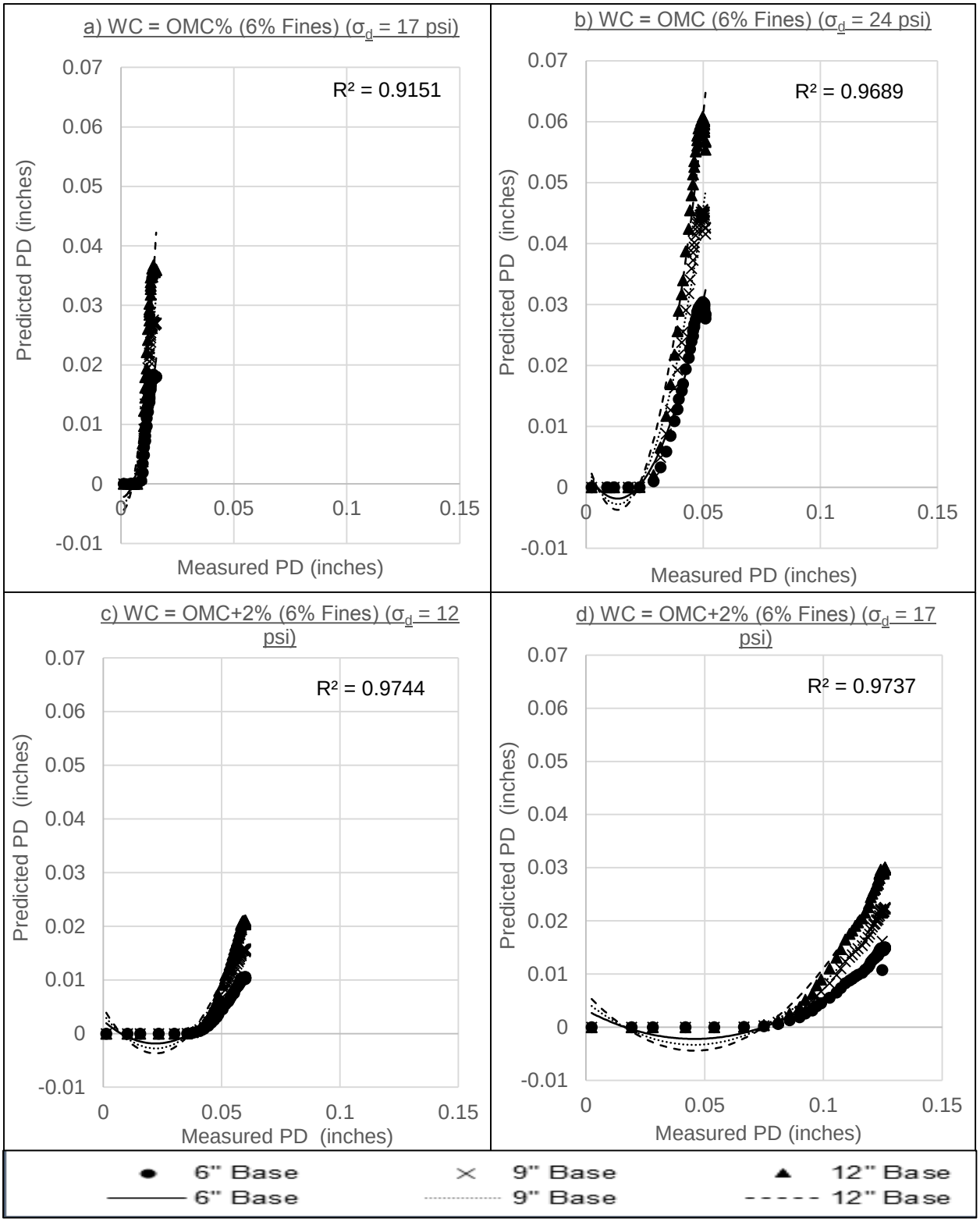

Figure 5.12. Measured versus Predicted PD of Single-stage RTL for 50% RAP TH 10 + 50% Class 5 with 6% Added Fines

Finally, the PD-MEPDG model seems better than the resilient modulus test in terms of predicting PD for data collected from single-stage RTL test. It is highly significant for the case of using RAP in base layer blends as shown in 50% RAP samples. However, there is a need to achieve this model on test data collected from multi-stage RTL for RAP samples used as a base layer taking in consideration the effect of stress history as M_R test. This high accurate prediction is found also for Class 5 granular aggregate in OMC% at 17 psi deviator stress level. Best results of the high accuracy of the PD prediction is shown in 50% RAP blend at OMC% water content level under 17 and 37 psi deviator stress levels. By adding 6% fines to the 50% RAP blend, the prediction accuracy is affected significantly. As the prediction under-estimates the PD values except at OMC% under 17 psi deviator stress level it is overestimated.

5.4.3. Multi-stage RTL test

In this stage, a comparison also is made between measured and predicted PD values for data collected from multi-stage RTL test. This test is more reflecting the field situation by applying different deviator stresses for each stage of loading for 5000 loading cycles. Nevertheless, it has the same problem of stress history as M_R test coming from the previous loading stages. This comparison is achieved at three water contents: OMC-2%, OMC% and OMC+2% for Class 5, 50% RAP TH 10 + 50% Class 5 and 50% RAP case with 3.5% high plasticity clay fines. This fine content and type are chosen to avoid the problem of PD increase, while at the same time gains the advantage of M_R increase. From the comparison in Class 5, as shown in Figure 5.13, for all water content levels, the measured PD values are much higher than the predicted PD values at all deviator stress levels. However, all R^2 values are high exceeding 0.9 and approaching to 1 as shown in Table 5.1. This model is not accurate in predicting PD values for granular base layer for measured data from multi-stage RTL test.

Table 5.1. R^2 for Multi-Stage RTL Test

Material	W.C%	Deviator Stress (psi)							
		6	12	17	24	37	53	63	73
Class 5	OMC-2%	0.94	0.97	0.98	0.98	NA	NA	NA	NA
	OMC%	NA	NA	0.97	0.98	0.99	NA	NA	NA
	OMC+2%	0.96	0.98	0.98	0.99	NA	NA	NA	NA
50% RAP + 50% Class 5	OMC-2%	NA	NA	0.96	0.97	0.99	1	0.99	0.85
	OMC%	NA	NA	NA	0.98	0.99	0.99	0.99	NA
	OMC+2%	0.97	0.99	0.99	0.99	0.99	0.99	NA	NA
50% RAP +50% Class 5 (3.5% fines)	OMC-2%	NA	NA	0.95	0.98	0.95	0.98	0.96	0.92
	OMC%	NA	NA	0.84	0.90	0.97	0.99	1	0.92
	OMC+2%	0.91	0.98	0.99	0.97	0.98	NA	NA	NA

For 50% RAP case, as shown in Figure 5.14, the difference between the predicted and measured PD values become lower especially at the OMC-2% case (Figure 5.14-a). By increasing the water content to OMC% and OMC+2%, the difference increases significantly and predicted PD values become much smaller than the measured values, opposite to the trend of OMC-2%. Adding RAP to the base layer blend shows better prediction for PD than Class 5 aggregates. Still the model seems to be un-significant in predicting PD for data collected from multi-stage RTL test. Adding 3.5% plastic fines significantly decreases the measured PD values, as shown in Figure 5.15, for all three levels of water contents.

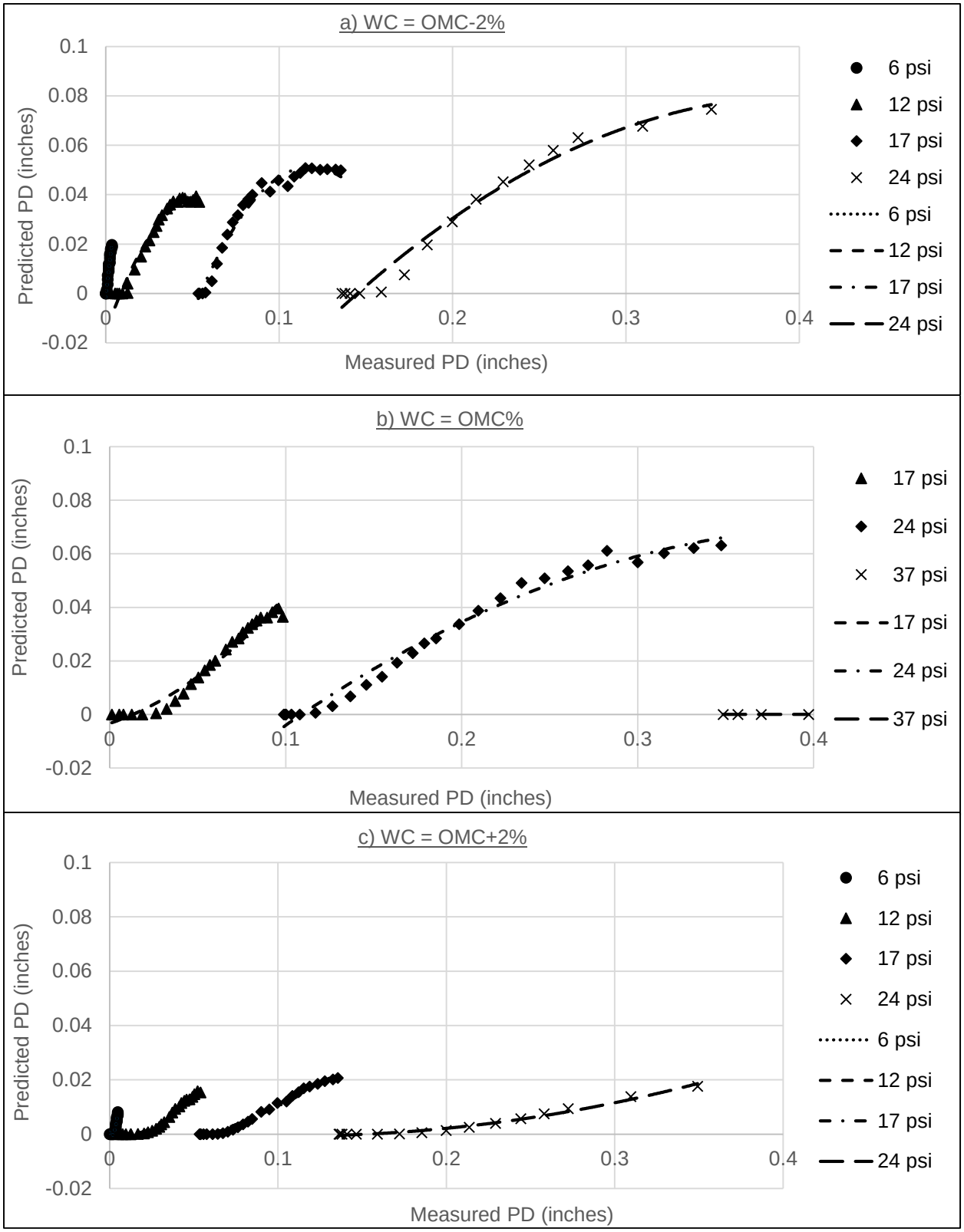

Figure 5.13. Measured versus Predicted PD of Multi-stage RTL for Class 5

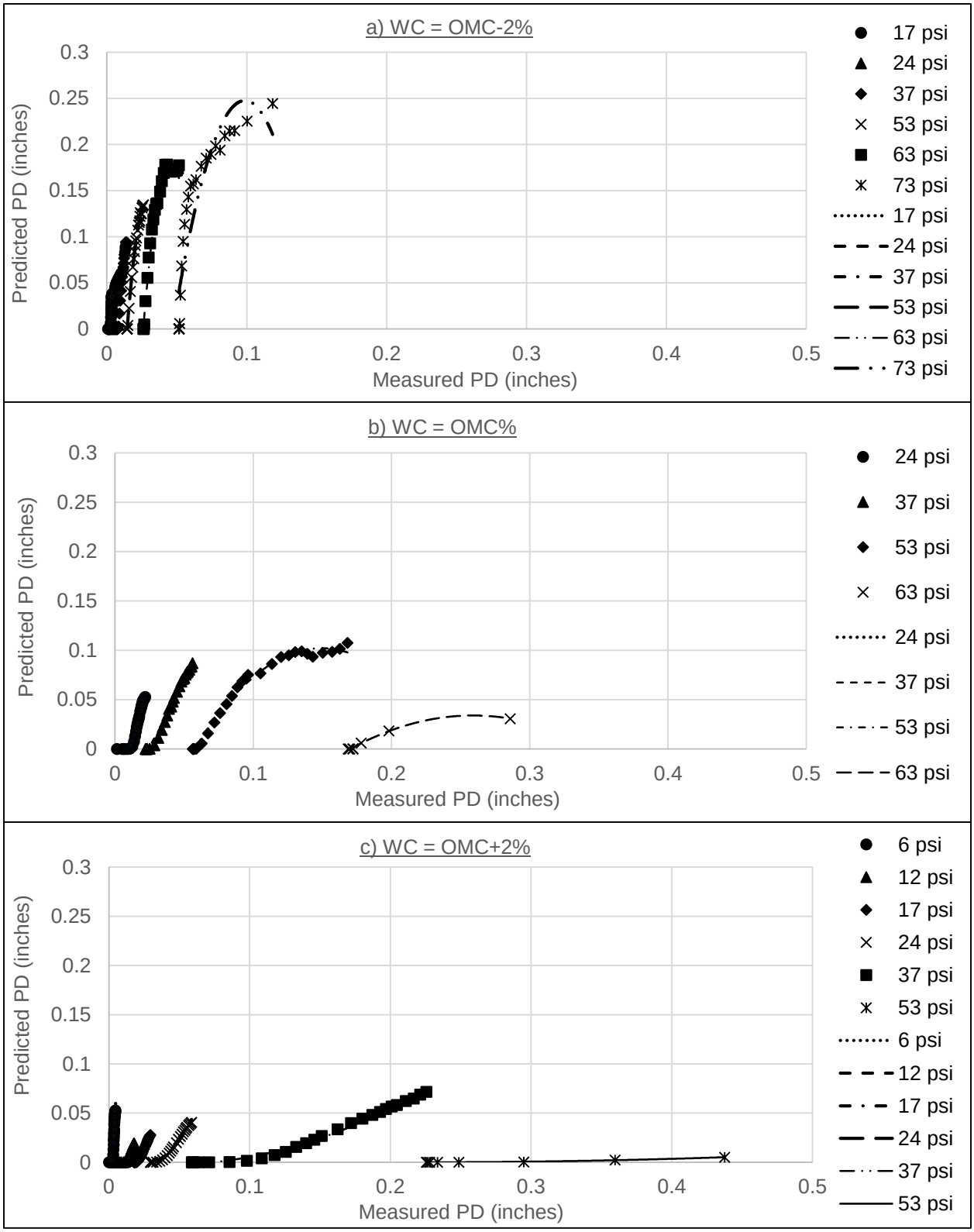

Figure 5.14. Measured versus Predicted PD of Multi-stage RTL for 50% RAP TH 10 + 50% Class 5

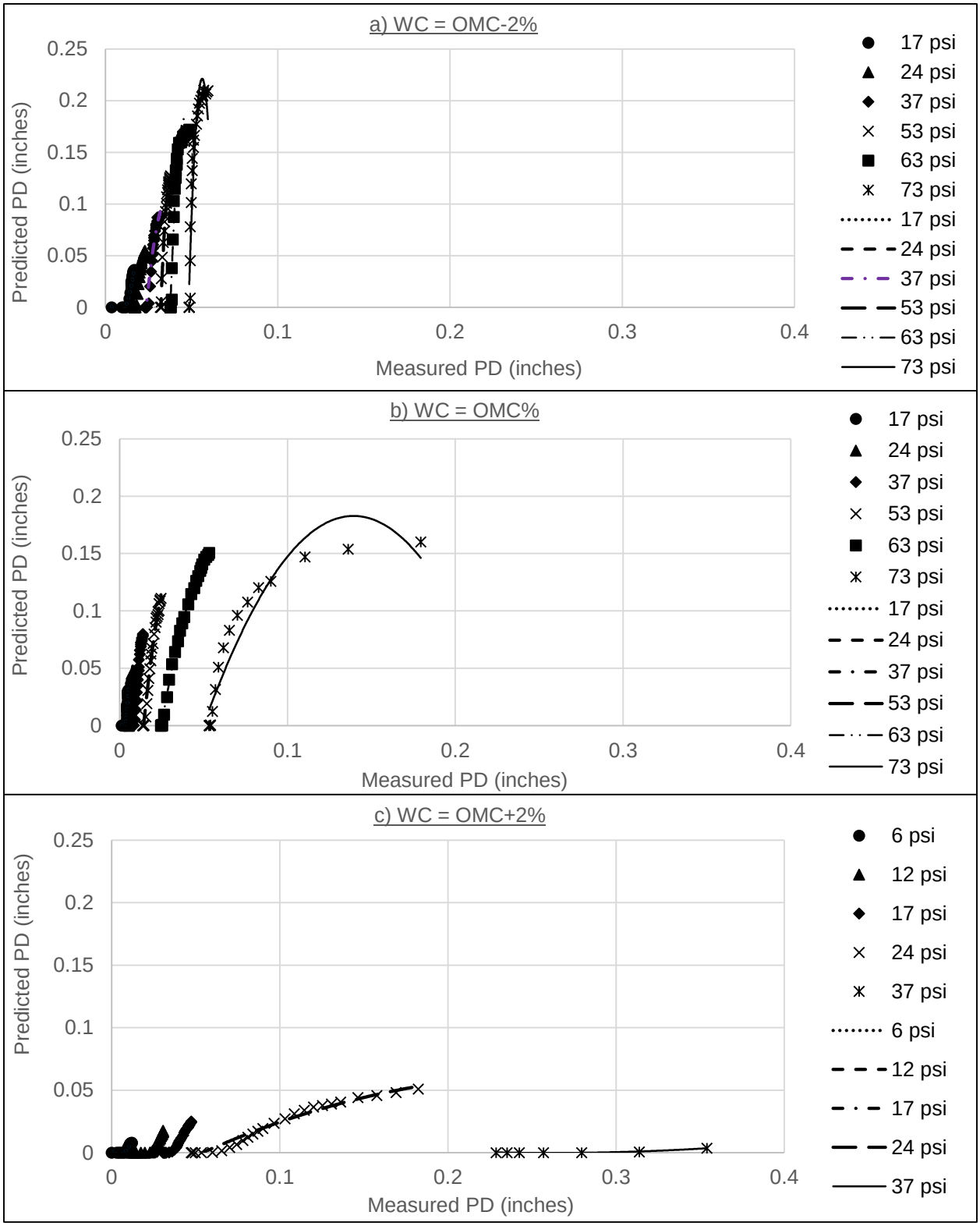

Figure 5.15. Measured versus Predicted PD of Multi-stage RTL for 50% RAP TH 10 + 50% Class 5 with 3.5% Added Fines

This result is expected from the literature survey results on the effect of adding clay on PD for base layer in general. In addition, the predicted PD values become too close to the measured ones only in the OMC% case. Nevertheless, by changing the water contents to the other two levels OMC-2% and OMC%, the difference between predicted and measured PD values significantly increases. In the OMC-2%, the model is over-estimating PD significantly, while in OMC+2% the model is underestimating the PD significantly.

Finally, it is obvious that PD-MEPDG model is significant in prediction for the measured PD data by single-stage RTL test only while very un-significant for the other two tests, M_R and multi-stage RTL tests. This finding is attributed to the effect of the stress history from applying successive stages of loading on base layer blends in both tests. The model is highly accurate for single-stage RTL test at water contents close to OMC% and at deviator stresses lower than 24 psi.

5.5. PD Modeling Task Summary

Several points are concluded from prediction of permanent deformation for RAP using the rutting MEPDG for the two measured laboratory data sets included in this task. It can be concluded from the resilient modulus test, that the PD-MEPDG model is found highly significant in two cases only: 50% and 100% RAP at OMC-2% as predicted values are so close to those measured. However, the predicted values for the other RAP contents are significantly less than those measured at different water contents. These results are expect to be related to the stress history of resilient modulus test procedure used for collecting PD data. All of the field RAP sources studied using the PD data collected from M_R test in this task have the same insignificant prediction trend of RAP TH 10 with more similarity with RAP TH 22. Generally, the PD predicted values are much lower than the measured values at different testing conditions such as RAP content and water content level. This result is due to the low load repetitions (100 cycles) applied in each sequence

and the effect of stress history from successive sequences of loading. Both RAP's TH 10 and TH 22, are the only sources that give a significant prediction but at OMC-2% water content only. The RAP content for both RAP sources is 50% mixed with another 50% traditional granular aggregate sources. Regression analysis from comparing predicted and measured PD values gives high correlation. However, it does not give an accurate prediction of PD.

For the single-stage RTL testing, the PD-MEPDG model seems better than the resilient modulus test in terms of predicting PD for data collected from single-stage RTL test. It is highly significant for the case of using RAP in base layer blends as shown in 50% RAP samples. However, same insignificance is found for this model on test data collected from multi-stage RTL for RAP samples used as a base layer due to the effect of stress history as M_R test. This high accurate prediction is found also for Class 5 granular aggregate in OMC% at 17 psi deviator stress level. Best results of the high accuracy of the PD prediction is shown in 50% RAP blend at OMC% water content level under 17 and 37 psi deviator stress levels. By adding 6% fines to the 50% RAP blend, the prediction accuracy is affected significantly. As the prediction under-estimates the PD values except at OMC% under 17 psi deviator stress level it is overestimated.

Finally, it is found from this task that the PD-MEPDG model is statistically significant in prediction PD compared to the measured PD values from the single-stage RTL test especially at OMC% condition with different stress levels. While the predicted PD values are much below the corresponding measured PD values from the resilient modulus and multi-stage RTL tests due to the effect of stress history from subsequent sequences or stages of loading.

CHAPTER 6. CORRELTION OF RESILIENT MODULUS AND PERMANENT DEFORMATION

6.1. Introduction

Previous researches summarized in the literature survey on RAP used as a base layer concluded that no exact optimum content of RAP to be in the granular blend. The previous results showed that increasing RAP content in granular layer blends, leads to increased M_R values. However PD results were different. Both parameters M_R and PD, are very important in the design process of the base layer and choosing the optimum RAP content. M_R is the responsible parameter of estimating the stiffness of the base layer blend under repetitive loads. The PD represents the accumulation of the permanent strain that happens in the base layer and participates in the rutting distress that will occur in the top asphalt layer.

Therefore, there is a need to correlate between both parameters under the most expected field conditions that could happen for base layer. Previous studies concluded that the state of stresses is the most effective parameter on the strength of the base layer. The moisture content variation was the second main effective parameter. In addition, this M_R-PD correlation was never studied before assuming M_R as the response of base layer blend and PD as an effective parameter on M_R values under the variation of different testing conditions. Therefore, correlating between these two parameters is highly required to study RAP behavior in base layer. The study focuses on the effect of main parameters on M_R, including accumulated permanent deformation after several load cycles responsible of rutting of the whole pavement section.

6.2. Correlation Approach

This task focuses on studying M_R-PD relationship for different sources of RAP used as a base layer under the variable confining pressure, moisture content and RAP contents. The

confining pressure is the most effective state of stresses on the structural behavior of the base layer. Firstly, this relation is important to be investigate in terms of how the PD affects M_R values under the variable testing conditions mentioned above. In addition, this task shall indicate whether a typical relation for the M_R-PD behavior is understood or not for the RAP in base layer. Secondly, this task aims at deciding the optimum RAP content, which has the highest M_R values with acceptable PD percentage not causing rutting in the future. Finally, it is important to recommend if the PD can be used as an effective parameter in M_R modeling or not. This approach is followed in the mechanistic empirical pavement design guide (MEPDG) (Guide, 2008). As the resilient strain is used as an effective parameter in PD modeling for granular base layer, while the permanent strain is not used in M_R modeling for the same layer.

6.3. Stages of Work

The first stage of this task is concerned with PD accumulated from the resilient modulus determination test. The PD is calculated as a percentage of the accumulated permanent strain from the total strain for the sample tested during M_R determination. Almost all other previous studies, measure PD by performing the repeated tri-axial loading (RTL) test either single or multiple stage as a separate test. However, this test was found very time consuming to cover all data previously measured for M_R through the project with MN/DOT (M. Attia et al., 2009). Firstly, the comparison between M_R and PD is achieved on the main RAP source (TH 10). The comparison is achieved at three levels of water content varying from optimum moisture content (OMC %); OMC-2%, OMC% and OMC+2%. This comparison comprised different levels of confining pressure which is well-known before as the most effective parameter on M_R. Each point on the same graph has a different percent of RAP (0, 50, 75 and 100%) in the blend with MN/DOT Class 5 granular aggregates. This aggregates type is used traditionally before as unbound granular base layer. The

comparison for this RAP source is divided into two steps. The first is under same confining pressure level (Figure 6.1) and the second under the same RAP content (Figure 6.2). Therefore, each factor is individually studied for each moisture content. For each condition in both steps, there is a best-fit regression to compare R^2 values.

It is important to achieve the comparison between M_R and PD on different RAP sources to take into consideration the RAP variability factor, one of the main problems facing the reuse of RAP as a base layer. Therefore, the data of the other four different RAP sources tested in MN/DOT project (M. Attia et al., 2009) are collected for this research in addition to the main source TH 10. These RAP sources are analyzed under the same testing conditions discussed before. Three from those four RAP samples (TH 19-101, TH 19-104 and TH 22) are collected from the field containing 50% RAP and 50% granular aggregates, as shown in Figure 6.3.

The first number refers to the truck highway number in Minnesota and the second number refers to the mileage station in each road. The fourth RAP source consists of 100% RAP collected from Cell 18 (Minnesota Destination) as shown in Figure 6.4. All four RAP sources are compared with TH 10 (main RAP source) at the equivalent percentage, 50% RAP (Figure 6.3) or 100% (Figure 6.4). This approach is followed to avoid the problem of different gradations, which may have effect on both measured parameters M_R and PD. For both Figures 6.3 and 6.4, each point on the graph is for a different confining pressure level (3, 6, 10, 15 and 20 psi). Also, for each RAP in both figures there is a best-fit regression to compare between R^2 values.

In the second stage, the comparison is achieved on PD results collected from the single-stage RTL for Class 5 and 50% RAP TH 10 + 50% Class 5. The analysis of this stage is shown in two figures (6.5 and 6.6) with an emphasis on stabilizing the 50% RAP sample with adding plastic fines. Figure 6.5 is for both blends at OMC% and Figure 6.6 is for both blends at OMC+2%. In

the third and last stage of this task, M_R-PD comparison is achieved on PD values collected from multi-stage RTL for the same samples tested before in the previous stage. Figure 6.7 is for the Class 5 aggregates and Figure 6.8 is for 50% RAP TH 10 + 50% Class 5 blends and Figure 6.9 for 50% RAP blend with added fines. Therefore, finally the work performed in this task is divided into three main stages. The first stage is achieved on five different RAP sources collected and tested before in previous researches. On the other hand, both second and third stages are performed on the main RAP source TH 10 with its blends with MN/DOT Class 5 granular aggregates.

6.4. Analysis of Results

6.4.1 Resilient modulus test

Firstly, the comparison between M_R and PD is achieved on RAP TH 10, as shown in Figures 6.1 and 6.2. In Figure 6.1, the comparison is accomplished at different confining pressure levels and each point on the same graph has a different content of RAP (0, 50, 75 and 100%) in the blend with Class 5 aggregates. On the other hand in Figure 6.2, the comparison is performed at different RAP concentrations and the relation is reversed as each point on the same graph has a different confining pressure level (3, 6, 10, 15 and 20 psi). The regression values R^2 for both figures are shown in Table 6.1.

From Figure 6.1, there is an obvious relation that appears at OMC% (Figure 6.1-b), as M_R decreases by increasing PD until a certain point for all confining pressure levels, except at 20 psi which has the opposite relation. This certain point at 0% RAP blends for 3, 6, 10 and 15 confining pressure (C.P). However, for 20 psi the highest point at 100% RAP. This relation shows that as the percentage of RAP exceeds 50%, M_R increases and PD decreases, a result that may be recommended for base layer design considerations. Also, this relation works well on confining pressure levels less than 15 psi with highest correlation R^2.

By decreasing the moisture level to OMC-2% (Figure 6.1-a), as may be expected, M_R values generally increase and PD decrease. On the other hand, the typical relation found before at OMC% almost disappears from most of confining pressure levels except at 3 psi. In addition, PD increases when RAP content increases and M_R does not markedly increase after exceeding 75% RAP for all confining pressure levels, except for 20 psi. By increasing the moisture level to OMC+2% (Figure 6.1-c), generally M_R values decrease and PD increase approaching the failure limit 5% accumulated PD (M. I. E.-S. Attia, 2010), which is also expected. The typical relation for OMC% also disappears except at 6 psi confining pressure level with the highest correlation (R^2 = 0.71). But, the only exception at this moisture level is that the PD values at 75% RAP are higher than those at 50% and 100% RAP.

For the same data analyzed before in Figure 6.1, but at different RAP contents as in Figure 6.2, it is obvious at OMC% (Figure 6.2-b) that both 100% and extracted (without aged binder) RAP's have the highest M_R and lowest PD values with higher correlation to 100% RAP (R^2 = 0.92). The removal of aged binder affected M_R negatively and the effect on PD was minimal. For other RAP contents, M_R has lowest values at 3 and 6 psi, and increases with the increase of confining pressure levels with high contribution on PD at 20 psi. By decreasing the moisture level to OMC-2% (Figure 6.2-a), the relation is more clear with high correlation and close to the trend of 100% RAP at OMC%, M_R increases with increasing confining pressure levels and PD also increases. On the other hand, by increasing the moisture level to OMC+2% (Figure 6.2-c), the relation is not clear and the correlation is too weak. Both 50% and 100% RAP blends have the highest M_R and lowest PD values.

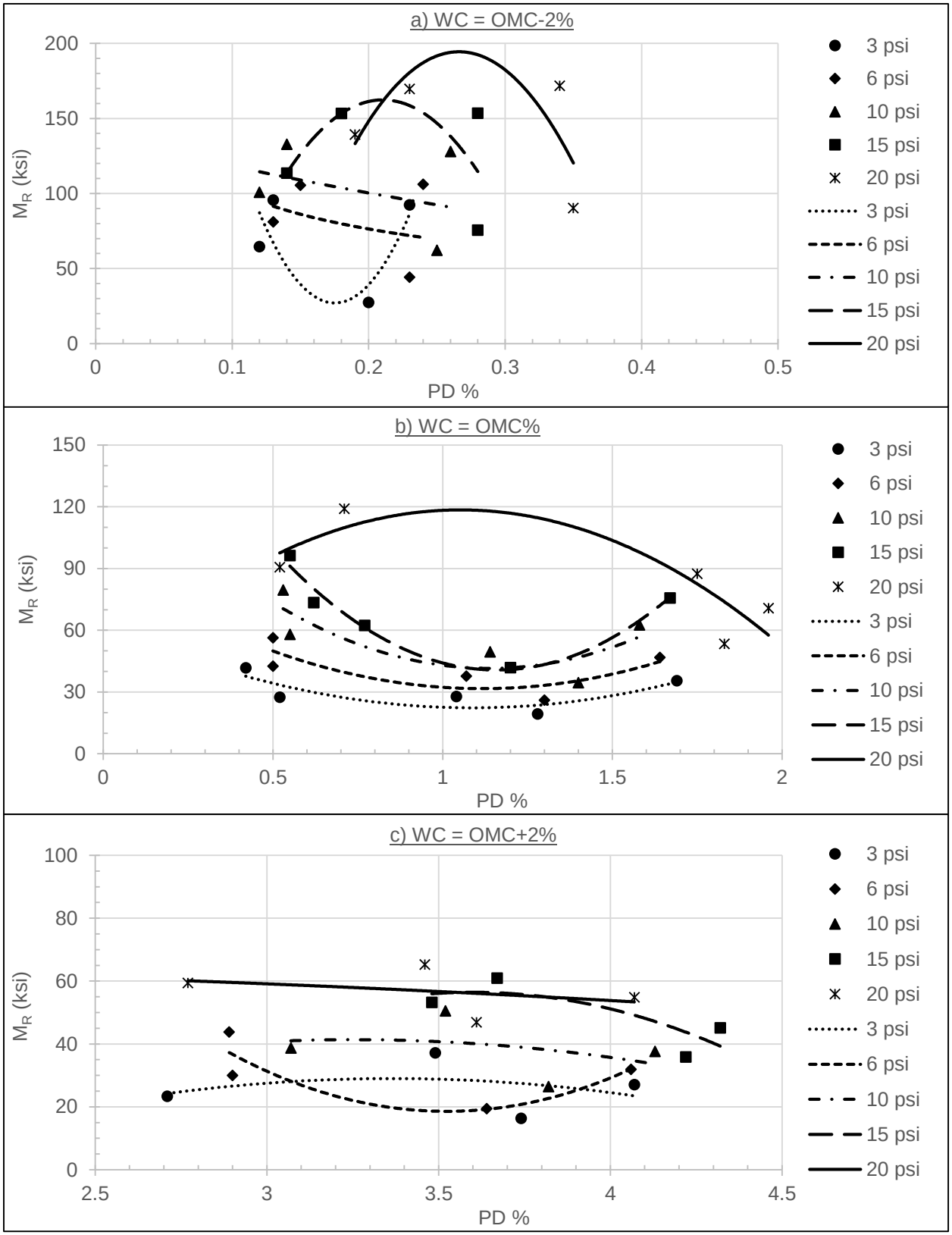

Figure 6.1. M_R versus PD for RAP TH 10 at Several Confining Pressure Levels

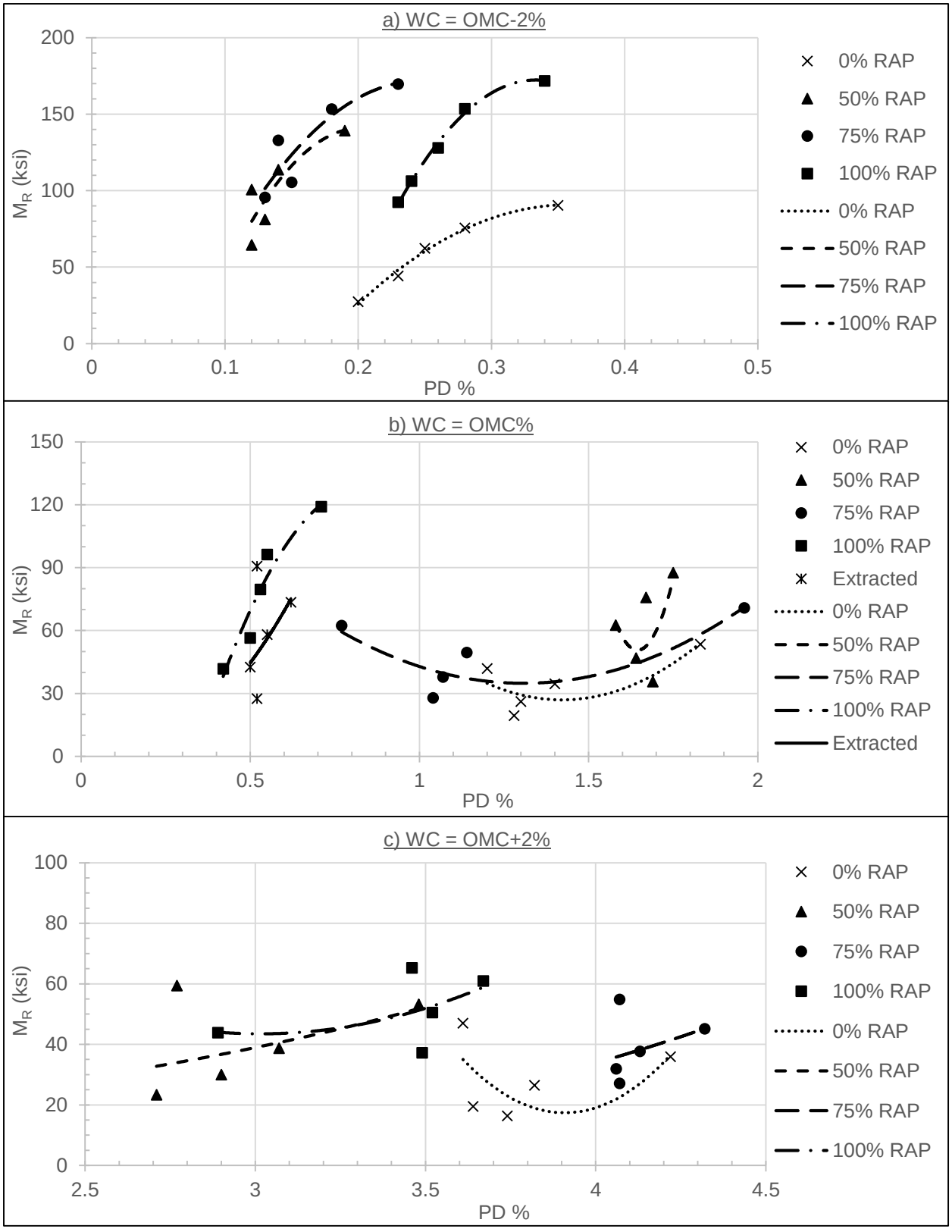

Figure 6.2. M_R versus PD for RAP TH 10 at Several RAP Percentages

Table 6.1. R^2 for M_R-PD Relation of Resilient Modulus Test for RAP TH 10

Water Content	Confining Pressure (psi) (*Figure 6.1*)				
	3	6	10	15	20
OMC-2%	0.5	0.1	0.12	0.27	0.48
OMC%	0.66	0.63	0.6	0.95	0.69
OMC+2%	0.09	0.71	0.12	0.64	0.13
Water Content	RAP Content % (*Figure 6.2*)				
	0%	50%	75%	100%	Extracted
OMC-2%	0.99	0.73	0.8	0.99	N/A
OMC%	0.67	0.43	0.73	0.92	0.19
OMC+2%	0.38	0.22	0.13	0.21	N/A

Other RAP sources are investigated to take into consideration the RAP variability and compare the trend of M_R-PD for RAP TH 10 with other sources tested at the same testing conditions: RAP content, water content and confining pressure levels. The comparison is completed first with 50% RAP sources, as shown in Figure 6.3. Then, it is achieved with other RAP 100% source, as shown in Figure 6.4. The regression parameter R^2 for both comparisons is shown in Table 6.2.

In (Figure 6.3-a) at OMC-2%, all other RAP sources have the same pattern as RAP TH 10 with high correlation, except RAP TH 19-104. RAP TH 10 has lowest PD with highest M_R values, as shown also for TH 22, better in terms of the base layer behavior. On the other hand, the trend of RAP TH 10 is different from other RAP sources at OMC% (Figure 6.3-b). This is because the comparison is made at 50% RAP TH 10, which is the same RAP content of the other RAP sources. However, if the comparison is made with 100% RAP TH 10, the trend is almost the same with a

little increase of M_R and PD values from RAP TH 19-101. The trend of 50% RAP TH 10 is found before in Figure 6.2 to be different than other RAP contents and has the lowest correlation, which may be related to the test accuracy for this sample. At OMC+2% (Figure 6.3-c) the trend of RAP TH 10 is so close to the trend of RAP TH 19-101 but RAP TH 10 has higher PD and lower correlation than RAP TH 19-101. Contrary, the other two RAP sources TH 19-104 and TH 22 have almost the same trend.

Then, a comparison is carried out between RAP TH 10 and Cell 18 at 100% RAP for both. The comparison shows that both RAP's almost have the same trend especially at OMC% (Figure 6.4-b) with high correlation for both. However, Cell 18 has much lower correlation at OMC-2% (Figure 6.4-b) and also RAP TH 10 at OMC+2% (Figure 6.4-c). Finally, for this stage all work done on PD accumulated from resilient modulus test for each sequence of loading after 100 load repetitions taking into consideration the effect of stress history for each sequence to the sequence after. The M_R-PD comparison here is taken under the effect of confining pressure levels, RAP contents and water content levels at low number of load repetitions (100 cycles). Therefore, it is essential to study the same comparison under higher number of load repetitions and different deviator stress levels, well-known as the most effective parameters on PD for base layer.

The results of this comparison for the five RAP sources collected can be concluded in this following points:

- From resilient modulus testing at OMC%, it is found that as the percentage of RAP TH 10 (the main RAP source) exceeds 50%, M_R increases and PD decreases. This result is recommended for base layer design considerations. This relation is more significant at confining pressure levels below 15 psi.

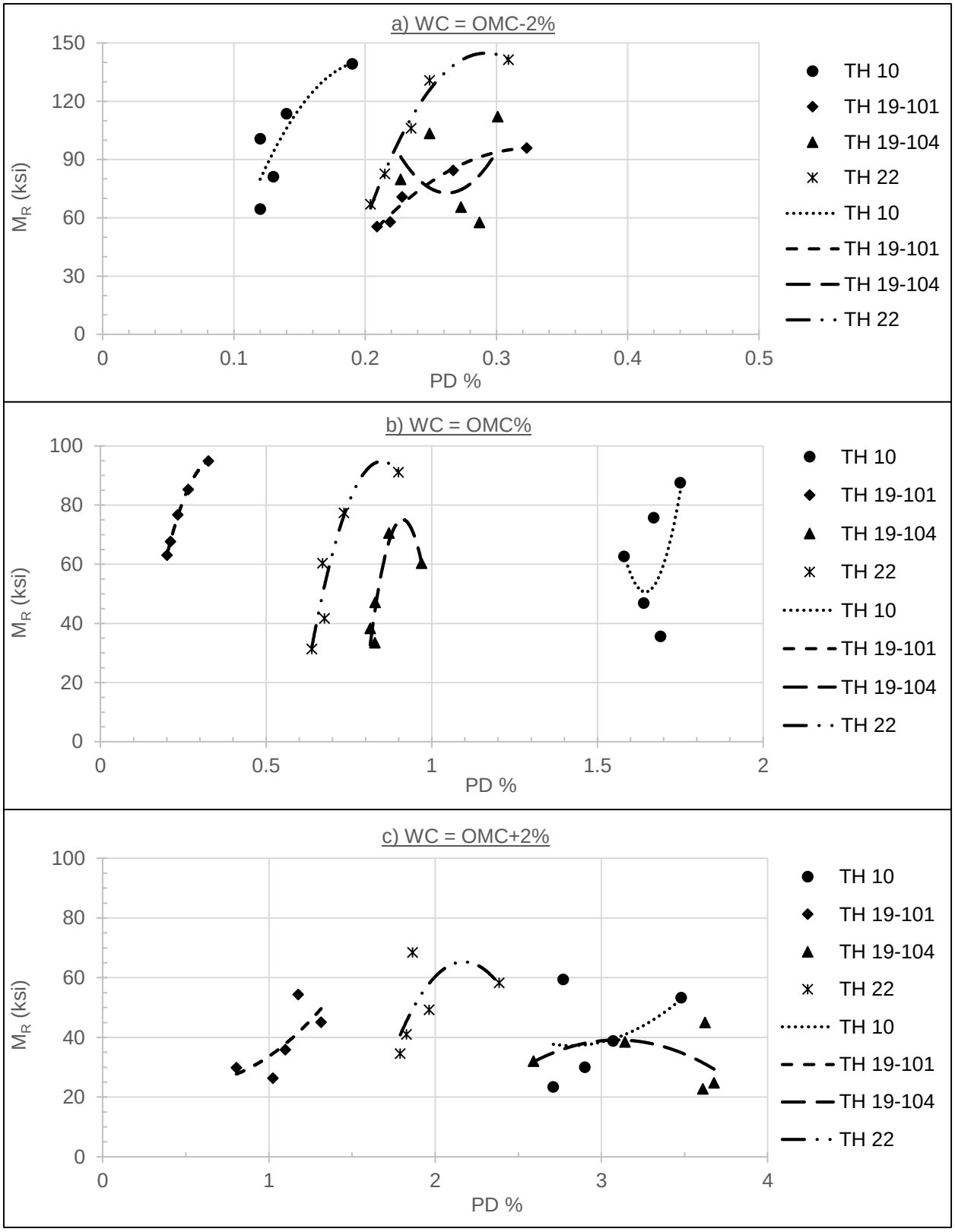

Figure 6.3. M_R versus PD for all RAP Sources at 50% RAP

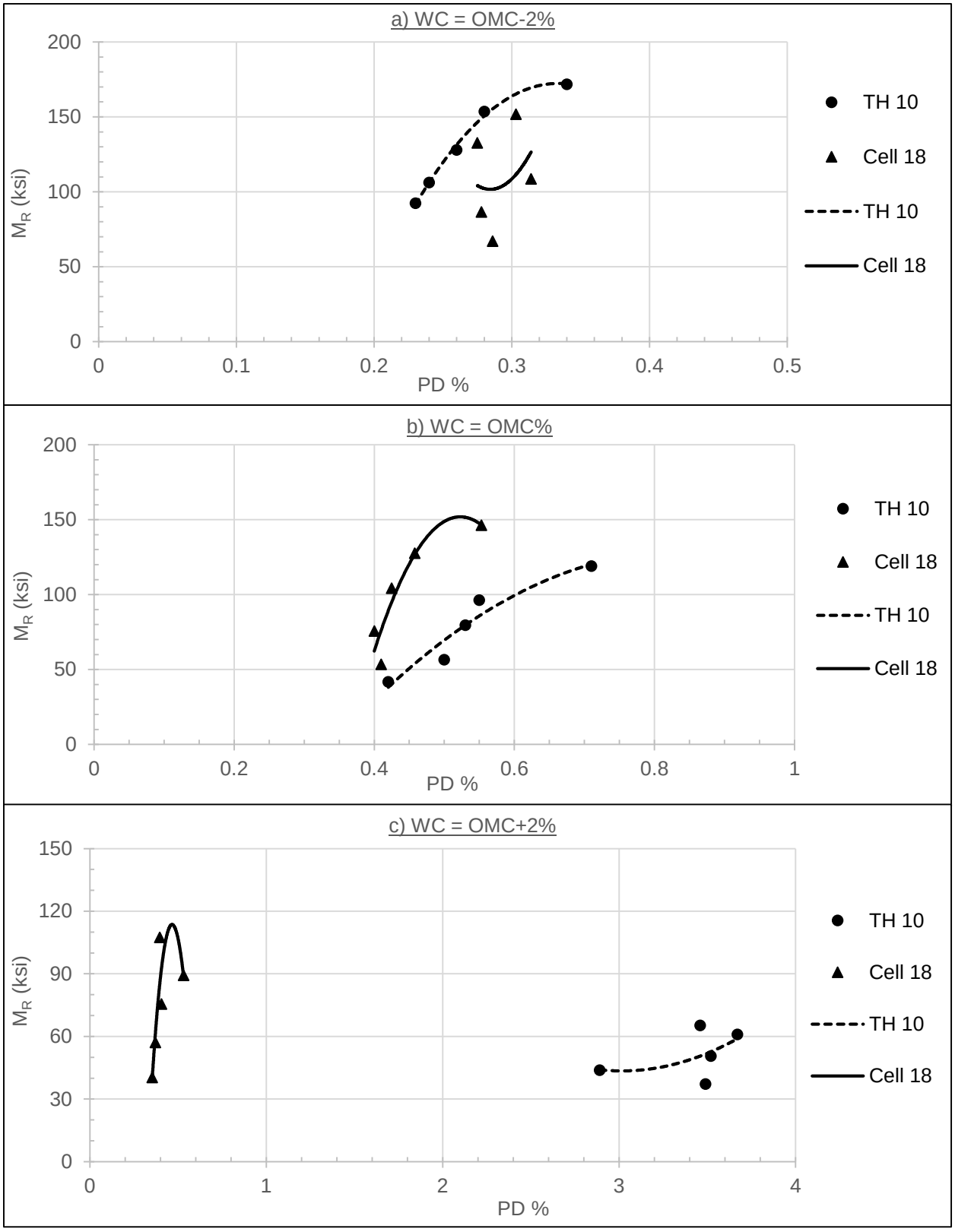

Figure 6.4. M_R versus PD for all RAP Sources at 100% RAP

Table 6.2. R^2 for M_R-PD Relation of Resilient Modulus Test for All RAP Sources

RAP Content%	Water Content	RAP Source				
		TH 10	TH 19-101	TH 19-104	TH 22	Cell 18
50% (*Fig. 6.3*)	OMC-2%	0.73	0.98	0.16	0.99	N/A
	OMC%	0.43	0.99	0.84	0.9	N/A
	OMC+2%	0.19	0.51	0.16	0.31	N/A
100% (*Fig. 6.4*)	OMC-2%	0.99	N/A	N/A	N/A	0.09
	OMC%	0.92	N/A	N/A	N/A	0.86
	OMC+2%	0.21	N/A	N/A	N/A	0.72

- For the same water content, both 100% and extracted RAP TH 10 have the highest M_R and the lowest PD with a small decrease in M_R values after extraction.
- The trend of RAP TH 10 is close to most of the other field RAP samples (TH 19-101, TH 19-104 and TH 22) with 50% content especially at OMC-2%. However, a little difference is found at OMC% when compared with same 50% content.
- The trend of 50% RAP TH 10 is found to be different from other RAP contents for the same source TH 10. This may be attributed to the test accuracy for this sample. However, the trend of 100% RAP TH 10 is too close to the other field RAP sources.
- In addition, the trend of RAP TH 10 is too close to the other 100% RAP source (Cell 18) especially at OMC%.
- The trend of all RAP sources at OMC+2% do not have a typical pattern and this is due to the high values of PD approaching to the 5% failure limit.

6.4.2. Single-stage RTL test

In this testing method, both parameters M_R and PD are measured during 5000 load repetitions. As load repetitions increases, both parameters increase, as shown in Figures 6.5 and 6.6. As deviator stress increases for both Class 5 and 50% RAP blends, PD increases without a significant difference in M_R values. It is very clear from comparing both Figures (6.5-a) and (6.5-b) that by adding 50% RAP, PD decreases and M_R increases. This finding is very useful for the base layer behavior.

From comparing both Figures (6.5-b) and (6.5-c), it is obvious that modifying the 50% RAP blend by adding 6% fines have a negative behavior on base layer characteristics. As for both levels of deviator stress 17 and 24 psi, M_R decreases and PD increases. This comparison is repeated but at OMC+2%, as shown in Figure 6.6. From Figure (6.6-a), it is obvious that as deviator stress increases from 12 to 17 psi, PD decreases without significant change in M_R contrary to the OMC% case. For the 50% RAP at OMC+2% (Figure 6.6-b), the increase of deviator stress increases the PD and negatively decreases M_R. From comparing both Figures (6.6-b) and (6.6-c), no significant difference is found after adding fines to the 50% RAP blend. However, there is a little decrease in M_R especially at the low deviator stress level of 12 psi.

In this testing method, both parameters M_R and PD were measured during 5000 load repetitions. As load repetitions increase, both parameters increase, as shown in Figures 6.5 and 6.6. It is obvious from Figure 6.5 that as deviator stress increases for both Class 5 and 50% RAP blends, PD increase without a significant difference in M_R values. It is very clear from comparing both Figures (6.5-a) and (6.5-b) that by adding 50% RAP to the blend, PD decreases and M_R increases. Again, this conclusion is very useful to the base layer behavior.

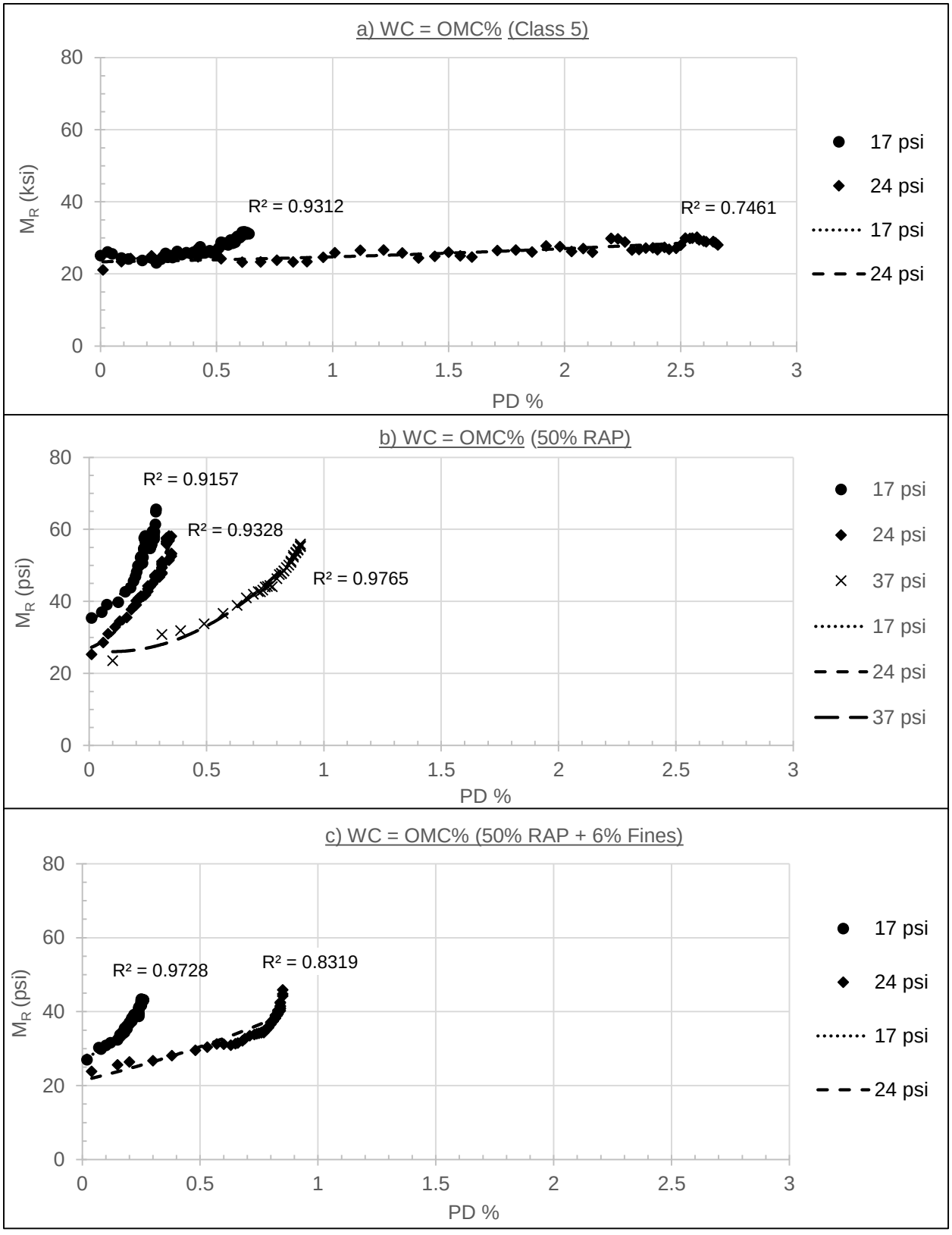

Figure 6.5. M_R versus PD for Single-stage RTL at OMC%

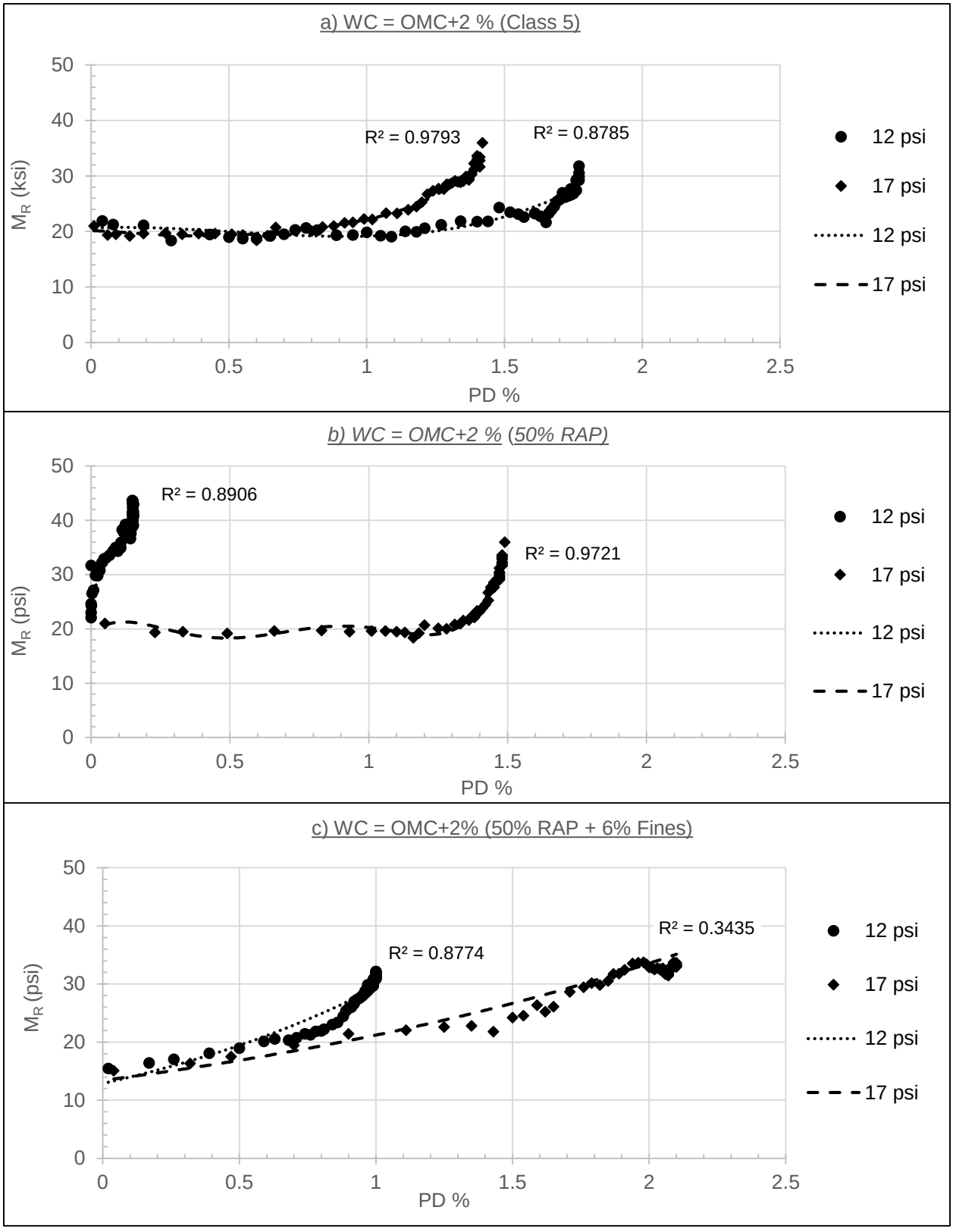

Figure 6.6. M_R versus PD for Single-stage RTL at OMC+2%

From comparing both Figures (6.5-b) and (6.5-c), modifying the 50% RAP blend by adding 6% fines have a negative behavior on base layer characteristics. As for both levels of deviator stress 17 and 24 psi, M_R decreases and PD increases. This comparison is repeated but at OMC+2%, as shown in Figure 6.6. From Figure (6.6-a), it is obvious that as deviator stress increases from 12 to 17 psi, PD decreases without significant change in M_R contrary to the OMC% case. For the 50% RAP at OMC+2% (Figure 6.6-b), the increase of deviator stress, increases the PD and negatively decreases M_R. From comparing both Figures (6.6-b) and (6.6-c), no significant difference is found after adding fines to the 50% RAP blend. However, there is a little decrease in M_R especially at the low deviator stress level of 12 psi.

Finally, it can be concluded from the data analysis for single-stage RTL test that, as the deviator stress increases for both Class 5 and 50% RAP blends, PD increases without a significant difference in M_R values for both water content levels OMC-2% and OMC%. Adding RAP to the base layer has a positive effect for base layer by decreasing PD and increasing M_R values. Modifying the 50% RAP blends by 6% plastic fines does not have any positive effects on base layer performance for both water content levels OMC-2% and OMC%.

6.4.3. Multi-stage RTL test

In this stage, the same effort is repeated but on different type of RTL testing. This stage is more close to the methodology of resilient modulus testing by applying stages of loading with different deviator stresses (D.S) but at higher number of load repetitions (5000 compared to 100 cycles). Confining pressure is kept the same (3 psi for all stages of loading). Figures 6.7, 6.8 and 6.9 show the M_R-PD trend for different RAP TH 10/Class 5 blends at three different water content levels: OMC-2%, OMC% and OMC+2% and the regression parameter R^2 for this relation is shown in Table 6.3. For Class 5 aggregates (Figure 6.7), the general trend is that both parameters M_R and

PD increase with the increase of deviator stress until reaching the highest stage of loading where the sample fails when reaching 5% PD and the M_R decreases when increasing PD. It is obvious that for all water content levels (Figures 6.7-a, 6.7-b and 6.7-c), Class 5 aggregates begin to fail when deviator stress reaches 24 psi without a significant difference in M_R values.

By adding 50% RAP to Class 5 aggregates (Figure 6.8), M_R values increase while PD values decrease. This finding proves that adding RAP is better for base layer performance. However, the trend shown before with Class 5 changes with adding RAP at low water content level of OMC-2% (Figure 6.8-a). The M_R values change un-expectedly with the increase of PD. On the other hand, the trend shown before with Class 5 is almost the same for the other two water content levels OMC% and OMC+2% (Figures 6.8-b and 6.8-c). Nevertheless, in this case the samples fails at higher deviator stress levels 59 and 48 psi for OMC% and OMC+2% respectively.

From comparing both Figures 6.8 and 6.9 for both cases of 50% RAP, the general trend of M_R-PD is almost the same. However, the significant result from this comparison is that adding 3.5% fines to the 50% RAP samples has remarkably positive effect on the behavior of the samples. It is found for all water content levels that PD values do not reach the 5% failure limit. The M_R values are significantly higher than those samples shown before stabilization. This result is completely different to samples tested before by single-stage RTL test with 6% fines added**.**

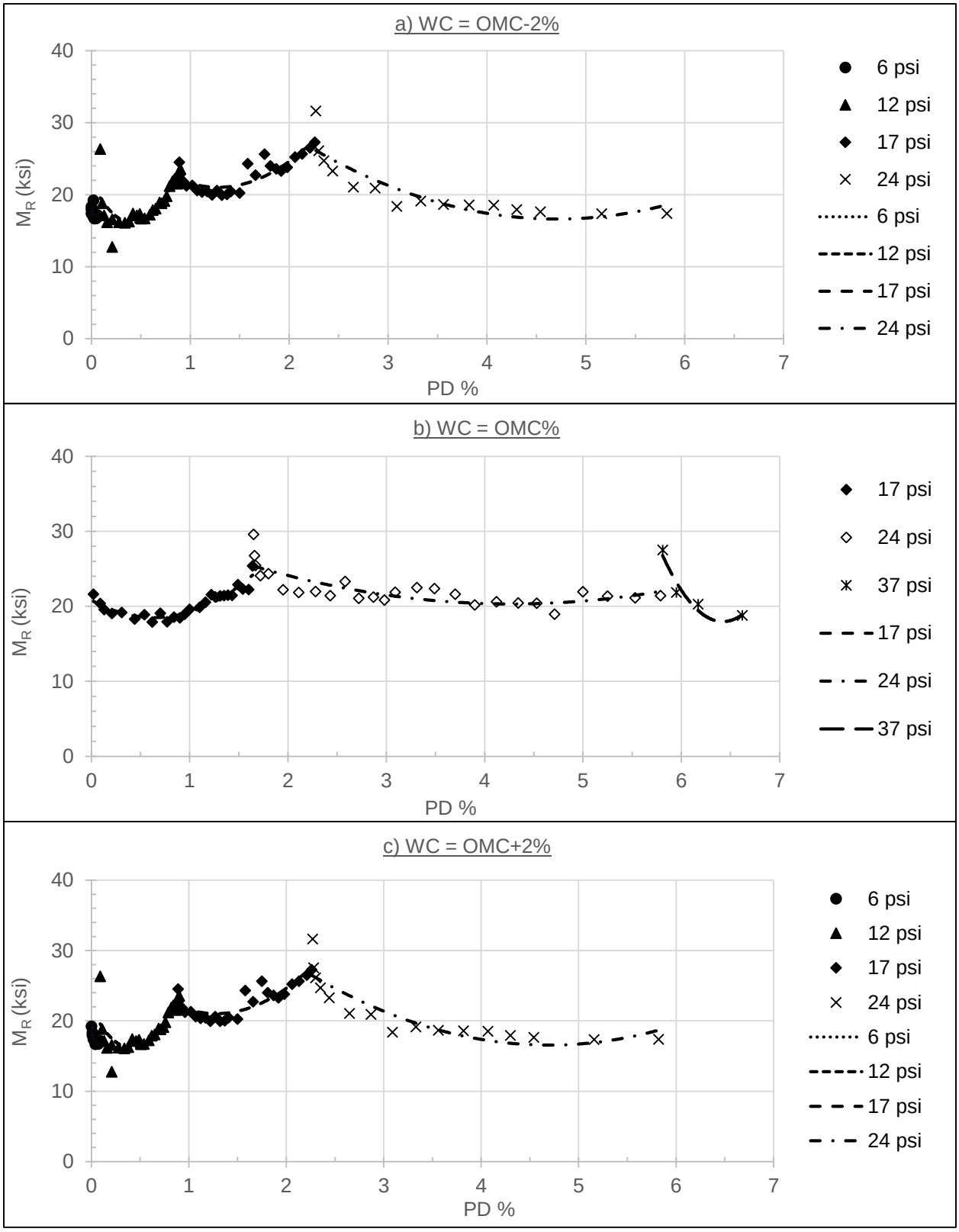

Figure 6.7. M_R versus PD for Multi-stage RTL of Class 5

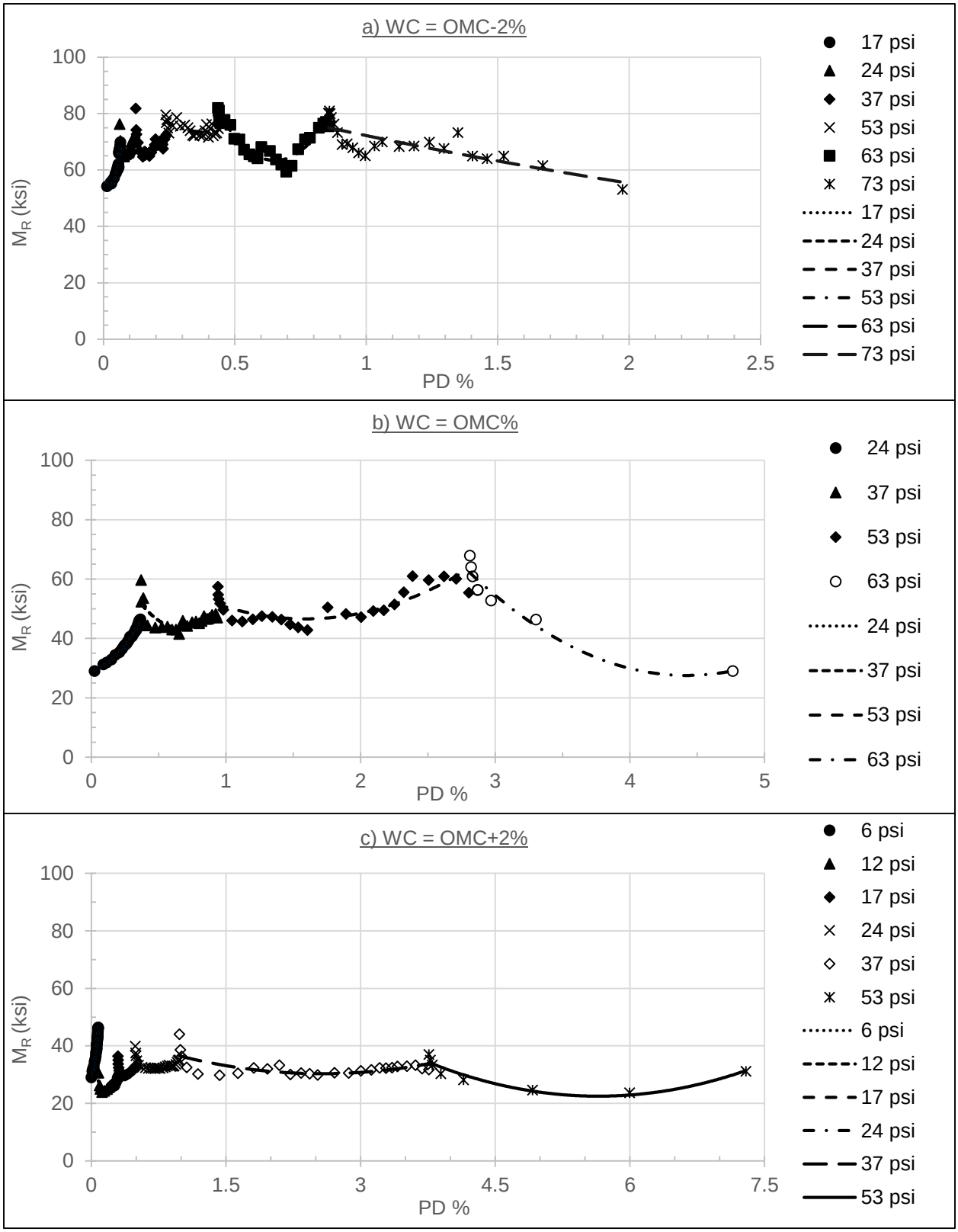

Figure 6.8. M_R versus PD for Multi-stage RTL of 50% RAP TH 10/50% Class 5

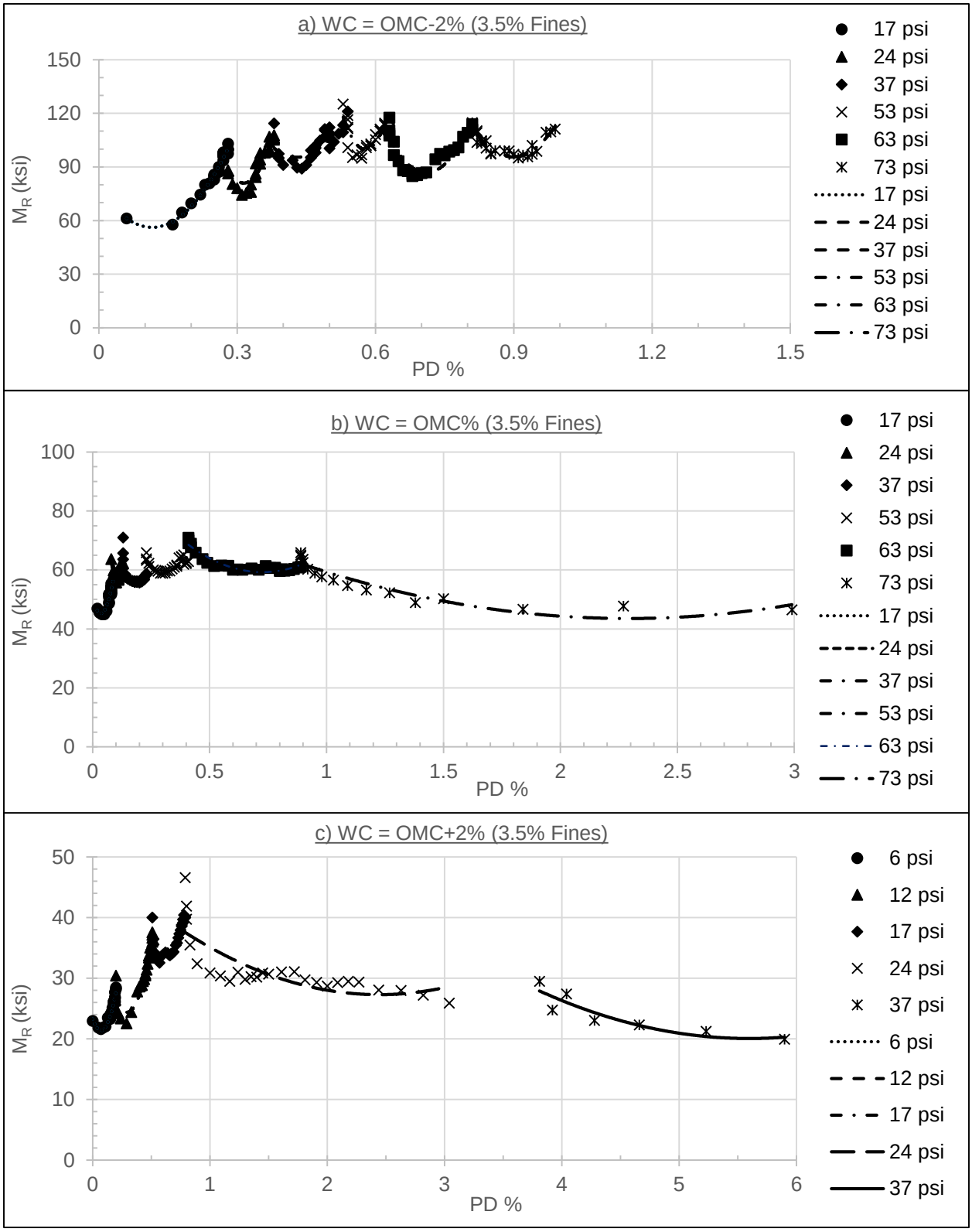

Figure 6.9. M_R versus PD for Multi-stage RTL of 50% RAP TH10/50% Class 5 + 3.5% Plastic Fines

Table 6.3. R^2 for M_R-PD relation of Multi-Stage RTL Test for RAP TH 10

Material Condition	Water Content	Deviator Stress (psi)							
		6	12	17	24	37	53	63	73
0% RAP	OMC-2%	0.37	0.59	0.74	0.78	N/A	N/A	N/A	N/A
	OMC%	N/A	N/A	0.88	0.64	0.93	N/A	N/A	N/A
	OMC+2%	0.87	0.59	0.74	0.8	N/A	N/A	N/A	N/A
50% RAP	OMC-2%	N/A	N/A	0.9	0.63	0.5	0.4	0.9	0.66
	OMC%	N/A	N/A	N/A	0.99	0.53	0.65	0.93	N/A
	OMC+2%	0.99	0.85	0.72	0.72	0.45	0.89	N/A	N/A
50% RAP + 3.5% Fines	OMC-2%	N/A	N/A	0.98	0.79	0.63	0.66	0.79	0.87
	OMC%	N/A	N/A	0.9	0.75	0.74	0.58	0.9	0.88
	OMC+2%	0.96	0.94	0.86	0.61	0.83	N/A	N/A	N/A

Finally, it can be concluded from the data analysis for single-stage RTL test that for Class 5 aggregates, both M_R and PD increase by increasing deviator stress until reaching the failure limit at the highest stage of loading, the M_R decreases. Adding 50% RAP to the base layer improves the performance by increasing M_R and decreasing PD values. The trend of M_R-PD of 50% RAP is almost the same as Class 5 especially at OMC% and OMC+2%, but the samples fails at higher deviator stress levels. Modifying the 50% RAP samples by 3.5% plastic fines has a significant positive effect on the performance of the samples at the three water contents; OMC-2%, OMC% and OMC+2%.

6.5. Correlation Task Summary

By comparing the two most important parameters (M_R and PD) in the RAP base layer performance, several findings are concluded from the three different testing procedures included in this study resilient modulus, single-stage RTL and multi-stage RTL tests. These findings may be summarized as follows:

6.5.1. Resilient modulus testing

- From resilient modulus testing at OMC%, it was found that as the percentage of RAP TH 10 (the main RAP source) exceeds 50%, M_R increases and PD decreases. This result is positive for base layer strength. This relation is more significant at confining pressure levels below 15 psi.
- For the same water content, both 100% and extracted RAP TH 10 have the highest M_R and the lowest PD with a small decrease in M_R values after extraction.
- The trend of RAP TH10 is close to most of the other field RAP samples (TH 19-101, TH 19-104 and TH 22) with 50% content especially at OMC-2%. However, a little difference is found at OMC% when compared with same 50% content.
- The trend of 50% RAP TH 10 is found to be different than other RAP contents for the same source TH10. This may be attributed to the test accuracy for this sample. However, the trend of 100% RAP TH 10 is too close to the other field RAP sources.
- Also, the trend of RAP TH 10 is too close to the other 100% RAP source (Cell 18) especially at OMC%.
- The trend of all RAP sources at OMC+2% do not have a typical pattern and this is due to the approach of the PD from the failure limit (5%) and the lowest correlation found (R^2 is low) as shown in Tables 3 and 4. This behavior is changed for single and multi-stage RTL test, because

the effect of stress history in resilient modulus test by applying 30 different sequences of loading with variable deviator and confining stresses.

6.5.2. Single-Stage RTL Testing

- As the deviator stress increases for both Class 5 and 50% RAP blends, PD increases without a significant difference in M_R values for both water content levels OMC-2% and OMC%.
- Adding RAP to the base layer has a positive effect for base layer by decreasing PD and increasing M_R values.
- Modifying the 50% RAP blends by 6% plastic fines do not have any positive effects on base layer performance for both water content levels OMC-2% and OMC%.

6.5.3. Multi-Stage RTL Testing

- For Class 5 aggregates, both M_R and PD increase by increasing deviator stress until reaching the failure limit at the highest stage of loading, the M_R decreases.
- Adding 50% RAP to the base layer improves the performance by increasing M_R and decreasing PD values.
- The trend of M_R-PD of 50% RAP is almost the same as Class 5 especially at OMC% and OMC+2% but the samples fails at higher deviator stress levels.
- Modifying the 50% RAP samples by 3.5% plastic fines has a significant positive effect on the performance of the samples at the three water contents; OMC-2%, OMC% and OMC+2%.

CHAPTER 7. POSSOIN'S RATIO MEASUREMENT

7.1. Introduction

Based on the results of Maher et. al. (Maher & Bennert, 2008) study, Poisson's ratio measured values during the dynamic modulus test are very close to the MEPDG predicted values for several HMA mixes tested at this study. However, this study showed that unbound granular aggregates used for base layer have identical resilient modulus at different levels of Poisson's Ratio values. For example, a Poisson's ratio value of approximately 0.15 occurred at all five confining pressures and had resilient modulus values that ranged from 22,000 to almost 90,000 psi (Maher & Bennert, 2008). In addition, it is not accurate to measure Poisson's ratio for confined materials during uniaxial loading as the confining pressure applied to samples during testing affect on the real lateral strain that happens to the sample. Even if there is a confining pressure in the field, but in this study the material is assumed totally elastic especially in the linear stress-strain relationship to measure accurate Poisson's ratio value and avoid the variation found from the above mentioned study.

Therefore, there is a need to measure Poisson's ratio for RAP/Aggregate blends in a base layer with another testing procedure, especially when it is still in elastic region just before failure or permanent deformation accumulation. The un-confined compression test seems to be the most suitable procedure to measure the lateral deformation of RAP samples during axial loading. Lateral strain gauges can be used to measure this deformation simultaneously with axial deformation measured without any confining pressure, which may affect on the accuracy of lateral deformation measurement. This test was used before in evaluating the stiffness of cement treated base as by adding cement a pozzlanic reaction happens which changes the layer from elasto-plastic material

to totally elastic brittle material. In this case the treated material cannot be measured with the same methods used for granular base materials

Finally, the Poisson's ratio was not considered in previous studies as an important parameter affecting the structural capacity for granular base layer, especially during measuring any stiffness parameter either under dynamic or static loading. Usually, Poisson's ratio was estimated during all methods of pavement design including the MEPDG. However, effect of Poisson's ratio on both M_R and PD modeling behavior for RAP blends is essential to be studied to investigate its effectiveness on the structural capacity of base layer. This study is essentially needed to confirm the difference in behavior of RAP blends from granular aggregates, especially under variation of water content. Usually the accepted variation of water content in the field is 2% from the OMC%, therefore Poisson's ratio is measured within this range for all investigated RAP/Aggregate blends.

7.2. Scope of Task

The main objective of this task focuses on measuring Poisson's ratio and ultimate compressive strength for several RAP/Aggregate blends, tested before in the previous research tasks on resilient modulus and repeated tri-axial loading (RTL) tests to determine the values of both parameters M_R and PD, at various testing conditions. The target of this task is to evaluate the Poisson's ratio and compressive strength relationship, and its future effectiveness on the main design parameters of RAP blends used in base layer such as M_R and PD. Based on literature review results, this ratio cannot be measured during the M_R test. Therefore, the un-confined compression test is used to determine the respective results. This test is more suitable and practical to implement in measuring the lateral deformation without any effect of confining pressure like M_R or RTL tests.

7.3. Stages of Analysis

According to the literature review collected in this study, for each tested specimen an axial stress-strain curve is drawn and the linear elastic region is calculated as a range percentage from the ultimate compressive strength as shown in appendices. Generally, this linear relationship is varied from 15% to 90%, while the average midpoint for this relation varied from 40% to 65% of the ultimate compressive strength for analyzed samples. Usually, the Poisson's ratio should be constant in this linear elastic for homogenous specimens. However, these tested specimens are not truly homogenous due to many reasons such as; gradation, compaction, aggregate properties, aging characteristics and etc. Therefore, the Poisson's ratio is considered as the average midpoint of this linear elastic region for each sample condition. For all analyzed samples, the Poisson's ratio varied from 0.07 to 0.47, while the ultimate compressive strength varied from 1.92 to 32.83 psi. The analysis of this task is divided into three main stages according to the different testing conditions investigated.

7.3.1. Analysis versus RAP content

This stage is focusing on the condition of percentage of RAP with traditional Class 5 granular aggregates on Poisson's ratio and ultimate compressive strength values. Two RAP sources TH 29 and TH 10 are analyzed in this stage with the two different sources of Class 5 at three water content levels OMC-2%, OMC% and OMC+2%. The new Class 5 source used for this study is mixed with RAP TH 29, as shown in Figure 7.1. The old Class 5 source used before in MN/DOT project (M. Attia et al., 2009) is mixed with RAP TH 10, as shown in Figure 7.2.

For Figure 7.1 the general trend of both OMC-2% and OMC% is almost the same, as Poisson's ratio values increases significantly at 50% RAP then decreases significantly at 100% RAP with a little higher values at OMC% condition.

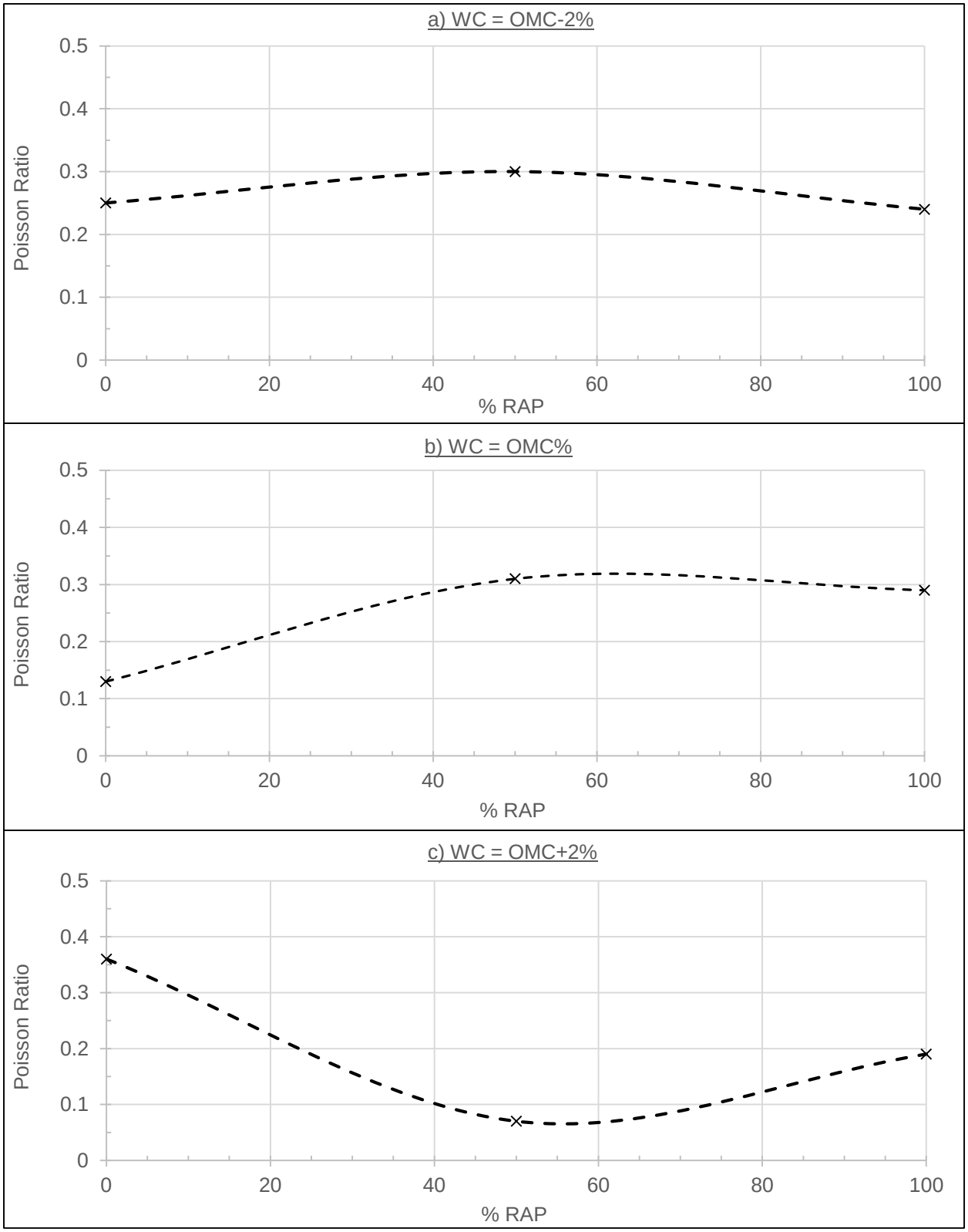

Figure 7.1. Poisson's Ratio for RAP TH 29/New Class 5 Blends versus RAP Content

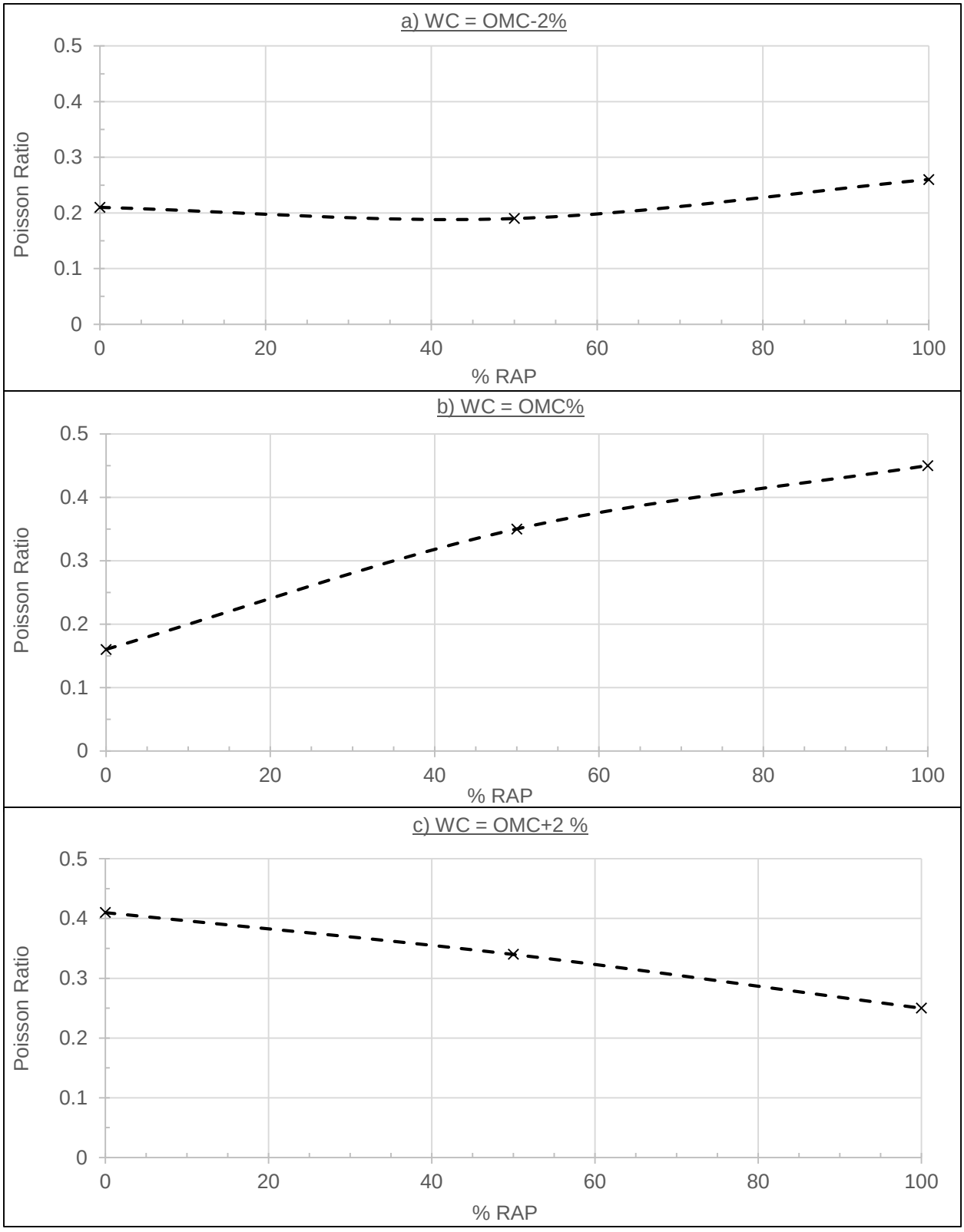

Figure 7.2. Poisson's Ratio for RAP TH 10/Old Class 5 Blends versus RAP Content

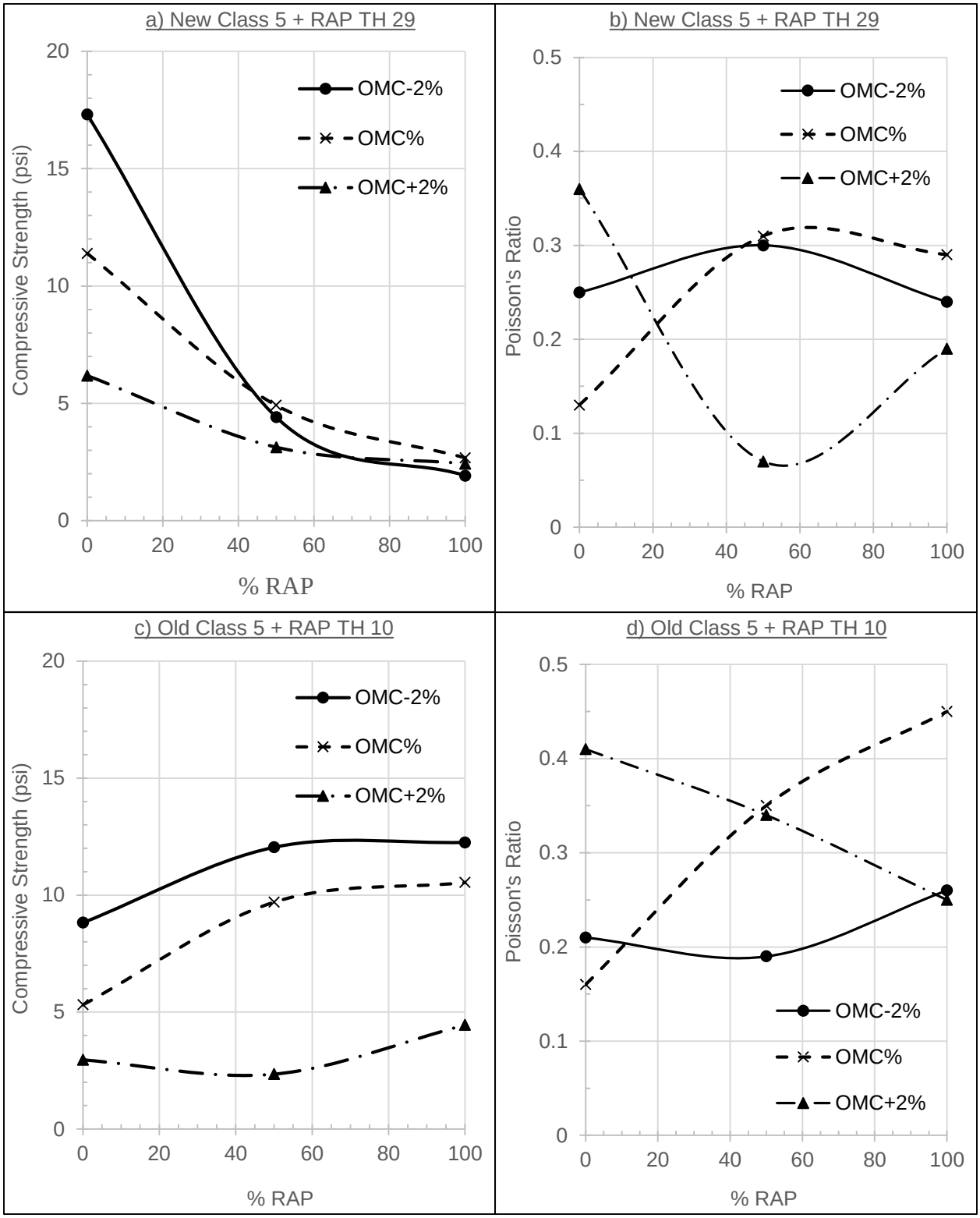

Figure 7.3. Comparison between Ultimate Compressive Strength and Poisson's Ratio for RAP/Aggregate blends versus RAP Content

This trend changes at OMC+2% as Poisson's ratio value is the lowest at 50% RAP. In Figure 7.2 the trend is obvious at OMC%, as Poisson's ratio increases with the increase of percentage of RAP significantly. However, the trend is opposite at OMC+2% as it decreases significantly with RAP content increase. And the change in Poisson's ratio is not significant at OMC-2% water content. In addition, a general comparison is achieved between the trend of both the ultimate compressive strength and Poisson's ratio values, at the three water content levels for both RAP/Class 5 blends versus RAP content, as shown in Figure 7.3.

Generally, the ultimate compressive strength decreases with the increase of RAP content for new Class 5 + RAP TH 10 blends. While on the other hand, the trend is opposite for old Class 5 + RAP TH 29 at all water content levels. This conclusion can be explained as new Class 5 (6-18 psi) is much stronger than the old Class 5 (3-9 psi). However, RAP TH 29 (2-3 psi) is much weaker than RAP TH 10 (5-13 psi), as this source of RAP is much older which means that more age hardening effect on the asphalt binder. This means that for the first case softening effect happens by increasing the RAP TH 29 content and the opposite for the second case by increasing RAP TH 10 content. Contrary, there is no typical shape from the Poisson's ratio relationship for both RAP blends. At OMC%, the Poisson's ratio increases from 0.13 to 0.29 for RAP TH 29 blend, and also it increases from 0.16 to 0.45 for RAP TH 10 blend with increasing RAP content. At OMC+2%, the trend of both blends is almost the same as Poisson's ratio decreases significantly from 0.4 to 0.2 approximately. On the other hand at OMC-2%, there isn't significant variation in Poisson's ratio values.

7.3.2. Analysis versus water content

In this stage, Poisson's ratio parameter is analyzed versus water content variation for the three main RAP/Aggregate blends. New Class 5/ RAP TH 29 blends are shown in Figure 7.4,

while old Class 5/RAP TH 10 are shown in Figure 7.5 and the other field RAP sources are shown in Figure 7.6. In addition, ultimate compressive strength parameter is analyzed also versus water content variation for the same RAP/Aggregate blends, as shown in Figure 7.7.

For Class 5, Poisson's ratio is are in its lowest value (0.15 approximately) at OMC% level, as shown in Figures (7.4-a) and (7.5-a) for both types. At 50% RAP TH 29, Poisson's ratio decreases significantly from 0.3 to 0.07 (Figure 7.4-b) by increasing water content, while it increases slightly from 0.19 to 0.35 (Figure 7.5-b) for 50% RAP TH 10. At 100% RAP, Poisson's ratio increases at OMC% then decreases at the other two water contents for both RAP blends with more significance for RAP TH 10 blend by comparing both Figures (7.4-c) and (7.5-c). As Poisson's ratio for 100% RAP TH 10 reaches 0.45 corresponding to 0.29 for 100% TH 29.

For the other field RAP sources, Poisson's ratio values almost has no significant change for RAP TH 19-101 (Figure 7.6-a) by increasing water content. However, for the other two RAP sources, Poisson's ratio for RAP TH 19-104 reaches its lowest value 0.15 (Figure 7.6-b), while for RAP TH 22 it reaches its optimum value 0.47 (Figure 7.6-c), both at OMC% level. On the other hand, for the ultimate compressive strength parameter (Figure 7.7), it decreases significantly for both RAP/Class 5 blends by increasing water content from 15 psi to 3 psi approximately especially for Class 5 blends, as shown in Figures (7.7-a) and (7.7-b).

Also for the other field RAP sources, RAP TH 22 is the only one which have the same behavior as RAP/Class 5 blends as its ultimate strength decreases significantly from 16 to 6 psi approximately (Figure 7.7-c). While for the other two RAP sources, their ultimate strength reach its optimum values 32 and 25 psi at OMC% for RAP's TH 19-101 and TH 19-104 respectively, as shown in Figure (7.7-c).

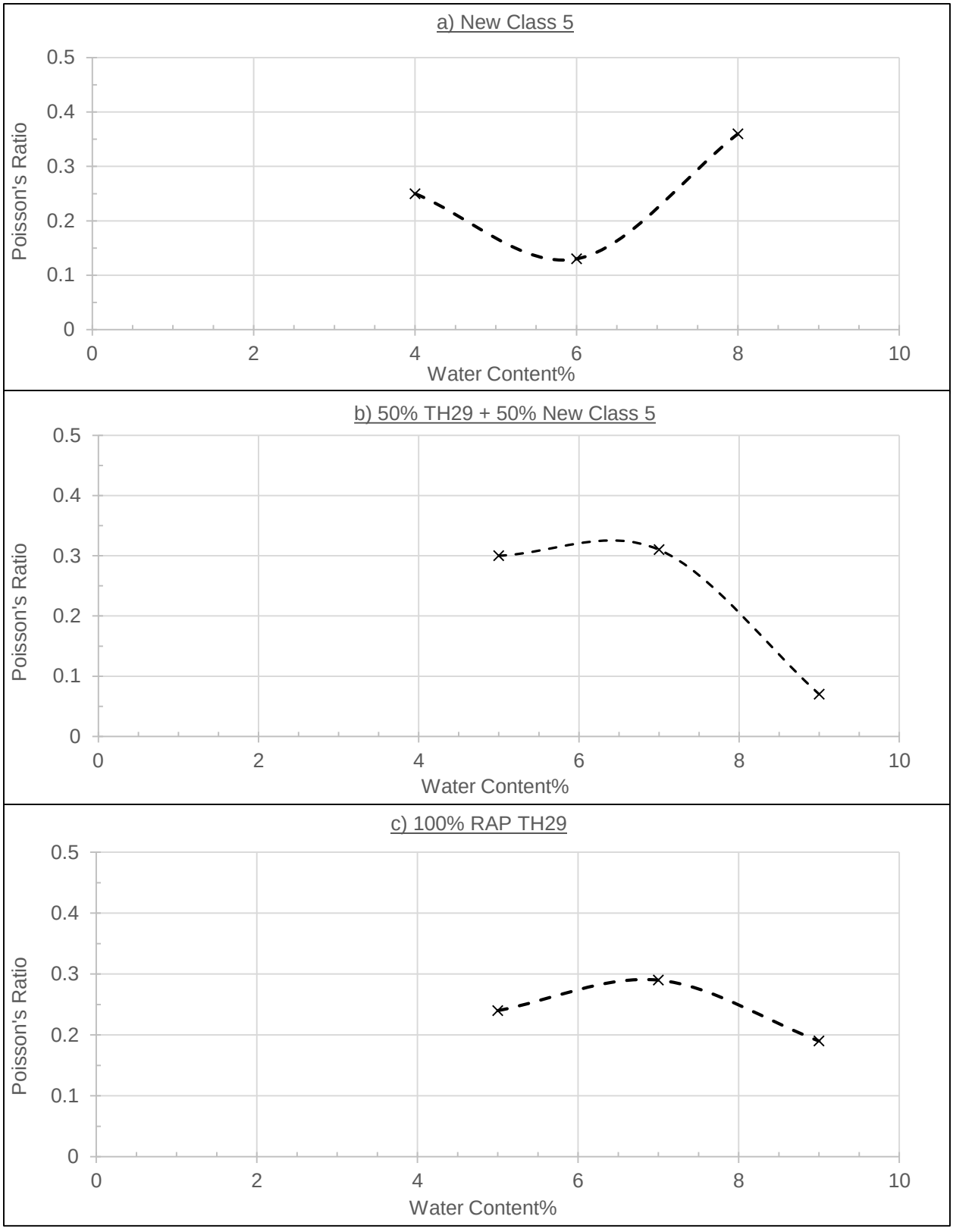

Figure 7.4. Poisson's Ratio for RAP TH 29 + New Class 5 Blends versus Water Content

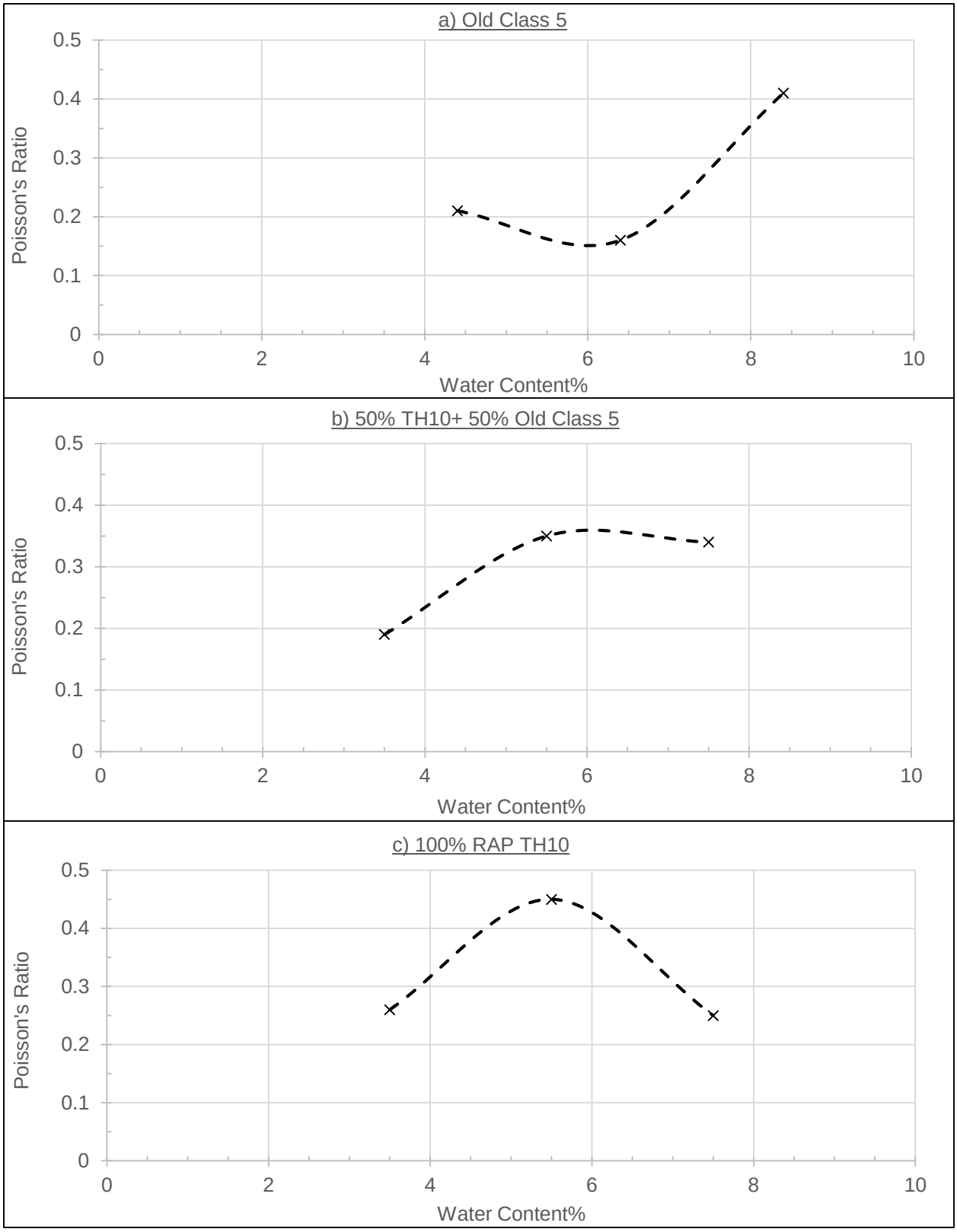

Figure 7.5. Poisson's Ratio for RAP TH 10 + Old Class 5 Blends versus Water Content

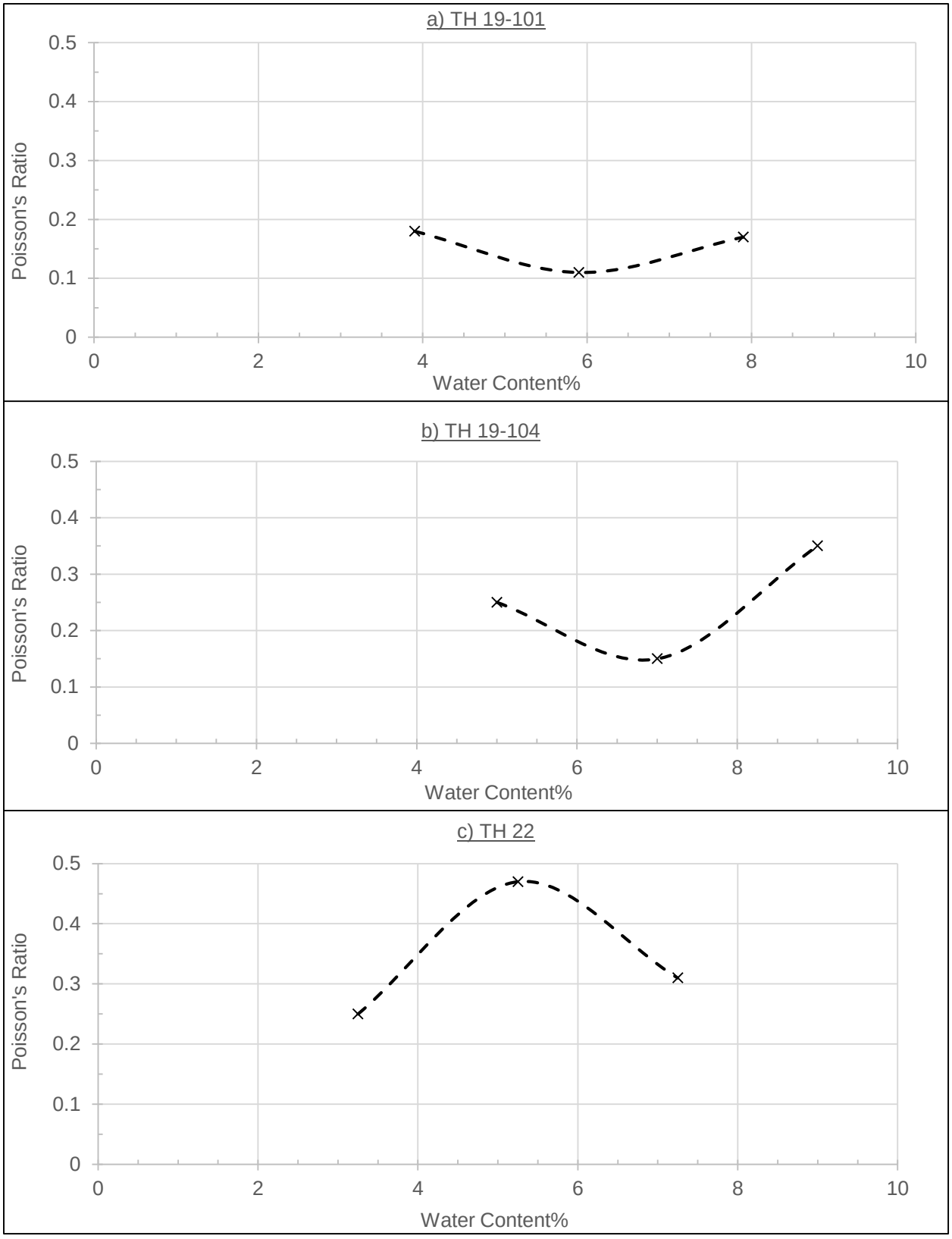

Figure 7.6. Poisson's Ratio for Field RAP Blends versus Water Content

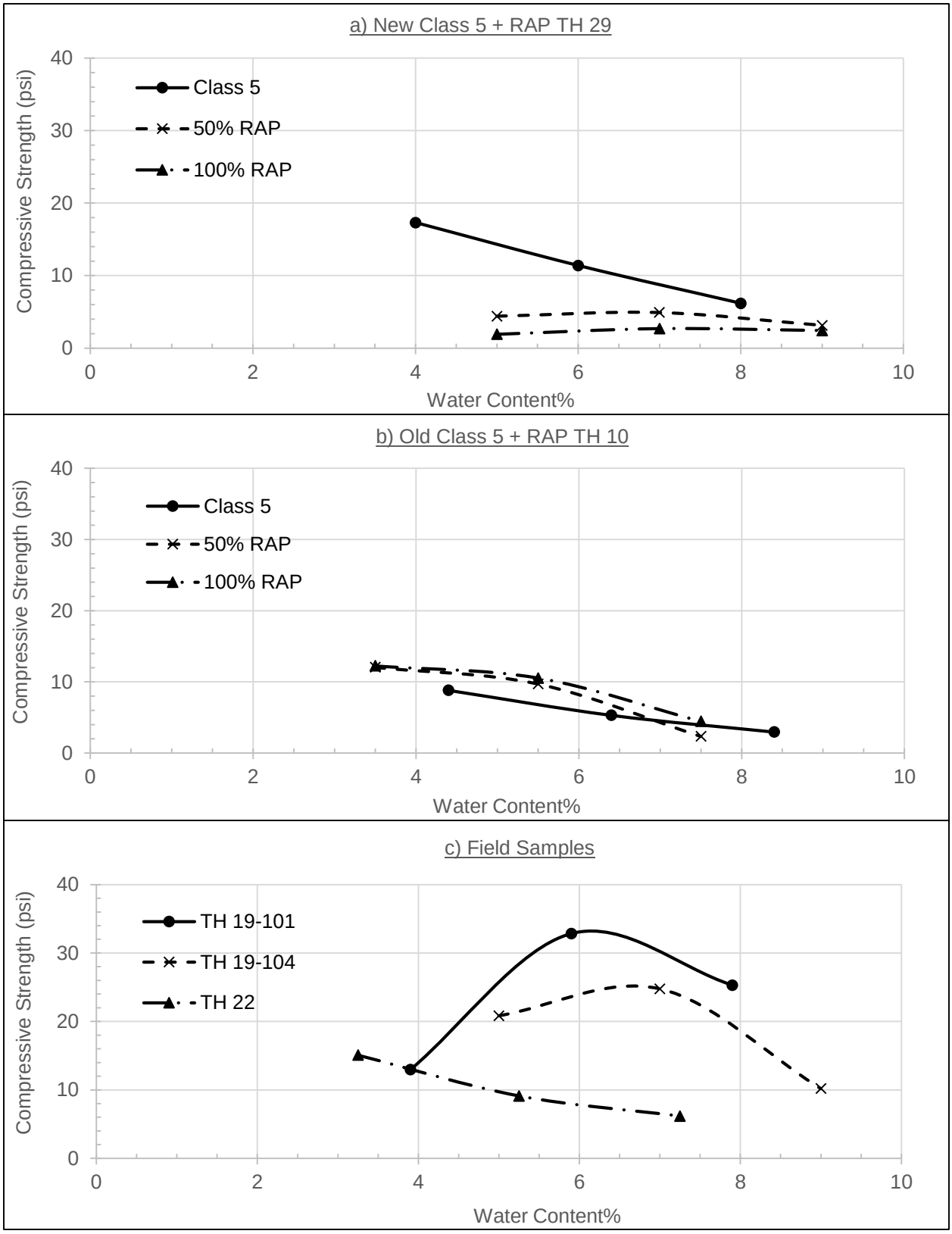

Figure 7.7. Ultimate Compressive Strength for RAP Blends versus Water Content

7.3.3. Correlation between lateral strain and compressive stress

At this third stage, a comparison is made between lateral strain to the compressive stress directly at four levels (25%, 50%, 75% and 100%) of the ultimate compressive strength for all RAP blends tested at investigated testing conditions. This stage is important to show the lateral strain increase during whole compression test. RAP TH 29/Class 5 blends are shown in Figure 7.8, RAP TH 10/Class 5 blends are shown in Figure 7.9 and field RAP blends are shown in Figure 7.10. The general trend is that increasing the compressive stress increases lateral strain. By decreasing water content, same lateral strain values are achieved at higher compressive stresses except for 50% RAP TH 29 (Figure 7.8-b) and field RAP's TH 19-101 & TH 19-104 (Figure 7.10-b & 7.10-c) blends. For those RAP blends, the highest stress values are achieved at OMC%. One sample is tested as a trial for RAP TH 10 by retesting the sample at OMC% after extracting the aged asphalt binder, as shown in Figure (7.9-c).

The extracted sample has slightly higher stress levels and smaller lateral strain than the original sample but the variation is insignificant. It is obvious from most of RAP blends tested that variation of water content have more effect on the compressive stress than lateral strain values. On the other hand, the RAP contents have contradicting effects on both parameters depending on the RAP source, aging characteristics, granular aggregate gradation and strength parameters.

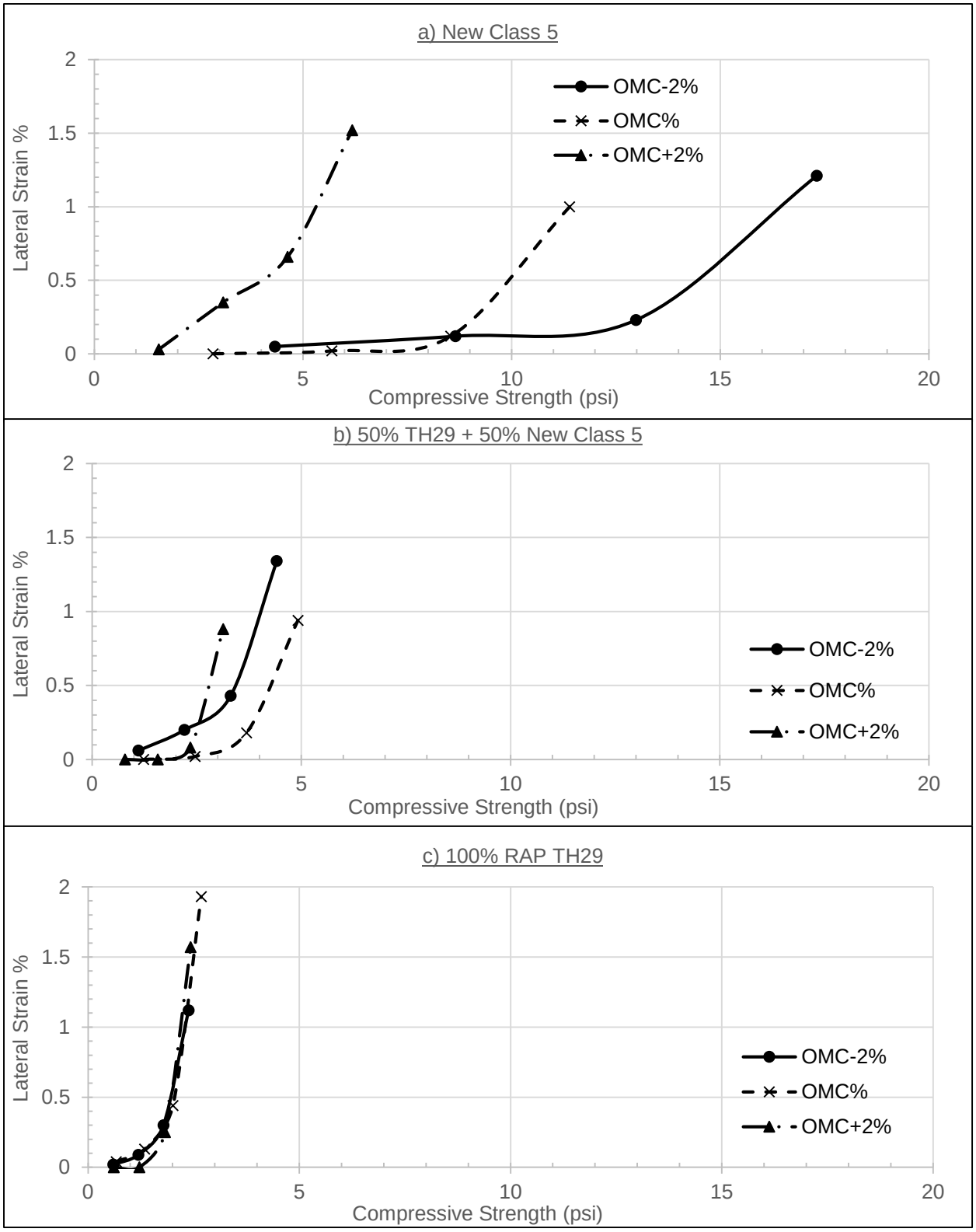

Figure 7.8. Comparison between Lateral Strain and Compressive Stress for RAP TH 29 + New Class 5 Blends

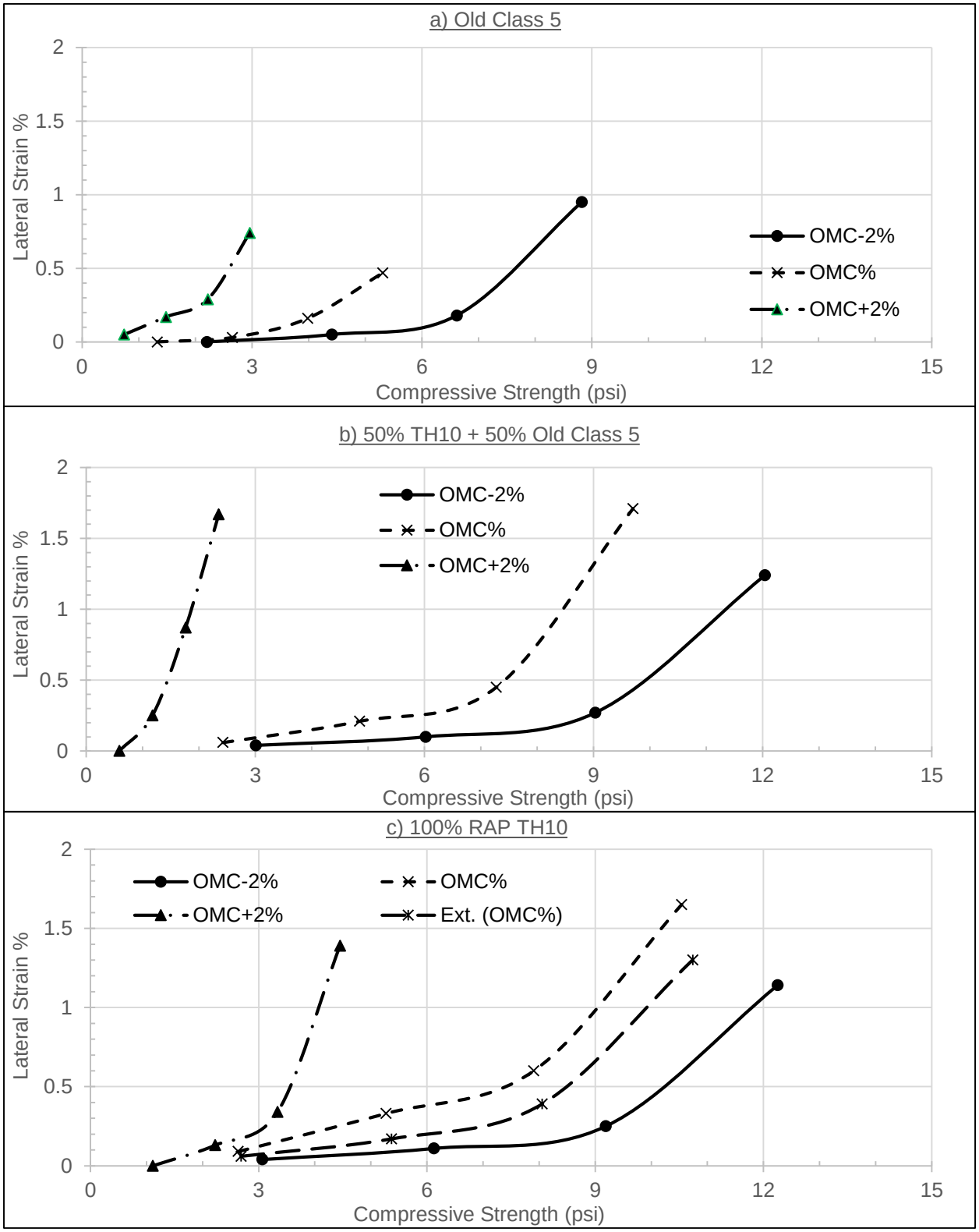

Figure 7.9. Comparison between Lateral Strain and Compressive Stress for RAP TH 10 + Old Class 5 Blends

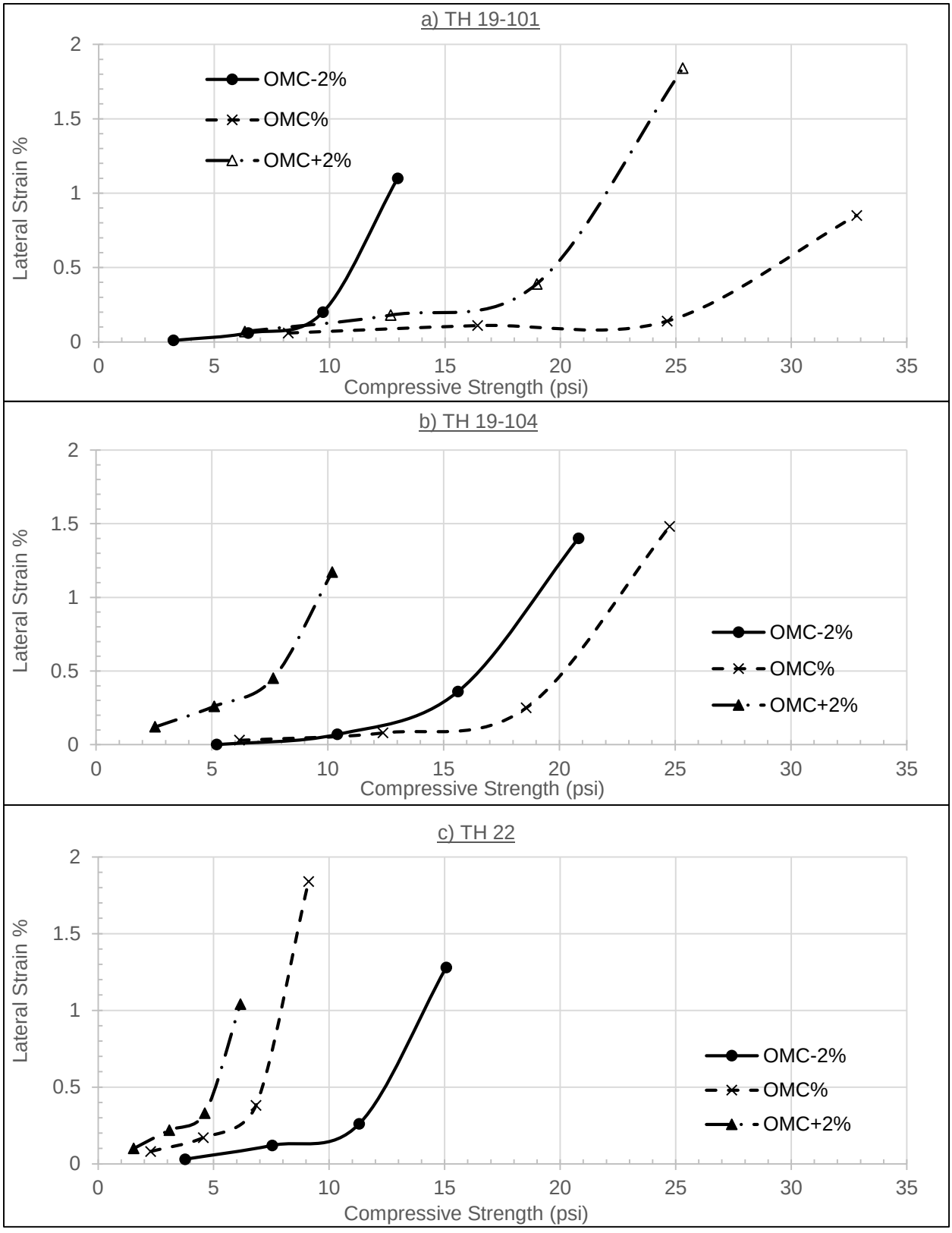

Figure 7.10. Lateral Strain versus Compressive Stress for Field RAP Blends

7.4. M_R Relationship with Un-confined Compression Test Parameters

It is known from NCHRP1-28A protocol used for measuring M_R, that 30 different sequences of loading are applied for each sample at every testing condition. However, to compare the M_R behavior of RAP/Aggregate blends with both parameters (Poisson's ratio and ultimate compressive strength) collected from un-confined compression test, average values of M_R are taken at each testing condition investigated corresponding to average Poisson's ratio and ultimate compressive strength values. Those average values shows only the general trend of M_R at different investigated testing conditions even they are not so much realistic due to the change of the stress condition for each replicate.

This comparison is made first for RAP TH 10/Old Class 5 blends at different RAP contents as shown in Figure 7.11. On the other hand, this comparison is made for same RAP/Aggregate blends versus water content variation as shown in Figure 7.12. Finally, this comparison is made for the other Field RAP blends (previously mixed with 50% granular aggregates) as shown in Figure 7.13. It is obvious from Figure (7.11-a) that M_R values increase significantly by increasing the RAP content for all water content levels. This relation is almost the same for ultimate compressive strength factor but with less significance as shown in Figure (7.11-c) especially at OMC+2% water level. On the other hand, there is no general trend for Poisson's ratio versus RAP content as shown in Figure (7.11-b).

At OMC%, Poisson's ratio increases significantly from 0.16 to 0.45 by increasing RAP content corresponding to an increase in both parameters M_R and ultimate compressive strength. However at OMC+2%, Poisson's ratio decreases significantly from 0.41 to 0.25 corresponding to a significant increase in M_R values and insignificant increases in ultimate compressive strength.

At OMC-2%, there isn't a significant increase (0.21-0.25) corresponding to an increase in both parameters M_R and ultimate compressive strength.

The same comparison is achieved between M_R behavior and un-confined strength parameters with water content variation for each RAP/Aggregate blend as shown in Figure 7.12. Both M_R and ultimate compressive strength have the same trend as each parameter decreases significantly with water content increase as shown in both figures (7.12-a) and (7.12-c). For Poisson's ratio parameter as shown in Figure (7.12-b), both RAP blends have the same behavior as it reaches their maximum values 0.35 and 0.45 for 50% and 100% RAP respectively then decreases significantly at the other two water contents. While Class 5 have an opposite trend as it reaches its lowest value 0.16 at OMC%.

For the other three field RAP's, the same comparison is conducted with water content variation only as those RAP's were already mixed with 50% granular aggregates. For M_R results as shown in Figure (7.13-a), the trend is the same for all RAP sources as M_R decreases by increasing water content. However, this trend is not the same for ultimate compressive strength parameter (Figure 7.13-c) as both RAP sources TH 19-101 and TH 19-104 reaches their maximum values 25 and 33 psi respectively at OMC%. Also, it is obvious for both RAP's that they have the same behavior for Poisson's ratio parameter (Figure 7.13-b). As they reach their lowest values 0.11 and 0.15 for RAP TH 19-101 and RAP TH 19-104 respectively. While for RAP TH 22, the Poisson's ratio behavior is more close to its M_R behavior than ultimate compressive strength. As it reaches its maximum value 0.47 at OMC%.

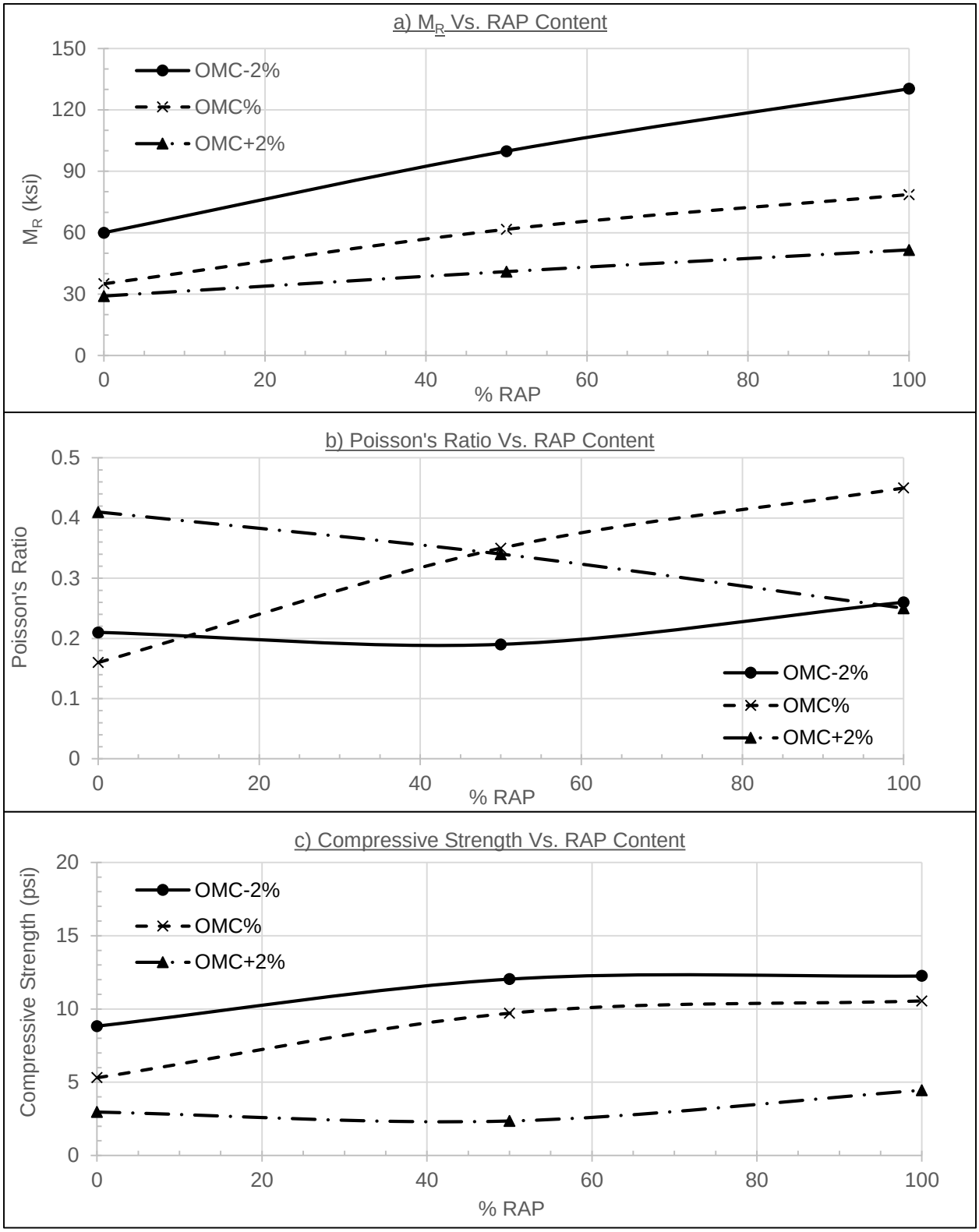

Figure 7.11. Comparison between M_R and Un-confined Compression Parameters versus RAP Content for RAP TH 10 + Old Class 5 Blends

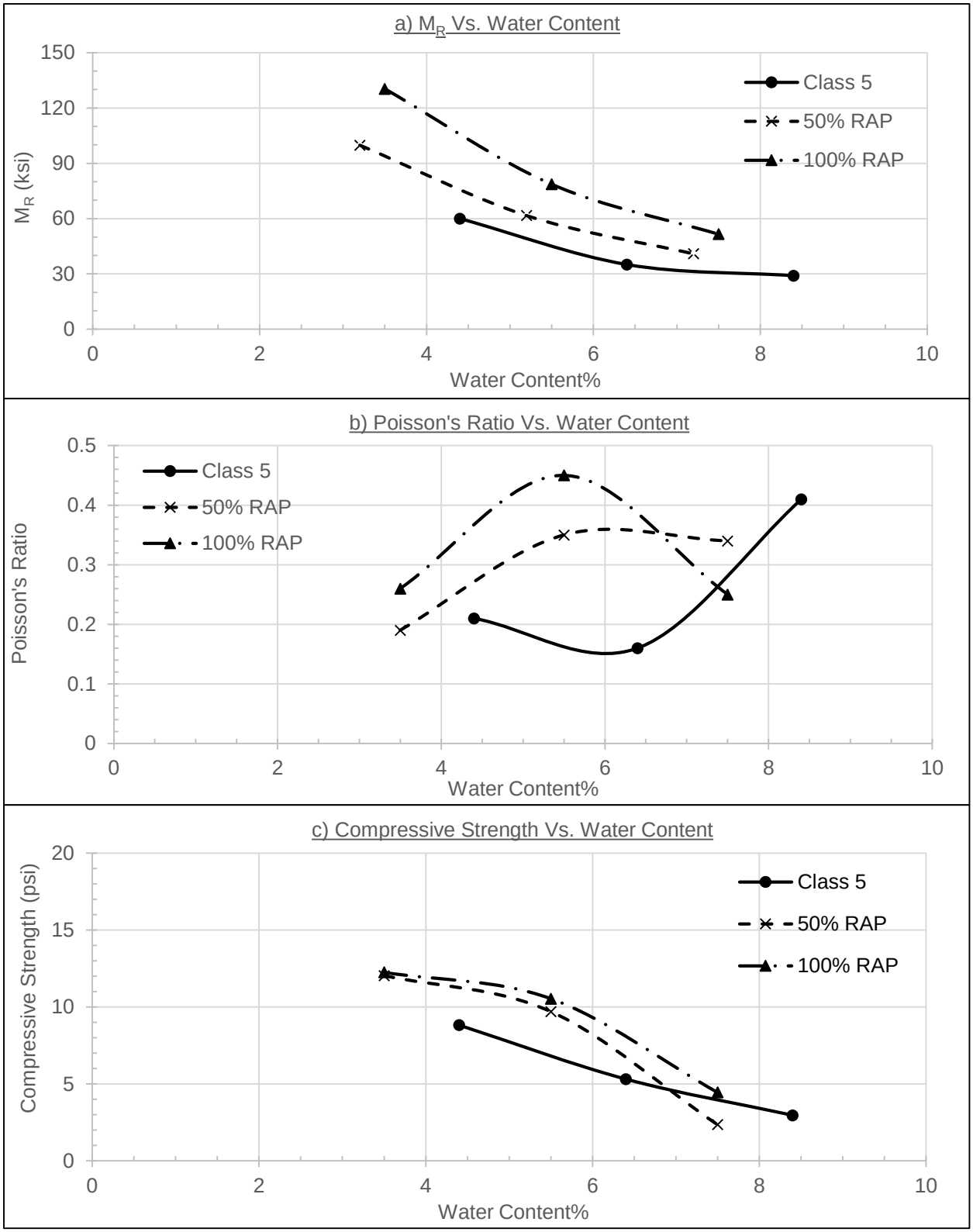

Figure 7.12. Comparison between M_R and Un-confined Compression Parameters versus Water Content for RAP TH 10 + Old Class 5 Blends

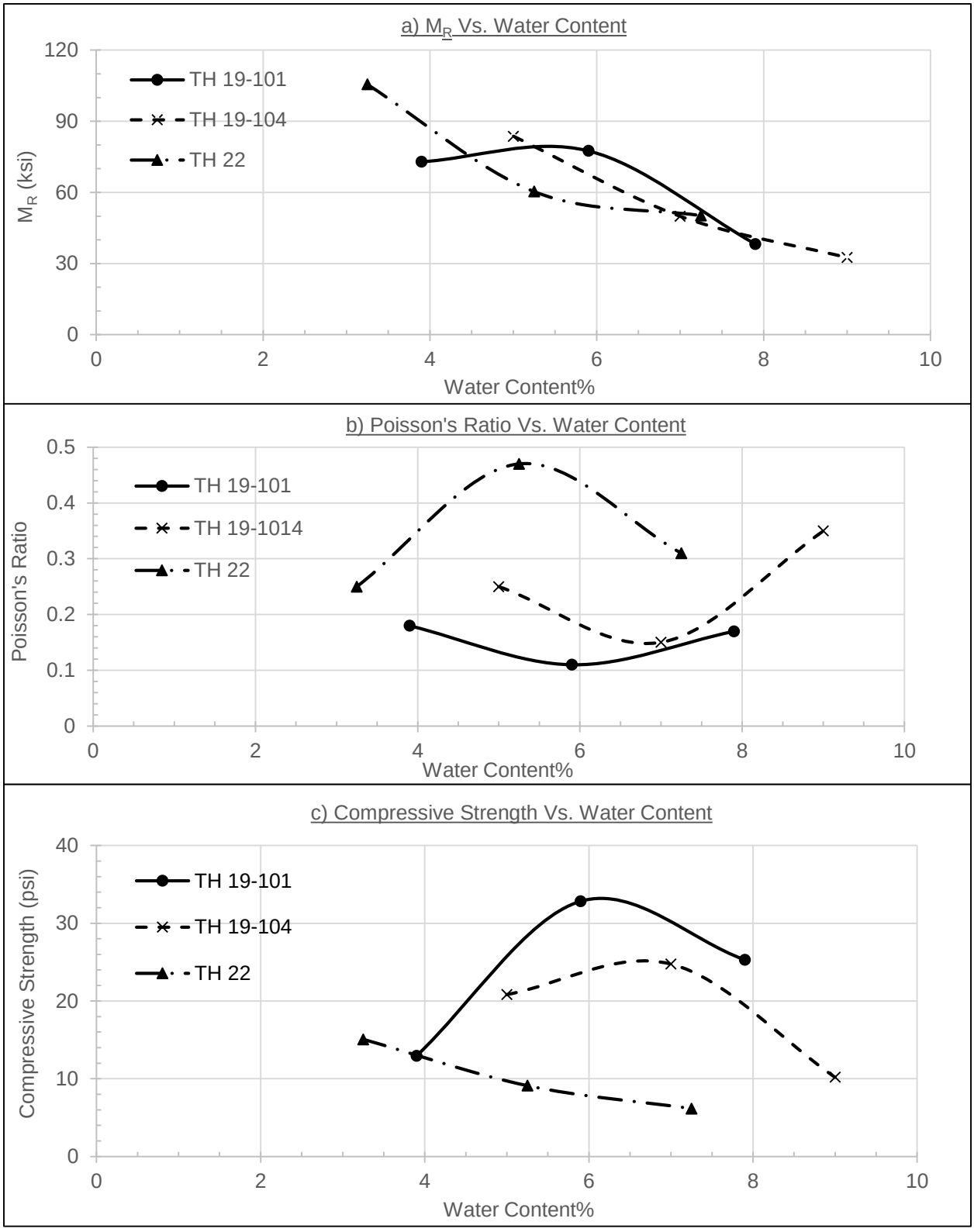

Figure 7.13. Comparison between M_R and Un-confined Compression Parameters versus Water Content for Other Field RAP Blends

7.5. PD Relationship with Un-confined Compression Test Parameters

During the resilient modulus test for collecting M_R values of RAP/Aggregate blends investigated, PD is accumulated for every sequence of loading. Those values are calculated as a percentage from whole sample height then an average value is taken for each sample as an indicator for PD values. PD values collected from both single-stage and multi-stage RTL test cannot be used as it didn't cover all the investigated testing conditions such as RAP content and water content for tested RAP/Aggregate blends analyzed in this chapter.

Generally, it seems that the RAP content is not significantly affect PD as water content by comparing both Figures (7.14-a) and (7.15-a). As increasing water content, increases PD accumulated for all RAP/Aggregate blend. However, increasing RAP content do not change PD accumulated significantly except at OMC%. At OMC% by increasing RAP content, PD decreases from 1.4% to 0.5% while Poisson's ratio increases significantly from 0.16 to 0.45. At OMC+2%, PD decreases insignificantly from 3.4% to 3.8% corresponding to a significant decrease for Poisson's ratio from 0.41 to 0.25. At OMC-2%, both parameters PD and Poisson's ratio do not change significantly by increasing RAP content.

By increasing water content, PD increases significantly for all RAP/Aggregate blends as shown in Figure (7.15-a). While the Poisson's ratio for both 50% and 100% RAP/Aggregate blends reach its maximum values 0.35 and 0.45 respectively, however Class 5 has an opposite trend (Figure 7.15-b). For the field RAP blends, increasing water content increases PD significantly as shown in Figure (7.16-a). And both RAP's TH 19-101 and TH 19-104 have a similar behavior for Poisson's ratio while RAP TH 22 have an opposite trend (Figure 7.16-b).

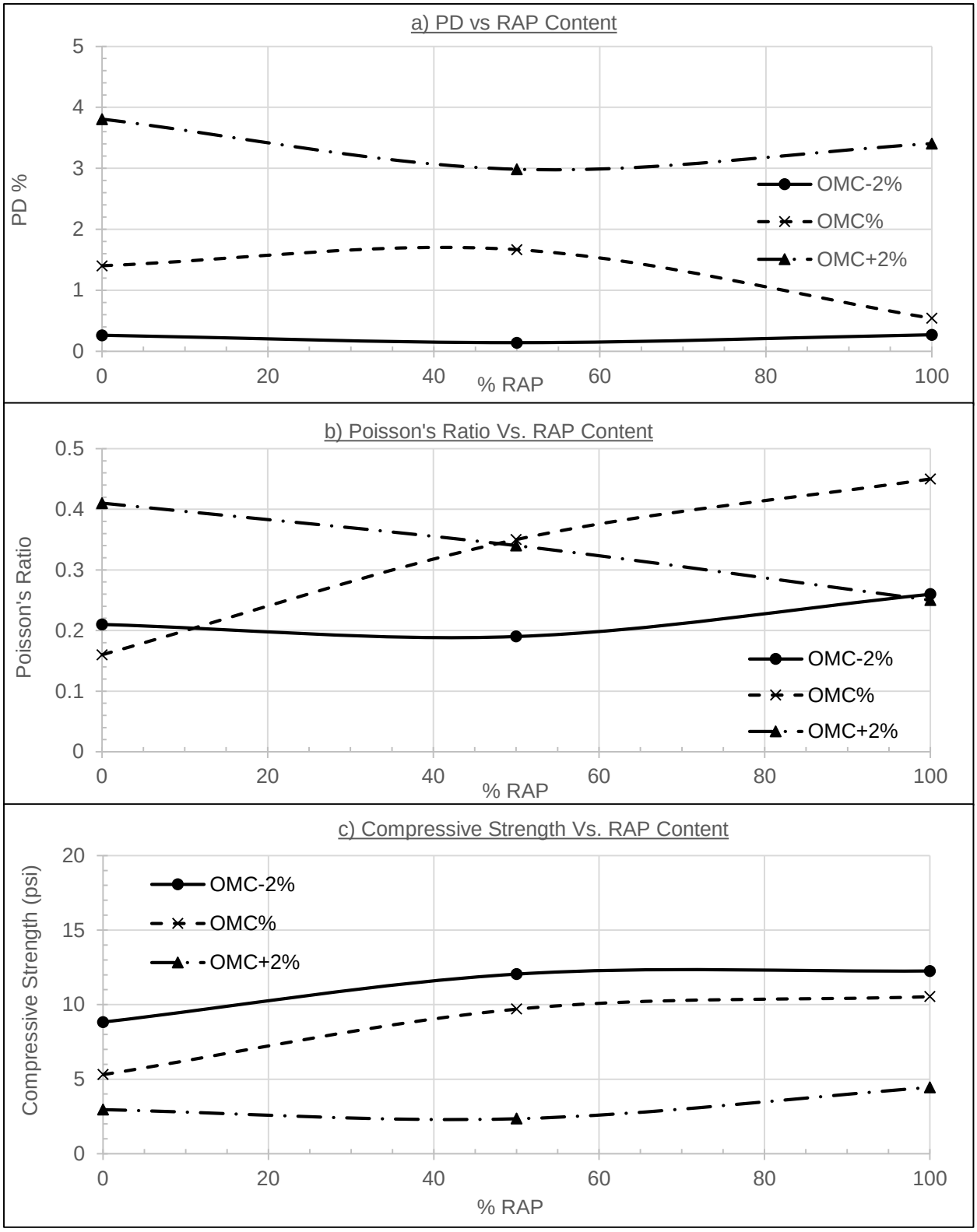

Figure 7.14. Comparison between PD and Un-confined Compression Parameters versus RAP Content for RAP TH 10 + Old Class 5 Blends

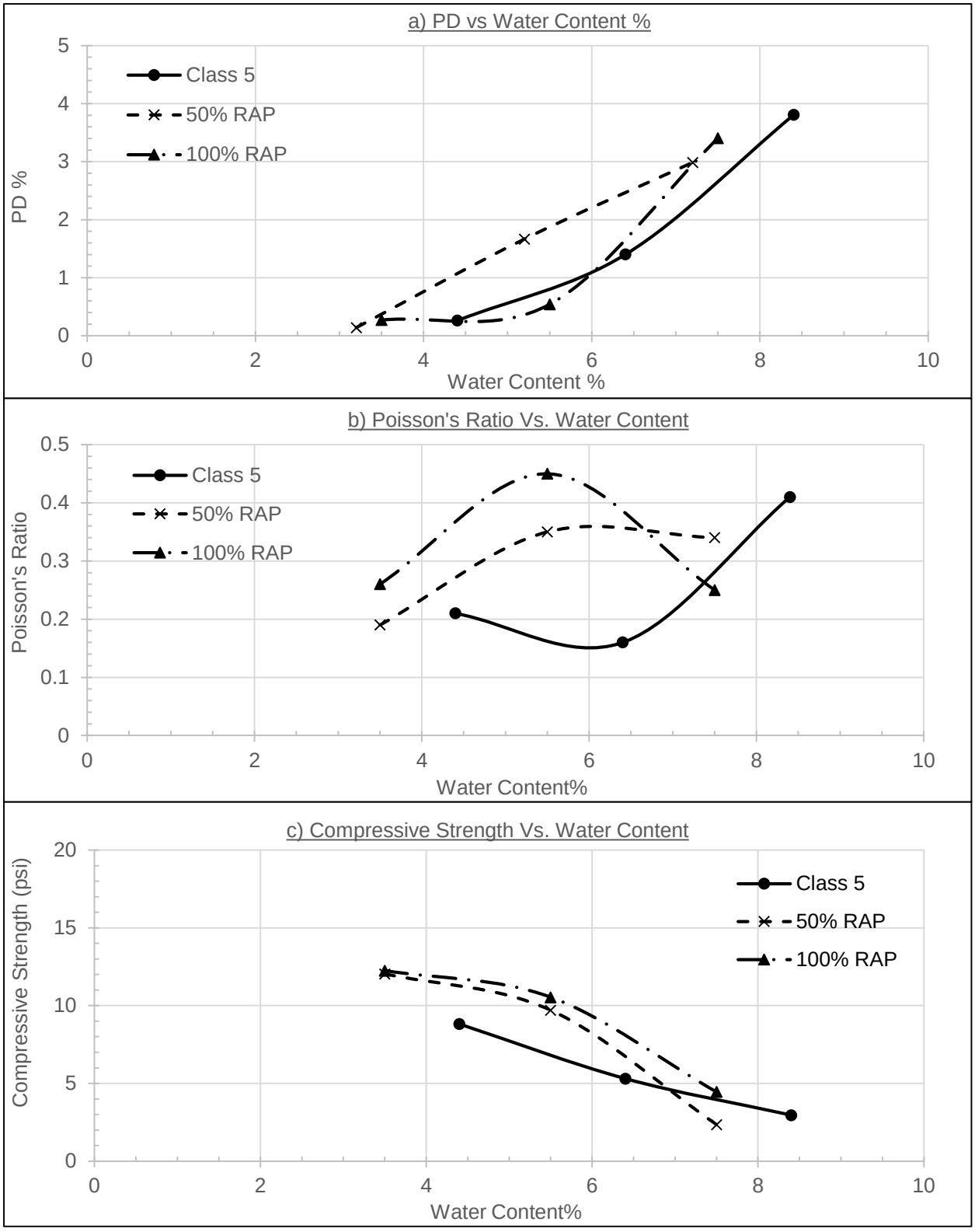

Figure 7.15. Comparison between PD and Un-confined Compression Parameters versus Water Content for RAP TH 10 + Old Class 5 Blends

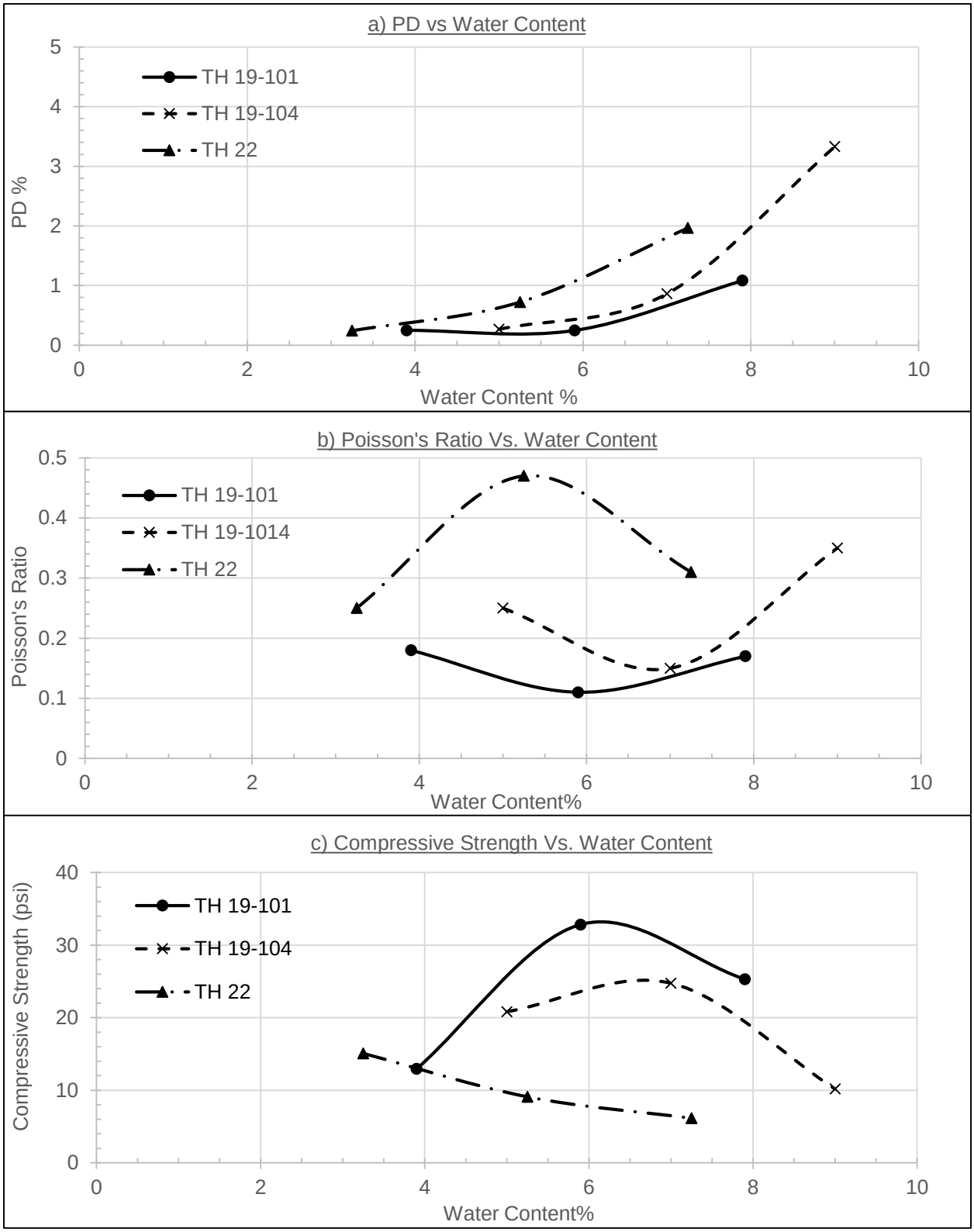

Figure 7.16. Comparison between PD and Un-confined Compression Parameters versus Water Content for Other Field RAP Blends

7.6. Poisson's Ratio Task Summary

By studying three different testing conditions for RAP/Aggregate blends on both measured parameters Poisson's ratio and ultimate compressive strength, several outcomes can be concluded for each condition. The first testing condition is the RAP content, it is proved that increasing RAP content affects positively or negatively on the compressive strength depending on the RAP aging characteristics and granular aggregate properties. No typical standard shape can be concluded for the Poisson's ratio relationship with RAP content. However, it seems to be that the 50% RAP content is a critical point in most cases, as Poisson's ratio reaches its maximum or minimum value at this point.

Water content variation is the second testing condition investigated. In most cases, it is found that increasing water content affects negatively on the compressive strength. However, two of the field RAP sources (TH19-101 & TH 19-104) achieved their ultimate compressive strength at OMC% level. Strength of RAP TH 29 blends is found to be un-affected by water content variation at both RAP contents 50% and 100%. Poisson's ratio for granular aggregates is found to be in its lowest value at OMC% level.

After adding RAP, Poisson's ratio have two main trends; as it reaches its highest optimum values at OMC% level as for RAP's TH 29, TH 10, TH 22 or lowest values at OMC% for TH 19-101 and TH 19-104 which the same trend of both types of Class 5 used. This can be explained by the role of the aged binder in the RAP. If it is still effective so it will cause softening effect to the whole blend by adding water. While if it is completely aged, RAP behaves the same as granular aggregate reaching its strongest point at OMC% with high strength and low Poisson's ratio values.

It can be concluded that aging of RAP and aggregate material strength properties have a significant and very important role for both tested parameters. When RAP is more aged it behaves

normally like granular aggregates, depending on its material strength compared to the aged RAP. At this case there is insignificant effect on Poisson's ratio and normal decreasing effect on compressive strength by increasing water content. And when RAP is not completely aged, it affects drastically on the compressive strength causing significant increase in Poisson's ratio. An additional conclusion can be understood that aging of RAP is related to the asphalt binder percentage. As field samples has higher strength than lab implemented samples with lower asphalt content as shown in Tables 3.1 and 3.2. This means that the ultimate compressive strength is indirect proportional to the percentage of aged asphalt binder in RAP/Aggregate blends.

Generally by comparing M_R with un-confined compression parameters, M_R has the same behavior with ultimate compressive strength as expected. As both parameters increase by increasing RAP content while they decrease by increasing water content. While on the other hand, no general trend is found from M_R and Poisson's ratio comparison especially with RAP content increase. However the variation with water content shows that OMC% level is a critical condition for Poisson's ratio parameter.

Finally by comparing PD with un-confined strength parameters, a typical direct relation is found for both parameters PD and Poisson's ratio with RAP content increase at three water contents investigated. This relation is significant for RAP content up to 50% then reversed to indirect relationship especially at OMC% and OMC+2% water levels. On the other hand, by comparing both parameters as PD was increasing with water content increase, Poisson's ratio has critical condition at OMC% level. From comparing PD with ultimate compressive strength, an indirect relation is found that as PD increase with water content increase, the compressive strength decreases. While a direct relationship is found for both parameters with RAP content increase.

CHAPTER 8. CONCLUSIONS AND RECOMMENDATIONS

8.1. RAP Effectiveness on M_R Modeling

From comparing the predicted and measured values of M_R for different prediction models, it is obvious that the MEPDG is considered the best-fit for RAP behavior under tested conditions. This result is understood to the relative closeness of the regression lines, obtained from this model, to the equity line. In addition, this conclusion is confirmed by results of the calculated R^2 as this model yield the highest values for all the tested conditions

This model is proceeded with an extra study for calculating dimensionless multiple regression constants K parameters. Generally, the parameters of this model are highly affected by the water content variation, slightly affected by decreasing the maximum dry density level and almost not affected by freeze-thaw cycles at all RAP contents. This model parameters (K's for Equation 4.1) are not highly affected by increasing the percentage of RAP. Also this model in general, gives the best prediction M_R values at 50% to 75% RAP in the base layer blend**.**

This model fits all four concentrations of RAP-Aggregate combinations (0%, 50%, 75% and 100%) especially for confining pressure levels below10 psi. As K_1 is dramatically affected by confining pressure levels however, this variation is minimized at water contents close to OMC%. Generally, K_1 increases by increasing percentage of RAP at confining pressure levels below 10 psi. While K_2 decreases with increasing percentage of RAP at low confining pressure levels (< 10 psi) and vice versa at high confining pressure (> 10 psi). Water content variation is an effective factor on K_2 values for the case of RAP. However, this effect diminishes when reaching the OMC%. K_2 values at high confining pressure levels above 10 psi are below zero which contradicts with the concept of stress stiffening related to this parameter confirmed by the literature survey.

The K_3 values are affected by confining pressure variation especially at intermediate level (10 psi). Nevertheless, this variation is the least at water content levels close to OMC% when using RAP. K_3 value is negative at low confining pressure levels (< 10 psi) and water contents close to OMC%. This finding seems to be reasonable and satisfy the concept of shear softening related to this parameter, as confirmed in the literature. K_3 values are almost the same for the two cases of with or without RAP in the base course.

8.2. RAP Effectiveness on PD Modeling

By studying the rutting model effectiveness in MEPDG on measured PD data from several tests, it can be concluded from the resilient modulus test, that this model is found highly significant in two cases only: 50% and 100% RAP at OMC-2% as predicted values are so close to those measured. However, the predicted values for the other RAP contents are significantly less than those measured at different water contents. These results are expect to be related to the stress history of resilient modulus test procedure used for collecting PD data.

The PD-MEPDG model seems better in terms of predicting PD for data collected from single-stage RTL test than the resilient modulus test. It is highly significant for the case of using RAP in base layer blends especially for 50% RAP content. This high accurate prediction is found also for Class 5 granular aggregate in OMC% at 17 psi deviator stress level. Best results of the high accuracy of the PD prediction is shown in 50% RAP blend at OMC% water content level under 17 and 37 psi deviator stress levels. By adding 6% fines to the 50% RAP blend, the prediction accuracy is affected significantly. As the prediction under-estimates the PD values except at OMC% under 17 psi deviator stress level it is overestimated.

For PD data collected from the multi-stage RTL test, it is obvious that PD-MEPDG model is more significant in prediction for the measured PD data by single-stage RTL test other than the

multi-stage. This finding is concluded to the effect of the stress history from applying successive stages of loading on base layer blends as the M_R test. Finally, it is found that the PD-MEPDG model is highly accurate for data measured by single-stage RTL test at water contents close to OMC% and at deviator stresses lower than 24 psi.

8.3. Correlation for Both M_R and PD Parameters

By achieving this comparison on data collected from several tests, few conclusions can be considered from each test individually. From resilient modulus testing, at OMC% it is found that as the percentage of RAP exceeds 50%, M_R increases and PD decreases which is recommended for base layer design considerations. While the trend at OMC+2% do not have a typical pattern and this is due to the approach of the PD from the failure limit. By increasing RAP content to 100%, M_R reaches its highest value while PD reaches its lowest.

For data collected of both parameters in RTL testing, as the deviator stress increases for both granular aggregates and RAP/Aggregate blends, PD increases without a significant difference in M_R values at both water content levels OMC-2% and OMC%. While adding 50% RAP to the base layer improves the performance by increasing M_R and decreasing PD values. For single-stage RTL test, modifying the 50% RAP blends by 6% plastic fines do not have any positive effects on base layer performance at both water content levels OMC-2% and OMC%. However for multi-stage RTL test, modifying the 50% RAP samples by 3.5% plastic fines has a significant positive effect on the performance of the samples at the three water contents; OMC-2%, OMC% and OMC+2%.

8.4. Poisson's Ratio Effectiveness on RAP behavior

It is proved that increasing RAP content affects on the compressive strength depending on the RAP aging characteristics and granular aggregate properties. For RAP/Aggregate blends, it is found that Poisson's ratio reaches its highest optimum values at OMC% level then decreases by varying water content from this level. On the other hand for granular aggregates, it is found to be in its lowest value at OMC% level. In most cases, it is found that increasing water content affects negatively on the compressive strength.

Generally by comparing M_R with Poisson's ratio, no general trend is found from this comparison especially with RAP content increase. However the variation against water content shows that OMC% level is a critical condition for Poisson's ratio parameter. While by comparing PD with Poisson's ratio parameter, a typical direct relation is found for both parameters PD and Poisson's ratio with RAP content increase at three water contents investigated. This relation is significant for RAP content up to 50% then reversed to indirect relationship especially at OMC% and OMC+2% water levels. On the other hand, by comparing both parameters with water content increase, PD increases while Poisson's ratio has critical condition at OMC% level.

8.5. Final Summary

Both models used in the MEPDG for prediction of both parameters M_R and PD are totally significant for RAP/Aggregate blends used for pavement base layer. The prediction is at the highest accuracy at water content levels close to OMC%, MDD and with 50% to 75% RAP content. Poisson's ratio is an effective parameter on both parameters especially with variation of water content as a typical relation is found between investigated parameters with this factor. The ultimate compressive strength have the same behavior like M_R parameter, which is expected as both

parameters evaluate strength of samples, the first is under static loading while the second is under dynamic loading.

8.6. Recommendations for Future Research

A further study is needed to investigate the aged properties of RAP before mixing with traditional granular aggregates. As there is a need to focus especially on aged binder to know if it is still effective or not. This point is very important with water content variation as the reaction between aged binder and water content may cause stress stiffening or shear softening depending on the chemical properties of the aged binder.

Also there is a need to evaluate statistical significance for both M_R and PD prediction models on stabilized RAP/Aggregate blends. These RAP blends are stabilized by modifying the gradation through adding fines and/or by adding different rejuvenating agents such as virgin binder or used motor oil. Stabilization of RAP blends is important to reactive the properties of the original asphalt mixes.

REFERENCES

Adu-Osei, A. (2000). Characterization of unbound granular layers in flexible pavements *Research Project Title: Evaluation of Superpave Aggregate Specifications.* (pp. 260 p.). Washington, DC.

Alam, T. B., Abdelrahman, M., & Schram, S. A. (2010). Laboratory characterisation of recycled asphalt pavement as a base layer. *International Journal of Pavement Engineering, 11*(2), 123-131.

Andrei, D., Witczak, M. W., Schwartz, C. W., & Uzan, J. (2004). Harmonized resilient modulus test method for unbound pavement materials. *Transportation Research Record: Journal of the Transportation Research Board, 1874*(1), 29-37.

Arnold, G. K. (2004). *Rutting of granular pavements.* (Ph.D.), University of Nottingham.

Astm, C. (2014). 469/469M *Standard test method for static modulus of elasticity and Poisson's ratio of concrete in compression. West Conshohochen: American Society for Testing and Materials*.

Attia, M., & Abdelrahman, M. (2011). Effect of state of stress on the resilient modulus of base layer containing reclaimed asphalt pavement. *Road Materials and Pavement Design, 12*(1), 79-97.

Attia, M., Abdelrahman, M., Alam, T., Section, M. D. o. T. R. S., & Department, N. D. S. U. C. E. (2009). Investigation of Stripping in Minnesota Class 7 (RAP) and Full-depth Reclamation Base Materials: Minnesota Department of Transportation, Research Services Section.

Attia, M. I. E.-S. (2010). *Characterization of the structural behavior of reclaimed asphalt pavement as pavement base layer*: North Dakota State University.

Bani Hashem, E., & Zapata, C. E. (2013). *Enhancement of Permanent Deformation Model for Unbound Materials Used by DARwin-ME.* Paper presented at the Transportation Research Board 92nd Annual Meeting.

Bennert, T., & Dongré, R. (2010). Backcalculation method to determine effective asphalt binder properties of recycled asphalt pavement mixtures. *Transportation Research Record: Journal of the Transportation Research Board, 2179*(1), 75-84.

Bennert, T., & Maher, A. (2005). The development of a performance specification for granular base and subbase material (C. f. A. I. T. (CAIT), Trans.). Piscataway, NJ 08854-8014: Rutgers, The State University

Bilodeau, J.-P., Doré, G., & Depatie, J. (2013). Mitigation of permanent deformation in base layer containing recycled asphalt aggregates. *Canadian Journal of Civil Engineering, 40*(2), 181-187.

Bowers, B. F., Huang, B., Shu, X., & Miller, B. C. (2014). Investigation of Reclaimed Asphalt Pavement blending efficiency through GPC and FTIR. *Construction and Building Materials, 50*, 517-523.

Chehab, G. R., & Daniel, J. S. (2006). Evaluating recycled asphalt pavement mixtures with mechanistic-empirical pavement design guide level 3 analysis. *Transportation Research Record: Journal of the Transportation Research Board, 1962*(1), 90-100.

Chesner, W., Collins, R., & MacKay, M. (1997). User Guidelines for Waste and By-product Materials in Pavement Construction, US Department of Transportation, Federal Highway Administration, Publication No: FHWA-RD-97-148.

Christopher, B., Schwartz, C., & Boudreau, R. (2006). Geotechnical aspects of pavements. *Report No. FHWA NHI-05-037. Washington, DC, US Department of Transportation, Federal Highway Administration*.

Cosentino, P., Kalajian, E., Shieh, C., Mathurin, W., Gomez, F., Cleary, E., & Treeratrakoon, A. (2003). Developing specifications for using recycled asphalt pavement as base, subbase or general fill materials, phase II (C. Engineering, Trans.) (pp. 272): Florida Institute of Technology.

Cosentino, P. J., Kalajian, E. H., Bleakley, A. M., Diouf, B. S., Misilo, T. J., Petersen, A. J., . . . Sajjadi, A. M. (2012). Improving the properties of reclaimed asphalt pavement for roadway base applications (C. Engineering, Trans.) (pp. 605): Florida Institute of Technology.

Cosentino, P. J., Kalajian, E. H., Dikova, D., Patel, M., & Sandin, C. (2008). Investigating the Statewide Variability and Long Term Strength Deformation Characteristics of RAP and RAP-Soil Mixtures (C. Engineering, Trans.) (pp. 411): Florida Institute of Technology.

Deniz, D., Tutumluer, E., & Popovics, J. S. (2009). Expansive characteristics of reclaimed asphalt pavement (RAP) used as base materials (I. C. f. Transportation, Trans.) (pp. 92): University of Illinois at Urbana-Champaign

El-Badawy, S. M. A. (2006). *Development of a Mechanistic Constitutive Model for the Repeated Load Permanent Deformation Behavior of Subgrade Pavement Materials.* Arizona State University.

El-Basyouny, M., Witczak, M., & Kaloush, K. (2005). *Development of the permanent deformation models for the 2002 design guide.* Paper presented at the Proc., Transportation Research Board 84th Annual Meeting.

El-Basyouny, M. M. (2004). *Calibration and validation of asphalt concrete pavements distress models for 2002 design guide.* Arizona State University.

Erlingsson, S., & Rahman, M. S. (2013). Evaluation of Permanent Deformation Characteristics of Unbound Granular Materials from Multi-Stage Repeated Load Triaxial Test. *in Transport Research Records: Journal of the Transportation Research Board*.

Garg, N., & Thompson, M. R. (1996). Lincoln Avenue reclaimed asphalt pavement base project. *Transportation Research Record: Journal of the Transportation Research Board, 1547*(1), 89-95.

Garg, N., & Thompson, M. R. (1997). Triaxial characterization of Minnesota road research project granular materials. *Transportation Research Record: Journal of the Transportation Research Board, 1577*(1), 27-36.

Guide, M. E. P. D. (2008). A Manual of Practice. *American Association of State Highway and Transportation Officials*.

Highway, A. A. o. S., & Officials, T. (1993). *AASHTO Guide for Design of Pavement Structures, 1993* (Vol. 1): AASHTO.

Highway, A. A. o. S., & Officials, T. (2011). *Standard specifications for transportation materials and methods of sampling and testing*: AASHTO.

Huang, Y. H. (1993). *Pavement analysis and design*: Prentice Hall.

Huesemann, M. H., Hausmann, T. S., & Fortman, T. J. (2005). Leaching of BTEX from aged crude oil contaminated model soils: Experimental and modeling results. *Soil & Sediment Contamination, 14*(6), 545-558.

Itani, S. Y. (1990). *Behavior of base materials containing large sized particles.* (Ph.D.), Georgia Institute of Technology.

Jennings, P., Pribanic, P., Campbell, W., Dawson, K., Shane, S., & Taylor, R. (1980). High pressure liquid chromatography as a method of measuring asphalt composition (D. o. Chemistry, Trans.) (pp. 82). Bozeman, MT: Montana State University.

Jeon, E., Steven, B., & Harvey, J. (2009). Laboratory testing and performance evaluation of recycled pulverized hot-mix asphalt material. *Transportation Research Record*(2014), 42-52.

Kang, D.-H., Gupta, S. C., Bloom, P., Ranaivoson, A. Z., Roberson, R., & Siekmeier, J. (2011). Recycled materials as substitutes for virgin aggregates in road construction: II. Inorganic contaminant leaching. *Soil Science Society of America Journal, 75*(4), 1276-1284.

Kang, D.-H., Gupta, S. C., Ranaivoson, A. Z., Siekmeier, J., & Roberson, R. (2011). Recycled materials as substitutes for virgin aggregates in road construction: I. Hydraulic and mechanical characteristics. *Soil Science Society of America Journal, 75*(4), 1265-1275.

Kim, W., & Labuz, J. (2007). Resilient modulus and strength of base course with recycled bituminous material (C. Engineering, Trans.) (pp. 270). Minneapolis, MN: University of Minnesota.

Lekarp, F., Isacsson, U., & Dawson, A. (2000a). State of the art. I: Resilient response of unbound aggregates. *Journal of transportation engineering, 126*(1), 66-75.

Lekarp, F., Isacsson, U., & Dawson, A. (2000b). State of the art. II: Permanent strain response of unbound aggregates. *Journal of transportation engineering, 126*(1), 76-83.

MacGregor, J. A., Highter, W. H., & DeGroot, D. J. (1999). Structural numbers for reclaimed asphalt pavement base and subbase course mixes. *Transportation Research Record: Journal of the Transportation Research Board, 1687*(1), 22-28.

Madjadoumbaye, J., & Tamo, T. (2012). Influence of Poisson's Ratio on the Stresses, Strains and Deflections in Pavement Design. *Electronic Journal of Geotechnical Engineering, 17*.

Maher, A., & Bennert, T. A. (2008). Evaluation of Poisson's ratio for use in the mechanistic empirical pavement design guide (MEPDG) (C. E. Engineering, Trans.) (pp. 60): Center for Advanced Infrastructure & Transportation (CAIT), Rutgers, The State University.

McDaniel, R., & Anderson, R. M. (2001). *Recommended use of reclaimed asphalt pavement in the superpave mix design method: guidelines*: Transportation Research Board, National Research Council.

McDaniel, R. S., & Shah, A. (2003). Use of reclaimed asphalt pavement (RAP) under Superpave specifications. *Asphalt Paving Technology, 72*, 226-252.

McDaniel, R. S., Soleymani, H., Anderson, R. M., Turner, P., & Peterson, R. (2000). Recommended use of reclaimed asphalt pavement in the Superpave mix design method. *NCHRP Web document, 30*.

Mohammad, L. N., Herath, A., Rasoulian, M., & Zhongjie, Z. (2006). Laboratory evaluation of untreated and treated pavement base materials: Repeated load permanent deformation test. *Transportation Research Record: Journal of the Transportation Research Board, 1967*(1), 78-88.

Mulvaney, R., & Worel, B. (2001). MnROAD Cell 26 Forensic Investigation. *Commercially Unpublished Report to the Office of Materials and Road Research. Minnesota Department of Transportation*.

Papp, W., Maher, M., Bennert, T., & Gucunski, N. (1998). *Behavior of construction and demolition debris in base and subbase applications.* Paper presented at the Recycled Materials in Geotechnical Applications.

Park, S.-W. (2000). *Evaluation of accelerated rut development in unbound pavement foundations and load limits on load-zoned pavements.* Texas A & M University.

Pezo, R. F. (1993). *A general method of reporting resilient modulus tests of soils, a pavement engineer's point of view.* Paper presented at the 72nd Annual Meeting of the Transportation Research Board, Washington, DC.

Protocol, L.-T. P. P. (1996). P46, Resilient Modulus of Unbound Granular Base/Subbase Materials and Subgrade Soils. *Long-Term Pavement Performance*.

Puppala, A. J., Hoyos, L. R., & Potturi, A. K. (2011). Resilient moduli response of moderately cement-treated reclaimed asphalt pavement aggregates. *Journal of Materials in Civil Engineering, 23*(7), 990-998.

Puppala, A. J., Saride, S., & Williammee, R. (2011). Sustainable reuse of limestone quarry fines and RAP in pavement base/subbase layers. *Journal of Materials in Civil Engineering, 24*(4), 418-429.

Seed, H. B., Chan, C., & Lee, C. E. (1962). *Resilience characteristics of subgrade soils and their relation to fatigue failures in asphalt pavements.* Paper presented at the International Conference on the Structural Design of Asphalt Pavements. Supplement.

Song, Y., & Ooi, P. (2010). Interpretation of shakedown limit from multistage permanent deformation tests. *Transportation Research Record: Journal of the Transportation Research Board*(2167), 72-82.

Tabaković, A., Gibney, A., McNally, C., & Gilchrist, M. D. (2010). Influence of recycled asphalt pavement on fatigue performance of asphalt concrete base courses. *Journal of Materials in Civil Engineering, 22*(6), 643-650.

Taha, R., Ali, G., Basma, A., & Al-Turk, O. (1999). Evaluation of reclaimed asphalt pavement aggregate in road bases and subbases. *Transportation Research Record: Journal of the Transportation Research Board, 1652*(1), 264-269.

Tam, W., & Brown, S. (1988). *Use of the falling weight deflectometer for insitu evaluation of granular materials in pavements.* Paper presented at the Australian Road Research Board (ARRB) Conference, 14th, 1988, Canberra.

Tayebali, A. A., Tsai, B.-w., & Monismith, C. L. (1994). *Stiffness of asphalt-aggregate mixes*: Strategic Highway Research Program, National Research Council Washington DC.

Townsend, T. (1998). Leaching characteristics of asphalt road waste (E. E. Sciences, Trans.) (pp. 77). Gainesville, FL: University Of Florida.

Tseng, K.-H., & Lytton, R. L. (1989). Prediction of permanent deformation in flexible pavement materials. *Implication of Aggregates in the Design, Construction, and Performance of Flexible Pavements, ASTM STP, 1016*, 154-172.

Tutumluer, E., & Meier, R. W. (1996). Attempt at resilient modulus modeling using artificial neural networks. *Transportation Research Record: Journal of the Transportation Research Board, 1540*(1), 1-6.

Uzan, J. (1985). Characterization of granular material. *Transportation Research Record*(1022).

Waldenmaier, A. J., Abdelrahman, M., & Attia, M. (2013). Strain Response of Reclaimed Asphalt Pavement Material Blends under Extended Loading Testing. *Journal of Materials in Civil Engineering*, *25*(11), 1674-1681.

Wen, H., & Wu, M. (2011). Evaluate high percentage recycled asphalt pavement as base materials (T. N. R. C. X. (TransNow), Trans.) (pp. 142). Seattle, Washington: University of Washington.

Werkmeister, S. (2004). *Permanent deformation behaviour of unbound granular materials in pavement constructions*: Techn. Univ., Fak. Bauingenieurwesen.

Witczak, M. (2003). NCHRP 1-28A: Harmonized Test Method for Laboratory Determination of Resilient Modulus for Flexible Pavement Design: Final Report. TRB, National Research Council, Washington, DC.

Witczak, M., Andrei, D., & Houston, W. (2000). Guide for mechanistic-empirical design of new and rehabilitated pavement structures. Appendix DD-1: Resilient modulus as function of soil moisture—Summary of predictive models. *Final report to National Cooperative Highway Research Program, Report*(1-37A).

Witczak, M., Andrei, D., & Houston, W. (2004). Guide for Mechanistic–Empirical Design of New and Rehabilitated Pavement Structures. *Transportation Research Board of the National Research Council*, 1-91.

Witczak, M., & Uzan, J. (1988). The universal airport pavement design system. *Report I of V: granular material characterization, Department of Civil Engineering, University of Maryland, College Park, MD*.

Witczak, M. W. (2003). Harmonized Test Methods for Laboratory Determination of Resilient Modulus For Flexible Pavement Design (N. C. H. R. Program, Trans.).

Witczak, M. W. (2004). *Laboratory determination of resilient modulus for flexible pavement design*: Transportation Research Board.

Yoder, E. J., & Witczak, M. W. (1975). *Principles of pavement design*: John Wiley & Sons.

Zahid Hossain, P. S., Musharraf Zaman, Sharon Lewis and Kenneth Habson. (2012). Influence of Recovery Processes on Properties of Binders and Aggregates Recovered from Recycled Asphalt Pavement (Vol. 9, No. 2).

Zak, J., Stastna, J., Vavricka, J., Milackova, K., Kasek, L., & Zanzotto, L. (2014). *Poisson's Ratio of Hot Asphalt Mixtures Determined by Relaxation and Small Amplitude Oscillation Tests.* Paper presented at the Design, Analysis, and Asphalt Material Characterization for Road and Airfield Pavements.

Zeng, X., & Hu, R. (2013). Developing an Economical and Reliable Test for Measuring the Resilient Modulus and Poisson's Ratio of Subgrade Soils. *Bridges, 10,* 9780784413128.9780784413006.

Zhang, X. Y., & Sun, D. Y. (2012). The Aging Rules of Asphalt and General Study on RAP. *Applied Mechanics and Materials, 105,* 1211-1214.

APPENDIX A. RESILIENT MODULUS DATA MODELING

Table A1. M_R data for Class 5 versus Water Content Variation

WC = OMC-3%			WC = OMC-2%			WC = OMC-1%		
Seq.	Meas. M_R (psi)	Pred. M_R (psi)	Seq.	Meas. M_R (psi)	Pred. M_R (psi)	Seq.	Meas. M_R (psi)	Pred. M_R (psi)
						2	28071	28774
			3	58487	53818	3	40147	42584
4	62935	76105	4	69275	72188	4	57105	57465
5	80361	91698	5	87745	87741	5	40225	70534
6	26926	26514	6	33871	22305	6	19507	18112
7	35327	43166	7	37185	38239	7	27263	30892
8	58325	60712	8	50515	55067	8	41581	44925
9	78040	78434	9	69540	71643	9	60605	59555
10	98346	93210	10	87979	84942	10	81929	72047
11	35581	30171	11	25794	25360	11	19544	20889
12	53215	47907	12	37582	41564	12	36585	34701
13	72208	65703	13	55585	57199	13	58450	49145
14	94981	82939	14	76057	71377	14	82687	63584
15	111812	96879	15	92548	82043	15	99725	75543
16	33846	33448	16	26421	28021	16		
17	54226	52051	17	41248	44289	17	41789	38073
18	75040	70099	18	60086	58984	18	68508	52900
19	92641	87162	19	78325	71632	19	80680	67366
20	113281	100765	20	89859	80818	20	92642	79172
21	38233	39157	21	29074	32465	21	28248	27865
22	59516	59102	22	45975	48567	22	45372	43896
23	81275	77664	23	63758	61886	23	60523	59440
24	95300	94798	24	73919	72695	24	70559	74237
25	104958	108304	25	88144	80290	25	81489	86171
26	36142	44044	26	28170	36066	26	27355	31749
27	57307	65024	27	46607	51849	27	45730	48866
28	78953	84106	28	64946	64214	28		
29	94945	101546	29	77651	73962	29	65049	80355
30	102933	115254	30	71755	80727	30	81547	92630

Table A1. M_R data for Class 5 versus Water Content Variation (Continued)

WC = OMC%			WC = OMC+1%			WC = OMC+2%		
Seq.	Meas. M_R (psi)	Pred. M_R (psi)	Seq.	Meas. M_R (psi)	Pred. M_R (psi)	Seq.	Meas. M_R (psi)	Pred. M_R (psi)
1	12796	12162						
2	19011	22847	2	13962	17483	2	16951	22530
3	25633	32964	3	21539	25915	3	22735	32874
4	37733	44239	4	32893	34845	4	34815	43485
5	50439	53658	5	43400	42518	5	48775	52315
6	17124	14413	6	11900	10852	6	18726	14098
7	19860	23990	7	16163	18567	7	16323	23626
8	28212	33830	8	24002	26843	8	24249	33427
9	42186	43692	9	36251	35185	9	38296	42851
10	55090	50940	10	47758	42055	10	49648	50253
11	17481	16520	11	14298	12409	11	15231	15901
12	25049	26334	12	20253	20449	12	19271	25442
13	36797	34942	13	30559	28466	13	28620	34355
14	44497	42497	14	40918	36039	14	37714	42194
15	58073	48110	15	50674	41976	15	42890	47931
16	19953	18000	16	16183	13788	16	13826	17450
17	28077	27522	17	22666	22045	17	19139	26899
18	37644	35669	18	31646	29862	18	42254	35120
19	46595	42187	19	38911	36960	19	33691	41946
20	54367	47010	20	46787	42386	20	42254	46745
21	20709	20130	21	18472	16150	21	16339	19994
22	29911	29613	22	25048	24664	22	20975	29126
23	37154	36570	23	30299	32202	23	28955	36340
24			24	38447	38766	24	37425	41942
25	53331	45954	25	38352	43675			
26	22707	23028	26	16463	18124			
27	30343	43533	27	19219	26776			
28	38559	37452						
30	49341	45568						

Table A2. M_R data for Class 5 at 90% Maximum Dry Density

WC = OMC-2%			WC = OMC%			WC = OMC+2%		
Seq.	Meas. M_R (psi)	Pred. M_R (psi)	Seq.	Meas. M_R (psi)	Pred. M_R (psi)	Seq.	Meas. M_R (psi)	Pred. M_R (psi)
						1	11431	8518
2	29536	27893	2	28073	26237	2	11858	13898
3	36935	40102	3	34731	37680	3	17103	19767
4	48448	52342	4	45425	48670	4	26439	25955
5	61459	62307	5	56418	57140	5	36067	31331
6	23610	17671	6	19812	16255	6	9672	9234
7	27104	29034	7	24516	26712	7	12704	14913
8	36491	40374	8	33882	36567	8	20324	20975
9	50965	50940	9	45241	44986	9	30237	27227
10	65642	58988	10	56875	50761	10	37025	32562
11	20243	19748	11	18765	17836	11	10408	10553
12	28233	30863	12	26054	27277	12	15516	16759
13	42564	40806	13	38362	34728	13	24490	23174
14	56424	49154	14	46339	39972	14	31277	29614
15	63947	54992	15	49935	42923	15	35306	35007
16	20172	21497	16	17988	19070	16	11621	11754
17	30088	32269	17	25895	27523	17	17486	18414
18	43427	41140	18	33013	33255	18	22166	25151
19	46967	48083	19	35170	36651			
20	54518	52693	20	43446	38204			
21	20647	24292	21	20398	20829			
22	33524	34303	22	25681	27532			
23	38112	41639	23	24252	31000			
24	43318	46898						

Table A3. M_R data for Class 5 after Two Freeze-Thaw Cycles

WC = OMC%			WC = OMC+2%		
Seq.	Meas. M_R (psi)	Pred. M_R (psi)	Seq.	Meas. M_R (psi)	Pred. M_R (psi)
1	19010	14271			
2	22387	24540			
3	32760	36104	3	26385	29820
4	45824	48482	4	37149	38965
5	61918	59288	5	48929	46668
6	16652	15537			
7	24217	26291	7	18667	22126
8	35396	37944	8	29345	30877
9	51313	50098	9	41143	39483
10	66916	60363	10	50358	46464
11	17078	17863	11	15954	15418
12	26897	29427	12	24465	24219
13	41042	41388	13	33894	32728
14	54203	53231	14	43465	40633
15	70871	62961	15	51066	46778
16	19519	19968	16	18365	16980
17	31025	32189	17	25851	25996
18	45814	44396	18	34742	34323
19	59917	56180	19	43629	41800
20	70066	65715	20	50129	47491
21	23925	23674	21	21649	19635
22	36149	36929	22	30110	28912
23	45031	49608	23	33839	36997
24	55500	61540	24	37678	44006
25	69005	71075			
26	23734	26882			

Table A4. M_R data for 50% Old Class 5/50% RAP TH 10 versus Water Content Variation

WC = OMC-3%			WC = OMC-2%			WC = OMC-1%		
Seq.	Meas. M_R (psi)	Pred. M_R (psi)	Seq.	Meas. M_R (psi)	Pred. M_R (psi)	Seq.	Meas. M_R (psi)	Pred. M_R (psi)
			3	79563	93197			
			4	96009	115717			
			5	115888	133289	5	158978	158039
			6	59511	48291	6		
			7	72912	72232	7	69655	65970
			8	106606	94318	8	89025	95677
9	166865	165353	9	128302	113703	9	118361	123676
10	195384	187132	10	172143	127986	10	147467	144873
11	88891	65093	11	68694	52756	11	56183	42121
12	106162	101246	12	75931	76859	12	69736	69676
13	120887	128830	13	103232	96162	13	90312	94579
14	155937	149476	14	116191	111406	14	114471	115047
15	176834	162548	15	132801	122069	15	148128	128804
16	79977	70908	16	57896	57623	16	50241	46106
17	98114	103494	17	68726	80619	17	65285	72337
18	124789	125288	18	89029	97447	18	93446	93610
19	146299	139778	19	109153	110403	19	108086	109446
20	153902	147853	20	121372	119177	20	135837	119252
21	74100	79567	21	51533	65029	21	50479	52354
22	93177	105139	22	68081	85221	22	73252	75809
23	115324	119668	23	89777	99370	23	90690	91981
24	126536	127403	24	104853	109666	24	100607	102442
25	143773	130595	25	123227	116331	25	117701	108209
26	63177	84464	26	57400	69801	26	43848	56999
27	81690	105391	27	77143	88457	27	65268	77882
28	106859	115980	28	98471	100810	28	84960	90654
29	128328	119512	29	117858	109596	29	97607	98112
30	132044	120495	30	127251	115172	30	103679	101861

Table A4. M_R data for 50% Class 5 + 50% RAP TH 10 versus Water Content Variation (Continued)

WC = OMC%			WC = OMC+1%			WC = OMC+2%		
Seq.	Meas. M_R (psi)	Pred. M_R (psi)	Seq.	Meas. M_R (psi)	Pred. M_R (psi)	Seq.	Meas. M_R (psi)	Pred. M_R (psi)
			1	35776	20538	1	23390	18175
2	43861	40327	2	35165	34363	2	25393	27921
3	58545	59785	3	43331	49283	3	32965	37954
4	79804	79924	4	60409	63710	4	46160	47774
5	95985	96487	5	78201	75029	5	59326	55564
6	33112	24328	6	28393	21430	6	21272	18988
7	42158	41870	7	31960	35373	7	27054	29149
8	55494	60023	8	42196	48580	8	35927	38964
9	74963	76579	9	60794	59840	9	50180	47719
10	93959	89093	10	77284	67937	10	63612	54362
11	31244	27275	11	27860	23904	11	23209	21143
12	41346	45324	12	37163	37224	12	32158	31820
13	60543	60374	13	48614	47384	13	42533	40620
14	77010	72606	14	58496	55151	14	52693	48009
15	90723	81280	15	70146	60117	15	61267	53461
16	29999	30818	16	27601	26263	16	24793	23362
17	43845	47784	17	35942	38202	17	32027	33537
18	61212	60556	18	47463	46564	18	41123	41712
19	74719	70534	19	57403	52338	19	49470	48447
20	83723	77175	20	65687	55685	20	48964	53271
21	31572	36096	21	29253	29376	21	26495	26746
22	44586	50474	22	37193	39219	22	33238	36210
23	58989	60786	23	45228	45247	23	41198	43545
24	69258	68116	24	50246	48756			
25	78508	72632	25	55411	50441			
26	30818	38971	26	23138	31458			
27	45439	52264	27	30793	39742			
28	60934	60927	28	37189	44137			
29	63537	66739						
30	71100	70152						

Table A5. M_R data for 50% Class 5 + 50% RAP TH 10 at 90% Maximum Dry Density

WC = OMC-2%			WC = OMC%			WC = OMC+2%		
Seq.	Meas. M_R (psi)	Pred. M_R (psi)	Seq.	Meas. M_R (psi)	Pred. M_R (psi)	Seq.	Meas. M_R (psi)	Pred. M_R (psi)
						1	21701	18606
						2	30286	34662
3	70723	69789	3	58071	61326	3	49155	53917
4	87194	89061	4	75966	80396	4	64792	74083
5	102843	103840	5	94131	95127	5	80249	89876
6	37654	31921	6	35592	25400	6	20597	18703
7	52304	50836	7	39925	42773	7	36056	34766
8	65114	68312	8	55178	59184	8	48567	50575
9	81882	82830	9	72435	72888	9	64721	63889
10	99358	92827	10	88667	82199	10	82967	72701
11	41450	34859	11	30422	27902	11	25899	20733
12	50391	52811	12	42581	44020	12	34367	35049
13	65309	65629	13	58092	55405	13	53031	44947
14	84659	74951	14	72473	63533	14	64815	51739
15	88335	80766	15	84300	68370	15	72065	55382
16	39352	38163	16	28440	30676	16	23223	22923
17	50470	53843	17	40265	44441	17	34493	34652
18	62877	63909	18	56043	53051	18	46878	41610
19	71939	70501	19	64625	58322	19	48292	45265
20	80860	74098	20	66176	60878	20	46749	46508
21	37215	42569	21	26127	34247	21	17090	25538
22	50221	54495	22	40619	44314	22	23665	33496
23	59831	61237	23	43367	49498	23	27844	36806
24	66761	64709	24	47015	51625			
25	71509	65966						
26	35429	44487						
27	49493	54569						
28	63196	59234						
29	59717	60962						

Table A6. M_R data for 50% Class 5 + 50% RAP TH 10 after Two Freeze-Thaw Cycles

WC = OMC%			WC = OMC+1%			WC = OMC+2%		
Seq.	Meas. M_R (psi)	Pred. M_R (psi)	Seq.	Meas. M_R (psi)	Pred. M_R (psi)	Seq.	Meas. M_R (psi)	Pred. M_R (psi)
1	36017	28731	1	35676	24497			
2	47589	44081	2	38718	38693	2	49043	53934
3	60123	61635	3	52507	55083	3	70379	79364
4	77780	79179	4	73641	71513	4	95321	104854
5	95899	93428	5	93414	84754	5	110984	124897
6	36195	28875	6	32053	24621	6	38980	32398
7	44413	45851	7	38070	40072	7	51546	55173
8	57127	62843	8	51968	55441	8	71177	77271
9	78098	78141	9	74277	69113	9	96035	96189
10	98444	89803	10	95546	79311	10	114944	109424
11	34778	32034	11	29182	27312	11	43002	35799
12	44056	50008	12	39837	43177	12	57017	57476
13	63201	65026	13	54654	56028	13	77194	73506
14	78809	77345	14	62114	66310	14	102103	85371
15	100978	86368	15	85198	73564	15	117643	92804
16	33592	35873	16	28923	30526	16	41300	39655
17	47657	53197	17	38436	45412	17	59240	58624
18	67089	66434	18	55428	56373	18	81779	71116
19	83996	77259	19	64236	64887	19	87890	79334
20	92174	84902	20	72881	70568	20	101777	83771
21	35735	41744	21	28663	35286	21	41864	44828
22	50460	57009	22	41134	47894	22	61971	59248
23	65505	68660	23	51649	56872	23	69400	67443
24	82197	77692	24	58499	63292	24	71749	71668
25	91564	83862	25	69082	67310	25	74638	73222
26	34629	45067	26	27154	37875	26	34136	47292
27	51489	59827	27	44500	49583	27	50571	59174
28	73622	70406	28	55466	57230	28	57099	64674
29	80864	78389	29	51955	62442	29	51234	66806
30	79660	83789	30	102696	65586			

Table A7. M_R data for 25% Class 5 + 75% RAP TH 10 versus Water Content Variation

WC = OMC-3%			WC = OMC-2%			WC = OMC-1%		
Seq.	Meas. M_R (psi)	Pred. M_R (psi)	Seq.	Meas. M_R (psi)	Pred. M_R (psi)	Seq.	Meas. M_R (psi)	Pred. M_R (psi)
8	10936	103661	8	89404	92430	8		
9	128288	127606	9	118157	123266	9	154995	157328
10	150974	145406	10	144571	146652	10	184287	177427
11	71570	54444	11			11		
12	78169	81280	12	67480	63488	12	111107	102048
13	94936	104289	13	86265	89194	13	124774	128672
14	127254	122996	14	114569	110071	14	156141	149398
15	141336	135755	15	134157	123608	15	169112	162916
16	62853	58707	16	49572	39430	16	91355	74726
17	78284	84436	17	67910	65462	17	105293	105104
18	103645	104751	18	90060	86527	18	126319	127903
19	121942	120139	19	104688	101516	19	145161	144199
20	134855	130090	20	117046	110119	20	155363	154108
21	59781	65410	21	45437	45121	21	82022	82341
22	78279	88907	22	63114	67621	22	97430	109115
23	101465	105401	23	78569	82325	23	117910	126579
24	114535	116817	24	91278	90781	24	137711	137649
25	135427	123755	25	102785	94649	25	154741	143754
26	62136	70462	26	40943	49228	26	79147	87889
27	80766	91936	27	57509	68510	27	93406	111553
28	98511	105850	28	72403	79104	28	115071	125478
29	124183	114968	29	85481	84096	29	139389	133577
30			30	89540	85769	30	148916	137724

Table A7. M_R data for 25% Class 5 + 75% RAP TH 10 versus Water Content Variation (Continued)

WC = OMC%			WC = OMC+1%			WC = OMC+2%		
Seq.	Meas. M_R (psi)	Pred. M_R (psi)	Seq.	Meas. M_R (psi)	Pred. M_R (psi)	Seq.	Meas. M_R (psi)	Pred. M_R (psi)
1	26966	21991	1			1		
2	33280	35841	2	27011	28766	2	32093	32125
3	44446	50203	3	34310	38846	3	37805	40149
4	62711	64288	4	46366	48209	4	45991	47197
5	79137	75583	5	56210	55897	5	54698	52393
6	27311	23468	6	22278	20168	6	27865	24159
7	34446	37206	7	28671	29892	7	31095	32785
8	46866	50532	8	37793	39719	8	37163	40029
9	65424	62711	9	49047	48379	9	46757	45951
10	78845	71871	10	59616	54994	10	56237	50035
11	27500	26020	11	23858	22033	11	28125	25775
12	37779	39387	12	34051	32792	12	34413	33774
13	53117	51056	13	45151	41984	13	41475	39806
14	58882	60704	14	53433	49068	14	46241	44238
15	76771	67388	15	59243	54518	15	53560	47021
16	28121	28156	16	24291	25232	16	25330	27061
17	39001	41060	17	34160	34994	17	30141	34472
18	52827	51463	18	44477	4123	18	34166	39607
19	62438	59503	19	51553	49778	19	41633	43096
20	67080	64803	20	59055	54762			
21	28235	31546	21	27315	28104			
22	39024	43477	22	35755	37751			
23	48530	52072	23	42791	45251			
24			24	43615	51250			
25	64106	61993						
26	28914	34132						
27	43056	45155						
28	51380	52523						
30	58588	60538						

Table A8. M_R data for 25% Class 5 + 75% RAP TH 10 after Two Freeze-Thaw Cycles

WC = OMC%			WC = OMC+2%		
Seq.	Meas. M_R (psi)	Pred. M_R (psi)	Seq.	Meas. M_R (psi)	Pred. M_R (psi)
2	37117	35873	2	41077	37131
3	49141	50568	3	47642	50587
4	63043	65157	4	60874	63352
5	75290	76822	5	71831	73107
6	29709	23101	6	30870	24802
7	36624	37092	7	35794	37986
8	47826	50817	8	46472	50010
9	62825	62905	9	58577	59981
10	76165	71847	10	69597	66925
11	28194	25538	11	28276	26973
12	37996	39816	12	36802	39722
13	52193	51212	13	50437	48925
14	64910	60241	14	63114	55716
15	74813	66557	15	68701	60094
16	28562	28432	16	28912	29442
17	37552	41758	17	37300	40778
18	52627	51435	18	48349	48207
19	62454	58865	19	54433	53310
20	72315	63773	20	60526	56298
21	30053	32686	21	27294	32823
22	41597	43890	22	37812	41705
23	51698	51745	23	39812	47062
24	58102	57284			
25	65299	60703			
26	27584	34981			
27	38936	45321			
28	50114	51959			
29	55448	56408			
30	58959	59045			

Table A9. M_R data for 100% RAP TH 10 versus Water Content Variation

WC = OMC-3%			WC = OMC-2%			WC = OMC-1%		
Seq.	Meas. M_R (psi)	Pred. M_R (psi)	Seq.	Meas. M_R (psi)	Pred. M_R (psi)	Seq.	Meas. M_R (psi)	Pred. M_R (psi)
						8	113980	111868
			9	182351	167007	9	150019	146229
			10	207135	188154	10	165701	175500
			11	113196	79431	11	57278	45398
12	108942	116183	12	118421	112378	12	81702	77906
13	143692	147389	13	133087	136942	13	106061	105082
14	182108	170969	14	159071	155408	14	136330	126611
15	193709	185894	15	170763	167342	15	149517	140608
16	104205	82713	16	93749	85632	16	58917	50762
17	123897	119125	17	107980	115597	17	79210	80340
18	142556	143012	18	126427	135081	18	101802	101068
19	160743	159005	19	141306	148570	19	122394	115409
20	167603	167539	20	158656	156321	20	130346	123170
21	93114	92940	21	80015	94763	21	53471	58755
22	106860	118903	22	98729	116825	22	70371	80064
23	130954	135479	23	130051	131438	23	88651	94266
24	142295	144294	24	148301	140026	24	104136	101943
25	158831	146403	25	160499	143357	25	112621	103713
26	88579	97907	26	82730	99343	26	46602	62709
27	98864	119237	27	99484	118250	27	66491	80276
28	119530	130182	28	122072	128794	28	87767	89549
29	131892	133606	29	136500	133659	29	95780	92392
30	144226	133948	30	161528	135582	30	100340	92587

Table A9. M_R data for 100% RAP TH 10 versus Water Content Variation (Continued)

WC = OMC%			WC = OMC+1%			WC = OMC+2%		
Seq.	Meas. M_R (psi)	Pred. M_R (psi)	Seq.	Meas. M_R (psi)	Pred. M_R (psi)	Seq.	Meas. M_R (psi)	Pred. M_R (psi)
1	47033	35294						
2	61104	59552	2	34042	34834	2	42335	40618
3	82772	84988	3	48302	52844	3	51449	55653
4	110569	110124	4	69769	71835	4	65446	70300
5	133005	130072	5	85290	87756	5	81438	81985
6	48736	37526	6	26493	20447	6	37605	27268
7	61979	60803	7	34457	36015	7	42642	41836
8	81407	83372	8	49116	52582	8	55390	55917
9	107000	102570	9	69432	67772	9	73107	68098
10	131346	118208	10	83481	80747	10	86847	78071
11	46937	42230	11	22857	23641	11	35320	30528
12	58247	63875	12	37888	38940	12	44340	44819
13	78392	80796	13	54521	52271	13	58735	56506
14	99390	93864	14	70395	63494	14	71143	66054
15	116946	102428	15	81284	71497	15	79814	72831
16	41671	46170	16	29483	26508	16	32088	33449
17	57345	65986	17	39555	41199	17	43675	47188
18	77479	79364	18	53334	52347	18	55435	57188
19	94283	88780	19	65889	61146	19	64303	65065
20	106317	94213	20	71209	66902	20	67710	70334
21	43029	52045	21	28428	31090	21	31264	38081
22	56256	66704	22	41126	42838	22	41312	49224
23	73266	76632	23	48280	51988	23	51515	57843
24	74208	82491	24	56607	58336	24	68549	63995
25	96743	84690	25	68649	61758	25	80570	67666
26	38920	55018	26	27653	33607	26	29294	40640
27	55830	67577	27	42830	44445	27	50383	51147
28	71744	74666	28	50297	51695			
29	83412	77857	29	50321	56280			
30	90322	79052						

Table A10. M_R data for 100% RAP TH 10 at 90% Maximum Dry Density

WC = OMC-2%			WC = OMC%			WC = OMC+2%		
Seq.	Meas. M_R (psi)	Pred. M_R (psi)	Seq.	Meas. M_R (psi)	Pred. M_R (psi)	Seq.	Meas. M_R (psi)	Pred. M_R (psi)
						2	52982	54169
						3	71500	79938
			4	104845	116980	4	89577	104664
			5			5	111323	122729
			6	126540	141088	6	41330	31690
			7	65045	56798	7	50636	54120
8	91811	98265	8	78758	81638	8	68106	73852
9	121412	123402	9	103176	102598	9	89613	88969
10	141241	140526	10	123110	116651	10	108537	97963
11	52704	42626	11	44883	34724	11	40339	34306
12	69134	70434	12	58919	57745	12	51726	52953
13	89548	90354	13	81406	73892	13	74628	63859
14	113458	104586	14	96105	85184	14	91764	70366
15	120596	112892	15	103270	91510	15	97520	73055
16	49224	47207	16	42721	38388	16	36786	36905
17	65315	70752	17	53769	57557	17	50370	51137
18	86038	85513	18	73254	69222	18	65301	58086
19	93383	94285	19	79265	75756	19	70056	60531
20	114781	98260	20	88221	78377	20	63228	60347
21	50956	53027	21	36497	42901	21	28246	39500
22	70623	69954	22	50309	56292	22	37273	48015
23	82280	78322	23	60353	62388	23	36771	49980
24	82142	81268	24	69525	63972	24	41374	48544
25	91311	81085	25	74013	63156			
26	47507	55353	26	33519	44617			
27	63326	68697	27	46369	54818			
28	69369	73172	28	51455	57569			
29	66513	73107	29	52624	56675			

Table A11. M_R data for 100% RAP TH 10 after Two Freeze-Thaw Cycles

WC = OMC%			WC = OMC+1%			WC = OMC+2%		
Seq.	Meas. M_R (psi)	Pred. M_R (psi)	Seq.	Meas. M_R (psi)	Pred. M_R (psi)	Seq.	Meas. M_R (psi)	Pred. M_R (psi)
2	60213	58920	2	37245	38948	2	59966	58140
3	78561	80410	3	52637	58516	3	87038	83309
4	114685	100920	4	73732	78789	4	121139	107732
5	87678	116721	5	91473	95322	5	126666	126346
6	53852	39347	6	29256	22960	6	44833	35996
7	61912	60408	7	39627	40245	7	61146	59086
8	76197	79844	8	55737	57991	8	78417	80383
9	98624	96139	9	74932	73964	9	94213	97868
10	123736	107641	10	90946	85770	10	106751	109587
11	53186	42888	11	29662	25705	11	48835	39329
12	65876	63525	12	40909	42997	12	58287	60583
13	83981	78737	13	63186	56966	13	75230	75229
14	102446	90141	14	74528	68017	14	89670	85521
15	110186	97653	15	84286	75548	15	94250	91545
16	42409	46957	16	28338	28947	16	42272	42992
17	59400	65529	17	41365	44792	17	54239	61010
18	77940	77983	18	59874	56269	18	70635	72024
19	91874	86793	19	68169	64752	19	80106	78612
20	104330	92139	20	76895	70042	20	78643	81712
21	41521	52628	21	29990	33615	21	38057	47640
22	58387	67448	22	43038	46533	22	50841	60680
23	75585	76752	23	54378	55132	23	65392	67188
24	81462	82558	24	61532	60680	24	70377	69827
25	95872	85658	25	66594	63700	25	78791	70194
26	39938	55509	26	29071	36050	26	38365	49690
27	57875	68517	27	42299	47514	27	55447	59852
28	72617	75767	28	53037	54228	28	62055	63612
29	81247	79889	29	55717	58147	29	65471	64251
			30	56496	60026	30	71097	63017

Table A12. K's Parameters versus Water Content Variation

% RAP	W.C Condition	M_R-MEPDG Model		
		K_1	K_2	K_3
0% (Class 5)	OMC-3%	2118	0.76	-0.4
	OMC-2%	1880	0.88	-0.72
	OMC-1%	1466	0.83	-0.42
	OMC%	1185	0.85	-0.74
	OMC+1%	900	0.86	-0.6
	OMC+2%	988	0.8	-0.64
50% (TH 10)	OMC-3%	5310	0.82	-1
	OMC-2%	4032	0.62	-0.56
	OMC-1%	3309	0.97	-1.05
	OMC%	2209	0.85	-0.85
	OMC+1%	1943	0.78	-0.9
	OMC+2%	1616	0.63	-0.48
75% (TH 10)	OMC-3%	4083	0.75	-0.74
	OMC-2%	5278	0.73	-0.78
	OMC-1%	2939	1.14	-1.34
	OMC%	1949	0.77	-0.74
	OMC+1%	1656	0.61	-0.44
	OMC+2%	1893	0.52	-0.56
100% (TH 10)	OMC-3%	6102	0.84	-1.05
	OMC-2%	6125	0.66	-0.77
	OMC-1%	3830	1.06	-1.33
	OMC%	3342	0.79	-0.93
	OMC+1%	1880	0.91	-0.95
	OMC+2%	2313	0.68	-0.65

Table A13. K's Parameters versus 90% Maximum Dry Density

% RAP	W.C Condition	M_R-MEPDG Model		
		K_1	K_2	K_3
0%	OMC-2%	1491	0.83	-0.8
	OMC%	1436	0.88	-1.15
	OMC+2%	724	0.73	-0.27
50%	OMC-2%	2834	0.75	-0.92
	OMC%	2349	0.85	-1.12
	OMC+2%	1864	1.03	-1.5
100%	OMC-2%	3700	0.95	-1.29
	OMC%	3059	0.98	-1.38
	OMC+2%	3053	0.91	-1.48

Table A14. K's Parameters versus Two Freeze-Thaw Cycles

% RAP	W.C Condition	M_R-MEPDG Model		
		K_1	K_2	K_3
0%	OMC%	1257	0.82	-0.43
	OMC+2%	1105	0.77	-0.51
50%	OMC%	2484	0.71	-0.6
	OMC+1%	2165	0.76	-0.74
	OMC+2%	2994	0.86	-1.07
75%	OMC%	2019	0.74	-0.73
	OMC+2%	2140	0.68	-0.78
100%	OMC%	3388	0.68	-0.75
	OMC+1%	2126	0.89	-0.98
	OMC+2%	3284	0.81	-1.08

Table A15. K's Parameters versus Water Content Variation for Class 5 at Different Confining Pressure Levels

W.C Condition	Conf. Pressure (psi)	M_R-MEPDG Model		
		K_1	K_2	K_3
OMC-3%	3	6208	3.27	-6.32
	6	130	10.79	-13.82
	10	$1.12 * 10^{-21}$	78.56	-79.7
	15	76500000	-9.08	7.94
	20	6460000	-5.31	4.12
OMC-2%	3	642	-3.25	6.69
	6	2086	0.36	-0.09
	10	2580000000	-18.82	19.39
	15	51063	-2.23	1.97
	20	542675	-3.36	2.41
OMC-1%	3	1678	1	-1.12
	6	522	4.74	-5.7
	10	$3.6 * 10^{-31}$	108.7	-110.5
	15	$3.21 * 10^{9}$	-12.63	10.74
	20	$1.02 * 10^{11}$	-13	10.07
OMC%	3	2173	1.83	-3.27
	6	711	2.42	-2.68
	10	$1.51 * 10^{-15}$	58.06	-58.92
	15	149645	-3.74	3.25
	20	118152	-2.6	1.9
OMC+1%	3	3403	3.75	-7.31
	6	98.55	9.65	-12.82
	10	$1.41 * 10^{-25}$	90.12	-91.78
	15	462482	-4.81	4
	20	$1.45 * 10^{12}$	-14.14	9.39
OMC+2%	3	79	-7.1	15.51
	6	917	0.64	-0.47
	10	$3.27 * 10^{-12}$	47.1	-47.84
	15	3277	-0.27	0.23
	20	11278	-0.83	0.34

Table A16. K's Parameters versus Water Content Variation for 50% RAP TH 10 + 50% Class 5 at Different Confining Pressure Levels

W.C Condition	Conf. Pressure (psi)	M_R-MEPDG Model		
		K_1	K_2	K_3
OMC-3%	3	7812	0.41	-1.66
	6	5132	1.66	-2.61
	10	$3.66 * 10^{-21}$	77.97	-79.48
	15	4560	0.97	-1.1
	20	5014	0.89	-1.01
OMC-2%	3	3899	-0.3	0.33
	6	8721	-2.16	2.92
	10	$6.11 * 10^{-6}$	28.93	-29.49
	15	88971	-2.31	1.96
	20	56053	-1.33	0.92
OMC-1%	3	4613	0.27	-1.18
	6	4224	0.44	-0.63
	10	$9.73 * 10^{-8}$	34.62	-35.3
	15	9176	-0.03	-0.17
	20	172388	-2	-1.2
OMC%	3	1598	-0.81	1.68
	6	3624	-0.95	1.39
	10	31.64	6.71	-6.79
	15	53006	-2.07	1.58
	20	31394	-1.12	0.62
OMC+1%	3	1872	-0.37	0.31
	6	1211	2.8	-3.92
	10	$7.68 * 10^{-16}$	59.78	-61.12
	15	213246	-3.57	2.75
	20	98963	-2.08	1.19
OMC+2%	3	1287	-0.34	1.3
	6	799	3.39	-4.42
	10	$4.71 * 10^{-15}$	56.89	-57.95
	15	$9.58 * 10^{8}$	-11.46	9.18
	20	$3.77 * 10^{9}$	-9.98	6.56

Table A17. K's Parameters versus Water Content Variation for 75% RAP TH 10 + 25% Class 5 at Different Confining Pressure Levels

W.C Condition	Conf. Pressure (psi)	M_R-MEPDG Model		
		K_1	K_2	K_3
OMC-3%	3	1445	-3.93	7.52
	6	7609	-1.29	1.73
	10	$2.77 * 10^{10}$	-21.08	21.41
	15	688	2.43	-2.14
	20	641	2.16	-1.74
OMC-2%	3	3935	-2.14	3.58
	6	12512	-1.31	1.37
	10	0.01	19.43	-19.89
	15	7480	0.39	-0.46
	20	1335	1.8	-1.56
OMC-1%	3	5461	1	-2.68
	6	1685	3.82	-5.3
	10	$3.73 * 10^{-9}$	39.25	-40.22
	15	68021	-1.85	1.25
	20	56444	-1.15	0.47
OMC%	3	1871	0.06	0.0006
	6	1727	0.98	-1.02
	10	$1.97 * 10^{-10}$	42.35	-43.09
	15	492	2	-1.68
	20	22937	-1.01	0.52
OMC+1%	3	1453	-0.03	0.06
	6	855	3.28	-4.21
	10	$2.09 * 10^{-19}$	70.93	-72.3
	15	$2.33 * 10^{7}$	-8.12	6.61
	20	63953	-2.06	1.45
OMC+2%	3	18921	5.3	-13.6
	6	468	6.69	-9.83
	10	$6.67 * 10^{-41}$	140.26	-143.86
	15	$5.03 * 10^{7}$	-8.81	6.95
	20	$4.9 * 10^{6}$	-5.24	3.46

Table A18. K's Parameters versus Water Content Variation for 100% RAP TH 10 at Different Confining Pressure Levels

W.C Condition	Conf. Pressure (psi)	M_R-MEPDG Model		
		K_1	K_2	K_3
OMC-3%	3	6476	-0.78	0.96
	6	831	7.9	-10.55
	10	$5.32 * 10^{-13}$	52.18	-53.33
	15	175	4.37	-4.21
	20	1075	2.2	-2.06
OMC-2%	3	2424	-3.62	6.63
	6	29932	-4.14	5.08
	10	191	5.41	-5.59
	15	128	4.36	-3.94
	20	66	4.15	-3.35
OMC-1%	3	9915	2.41	-5.5
	6	5243	0.68	-1.28
	10	18909	-1.11	0.82
	15	27178	-0.74	0.2
	20	37911	-0.76	0.15
OMC%	3	3232	-0.06	-0.26
	6	4803	-0.53	0.6
	10	1670	1.73	-1.9
	15	5060	0.43	-0.65
	20	15364	-0.32	-0.05
OMC+1%	3	2164	0.63	-1.11
	6	1835	0.88	-0.92
	10	$1.06 * 10^{-6}$	30.53	-31.15
	15	891795	-4.75	3.71
	20	18347	-0.8	0.37
OMC+2%	3	1970	-0.72	1.05
	6	3913	-1.31	1.93
	10	$1.16 * 10^{-14}$	56.27	-57.57
	15	38269	-1.93	1.56
	20	547	1.75	-1.34

Table A19. K's Parameters versus 90% Maximum Dry Density for Class 5 at Different Confining Pressure Levels

W.C Condition	Conf. Pressure (psi)	M_R-MEPDG Model		
		K_1	K_2	K_3
OMC-2%	3	424	-3.42	7.3
	6	0.007	52.91	-74.1
	10	$9.15 * 10^{-22}$	78.5	-80.12
	15	$4.29 * 10^{7}$	-8.67	7.02
	20	$1.05 * 10^{9}$	-9.11	6.16
OMC%	3	378	-3.17	7.22
	6	2846	-1.83	2.49
	10	$1.11 * 10^{-38}$	132.96	-136.3
	15	$1.08 * 10^{13}$	-20	15.76
	20	7647791	-5.49	3.44
OMC+2%	3	24.4	-7.67	19.73
	6	633	0.39	0.56
	10	$3.46 *10^{-69}$	230	-235.2
	15	$1.66 *10^{12}$	-18.87	15.27
	20	2431748	-5.03	3.32

Table A20. K's Parameters versus 90% Maximum Dry Density for 50% RAP TH 10 + 50% Class 5 at Different Confining Pressure Levels

W.C Condition	Conf. Pressure (psi)	M_R-MEPDG Model		
		K_1	K_2	K_3
OMC-2%	3	2834	0.75	-0.92
	6	3981	-0.43	0.52
	10	$1.13 * 10^{9}$	-17.28	17.53
	15	100220	-2.54	1.83
	20	23750	-0.83	0.28
OMC%	3	1177	-1.8	3.31
	6	1917	1.48	-2.05
	10	$1.75 * 10^{-18}$	68.74	-70.59
	15	$1.05 * 10^{8}$	-9	6.95
	20	$2.38 * 10^{7}$	-5.93	3.66
OMC+2%	3	13662	5.1	-12.45
	6	215	10.14	-14.69
	10	$1.42 * 10^{-48}$	165.42	-169.77
	15	$4.02 * 10^{11}$	-16.6	12.9
	20	$8.68 * 10^{12}$	-15.34	9.85

Table A21. K's Parameters versus 90% Maximum Dry Density for 100% RAP TH 10 at Different Confining Pressure Levels

W.C Condition	Conf. Pressure (psi)	M_R-MEPDG Model		
		K_1	K_2	K_3
OMC-2%	3	3435	-0.16	0.14
	6	2921	1.7	-2.3
	10	$5.44 * 10^{-9}$	38.79	-39.81
	15	563883	-3.72	2.61
	20	97375	-1.58	0.72
OMC%	3	4222	0.58	-1.99
	6	5489	-0.6	0.35
	10	$4.58 * 10^{-19}$	71.02	-72.87
	15	$3.62 * 10^{6}$	-5.6	4.15
	20	94065	-1.65	0.7
OMC+2%	3	5960	1.58	-4.72
	6	791	6.59	-9.74
	10	$2.24 * 10^{-50}$	171.75	-176.34
	15	$3.93 * 10^{12}$	-18.39	14.38
	20	$7.92 * 10^{11}$	-13.36	8.49

Table A22. K's Parameters versus Two Freeze-Thaw Cycles for Class 5 at Different Confining Pressure Levels

W.C Condition	Conf. Pressure (psi)	M_R-MEPDG Model		
		K_1	K_2	K_3
OMC%	3	694	-1.2	3.37
	6	1244	0.4	0.29
	10	$1.15 * 10^{-17}$	65.08	-66.07
	15	$5.96 * 10^{6}$	-7	6
	20	138456	-2.61	2
OMC+2%	3	1929	2.43	-3.75
	6	217	6.25	-7.67
	10	$6.92 * 10^{-23}$	81.62	-83.09
	15	$1.08 * 10^{8}$	-9.8	8.12
	20	50304	-2	1.43

Table A23. K's Parameters versus Two Freeze-Thaw Cycles for 50% Class 5 + 50% RAP TH 10 at Different Confining Pressure Levels

W.C Condition	Conf. Pressure (psi)	M_R-MEPDG Model		
		K_1	K_2	K_3
OMC%	3	1921	-0.58	1.23
	6	4392	-1.52	2.26
	10	722525	-7.3	7.65
	15	14227	-0.92	0.81
	20	121317	-2.14	1.46
OMC+1%	3	1408	-1.2	2.22
	6	3468	-1.26	1.9
	10	71.68	5.45	-5.53
	15	12468	-0.77	0.38
	20	14.56	4.56	-3.44
OMC+2%	3	6585	2.13	-4.87
	6	1231	4.28	-5.79
	10	$1.68 * 10^{-20}$	75.45	-77.17
	15	$1.07 * 10^{9}$	-10.92	8.67
	20	$9.91 * 10^{7}$	-6.91	4.63

Table A24. K's Parameters versus Two Freeze-Thaw Cycles for 25% Class 5 + 75% RAP TH 10 at Different Confining Pressure Levels

W.C Condition	Conf. Pressure (psi)	M_R-MEPDG Model		
		K_1	K_2	K_3
OMC%	3	2033	0.055	-0.18
	6	2377	0.18	-0.14
	10	0.005	18.7	-19.04
	15	74409	-2.6	2.07
	20	87861	-2.07	1.36
OMC+2%	3	1675	-0.54	0.96
	6	4535	-2.33	3.26
	10	$1.78 * 10^{-17}$	65.21	-66.86
	15	$3.19 * 10^{6}$	-6.04	4.72
	20	345000	-3.08	1.92

Table A25. K's Parameters versus Two Freeze-Thaw Cycles for 100% RAP TH 10 at Different Confining Pressure Levels

W.C Condition	Conf. Pressure (psi)	M_R-MEPDG Model		
		K_1	K_2	K_3
OMC%	3	2308	-1.28	2.1
	6	3179	1.21	-1.75
	10	0.0007	22.22	-22.74
	15	5731	0.31	-0.52
	20	$9.25 * 10^{6}$	-5.35	3.83
OMC+1%	3	1895	-0.12	0.27
	6	1975	1.11	-1.39
	10	$5.42 * 10^{-13}$	50.91	-52
	15	334695	-3.79	2.94
	20	172903	-2.38	1.42
OMC+2%	3	3458	0.13	-0.75
	6	5493	-1.13	1.39
	10	890543	-6.98	6.82
	15	598	2.45	-2.48
	20	556	2.1	-1.94

APPENDIX B. PERMANENT DEFORMATION DATA MODELING

Table B1. PD Measured Data from M_R Test for Class 5 (OMC-2%)

Seq.	Measured M_R (psi)	Measured PD (inches)	Pred. PD (inches)		
			H = 6 in.	H = 9 in.	H = 12 in
4	63010	0.0096	7.4931E-05	0.0001124	0.00014986
5	80403	0.01008	0.00010066	0.00015098	0.00020131
6	26926	0.00612	3.4574E-05	5.1862E-05	6.9149E-05
7	34455	0.00858	6.2239E-05	9.3358E-05	0.00012448
8	46727	0.00912	9.3779E-05	0.00014067	0.00018756
9	64814	0.00984	0.00013334	0.00020002	0.00026669
10	83747	0.01038	0.00018198	0.00027297	0.00036396
11	24551	0.00822	6.9856E-05	0.00010478	0.00013971
12	42634	0.00846	0.00010181	0.00015272	0.00020362
13	61387	0.00924	0.00015545	0.00023317	0.0003109
14	82326	0.01002	0.00024157	0.00036235	0.00048313
15	98613	0.01104	0.00036178	0.00054267	0.00072356
16	25425	0.00912	0.00010083	0.00015125	0.00020166
17	44821	0.0096	0.00014922	0.00022383	0.00029844
18	63824	0.01062	0.0002374	0.00035611	0.00047481
19	80972	0.01242	0.0003936	0.00059041	0.00078721
20	94180	0.01488	0.00061572	0.00092359	0.00123145
21	30261	0.0126	0.00014852	0.00022279	0.00029705
22	48693	0.01434	0.00024959	0.00037439	0.00049919
23	67823	0.0174	0.00043002	0.00064503	0.00086003
24	80901	0.02214	0.00079139	0.00118709	0.00158278
25	95115	0.0276	0.00132384	0.00198575	0.00264767
26	29988	0.02508	0.00021612	0.00032419	0.00043225
27	50503	0.02682	0.00036734	0.00055101	0.00073467
28	71442	0.02958	0.00066778	0.00100167	0.00133557
29	81753	0.03696	0.00134908	0.00202362	0.00269815
30	89707	0.05202	0.00248566	0.00372849	0.00497132

Table B2. PD Measured Data from M_R Test for Class 5 (OMC%)

Seq.	Measured M_R (psi)	Measured PD (inches)	Pred. PD (inches)		
			H = 6 in.	H = 9 in.	H = 12 in
1	18235	0.0573	2.7139E-07	4.0709E-07	5.4278E-07
2	19011	0.0573	5.6625E-07	8.4938E-07	1.1325E-06
3	25633	0.0576	8.1371E-07	1.2206E-06	1.6274E-06
4	37734	0.0582	1.0277E-06	1.5415E-06	2.0553E-06
5	50439	0.0585	1.2758E-06	1.9138E-06	2.5517E-06
6	17124	0.0573	4.9689E-07	7.4534E-07	9.9379E-07
7	19860	0.0576	9.5477E-07	1.4321E-06	1.9095E-06
8	28212	0.0579	1.3367E-06	2.0051E-06	2.6734E-06
9	42186	0.0585	1.7137E-06	2.5706E-06	3.4274E-06
10	55090	0.0588	2.2197E-06	3.3296E-06	4.4395E-06
11	17481	0.0579	9.1379E-07	1.3707E-06	1.8276E-06
12	25050	0.0585	1.5009E-06	2.2513E-06	3.0017E-06
13	36798	0.0591	2.14E-06	3.21E-06	4.2801E-06
14	44497	0.0597	3.3659E-06	5.0489E-06	6.7318E-06
15	58073	0.0618	4.5408E-06	6.8111E-06	9.0815E-06
16	19954	0.0609	1.2099E-06	1.8149E-06	2.4199E-06
17	28077	0.0621	2.0752E-06	3.1129E-06	4.1505E-06
18	37644	0.0645	3.2854E-06	4.928E-06	6.5707E-06
19	46596	0.069	5.2755E-06	7.9133E-06	1.0551E-05
20	54368	0.0744	7.9234E-06	1.1885E-05	1.5847E-05
21	20709	0.0747	1.9871E-06	2.9806E-06	3.9741E-06
22	29911	0.078	3.4903E-06	5.2355E-06	6.9807E-06
23	37155	0.0873	6.2114E-06	9.3171E-06	1.2423E-05
24	38398	0.114	1.2158E-05	1.8237E-05	2.4317E-05
25	53331	0.1497	1.7302E-05	2.5953E-05	3.4604E-05
26	22707	0.1512	2.6546E-06	3.9819E-06	5.3091E-06
27	34553	0.1557	4.7032E-06	7.0548E-06	9.4064E-06
28	41748	0.1773	9.1037E-06	1.3656E-05	1.8207E-05
29	49341	0.2538	3.3443E-05	5.0165E-05	6.6887E-05
30	18235	0.0573	2.7139E-07	4.0709E-07	5.4278E-07

Table B3. PD Measured Data from M_R Test for Class 5 (OMC+2%)

Seq.	Measured M_R (psi)	Measured PD (inches)	Pred. PD (inches)		
			H = 6 in.	H = 9 in.	H = 12 in
2	15521	0.1992	3.7135E-11	5.5703E-11	7.4271E-11
3	20093	0.1986	5.4798E-11	8.2197E-11	1.096E-10
4	32120	0.1986	6.3699E-11	9.5548E-11	1.274E-10
5	44648	0.1992	7.5954E-11	1.1393E-10	1.5191E-10
6	16542	0.1998	6.1446E-11	9.2169E-11	1.2289E-10
7	23629	0.1998	8.4809E-11	1.2721E-10	1.6962E-10
8	33527	0.1998	1.114E-10	1.671E-10	2.228E-10
9	47572	0.201	1.3385E-10	2.0078E-10	2.6771E-10
10	14783	0.201	5.8172E-11	8.7258E-11	1.1634E-10
11	19613	0.2022	1.0126E-10	1.519E-10	2.0253E-10
12	28818	0.2034	1.4184E-10	2.1276E-10	2.8368E-10
13	37630	0.2058	2.0819E-10	3.1229E-10	4.1638E-10
14	46849	0.21	2.8569E-10	4.2853E-10	5.7138E-10
15	15555	0.2112	8.2582E-11	1.2387E-10	1.6516E-10
16	21716	0.2142	1.4084E-10	2.1126E-10	2.8167E-10
17	30777	0.2202	2.1019E-10	3.1529E-10	4.2038E-10
18	38815	0.2328	3.2918E-10	4.9377E-10	6.5836E-10
19	48701	0.2556	4.6653E-10	6.9979E-10	9.3306E-10
20	18655	0.261	1.1928E-10	1.7892E-10	2.3856E-10
21	23891	0.2772	2.2991E-10	3.4487E-10	4.5983E-10
22	28955	0.3246	4.1309E-10	6.1963E-10	8.2618E-10
23	37425	0.4284	6.7962E-10	1.0194E-09	1.3592E-09
24	15521	0.1992	3.7135E-11	5.5703E-11	7.4271E-11

Table B4. PD Measured Data from M_R Test for 50% RAP TH 10 (OMC-2%)

Seq.	Measured M_R (psi)	Measured PD (inches)	Pred. PD (inches)		
			H = 6 in.	H = 9 in.	H = 12 in
3	79563	0.00162	0.00020217	0.00030325	0.00040433
4	96009	0.00234	0.00032097	0.00048145	0.00064194
5	115888	0.00288	0.0004637	0.00069555	0.0009274
6	106606	0.00372	0.00032303	0.00048454	0.00064605
7	128302	0.00432	0.00054273	0.00081409	0.00108546
8	172143	0.00684	0.00084724	0.00127086	0.00169447
9	68694	0.00312	0.00017599	0.00026399	0.00035199
10	87005	0.0042	0.00035224	0.00052835	0.00070447
11	112236	0.00606	0.00062775	0.00094163	0.00125551
12	130895	0.00546	0.00110425	0.00165638	0.0022085
13	148482	0.00642	0.00176205	0.00264308	0.00352411
14	66120	0.00444	0.00026688	0.00040032	0.00053376
15	79487	0.00498	0.00055554	0.00083331	0.00111108
16	102830	0.00576	0.00100249	0.00150374	0.00200498
17	122593	0.00702	0.00180095	0.00270142	0.0036019
18	132155	0.00882	0.00296412	0.00444618	0.00592824
19	61594	0.00672	0.00047081	0.00070622	0.00094163
20	77286	0.0075	0.0009956	0.0014934	0.00199121
21	98436	0.009	0.00190221	0.00285331	0.00380441
22	79106	0.01218	0.00415394	0.00623091	0.00830788
23	132971	0.01638	0.00639151	0.00958727	0.01278302
24	61665	0.01392	0.00067975	0.00101963	0.00135951
25	80782	0.01482	0.001471	0.0022065	0.00294201
26	104740	0.01632	0.00297907	0.0044686	0.00595813
27	124768	0.01986	0.00618289	0.00927434	0.01236578
28	133546	0.0276	0.01174529	0.01761793	0.02349058
29	79563	0.00162	0.00020217	0.00030325	0.00040433
30	96009	0.00234	0.00032097	0.00048145	0.00064194

Table B5. PD Measured Data from M_R Test for 50% RAP TH 10 (OMC%)

Seq.	Measured M_R (psi)	Measured PD (inches)	Pred. PD (inches)		
			H = 6 in.	H = 9 in.	H = 12 in
1	33848	0.129	3.7488E-06	5.6232E-06	7.4975E-06
2	42470	0.10638	6.8611E-06	1.0292E-05	1.3722E-05
3	61834	0.08268	9.9707E-06	1.4956E-05	1.9941E-05
4	80487	0.0828	1.4901E-05	2.2351E-05	2.9801E-05
5	97437	0.0831	2.1034E-05	3.1551E-05	4.2068E-05
6	39487	0.0825	5.7887E-06	8.6831E-06	1.1577E-05
7	46181	0.08268	1.1336E-05	1.7004E-05	2.2672E-05
8	59228	0.08298	1.8158E-05	2.7238E-05	3.6317E-05
9	78816	0.0831	2.7193E-05	4.079E-05	5.4387E-05
10	96998	0.08328	3.8763E-05	5.8144E-05	7.7526E-05
11	35893	0.0828	1.1634E-05	1.7451E-05	2.3267E-05
12	45905	0.08328	2.1774E-05	3.2661E-05	4.3548E-05
13	64737	0.08328	3.3962E-05	5.0943E-05	6.7923E-05
14	81937	0.08388	5.4495E-05	8.1742E-05	0.00010899
15	94831	0.08448	8.251E-05	0.00012377	0.00016502
16	34664	0.08388	1.7747E-05	2.662E-05	3.5494E-05
17	48209	0.0843	3.1972E-05	4.7958E-05	6.3944E-05
18	65324	0.0849	5.2763E-05	7.9144E-05	0.00010553
19	77264	0.08658	9.0515E-05	0.00013577	0.00018103
20	86139	0.08988	0.00014337	0.00021505	0.00028673
21	35061	0.0897	2.9832E-05	4.4748E-05	5.9664E-05
22	49437	0.09078	5.563E-05	8.3444E-05	0.00011126
23	62106	0.0945	0.00010163	0.00015244	0.00020325
24	72103	0.10842	0.00018812	0.00028217	0.00037623
25	78726	0.13158	0.00032153	0.0004823	0.00064307
26	34545	0.14118	4.3588E-05	6.5382E-05	8.7175E-05
27	48854	0.14268	8.4521E-05	0.00012678	0.00016904
28	62507	0.13998	0.00016154	0.00024231	0.00032308
29	63857	0.15642	0.00034361	0.00051542	0.00068723
30	71100	0.1572	0.00062088	0.00093131	0.00124175

Table B6. PD Measured Data from M_R Test for 50% RAP TH 10 (OMC+2%)

Seq.	Measured M_R (psi)	Measured PD (inches)	Pred. PD (inches)		
			H = 6 in.	H = 9 in.	H = 12 in
1	23390	0.1449	1.1205E-08	1.6808E-08	2.241E-08
2	25394	0.1458	2.2642E-08	3.3963E-08	4.5284E-08
3	32965	0.1458	3.4017E-08	5.1025E-08	6.8034E-08
4	46160	0.1455	4.5508E-08	6.8261E-08	9.1015E-08
5	59323	0.1455	5.8949E-08	8.8424E-08	1.179E-07
6	21272	0.1455	2.1037E-08	3.1556E-08	4.2074E-08
7	27054	0.1461	3.7645E-08	5.6468E-08	7.5291E-08
8	35926	0.1464	5.6584E-08	8.4876E-08	1.1317E-07
9	50180	0.147	7.7811E-08	1.1672E-07	1.5562E-07
10	63612	0.1473	1.042E-07	1.5631E-07	2.0841E-07
11	23209	0.1473	3.6595E-08	5.4893E-08	7.319E-08
12	32158	0.1491	6.2758E-08	9.4137E-08	1.2552E-07
13	42533	0.1503	9.8448E-08	1.4767E-07	1.969E-07
14	52693	0.1533	1.5373E-07	2.3059E-07	3.0746E-07
15	61266	0.1584	2.2488E-07	3.3732E-07	4.4976E-07
16	24793	0.159	5.1459E-08	7.7188E-08	1.0292E-07
17	32027	0.1623	9.5551E-08	1.4333E-07	1.911E-07
18	41123	0.1686	1.5744E-07	2.3616E-07	3.1488E-07
19	49470	0.1839	2.5905E-07	3.8857E-07	5.1809E-07
20	53365	0.2124	4.0971E-07	6.1456E-07	8.1941E-07
21	24158	0.2163	8.9154E-08	1.3373E-07	1.7831E-07
22	33238	0.2664	1.6426E-07	2.4639E-07	3.2852E-07
23	41198	0.3084	2.944E-07	4.416E-07	5.8881E-07
24	67781	0.4146	4.3123E-07	6.4684E-07	8.6246E-07

Table B7. PD Measured Data from M_R Test for 75% RAP TH 10 (OMC-2%)

Seq.	Measured M_R (psi)	Measured PD (inches)	Pred. PD (inches)		
			H = 6 in.	H = 9 in.	H = 12 in
8	166416	0.00342	0.00016887	0.0002533	0.00033774
9	174602	0.00666	0.00029646	0.00044468	0.00059291
10	202458	0.00708	0.00047951	0.00071926	0.00095902
11	123215	0.003	7.7198E-05	0.0001158	0.0001544
12	119481	0.00606	0.0001733	0.00025995	0.0003466
13	132315	0.00648	0.00033025	0.00049537	0.0006605
14	166513	0.00702	0.00059936	0.00089904	0.00119873
15	182814	0.00792	0.00097943	0.00146914	0.00195886
16	95941	0.0063	0.00012201	0.00018302	0.00024402
17	108771	0.00666	0.00026831	0.00040247	0.00053663
18	130924	0.0075	0.00051613	0.00077419	0.00103225
19	153410	0.00822	0.0009613	0.00144195	0.0019226
20	164140	0.01002	0.00160699	0.00241048	0.00321398
21	85771	0.0081	0.00021571	0.00032357	0.00043142
22	101500	0.00864	0.00048379	0.00072568	0.00096758
23	121174	0.00978	0.00097613	0.0014642	0.00195227
24	136311	0.01254	0.00193218	0.00289827	0.00386435
25	151939	0.0165	0.00344261	0.00516392	0.00688523
26	77600	0.01422	0.00032556	0.00048834	0.00065111
27	91835	0.01482	0.000754	0.001131	0.001508
28	113448	0.01602	0.00157693	0.0023654	0.00315386
29	135549	0.01944	0.00331005	0.00496508	0.0066201
30	147222	0.02664	0.00632183	0.00948275	0.01264367

Table B8. PD Measured Data from M_R Test for 75% RAP TH 10 (OMC%)

Seq.	Measured M_R (psi)	Measured PD (inches)	Pred. PD (inches)		
			H = 6 in.	H = 9 in.	H = 12 in
1	26966	0.0405	1.4184E-06	2.1276E-06	2.8368E-06
2	33281	0.0414	2.5974E-06	3.8961E-06	5.1948E-06
3	44446	0.042	3.8886E-06	5.8328E-06	7.7771E-06
4	62712	0.0426	5.3467E-06	8.02E-06	1.0693E-05
5	79137	0.0432	7.2143E-06	1.0821E-05	1.4429E-05
6	27311	0.0411	2.4322E-06	3.6483E-06	4.8645E-06
7	34446	0.0417	4.43E-06	6.6451E-06	8.8601E-06
8	46866	0.0426	6.6603E-06	9.9904E-06	1.3321E-05
9	65424	0.0435	9.4405E-06	1.4161E-05	1.8881E-05
10	78845	0.0441	1.3298E-05	1.9947E-05	2.6595E-05
11	27500	0.0417	4.5295E-06	6.7942E-06	9.059E-06
12	37779	0.0429	7.9068E-06	1.186E-05	1.5814E-05
13	53117	0.0438	1.2075E-05	1.8112E-05	2.415E-05
14	58882	0.0447	2.0442E-05	3.0663E-05	4.0884E-05
15	76771	0.0477	2.8439E-05	4.2658E-05	5.6878E-05
16	28121	0.0453	6.6095E-06	9.9143E-06	1.3219E-05
17	39001	0.0468	1.1723E-05	1.7584E-05	2.3445E-05
18	52828	0.0489	1.8918E-05	2.8377E-05	3.7836E-05
19	62439	0.0534	3.1959E-05	4.7939E-05	6.3919E-05
20	67081	0.0615	5.1016E-05	7.6524E-05	0.00010203
21	28236	0.0603	1.117E-05	1.6755E-05	2.234E-05
22	39025	0.0642	2.0731E-05	3.1096E-05	4.1461E-05
23	48530	0.0732	3.7431E-05	5.6147E-05	7.4862E-05
24	64106	0.1443	0.00011283	0.00016924	0.00022566
25	28915	0.1437	1.5833E-05	2.375E-05	3.1666E-05
26	43057	0.1479	2.9125E-05	4.3687E-05	5.8249E-05
27	51381	0.1608	5.7526E-05	8.6289E-05	0.00011505
28	58588	0.3651	0.00021845	0.00032768	0.00043691
29	26966	0.0405	1.4184E-06	2.1276E-06	2.8368E-06
30	33281	0.0414	2.5974E-06	3.8961E-06	5.1948E-06

Table B9. PD Measured Data from M_R Test for 75% RAP TH 10 (OMC+2%)

Seq.	Measured M_R (psi)	Measured PD (inches)	Pred. PD (inches)		
			H = 6 in.	H = 9 in.	H = 12 in
2	32093	0.2334	1.759E-09	2.6386E-09	3.5181E-09
3	37805	0.234	2.8751E-09	4.3127E-09	5.7503E-09
4	45991	0.234	4.2767E-09	6.4151E-09	8.5534E-09
5	54698	0.234	5.8049E-09	8.7074E-09	1.161E-08
6	27865	0.234	1.5756E-09	2.3635E-09	3.1513E-09
7	31095	0.2346	3.1573E-09	4.7359E-09	6.3146E-09
8	37163	0.2352	5.1718E-09	7.7577E-09	1.0344E-08
9	46757	0.2358	7.6453E-09	1.1468E-08	1.5291E-08
10	56237	0.2364	1.0501E-08	1.5751E-08	2.1001E-08
11	28125	0.2364	2.9287E-09	4.393E-09	5.8574E-09
12	34413	0.2388	5.5839E-09	8.3759E-09	1.1168E-08
13	41475	0.2418	9.3953E-09	1.4093E-08	1.8791E-08
14	46241	0.249	1.5706E-08	2.3559E-08	3.1412E-08
15	53560	0.2622	2.2864E-08	3.4296E-08	4.5727E-08
16	25330	0.2628	4.7392E-09	7.1088E-09	9.4784E-09
17	30141	0.2676	9.3946E-09	1.4092E-08	1.8789E-08
18	34166	0.279	1.6931E-08	2.5396E-08	3.3861E-08
19	41633	0.3168	2.7334E-08	4.1002E-08	5.4669E-08

Table B10. PD Measured Data from M_R Test for 100% RAP TH 10 (OMC-2%)

Seq.	Measured M_R (psi)	Measured PD (inches)	Pred. PD (inches)		
			H = 6 in.	H = 9 in.	H = 12 in
9	182351	0.00978	0.00037049	0.00055574	0.00074098
10	207135	0.01038	0.00059888	0.00089832	0.00119776
11	113196	0.00876	9.7009E-05	0.00014551	0.00019402
12	118421	0.00906	0.00021474	0.00032212	0.00042949
13	133087	0.0096	0.00040838	0.00061257	0.00081675
14	159071	0.01098	0.00073731	0.00110597	0.00147462
15	170763	0.0123	0.00119362	0.00179043	0.00238724
16	93750	0.01026	0.00015216	0.00022824	0.00030431
17	107980	0.01074	0.00033256	0.00049884	0.00066512
18	126428	0.01152	0.00064102	0.00096154	0.00128205
19	141306	0.01302	0.0011876	0.0017814	0.00237519
20	158656	0.0162	0.00198038	0.00297057	0.00396076
21	80016	0.01428	0.00027492	0.00041237	0.00054983
22	98729	0.01518	0.00060366	0.0009055	0.00120733
23	130051	0.0168	0.00119637	0.00179456	0.00239274
24	148301	0.0204	0.0023869	0.00358035	0.0047738
25	160499	0.02532	0.00427756	0.00641633	0.00855511
26	82730	0.0228	0.00039142	0.00058713	0.00078285
27	99484	0.02358	0.00090783	0.00136174	0.00181566
28	122072	0.0252	0.0019244	0.0028866	0.00384881
29	136500	0.0297	0.00409338	0.00614006	0.00818675
30	161528	0.03774	0.00786894	0.01180341	0.01573788

Table B11. PD Measured Data from M_R Test for 100% RAP TH 10 (OMC%)

Seq.	Measured M_R (psi)	Measured PD (inches)	Pred. PD (inches)		
			H = 6 in.	H = 9 in.	H = 12 in
1	35765	0.0015	1.6876E-06	2.5314E-06	3.3752E-06
2	48278	0.0252	2.9492E-06	4.4238E-06	5.8984E-06
3	84285	0.0237	4.0097E-06	6.0145E-06	8.0194E-06
4	122364	0.0243	6.1441E-06	9.2162E-06	1.2288E-05
5	152522	0.0249	9.2282E-06	1.3842E-05	1.8456E-05
6	45733	0.0225	2.4496E-06	3.6744E-06	4.8992E-06
7	59907	0.0231	4.51E-06	6.765E-06	9.0199E-06
8	84111	0.024	7.1278E-06	1.0692E-05	1.4256E-05
9	111785	0.0249	1.1302E-05	1.6953E-05	2.2604E-05
10	139704	0.0258	1.6968E-05	2.5453E-05	3.3937E-05
11	46111	0.0234	4.5617E-06	6.8426E-06	9.1235E-06
12	59317	0.024	8.6777E-06	1.3017E-05	1.7355E-05
13	80740	0.0252	1.4276E-05	2.1414E-05	2.8553E-05
14	53423	0.0264	3.2219E-05	4.8329E-05	6.4439E-05
15	122797	0.0282	3.6285E-05	5.4427E-05	7.2569E-05
16	41514	0.0252	7.293E-06	1.094E-05	1.4586E-05
17	58550	0.0258	1.3272E-05	1.9908E-05	2.6545E-05
18	80368	0.0276	2.2336E-05	3.3504E-05	4.4672E-05
19	97320	0.0297	3.8745E-05	5.8118E-05	7.749E-05
20	109269	0.033	6.2244E-05	9.3366E-05	0.00012449
21	42211	0.0303	1.222E-05	1.8331E-05	2.4441E-05
22	56228	0.0318	2.4062E-05	3.6093E-05	4.8124E-05
23	74831	0.0351	4.323E-05	6.4845E-05	8.646E-05
24	99678	0.0519	0.00013777	0.00020665	0.00027554
25	39445	0.0486	1.8536E-05	2.7804E-05	3.7072E-05
26	56349	0.0507	3.6226E-05	5.4338E-05	7.2451E-05
27	73487	0.0546	6.9582E-05	0.00010437	0.00013916
28	96697	0.06	0.00013364	0.00020046	0.00026728
29	90323	0.0912	0.000262	0.000393	0.000524
30	35765	0.0015	1.6876E-06	2.5314E-06	3.3752E-06

Table B12. PD Measured Data from M_R Test for 100% RAP TH 10 (OMC+2%)

Seq.	Measured M_R (psi)	Measured PD (inches)	Pred. PD (inches)		
			H = 6 in.	H = 9 in.	H = 12 in
2	45187	0.1644	3.0816E-09	4.6224E-09	6.1632E-09
3	51199	0.1644	5.2475E-09	7.8713E-09	1.0495E-08
4	59162	0.165	8.205E-09	1.2307E-08	1.641E-08
5	70708	0.165	1.1302E-08	1.6953E-08	2.2604E-08
6	44102	0.1656	2.5095E-09	3.7643E-09	5.0191E-09
7	47283	0.1656	5.2323E-09	7.8484E-09	1.0465E-08
8	55026	0.1662	8.9042E-09	1.3356E-08	1.7808E-08
9	67053	0.1668	1.3821E-08	2.0731E-08	2.7642E-08
10	74242	0.1674	2.0297E-08	3.0445E-08	4.0594E-08
11	39975	0.1674	5.0391E-09	7.5587E-09	1.0078E-08
12	45928	0.1686	1.0208E-08	1.5312E-08	2.0417E-08
13	54139	0.1704	1.7701E-08	2.6552E-08	3.5403E-08
14	64733	0.177	2.8725E-08	4.3088E-08	5.7451E-08
15	66262	0.1914	4.5463E-08	6.8194E-08	9.0925E-08
16	34883	0.1914	8.2834E-09	1.2425E-08	1.6567E-08
17	44083	0.195	1.5937E-08	2.3906E-08	3.1875E-08
18	47731	0.207	2.9991E-08	4.4986E-08	5.9982E-08
19	52918	0.243	5.2387E-08	7.8581E-08	1.0477E-07
20	49955	0.3072	9.03E-08	1.3545E-07	1.806E-07
21	29747	0.312	1.5896E-08	2.3844E-08	3.1792E-08
22	36612	0.3186	3.2242E-08	4.8364E-08	6.4485E-08
23	44434	0.348	5.8962E-08	8.8444E-08	1.1792E-07

Table B13. PD Measured Data from M_R Test for Extracted 100% RAP TH 10 (OMC%)

Seq.	Measured M_R (psi)	Measured PD (inches)	Pred. PD (inches)		
			H = 6 in.	H = 9 in.	H = 12 in
4	78504	0.0192	2.1589E-06	3.2383E-06	4.3178E-06
5	96907	0.0198	3.0188E-06	4.5283E-06	6.0377E-06
6	37545	0.018	1.8819E-06	2.8229E-06	3.7639E-06
7	49068	0.0186	2.9273E-06	4.391E-06	5.8546E-06
8	68864	0.0192	4.1627E-06	6.244E-06	8.3253E-06
9	91113	0.0198	5.6766E-06	8.5149E-06	1.1353E-05
10	25325	0.018	2.1959E-06	3.2939E-06	4.3919E-06
11	35925	0.0186	3.7205E-06	5.5808E-06	7.441E-06
12	54936	0.0192	5.3583E-06	8.0374E-06	1.0717E-05
13	74920	0.0204	8.1345E-06	1.2202E-05	1.6269E-05
14	88353	0.0222	1.2132E-05	1.8199E-05	2.4265E-05
15	26811	0.0192	3.1137E-06	4.6705E-06	6.2273E-06
16	40331	0.0204	5.1852E-06	7.7779E-06	1.037E-05
17	56334	0.0222	8.2377E-06	1.2357E-05	1.6475E-05
18	74686	0.0252	1.3179E-05	1.9768E-05	2.6357E-05
19	93293	0.0306	1.9925E-05	2.9888E-05	3.9851E-05
20	29794	0.0282	4.8498E-06	7.2746E-06	9.6995E-06
21	48644	0.0306	8.0555E-06	1.2083E-05	1.6111E-05
22	64216	0.0348	1.4288E-05	2.1432E-05	2.8576E-05
23	69942	0.0468	2.7372E-05	4.1058E-05	5.4743E-05
24	83926	0.0624	4.4791E-05	6.7187E-05	8.9582E-05
25	28004	0.06	7.3629E-06	1.1044E-05	1.4726E-05
26	45343	0.063	1.2734E-05	1.9101E-05	2.5468E-05
27	65675	0.069	2.2514E-05	3.3772E-05	4.5029E-05
28	73749	0.0912	4.564E-05	6.846E-05	9.128E-05
29	78504	0.0192	2.1589E-06	3.2383E-06	4.3178E-06

Table B14. PD Measured Data from M_R Test for RAP TH 19-101 (OMC-2%)

Seq.	Measured M_R (psi)	Measured PD (inches)	Pred. PD (inches)		
			H = 6 in.	H = 9 in.	H = 12 in
3	90464	0.01032	7.88E-05	0.000118	0.000158
4	105556	0.01116	0.000128	0.000192	0.000256
5	124349	0.01188	0.000188	0.000282	0.000377
6	72609	0.00942	3.75E-05	5.63E-05	7.51E-05
7	71999	0.00984	8.24E-05	0.000124	0.000165
8	79246	0.01056	0.000148	0.000222	0.000296
9	93611	0.01362	0.000241	0.000361	0.000481
10	108745	0.01224	0.000356	0.000534	0.000711
11	58879	0.00954	7.88E-05	0.000118	0.000158
12	60720	0.01008	0.000173	0.000259	0.000346
13	68176	0.01098	0.000313	0.00047	0.000627
14	87061	0.012	0.000504	0.000756	0.001008
15	95112	0.01344	0.000782	0.001173	0.001564
16	51518	0.0102	0.000127	0.000191	0.000255
17	56342	0.01092	0.000274	0.000412	0.000549
18	66878	0.01194	0.000494	0.000741	0.000988
19	79211	0.0135	0.000849	0.001273	0.001698
20	85637	0.01608	0.001363	0.002045	0.002726
21	48981	0.0126	0.000223	0.000335	0.000446
22	51488	0.01326	0.000514	0.000771	0.001028
23	61123	0.01488	0.000973	0.001459	0.001946
24	70208	0.0186	0.001809	0.002713	0.003617
25	80041	0.02568	0.003027	0.004541	0.006054
26	45535	0.02088	0.000338	0.000508	0.000677
27	48973	0.0216	0.0008	0.001201	0.001601
28	58857	0.02322	0.001587	0.00238	0.003174
29	70782	0.02724	0.003085	0.004627	0.006169
30	81916	0.0369	0.005508	0.008263	0.011017

Table B15. PD Measured Data from M_R Test for RAP TH 19-101 (OMC%)

Seq.	Measured M_R (psi)	Measured PD (inches)	Pred. PD (inches)		
			H = 6 in.	H = 9 in.	H = 12 in
1	55027	0.0096	5.02E-07	7.54E-07	1E-06
2	69464	0.01008	9.51E-07	1.43E-06	1.9E-06
3	85356	0.01074	1.6E-06	2.4E-06	3.2E-06
4	100191	0.0117	2.58E-06	3.87E-06	5.16E-06
5	122151	0.01218	3.75E-06	5.62E-06	7.49E-06
6	74839	0.00942	7.34E-07	1.1E-06	1.47E-06
7	82031	0.00996	1.54E-06	2.31E-06	3.08E-06
8	88696	0.01074	2.8E-06	4.2E-06	5.6E-06
9	97109	0.01158	4.71E-06	7.07E-06	9.43E-06
10	110689	0.01254	7.03E-06	1.05E-05	1.41E-05
11	70195	0.00966	1.42E-06	2.13E-06	2.84E-06
12	72645	0.0102	3.12E-06	4.67E-06	6.23E-06
13	85566	0.01206	5.59E-06	8.38E-06	1.12E-05
14	90406	0.01224	9.86E-06	1.48E-05	1.97E-05
15	97478	0.01386	1.54E-05	2.31E-05	3.08E-05
16	66045	0.0105	2.18E-06	3.27E-06	4.36E-06
17	68163	0.0111	4.89E-06	7.33E-06	9.77E-06
18	73441	0.01212	9.34E-06	1.4E-05	1.87E-05
19	82446	0.01386	1.65E-05	2.48E-05	3.31E-05
20	85986	0.01674	2.7E-05	4.05E-05	5.4E-05
21	57630	0.01284	3.99E-06	5.99E-06	7.99E-06
22	59392	0.01362	9.34E-06	1.4E-05	1.87E-05
23	66793	0.01524	1.84E-05	2.76E-05	3.67E-05
24	71692	0.0189	3.55E-05	5.33E-05	7.1E-05
25	77090	0.02484	6.11E-05	9.17E-05	0.000122
26	54809	0.02028	5.95E-06	8.92E-06	1.19E-05
27	54365	0.02106	1.49E-05	2.23E-05	2.97E-05
28	60360	0.0228	3.1E-05	4.65E-05	6.21E-05
29	69789	0.02694	6.17E-05	9.25E-05	0.000123
30	75818	0.03732	0.000113	0.00017	0.000226

Table B16. PD Measured Data from M_R Test for RAP TH 19-101 (OMC+2%)

Seq.	Measured M_R (psi)	Measured PD (inches)	Pred. PD (inches)		
			H = 6 in.	H = 9 in.	H = 12 in
2	35693	0.04098	5.49E-10	8.24E-10	1.1E-09
3	49109	0.04584	8.1E-10	1.22E-09	1.62E-09
4	56813	0.04758	1.26E-09	1.9E-09	2.53E-09
5	70762	0.04896	1.7E-09	2.55E-09	3.4E-09
6	30247	0.04038	5E-10	7.5E-10	9.99E-10
7	36703	0.04494	9.42E-10	1.41E-09	1.88E-09
8	36383	0.0465	1.78E-09	2.67E-09	3.56E-09
9	46059	0.04836	2.62E-09	3.92E-09	5.23E-09
10	57518	0.04998	3.51E-09	5.26E-09	7.02E-09
11	29831	0.04488	9.46E-10	1.42E-09	1.89E-09
12	26581	0.04602	2.32E-09	3.48E-09	4.64E-09
13	31976	0.04776	3.86E-09	5.8E-09	7.73E-09
14	44109	0.05016	5.49E-09	8.24E-09	1.1E-08
15	55032	0.05334	7.61E-09	1.14E-08	1.52E-08
16	24684	0.04752	1.64E-09	2.46E-09	3.28E-09
17	24969	0.04872	3.71E-09	5.56E-09	7.41E-09
18	32387	0.05124	5.97E-09	8.96E-09	1.19E-08
19	41268	0.05598	9.31E-09	1.4E-08	1.86E-08
20	46693	0.06486	1.42E-08	2.13E-08	2.84E-08
21	22117	0.05856	3.05E-09	4.57E-09	6.1E-09
22	25023	0.06006	6.54E-09	9.82E-09	1.31E-08
23	31609	0.06606	1.14E-08	1.71E-08	2.28E-08
24	40556	0.08658	1.9E-08	2.84E-08	3.79E-08
25	43746	0.13566	3.2E-08	4.8E-08	6.41E-08
26	24602	0.11574	4.03E-09	6.04E-09	8.05E-09
27	33565	0.1377	1.74E-08	2.6E-08	3.47E-08
28	41571	0.18432	3.19E-08	4.78E-08	6.38E-08
29	35693	0.04098	5.49E-10	8.24E-10	1.1E-09

Table B17. PD Measured Data from M_R Test for RAP TH 19-104 (OMC-2%)

Seq.	Measured M_R (psi)	Measured PD (inches)	Pred. PD (inches)		
			H = 6 in.	H = 9 in.	H = 12 in
4	112397	0.01206	2E-05	3.01E-05	4.01E-05
5	136712	0.01254	2.96E-05	4.44E-05	5.92E-05
6	76672	0.0111	1.27E-05	1.9E-05	2.54E-05
7	85042	0.01164	2.28E-05	3.41E-05	4.55E-05
8	97755	0.01224	3.76E-05	5.65E-05	7.53E-05
9	117266	0.0123	5.56E-05	8.33E-05	0.000111
10	68554	0.01092	1.15E-05	1.72E-05	2.3E-05
11	68839	0.0111	2.56E-05	3.84E-05	5.12E-05
12	77127	0.01194	4.68E-05	7.02E-05	9.35E-05
13	120043	0.0126	7.29E-05	0.000109	0.000146
14	108081	0.01392	0.000119	0.000179	0.000239
15	59069	0.01194	1.86E-05	2.79E-05	3.71E-05
16	63709	0.01242	4.06E-05	6.08E-05	8.11E-05
17	76575	0.0132	7.33E-05	0.00011	0.000147
18	99930	0.01488	0.000123	0.000185	0.000247
19	102751	0.01818	0.000203	0.000305	0.000406
20	51439	0.01566	3.43E-05	5.14E-05	6.86E-05
21	59493	0.01632	7.46E-05	0.000112	0.000149
22	80407	0.01764	0.000134	0.000201	0.000268
23	86896	0.02304	0.00026	0.000391	0.000521
24	95783	0.0333	0.000448	0.000672	0.000896
25	51333	0.03024	4.96E-05	7.44E-05	9.92E-05
26	58801	0.03084	0.000113	0.00017	0.000227
27	112397	0.01206	2E-05	3.01E-05	4.01E-05

Table B18. PD Measured Data from M_R Test for RAP TH 19-104 (OMC%)

Seq.	Measured M_R (psi)	Measured PD (inches)	Pred. PD (inches)		
			H = 6 in.	H = 9 in.	H = 12 in
2	49164	0.03864	3.15E-08	4.73E-08	6.31E-08
3	60073	0.03966	5.15E-08	7.73E-08	1.03E-07
4	79491	0.04068	7.61E-08	1.14E-07	1.52E-07
5	96164	0.04152	1.07E-07	1.61E-07	2.15E-07
6	44985	0.03834	2.68E-08	4.02E-08	5.36E-08
7	43203	0.03888	6.03E-08	9.05E-08	1.21E-07
8	52170	0.04008	9.98E-08	1.5E-07	2E-07
9	65118	0.04122	1.52E-07	2.28E-07	3.04E-07
10	81255	0.04224	2.11E-07	3.16E-07	4.22E-07
11	36998	0.03876	5.78E-08	8.67E-08	1.16E-07
12	37156	0.0396	1.29E-07	1.93E-07	2.57E-07
13	44533	0.04092	2.18E-07	3.27E-07	4.36E-07
14	57178	0.04242	3.34E-07	5.02E-07	6.69E-07
15	64114	0.04446	5.02E-07	7.52E-07	1E-06
16	31036	0.04026	9.82E-08	1.47E-07	1.96E-07
17	33939	0.04128	2.09E-07	3.14E-07	4.18E-07
18	42796	0.04296	3.5E-07	5.25E-07	7E-07
19	51059	0.04644	5.81E-07	8.71E-07	1.16E-06
20	58532	0.05286	8.86E-07	1.33E-06	1.77E-06
21	26235	0.04806	1.91E-07	2.86E-07	3.81E-07
22	32498	0.04998	3.83E-07	5.74E-07	7.65E-07
23	42364	0.0537	6.6E-07	9.91E-07	1.32E-06
24	49846	0.0663	1.19E-06	1.78E-06	2.37E-06
25	52648	0.08034	2.04E-06	3.06E-06	4.08E-06
26	27936	0.08304	2.62E-07	3.92E-07	5.23E-07
27	34022	0.08454	5.57E-07	8.35E-07	1.11E-06
28	40704	0.08094	1.08E-06	1.63E-06	2.17E-06
29	59440	0.11172	1.82E-06	2.73E-06	3.64E-06

Table B19. PD Measured Data from M_R Test for RAP TH 19-104 (OMC+2%)

Seq.	Measured M_R (psi)	Measured PD (inches)	Pred. PD (inches)		
			H = 6 in.	H = 9 in.	H = 12 in
3	36595	0.16698	4.12E-13	6.18E-13	8.24E-13
4	41426	0.16776	6.44E-13	9.66E-13	1.29E-12
5	50277	0.168	8.57E-13	1.29E-12	1.71E-12
6	32494	0.16644	1.95E-13	2.93E-13	3.9E-13
7	25072	0.16716	5.26E-13	7.88E-13	1.05E-12
8	29407	0.16806	8.67E-13	1.3E-12	1.73E-12
9	37943	0.1689	1.24E-12	1.86E-12	2.48E-12
10	48145	0.16962	1.62E-12	2.43E-12	3.25E-12
11	23022	0.16794	4.83E-13	7.25E-13	9.67E-13
12	24912	0.16932	1.01E-12	1.52E-12	2.02E-12
13	35033	0.17136	1.49E-12	2.23E-12	2.98E-12
14	38336	0.17568	2.51E-12	3.77E-12	5.02E-12
15	43522	0.1884	3.67E-12	5.51E-12	7.35E-12
16	18414	0.18684	8.7E-13	1.3E-12	1.74E-12
17	24539	0.1905	1.55E-12	2.33E-12	3.11E-12
18	29577	0.19986	2.65E-12	3.98E-12	5.3E-12
19	36197	0.2418	4.24E-12	6.36E-12	8.47E-12
20	37910	0.34356	6.8E-12	1.02E-11	1.36E-11
21	17001	0.34518	1.58E-12	2.37E-12	3.16E-12
22	24520	0.35574	2.75E-12	4.13E-12	5.5E-12
23	29218	0.4191	5.01E-12	7.52E-12	1E-11

Table B20. PD Measured Data from M_R Test for RAP TH 22 (OMC-2%)

Seq.	Measured M_R (psi)	Measured PD (inches)	Pred. PD (inches)		
			H = 6 in.	H = 9 in.	H = 12 in
14	147783	0.0096	0.001037	0.001556	0.002075
15	155775	0.01062	0.001667	0.002501	0.003334
16	68469	0.00858	0.000247	0.000371	0.000494
17	90046	0.00906	0.000498	0.000747	0.000996
18	114406	0.00978	0.000921	0.001382	0.001843
19	129331	0.01098	0.001688	0.002532	0.003376
20	143504	0.01302	0.002787	0.00418	0.005573
21	71920	0.0108	0.000409	0.000613	0.000817
22	84156	0.01134	0.000905	0.001357	0.00181
23	102441	0.01272	0.001774	0.002661	0.003547
24	117263	0.0159	0.003443	0.005164	0.006885
25	130202	0.02034	0.006044	0.009067	0.012089
26	60671	0.01728	0.000648	0.000971	0.001295
27	73701	0.01824	0.001449	0.002174	0.002898
28	101452	0.01986	0.002838	0.004257	0.005676
29	128449	0.02328	0.005815	0.008722	0.011629
30	135875	0.03006	0.011073	0.016609	0.022146

Table B21. PD Measured Data from M_R Test for RAP TH 22 (OMC%)

Seq.	Measured M_R (psi)	Measured PD (inches)	Pred. PD (inches)		
			H = 6 in.	H = 9 in.	H = 12 in
2	30670	0.04458	7.87E-06	1.18E-05	1.57E-05
3	59994	0.0306	9.12E-06	1.37E-05	1.82E-05
4	82447	0.03144	1.33E-05	1.99E-05	2.65E-05
5	103832	0.0321	1.85E-05	2.78E-05	3.71E-05
6	31386	0.0294	6.19E-06	9.28E-06	1.24E-05
7	42192	0.03024	1.08E-05	1.63E-05	2.17E-05
8	58394	0.03108	1.65E-05	2.47E-05	3.29E-05
9	79278	0.03198	2.44E-05	3.66E-05	4.88E-05
10	98688	0.03282	3.46E-05	5.2E-05	6.93E-05
11	31478	0.03	1.16E-05	1.73E-05	2.31E-05
12	413215	0.03102	2.75E-05	4.12E-05	5.5E-05
13	61425	0.03204	3.14E-05	4.72E-05	6.29E-05
14	79852	0.03336	4.95E-05	7.43E-05	9.91E-05
15	91948	0.0351	7.5E-05	0.000112	0.00015
16	30835	0.03192	1.75E-05	2.62E-05	3.49E-05
17	43152	0.03312	3.1E-05	4.65E-05	6.2E-05
18	60279	0.03468	4.96E-05	7.44E-05	9.93E-05
19	75120	0.03726	8.24E-05	0.000124	0.000165
20	85665	0.04128	0.000129	0.000194	0.000258
21	31436	0.03804	2.92E-05	4.37E-05	5.83E-05
22	44345	0.04032	5.38E-05	8.07E-05	0.000108
23	59650	0.04422	9.35E-05	0.00014	0.000187
24	72687	0.05322	0.000168	0.000253	0.000337
25	85193	0.06516	0.000279	0.000419	0.000559
26	31642	0.06192	4.19E-05	6.29E-05	8.38E-05
27	46566	0.06408	7.85E-05	0.000118	0.000157
28	62425	0.06864	0.000145	0.000218	0.000291
29	74845	0.08346	0.000284	0.000426	0.000569
30	81380	0.11724	0.000523	0.000785	0.001047

Table B22. PD Measured Data from M_R Test for RAP TH 22 (OMC+2%)

Seq.	Measured M_R (psi)	Measured PD (inches)	Pred. PD (inches)		
			H = 6 in.	H = 9 in.	H = 12 in
1	40211	0.08934	5.89E-09	8.84E-09	1.18E-08
2	42886	0.08958	1.22E-08	1.83E-08	2.44E-08
3	50335	0.0897	2.02E-08	3.03E-08	4.04E-08
4	62065	0.08994	3.04E-08	4.56E-08	6.08E-08
5	77740	0.09006	4.11E-08	6.17E-08	8.23E-08
6	37592	0.08976	1.07E-08	1.61E-08	2.15E-08
7	40501	0.09012	2.22E-08	3.33E-08	4.44E-08
8	47931	0.09042	3.71E-08	5.56E-08	7.42E-08
9	59133	0.09066	5.65E-08	8.48E-08	1.13E-07
10	71678	0.09108	7.87E-08	1.18E-07	1.57E-07
11	34141	0.0906	2.16E-08	3.24E-08	4.32E-08
12	42494	0.0915	4.11E-08	6.16E-08	8.21E-08
13	53130	0.09324	6.83E-08	1.02E-07	1.37E-07
14	60148	0.096	1.14E-07	1.71E-07	2.28E-07
15	66152	0.10266	1.73E-07	2.6E-07	3.47E-07
16	31619	0.10248	3.41E-08	5.11E-08	6.81E-08
17	40770	0.1047	6.42E-08	9.63E-08	1.28E-07
18	49940	0.11064	1.11E-07	1.66E-07	2.22E-07
19	53686	0.12768	1.98E-07	2.97E-07	3.96E-07
20	58197	0.1635	3.13E-07	4.69E-07	6.25E-07
21	29022	0.16482	6.18E-08	9.27E-08	1.24E-07
22	38291	0.17226	1.19E-07	1.78E-07	2.38E-07
23	44465	0.2049	2.25E-07	3.37E-07	4.49E-07
24	56003	0.31116	3.87E-07	5.81E-07	7.75E-07

Table B23. PD Measured Data from M_R Test for Cell 18 (OMC-2%)

Seq.	Measured M_R (psi)	Measured PD (inches)	Pred. PD (inches)		
			H = 6 in.	H = 9 in.	H = 12 in
5	170163	0.01272	0.000574	0.000861	0.001149
7	91074	0.01134	0.000226	0.000339	0.000452
8	117018	0.01188	0.000395	0.000593	0.000791
9	139380	0.01248	0.000674	0.001011	0.001348
10	162839	0.01314	0.00105	0.001575	0.0021
11	69136	0.01128	0.000219	0.000329	0.000438
12	87987	0.01176	0.000438	0.000657	0.000877
13	108490	0.01638	0.000791	0.001186	0.001582
14	132867	0.01338	0.001378	0.002068	0.002757
15	150656	0.01482	0.002203	0.003305	0.004407
16	66983	0.0126	0.000331	0.000497	0.000662
17	85440	0.01326	0.000673	0.00101	0.001346
18	108358	0.01422	0.001235	0.001853	0.002471
19	134056	0.01602	0.002228	0.003342	0.004456
20	144556	0.01872	0.00369	0.005535	0.00738
21	70996	0.01638	0.000545	0.000817	0.00109
22	88361	0.0174	0.001175	0.001762	0.00235
23	108337	0.01944	0.002313	0.00347	0.004626
24	124396	0.02418	0.004514	0.006772	0.009029
25	130925	0.03138	0.008	0.012	0.015999
26	61272	0.02844	0.000853	0.001279	0.001706
27	80080	0.0297	0.001846	0.002769	0.003691
28	100975	0.03228	0.003763	0.005645	0.007526

Table B24. PD Measured Data from M_R Test for Cell 18 (OMC%)

Seq.	Measured M_R (psi)	Measured PD (inches)	Pred. PD (inches)		
			H = 6 in.	H = 9 in.	H = 12 in
4	138283	0.0183	1.95E-05	2.92E-05	3.89E-05
5	170158	0.01872	3E-05	4.5E-05	6E-05
7	77267	0.01758	1.26E-05	1.9E-05	2.53E-05
8	104081	0.01746	2.12E-05	3.18E-05	4.24E-05
9	135208	0.01794	3.52E-05	5.29E-05	7.05E-05
10	160721	0.01854	5.47E-05	8.21E-05	0.000109
11	55714	0.01692	1.29E-05	1.94E-05	2.59E-05
12	78125	0.0174	2.41E-05	3.61E-05	4.81E-05
13	106273	0.018	4.15E-05	6.23E-05	8.3E-05
14	131834	0.0189	7.2E-05	0.000108	0.000144
15	149020	0.02028	0.000115	0.000172	0.00023
16	54460	0.01842	1.95E-05	2.93E-05	3.9E-05
17	70738	0.01896	3.83E-05	5.75E-05	7.67E-05
18	104029	0.01998	6.52E-05	9.78E-05	0.00013
19	122728	0.0219	0.000117	0.000176	0.000235
20	138843	0.02496	0.000193	0.000289	0.000386
21	52780	0.0228	3.37E-05	5.06E-05	6.75E-05
22	77642	0.02412	6.48E-05	9.72E-05	0.00013
23	104116	0.027	0.000122	0.000183	0.000244
24	117729	0.03294	0.000238	0.000357	0.000476
25	139599	0.04068	0.000416	0.000624	0.000832
26	50588	0.04032	5.01E-05	7.51E-05	0.0001
27	74971	0.04182	9.94E-05	0.000149	0.000199
28	102947	0.04518	0.000195	0.000293	0.000391
29	119916	0.05496	0.000406	0.000609	0.000812
30	119071	0.07584	0.000778	0.001167	0.001556

Table B25. PD Measured Data from M_R Test for Cell 18 (OMC+2%)

Seq.	Measured M_R (psi)	Measured PD (inches)	Pred. PD (inches)		
			H = 6 in.	H = 9 in.	H = 12 in
5	115782	0.0129	1.02E-07	1.53E-07	2.04E-07
6	46702	0.01074	2.61E-08	3.92E-08	5.23E-08
7	56156	0.01122	5.07E-08	7.61E-08	1.01E-07
8	72440	0.01194	8.26E-08	1.24E-07	1.65E-07
9	92492	0.0126	1.29E-07	1.94E-07	2.59E-07
10	111257	0.01332	1.89E-07	2.84E-07	3.79E-07
11	38461	0.01098	5.62E-08	8.42E-08	1.12E-07
12	54180	0.01164	9.93E-08	1.49E-07	1.99E-07
13	73191	0.01248	1.62E-07	2.43E-07	3.24E-07
14	93974	0.01368	2.62E-07	3.94E-07	5.25E-07
15	105526	0.01554	4.06E-07	6.08E-07	8.11E-07
16	37626	0.01302	8.48E-08	1.27E-07	1.7E-07
17	56233	0.01386	1.47E-07	2.21E-07	2.94E-07
18	75356	0.01506	2.49E-07	3.74E-07	4.98E-07
19	88983	0.01848	4.33E-07	6.5E-07	8.66E-07
20	102059	0.02268	6.86E-07	1.03E-06	1.37E-06
21	38814	0.01992	1.41E-07	2.11E-07	2.81E-07
22	58448	0.02136	2.54E-07	3.82E-07	5.09E-07
23	74516	0.02466	4.69E-07	7.03E-07	9.38E-07
24	85960	0.04086	8.82E-07	1.32E-06	1.76E-06
25	102491	0.05454	1.48E-06	2.22E-06	2.96E-06
26	39815	0.05142	1.99E-07	2.99E-07	3.99E-07
27	60308	0.05358	3.77E-07	5.65E-07	7.53E-07
28	81858	0.05766	7.16E-07	1.07E-06	1.43E-06
29	84655	0.07374	1.52E-06	2.28E-06	3.04E-06

Table B26. PD Measured Data from Single-stage RTL Test for Class 5 at OMC% (σ_d = 17 psi)

No. of Cycles	Measured M_R (psi)	Measured PD (inches)	Pred. PD (inches)		
			H = 6 in.	H = 9 in.	H = 12 in.
1	25070	0	0	0	0
10	26120	0.0018	5.177E-44	7.7655E-44	1.0354E-43
20	25550	0.003	3.2996E-23	4.9494E-23	6.5992E-23
50	24420	0.0054	1.0384E-10	1.5576E-10	2.0768E-10
100	24130	0.0072	1.5178E-06	2.2767E-06	3.0357E-06
200	23710	0.0108	0.00018422	0.00027633	0.00036844
300	24400	0.0132	0.00090442	0.00135663	0.00180884
400	23080	0.0144	0.00211609	0.00317413	0.00423217
500	24050	0.0156	0.00332303	0.00498454	0.00664605
600	24770	0.0162	0.00454024	0.00681037	0.00908049
700	25700	0.0168	0.00555481	0.00833222	0.01110963
800	24600	0.0174	0.00687571	0.01031356	0.01375141
900	25050	0.018	0.00778984	0.01168476	0.01557968
1000	24560	0.0186	0.00878911	0.01318366	0.01757821
1250	26220	0.0198	0.01015437	0.01523155	0.02030873
1500	25350	0.021	0.01186145	0.01779218	0.0237229
1750	25900	0.0222	0.01294956	0.01942434	0.02589911
2000	25610	0.0234	0.01395731	0.02093597	0.02791463
2250	26040	0.024	0.01450016	0.02175025	0.02900033
2500	26810	0.0252	0.01483434	0.02225151	0.02966867
2750	27480	0.0258	0.01502445	0.02253667	0.03004889
3000	25840	0.0264	0.01630705	0.02446058	0.03261411
3500	25810	0.027	0.01711859	0.02567788	0.03423718
4000	26450	0.0282	0.01731528	0.02597292	0.03463056
4500	25900	0.0288	0.01821285	0.02731927	0.0364257
5000	25820	0.0294	0.0186268	0.0279402	0.0372536
5500	26520	0.03	0.01851813	0.02777719	0.03703626
6000	27260	0.0306	0.01838471	0.02757707	0.03676942
6500	28110	0.0312	0.0183385	0.02750775	0.036677
7000	28770	0.0312	0.01821432	0.02732148	0.03642864
7500	28590	0.0318	0.0184247	0.02763704	0.03684939
8000	28570	0.0318	0.01854551	0.02781827	0.03709103
8500	28260	0.0324	0.01889142	0.02833713	0.03778283
9000	28480	0.033	0.01886664	0.02829996	0.03773328
9500	28060	0.033	0.01921359	0.02882038	0.03842717
10000	29280	0.0336	0.0187125	0.02806875	0.037425

Table B26. PD Measured Data from Single-stage RTL Test for Class 5 at OMC% (σ_d = 17 psi) (Continued)

No. of Cycles	Measured M_R (psi)	Measured PD (inches)	Pred. PD (inches)		
			H = 6 in.	H = 9 in.	H = 12 in.
10500	29410	0.0336	0.01873173	0.02809759	0.03746346
11000	28690	0.0336	0.01918591	0.02877886	0.03837182
11500	29240	0.0342	0.01890518	0.02835776	0.03781035
12000	28510	0.0342	0.01928121	0.02892182	0.03856242
12500	29390	0.0348	0.01894135	0.02841202	0.0378827
13000	28810	0.0348	0.01931509	0.02897264	0.03863018
13500	29810	0.0348	0.01903689	0.02855534	0.03807379
14000	29940	0.0354	0.0188557	0.02828355	0.0377114
14500	29870	0.0354	0.01887221	0.02830831	0.03774441
15000	30380	0.0354	0.01883684	0.02825526	0.03767368
15500	30320	0.036	0.01889263	0.02833895	0.03778526
16000	30050	0.036	0.01915232	0.02872847	0.03830463
16500	30640	0.0366	0.01883195	0.02824793	0.03766391
17000	31640	0.0366	0.01849225	0.02773837	0.03698449
17500	31370	0.0372	0.01852349	0.02778524	0.03704699
18000	31700	0.0372	0.01838822	0.02758232	0.03677643
18500	31200	0.0372	0.01874446	0.0281167	0.03748893
19000	31080	0.0378	0.01877704	0.02816556	0.03755408
19500	31470	0.0378	0.01865546	0.02798319	0.03731092
20000	31150	0.0384	0.01879119	0.02818678	0.03758238

Table B27. PD Measured Data from Single-stage RTL Test for Class 5 at OMC% (σ_d = 24 psi)

No. of Cycles	Measured M_R (psi)	Measured PD (inches)	Pred. PD (inches) – σ_d = 24 psi		
			H = 6 in.	H = 9 in.	H = 12 in.
1	21110	0.0006	0	0	0
10	23370	0.0054	2.574E-43	3.861E-43	5.148E-43
20	24260	0.0078	8.6305E-23	1.2946E-22	1.7261E-22
50	25040	0.0132	1.828E-10	2.742E-10	3.656E-10
100	24900	0.018	2.3274E-06	3.4911E-06	4.6548E-06
200	24720	0.0252	0.00028194	0.00042291	0.00056388
300	24220	0.0312	0.00139423	0.00209135	0.00278847
400	23280	0.0366	0.00320439	0.00480659	0.00640878
500	23360	0.0414	0.0051386	0.0077079	0.0102772
600	23780	0.0456	0.00697327	0.0104599	0.01394653
700	23300	0.0498	0.00891099	0.01336648	0.01782197
800	23430	0.0534	0.01051636	0.01577454	0.02103272
900	24600	0.0576	0.01154356	0.01731534	0.02308712
1000	25910	0.0606	0.01230942	0.01846413	0.02461884
1250	26550	0.0672	0.01466656	0.02199985	0.02933313
1500	26620	0.0732	0.01666863	0.02500295	0.03333726
1750	25840	0.078	0.01880292	0.02820438	0.03760584
2000	24410	0.0822	0.02103146	0.03154719	0.04206291
2250	24850	0.0864	0.02201753	0.03302629	0.04403506
2500	26000	0.09	0.02216633	0.03324949	0.04433265
2750	24980	0.093	0.02378253	0.03567379	0.04756505
3000	24690	0.096	0.02468638	0.03702958	0.04937277
3500	26480	0.1026	0.0244137	0.03662056	0.04882741
4000	26650	0.1074	0.02523448	0.03785171	0.05046895
4500	26120	0.1116	0.02652058	0.03978087	0.05304116
5000	27760	0.1152	0.02589001	0.03883502	0.05178003
5500	27580	0.1188	0.02638518	0.03957777	0.05277036
6000	26240	0.1218	0.02784545	0.04176817	0.05569089
6500	27050	0.1248	0.02764592	0.04146888	0.05529184
7000	25990	0.1272	0.02896257	0.04344386	0.05792514
7500	29810	0.132	0.026278	0.03941699	0.05255599
8000	29840	0.132	0.02642525	0.03963787	0.0528505
8500	29710	0.1338	0.02676828	0.04015241	0.05353655
9000	28870	0.1356	0.02758476	0.04137714	0.05516952
9500	26650	0.1374	0.02972294	0.04458441	0.05944588
10000	26750	0.1392	0.02972125	0.04458188	0.05944251
10500					
11000					

Table B27. PD Measured Data from Single-stage RTL Test for Class 5 at OMC% (σ_d = 24 psi) (Continued)

No. of Cycles	Measured M_R (psi)	Measured PD (inches)	Pred. PD (inches)		
			H = 6 in.	H = 9 in.	H = 12 in.
10500	27190	0.141	0.02947615	0.04421423	0.05895231
11000	27260	0.1428	0.02976907	0.0446536	0.05953813
11500	27190	0.141	0.02947615	0.04421423	0.05895231
12000	27260	0.1428	0.02976907	0.0446536	0.05953813
12500	26680	0.144	0.03036316	0.04554474	0.06072632
13000	27370	0.1458	0.02978242	0.04467362	0.05956483
13500	26850	0.147	0.03043552	0.04565329	0.06087105
14000	27110	0.1488	0.03025599	0.04538398	0.06051197
14500	27960	0.15	0.02963218	0.04444826	0.05926435
15000	29900	0.1512	0.0283614	0.0425421	0.05672281
15500	29840	0.1524	0.02841721	0.04262581	0.05683441
16000	29950	0.153	0.02843768	0.04265653	0.05687537
16500	30180	0.1542	0.02840646	0.04260969	0.05681292
17000	29480	0.1548	0.02905248	0.04357872	0.05810496
17500	29140	0.156	0.02936073	0.0440411	0.05872146
18000	28890	0.1566	0.02964242	0.04446363	0.05928484
18500	28950	0.1584	0.0296836	0.0445254	0.0593672
19000	28990	0.1584	0.02969535	0.04454302	0.0593907
19500	28670	0.159	0.03000304	0.04500455	0.06000607
20000	28070	0.1596	0.03069253	0.0460388	0.06138507

Table B28. PD Measured Data from Single-stage RTL Test for Class 5 at OMC+2% (σ_d = 12 psi)

No. of Cycles	Measured M_R (psi)	Measured PD (inches)	Pred. PD (inches) – σ_d = 12 psi		
			H = 6 in.	H = 9 in.	H = 12 in.
10	21900	0.0024	0	0	0
20	21240	0.0048	2.6806E-43	4.0209E-43	5.3612E-43
50	21130	0.0114	6.0125E-19	9.0187E-19	1.2025E-18
100	18350	0.0174	9.3238E-11	1.3986E-10	1.8648E-10
200	19470	0.0258	1.0542E-06	1.5813E-06	2.1084E-06
300	18950	0.03	2.4608E-05	3.6913E-05	4.9217E-05
400	18700	0.033	0.0001195	0.00017924	0.00023899
500	18730	0.036	0.00030531	0.00045796	0.00061062
600	19170	0.039	0.00056362	0.00084543	0.00112724
700	19510	0.042	0.0008679	0.00130185	0.00173581
800	20280	0.0444	0.00117549	0.00176323	0.00235098
900	20640	0.0468	0.00149625	0.00224437	0.0029925
1000	20230	0.0492	0.00187347	0.0028102	0.00374693
1250	19310	0.0534	0.00285745	0.00428617	0.00571489
1500	19370	0.057	0.00367103	0.00550654	0.00734205
1750	19850	0.06	0.00428091	0.00642136	0.00856181
2000	19230	0.063	0.00508004	0.00762007	0.01016009
2250	19070	0.0654	0.0056188	0.0084282	0.0112376
2500	20040	0.0684	0.0059272	0.0088908	0.0118544
2750	19950	0.0708	0.00634911	0.00952366	0.01269822
3000	20610	0.0726	0.00660023	0.00990034	0.01320046
3500	21180	0.0762	0.00700515	0.01050772	0.0140103
4000	21860	0.0804	0.00731199	0.01096799	0.01462399
4500	21780	0.084	0.00777255	0.01165883	0.0155451
5000	21800	0.0864	0.0081366	0.0122049	0.01627319
5500	24320	0.0888	0.00774747	0.01162121	0.01549495
6000	23490	0.0912	0.00821254	0.01231882	0.01642509
6500	23120	0.093	0.00850746	0.01276119	0.01701492
7000	22610	0.0942	0.00891041	0.01336562	0.01782082
7500	23300	0.0966	0.00893159	0.01339738	0.01786318
8000	23210	0.0966	0.00910126	0.01365189	0.01820251
8500	22750	0.0978	0.00943001	0.01414501	0.01886002
9000	21620	0.099	0.01002527	0.01503791	0.02005054
9500	23270	0.0996	0.00945976	0.01418965	0.01891953
10000	23880	0.1002	0.00949526	0.01424289	0.01899052

Table B28. PD Measured Data from Single-stage RTL Test for Class 5 at OMC+2% (σ_d = 12 psi) (Continued)

No. of Cycles	Measured M_R (psi)	Measured PD (inches)	Pred. PD (inches)		
			H = 6 in.	H = 9 in.	H = 12 in.
10500	24520	0.1008	0.00938953	0.01408429	0.01877906
11000	25400	0.1014	0.00920242	0.01380364	0.01840485
11500	25750	0.102	0.00914908	0.01372362	0.01829816
12000	26990	0.1026	0.00890646	0.0133597	0.01781293
12500	26200	0.1032	0.00916443	0.01374664	0.01832885
13000	26390	0.1038	0.00925128	0.01387693	0.01850257
13500	26680	0.1038	0.00928854	0.01393281	0.01857707
14000	26600	0.1044	0.00931305	0.01396958	0.0186261
14500	27190	0.1044	0.00931316	0.01396975	0.01862633
15000	27660	0.1044	0.00919814	0.01379721	0.01839628
15500	27660	0.105	0.00925263	0.01387894	0.01850525
16000	26830	0.105	0.00947523	0.01421284	0.01895046
16500	26910	0.105	0.00956671	0.01435006	0.01913342
17000	27390	0.1056	0.00947953	0.01421929	0.01895906
17500	29280	0.1056	0.00914796	0.01372194	0.01829592
18000	29140	0.1056	0.0092103	0.01381545	0.0184206
18500	29260	0.1062	0.00920592	0.01380888	0.01841184
19000	31790	0.1062	0.00861355	0.01292033	0.01722711
19500	30500	0.1062	0.00902862	0.01354294	0.01805725
20000	29840	0.1062	0.00914907	0.0137236	0.01829814

Table B29. PD Measured Data from Single-stage RTL Test for Class 5 at OMC+2% (σ_d = 17 psi)

No. of Cycles	Measured M_R (psi)	Measured PD (inches)	Pred. PD (inches)		
			H = 6 in.	H = 9 in.	H = 12 in.
1	21000	0.0006	0	0	0
10	19380	0.0036	0	0	0
20	19510	0.0054	4.7686E-43	7.1529E-43	9.5372E-43
50	19200	0.0084	1.072E-18	1.6079E-18	2.1439E-18
100	19640	0.0114	1.3695E-10	2.0543E-10	2.7391E-10
200	19730	0.0162	1.5714E-06	2.3571E-06	3.1428E-06
300	19490	0.0198	3.5613E-05	5.342E-05	7.1226E-05
400	19610	0.0234	0.00016871	0.00025307	0.00033742
500	19620	0.027	0.00042758	0.00064136	0.00085515
600	19500	0.0306	0.00080496	0.00120744	0.00160992
700	19350	0.033	0.00126437	0.00189656	0.00252875
800	18390	0.036	0.00186181	0.00279272	0.00372362
900	19250	0.0384	0.0023141	0.00347114	0.00462819
1000	20700	0.0402	0.00269943	0.00404914	0.00539886
1250	20140	0.0444	0.00402799	0.00604199	0.00805598
1500	20050	0.048	0.00520297	0.00780445	0.01040594
1750	20820	0.0504	0.00606323	0.00909484	0.01212645
2000	20980	0.0528	0.00691428	0.01037141	0.01382855
2250	21550	0.0552	0.00754145	0.01131218	0.0150829
2500	21660	0.057	0.00811703	0.01217554	0.01623405
2750	22260	0.0594	0.00852623	0.01278935	0.01705247
3000	22150	0.0612	0.00908749	0.01363123	0.01817498
3500	23320	0.0642	0.00953222	0.01429832	0.01906443
4000	23240	0.0666	0.01024937	0.01537405	0.02049873
4500	23900	0.069	0.01052979	0.01579468	0.02105957
5000	24490	0.0708	0.01085002	0.01627503	0.02170004
5500	25280	0.072	0.0109416	0.0164124	0.0218832
6000	26700	0.0732	0.01079347	0.0161902	0.02158693
6500	27310	0.0744	0.01090104	0.01635155	0.02180207
7000	27730	0.0756	0.01097461	0.01646191	0.02194921
7500	27760	0.0768	0.01126684	0.01690026	0.02253368
8000	27630	0.0768	0.01146245	0.01719367	0.02292489
8500	28510	0.0774	0.0114777	0.01721655	0.02295541
9000	28520	0.078	0.01153291	0.01729937	0.02306583
9500	28750	0.0786	0.01171744	0.01757615	0.02343487
10000	29110	0.0792	0.01169109	0.01753663	0.02338217

Table B29. PD Measured Data from Single-stage RTL Test for Class 5 at OMC+2% (σ_d = 17 psi) (Continued)

No. of Cycles	Measured M_R (psi)	Measured PD (inches)	Pred. PD (inches)		
			H = 6 in.	H = 9 in.	H = 12 in.
10500	28950	0.0798	0.01183084	0.01774626	0.02366168
11000	28850	0.0804	0.01202802	0.01804204	0.02405605
11500	29080	0.0804	0.01205749	0.01808624	0.02411499
12000	29070	0.081	0.01215131	0.01822697	0.02430262
12500	29580	0.0816	0.01208437	0.01812655	0.02416874
13000	29910	0.0816	0.01210685	0.01816028	0.02421371
13500	29310	0.0822	0.01234321	0.01851481	0.02468642
14000	29490	0.0822	0.01233531	0.01850297	0.02467063
14500	30480	0.0828	0.01213998	0.01820998	0.02427997
15000	30270	0.0828	0.01223327	0.0183499	0.02446654
15500	31210	0.0834	0.01196495	0.01794743	0.02392991
16000	32260	0.0834	0.01178611	0.01767917	0.02357223
16500	32230	0.0834	0.01183645	0.01775468	0.0236729
17000	31980	0.084	0.01199825	0.01799738	0.02399651
17500	33640	0.084	0.01159015	0.01738522	0.0231803
18000	33070	0.084	0.01174569	0.01761854	0.02349139
18500	31670	0.0846	0.01230005	0.01845008	0.0246001
19000	32790	0.0846	0.01202897	0.01804346	0.02405795
19500	33390	0.0846	0.0118754	0.0178131	0.0237508
20000	36000	0.0852	0.0114442	0.01716631	0.02288841

Table B30. PD Measured Data from Single-stage RTL Test for 50% Class 5 + 50% RAP TH 10 at OMC% (σ_d = 17 psi)

No. of Cycles	Measured M_R (psi)	Measured PD (inches)	Pred. PD (inches)		
			H = 6 in.	H = 9 in.	H = 12 in.
1	35357	0.0006	0	0	0
10	36971	0.00324	1.1231E-30	1.6846E-30	2.2462E-30
20	39084	0.0045	1.4243E-16	2.1365E-16	2.8487E-16
50	39769	0.00744	4.2653E-08	6.398E-08	8.5306E-08
100	42627	0.00924	2.7291E-05	4.0937E-05	5.4582E-05
200	43782	0.01062	0.00070434	0.00105651	0.00140869
300	45643	0.01134	0.00203565	0.00305348	0.0040713
400	46874	0.01182	0.00347942	0.00521913	0.00695883
500	48209	0.01212	0.00474586	0.0071188	0.00949173
600	49848	0.01248	0.00581427	0.00872141	0.01162854
700	49832	0.01272	0.00677869	0.01016803	0.01355738
800	50258	0.01296	0.00758912	0.01138368	0.01517824
900	52176	0.01314	0.00817863	0.01226795	0.01635727
1000	52435	0.01326	0.00876313	0.0131447	0.01752626
1250	51152	0.01344	0.01013458	0.01520187	0.02026915
1500	50584	0.01362	0.01102968	0.01654452	0.02205936
1750	52188	0.01374	0.01151633	0.01727449	0.02303265
2000	54621	0.01392	0.01166028	0.01749042	0.02332056
2250	54247	0.01398	0.01208438	0.01812657	0.02416876
2500	57578	0.0141	0.01195852	0.01793778	0.02391704
2750	57410	0.01416	0.01217157	0.01825735	0.02434313
3000	57617	0.01422	0.01247292	0.01870938	0.02494585
3500	58172	0.01434	0.01275398	0.01913097	0.02550796
4000	56297	0.0144	0.01331368	0.01997053	0.02662737
4500	57400	0.01452	0.01340531	0.02010796	0.02681061
5000	56366	0.01464	0.01381294	0.02071941	0.02762588
5500	55121	0.01518	0.0141825	0.02127376	0.02836501
6000	55679	0.01554	0.01424245	0.02136368	0.0284849
6500	54726	0.0156	0.01450531	0.02175796	0.02901062
7000	56185	0.01572	0.01437874	0.02156811	0.02875748
7500	55519	0.01584	0.01461267	0.02191901	0.02922534
8000	55939	0.01584	0.01461926	0.02192889	0.02923853
8500	57094	0.0159	0.0144798	0.0217197	0.02895959
9000	57166	0.01596	0.01456184	0.02184276	0.02912369
9500	55851	0.01602	0.01484852	0.02227278	0.02969704
10000	58172	0.01614	0.01450278	0.02175418	0.02900557

Table B30. PD Measured Data from Single-stage RTL Test for 50% Class 5 + 50% RAP TH 10 at OMC% (σ_d = 17 psi) (Continued)

No. of Cycles	Measured M_R (psi)	Measured PD (inches)	Pred. PD (inches)		
			H = 6 in.	H = 9 in.	H = 12 in.
10500	59400	0.0162	0.01433251	0.02149876	0.02866502
11000	57780	0.01626	0.01466911	0.02200367	0.02933822
11500	57940	0.01626	0.01463432	0.02195148	0.02926864
12000	59040	0.01632	0.01449578	0.02174366	0.02899155
12500	58360	0.01632	0.0145699	0.02185485	0.0291398
13000	58080	0.01632	0.01473776	0.02210663	0.02947551
13500	59130	0.01638	0.014666	0.02199899	0.02933199
14000	58760	0.01644	0.01465922	0.02198882	0.02931843
14500	58640	0.01644	0.01470055	0.02205082	0.0294011
15000	58198	0.0165	0.01467255	0.02200882	0.02934509
15500	57835	0.0165	0.01481658	0.02222487	0.02963316
16000	58796	0.01656	0.014682	0.022023	0.02936399
16500	58646	0.01656	0.01475445	0.02213168	0.02950891
17000	57334	0.01662	0.01488953	0.02233429	0.02977905
17500	57727	0.01662	0.01491428	0.02237142	0.02982857
18000	57667	0.01662	0.01494689	0.02242033	0.02989377
18500	59300	0.01668	0.01473778	0.02210666	0.02947555
19000	61402	0.01692	0.01441772	0.02162658	0.02883543
19500	64847	0.01704	0.01401125	0.02101688	0.02802251
20000	65586	0.0171	0.01395056	0.02092584	0.02790113

Table B31. PD Measured Data from Single-stage RTL Test for 50% Class 5 + 50% RAP TH 10 at OMC% (σ_d = 24 psi)

No. of Cycles	Measured M_R (psi)	Measured PD (inches)	Pred. PD (inches)		
			H = 6 in.	H = 9 in.	H = 12 in.
1	25310	0.0006	0	0	0
10	28600	0.0036	2.0331E-30	3.0497E-30	4.0663E-30
20	30990	0.0048	2.5484E-16	3.8226E-16	5.0967E-16
50	32890	0.0066	7.2572E-08	1.0886E-07	1.4514E-07
100	34510	0.0078	4.722E-05	7.083E-05	9.4441E-05
200	35490	0.0096	0.00119535	0.00179302	0.0023907
300	37720	0.0108	0.00339997	0.00509996	0.00679995
400	38600	0.0114	0.00583909	0.00875864	0.01167819
500	39050	0.012	0.00805951	0.01208926	0.01611901
600	40190	0.012	0.0098736	0.0148104	0.01974719
700	40830	0.0126	0.01150644	0.01725966	0.02301288
800	41070	0.0132	0.01285529	0.01928293	0.02571058
900	41470	0.0132	0.01400601	0.02100902	0.02801203
1000	41410	0.0138	0.01514307	0.02271461	0.03028615
1250	41780	0.0144	0.01724295	0.02586443	0.03448591
1500	42810	0.015	0.01846418	0.02769628	0.03692837
1750	43430	0.015	0.01959514	0.02939271	0.03919028
2000	44290	0.015	0.02030539	0.03045808	0.04061077
2250	44150	0.0156	0.02124911	0.03187366	0.04249822
2500	44860	0.0162	0.02170318	0.03255478	0.04340637
2750	44990	0.0162	0.02226176	0.03339263	0.04452351
3000	45850	0.0168	0.02249594	0.03374392	0.04499189
3500	46800	0.0168	0.02306478	0.03459718	0.04612957
4000	47210	0.0168	0.0236105	0.03541575	0.04722099
4500	46790	0.0174	0.02438909	0.03658364	0.04877819
5000	46730	0.018	0.02483413	0.0372512	0.04966827
5500	47490	0.018	0.02492621	0.03738931	0.04985242
6000	47950	0.018	0.02524172	0.03786258	0.05048344
6500	47990	0.0186	0.02555533	0.03833299	0.05111065
7000	47710	0.0186	0.0259694	0.03895409	0.05193879
7500	49480	0.0186	0.02563359	0.03845039	0.05126719
8000	49310	0.0186	0.02579612	0.03869418	0.05159224
8500	50110	0.0186	0.02555409	0.03833113	0.05110817
9000	50630	0.0186	0.02552547	0.03828821	0.05105095
9500	51060	0.0186	0.02563321	0.03844981	0.05126642
10000	55930	0.0198	0.02433977	0.03650966	0.04867955

Table B31. PD Measured Data from Single-stage RTL Test for 50% Class 5 + 50% RAP TH 10 at OMC% (σ_d = 24 psi) (Continued)

No. of Cycles	Measured M_R (psi)	Measured PD (inches)	Pred. PD (inches)		
			H = 6 in.	H = 9 in.	H = 12 in.
10500	56170	0.0198	0.02431819	0.03647729	0.04863638
11000	56050	0.0198	0.02441865	0.03662797	0.04883729
11500	56590	0.0198	0.02444865	0.03667298	0.04889731
12000	56660	0.0198	0.02445471	0.03668206	0.04890941
12500	57270	0.0198	0.02445908	0.03668862	0.04891817
13000	56670	0.0198	0.02466507	0.0369976	0.04933014
13500	57450	0.0198	0.02449593	0.03674389	0.04899186
14000	57620	0.0198	0.02451648	0.03677472	0.04903296
14500	57520	0.0198	0.02455933	0.036839	0.04911866
15000	58120	0.0204	0.02441022	0.03661533	0.04882043
15500	56820	0.0204	0.02471311	0.03706967	0.04942622
16000	57070	0.0204	0.02478004	0.03717005	0.04956007
16500	57710	0.0204	0.02464411	0.03696616	0.04928822
17000	57180	0.0204	0.02478802	0.03718203	0.04957604
17500	51650	0.0204	0.02654962	0.03982442	0.05309923
18000	51380	0.0204	0.02669085	0.04003627	0.0533817
18500	53310	0.021	0.02601329	0.03901993	0.05202657
19000	52550	0.021	0.02633472	0.03950209	0.05266945
19500	53170	0.021	0.02619755	0.03929632	0.05239509
20000	58080	0.021	0.02485319	0.03727978	0.04970638

Table B32. PD Measured Data from Single-stage RTL Test for 50% Class 5 + 50% RAP TH 10 at OMC% (σ_d = 37 psi)

No. of Cycles	Measured M_R (psi)	Measured PD (inches)	Pred. PD (inches)		
			H = 6 in.	H = 9 in.	H = 12 in.
1	23551	0.006	0	0	0
10	30791	0.0186	3.1287E-30	4.693E-30	6.2574E-30
20	31910	0.0234	4.1526E-16	6.2288E-16	8.3051E-16
50	33779	0.0294	1.2305E-07	1.8457E-07	2.4609E-07
100	36671	0.0342	7.9279E-05	0.00011892	0.00015856
200	38861	0.0378	0.0020024	0.00300361	0.00400481
300	40968	0.0402	0.00577222	0.00865833	0.01154444
400	41968	0.042	0.00985129	0.01477693	0.01970258
500	42745	0.0432	0.01355967	0.0203395	0.02711934
600	42649	0.0438	0.016882	0.025323	0.03376401
700	43127	0.0444	0.0196817	0.02952255	0.0393634
800	43998	0.045	0.02186784	0.03280176	0.04373568
900	44152	0.0456	0.02390619	0.03585929	0.04781238
1000	44401	0.0462	0.02563768	0.03845652	0.05127536
1250	44085	0.0468	0.02945585	0.04418377	0.05891169
1500	46259	0.048	0.03132924	0.04699386	0.06265849
1750	47403	0.0486	0.03291078	0.04936616	0.06582155
2000	47806	0.0492	0.03434553	0.0515183	0.06869106
2250	47680	0.0492	0.03592556	0.05388833	0.07185111
2500	48478	0.0498	0.03641716	0.05462574	0.07283433
2750	48463	0.0498	0.03736788	0.05605182	0.07473576
3000	49414	0.0504	0.03780626	0.05670939	0.07561253
3500	50041	0.051	0.03871016	0.05806523	0.07742031
4000	50777	0.0516	0.03939535	0.05909303	0.07879071
4500	51233	0.0516	0.0398684	0.0598026	0.07973679
5000	52284	0.0522	0.04016788	0.06025182	0.08033576
5500	52763	0.0522	0.04022879	0.06034319	0.08045759
6000	53434	0.0528	0.04026418	0.06039627	0.08052836
6500	53657	0.0528	0.04072888	0.06109332	0.08145776
7000	54304	0.0534	0.04075262	0.06112893	0.08150524
7500	54503	0.0534	0.04089897	0.06134845	0.08179794
8000	54253	0.0534	0.0411601	0.06174016	0.08232021
8500	55163	0.054	0.04103636	0.06155454	0.08207272
9000	55618	0.054	0.04106809	0.06160214	0.08213619
9500	55933	0.054	0.04121286	0.06181929	0.08242573
10000	55296	0.054	0.04160694	0.06241041	0.08321388

Table B33. PD Measured Data from Single-stage RTL Test for 50% Class 5 + 50% RAP TH 10 at OMC+2% (σ_d = 12 psi)

No. of Cycles	Measured M_R (psi)	Measured PD (inches)	Pred. PD (inches)		
			H = 6 in.	H = 9 in.	H = 12 in.
1	31700	0.0012	0	0	0
10	24620	0.0054	7.7265E-57	1.159E-56	1.5453E-56
20	23020	0.0078	1.0117E-29	1.5176E-29	2.0234E-29
50	22110	0.0108	1.94E-13	2.91E-13	3.88E-13
100	24290	0.0132	4.805E-08	7.2076E-08	9.6101E-08
200	26540	0.0156	2.3462E-05	3.5193E-05	4.6924E-05
300	27130	0.0168	0.00019126	0.00028689	0.00038253
400	29870	0.018	0.00050979	0.00076469	0.00101959
500	29800	0.0186	0.00096197	0.00144295	0.00192393
600	30810	0.0186	0.00143477	0.00215216	0.00286954
700	32200	0.0192	0.00187585	0.00281377	0.00375169
800	32910	0.0198	0.00231096	0.00346644	0.00462192
900	33030	0.0198	0.00275314	0.00412971	0.00550627
1000	33560	0.0204	0.00312963	0.00469444	0.00625926
1250	34330	0.021	0.00396176	0.00594265	0.00792353
1500	34990	0.0216	0.00470142	0.00705213	0.00940284
1750	34340	0.0216	0.0053114	0.0079671	0.01062281
2000	34890	0.0222	0.00576297	0.00864446	0.01152594
2250	34940	0.0222	0.00621514	0.00932271	0.01243028
2500	35940	0.0222	0.00638379	0.00957568	0.01276757
2750	38250	0.0228	0.00642447	0.0096367	0.01284894
3000	37810	0.0228	0.00671059	0.01006589	0.01342118
3500	39270	0.0228	0.00701489	0.01052234	0.01402979
4000	39100	0.0234	0.00741104	0.01111656	0.01482208
4500	39230	0.0234	0.00765371	0.01148056	0.01530741
5000	37350	0.0234	0.00810676	0.01216014	0.01621352
5500	36670	0.024	0.00839925	0.01259887	0.01679849
6000	37350	0.024	0.00850448	0.01275673	0.01700897
6500	39120	0.024	0.00835958	0.01253937	0.01671916
7000	37610	0.024	0.00866874	0.01300311	0.01733748
7500	38990	0.0246	0.00859705	0.01289558	0.01719411
8000	38690	0.0246	0.00872823	0.01309234	0.01745646
8500	39140	0.0246	0.00878961	0.01318441	0.01757921
9000	39400	0.0246	0.00878727	0.0131809	0.01757453
9500	39090	0.0246	0.00893473	0.0134021	0.01786946
10000	39050	0.0246	0.00910529	0.01365794	0.01821059

Table B33. PD Measured Data from Single-stage RTL Test for 50% Class 5 + 50% RAP TH 10 at OMC+2% (σ_d = 12 psi) (Continued)

No. of Cycles	Measured M_R (psi)	Measured PD (inches)	Pred. PD (inches)		
			H = 6 in.	H = 9 in.	H = 12 in.
11000	39890	0.0246	0.00895504	0.01343256	0.01791009
11500	40060	0.0252	0.00895553	0.0134333	0.01791107
12000	40350	0.0252	0.00900567	0.0135085	0.01801133
12500	40960	0.0252	0.00895412	0.01343118	0.01790824
13000	41400	0.0252	0.00896791	0.01345186	0.01793582
13500	41600	0.0258	0.00907271	0.01360906	0.01814541
14000	41100	0.0258	0.00897182	0.01345773	0.01794364
14500	41620	0.0258	0.00905527	0.01358291	0.01811054
15000	40750	0.0258	0.0091379	0.01370685	0.0182758
15500	41080	0.0258	0.00918285	0.01377428	0.01836571
16000	41290	0.0258	0.00913991	0.01370986	0.01827981
16500	43040	0.0258	0.0088959	0.01334385	0.01779181
17000	43580	0.0258	0.00894046	0.01341069	0.01788093
17500	42950	0.0258	0.00901927	0.0135289	0.01803853
18000	42370	0.0258	0.00914841	0.01372262	0.01829683
18500	43030	0.0258	0.00898632	0.01347948	0.01797264
19000	43690	0.0264	0.00899391	0.01349087	0.01798783
19500	43590	0.0264	0.00888847	0.01333271	0.01777694
20000	43810	0.0264	0.00891899	0.01337848	0.01783797

Table B34. PD Measured Data from Single-stage RTL Test for 50% Class 5 + 50% RAP TH 10 at OMC+2% (σ_d = 17 psi)

No. of Cycles	Measured M_R (psi)	Measured PD (inches)	Pred. PD (inches)		
			H = 6 in.	H = 9 in.	H = 12 in.
1	23720	0.003	0	0	0
10	23980	0.0138	1.1139E-56	1.6708E-56	2.2277E-56
20	25910	0.0198	1.3443E-29	2.0164E-29	2.6885E-29
50	28700	0.0294	2.292E-13	3.438E-13	4.584E-13
100	28490	0.0396	6.2154E-08	9.3231E-08	1.2431E-07
200	28460	0.0498	3.2704E-05	4.9056E-05	6.5408E-05
300	27480	0.0558	0.00027396	0.00041094	0.00054792
400	26420	0.0606	0.00081003	0.00121504	0.00162005
500	27260	0.0636	0.00149086	0.00223629	0.00298172
600	28790	0.066	0.0021817	0.00327255	0.0043634
700	29790	0.0678	0.00287699	0.00431549	0.00575399
800	29910	0.0696	0.00359559	0.00539339	0.00719118
900	30470	0.0708	0.00422198	0.00633297	0.00844396
1000	31830	0.072	0.00471846	0.00707769	0.00943693
1250	31330	0.075	0.00617263	0.00925895	0.01234526
1500	31480	0.0768	0.00728685	0.01093027	0.0145737
1750	32270	0.0786	0.00809259	0.01213889	0.01618519
2000	32680	0.0798	0.0087722	0.01315831	0.01754441
2250	33530	0.0804	0.00932343	0.01398515	0.01864686
2500	34180	0.0816	0.00972391	0.01458586	0.01944782
2750	35010	0.0822	0.01002443	0.01503664	0.02004885
3000	35310	0.0828	0.01034346	0.01551519	0.02068692
3500	35980	0.0834	0.01087257	0.01630885	0.02174514
4000	35940	0.084	0.01137726	0.0170659	0.02275453
4500	37070	0.0846	0.01163927	0.01745891	0.02327854
5000	36920	0.0852	0.01201837	0.01802755	0.02403673
5500	36870	0.0858	0.0122577	0.01838656	0.02451541
6000	37590	0.0858	0.01234595	0.01851892	0.0246919
6500	38320	0.0864	0.01244171	0.01866257	0.02488343
7000	38940	0.0864	0.01244125	0.01866188	0.02488251
7500	40310	0.087	0.01239093	0.01858639	0.02478186
8000	40300	0.087	0.01250624	0.01875936	0.02501248
8500	41200	0.087	0.01245525	0.01868287	0.0249105
9000	41650	0.087	0.01240326	0.01860489	0.02480652
9500	42450	0.0876	0.01240735	0.01861102	0.02481469
10000	41760	0.0876	0.01265976	0.01898963	0.02531951

Table B34. PD Measured Data from Single-stage RTL Test for 50% Class 5 + 50% RAP TH 10 at OMC+2% (σ_d = 17 psi) (Continued)

No. of Cycles	Measured M_R (psi)	Measured PD (inches)	Pred. PD (inches)		
			H = 6 in.	H = 9 in.	H = 12 in.
10500	42580	0.0876	0.01250365	0.01875547	0.0250073
11000	42220	0.0876	0.01268009	0.01902014	0.02536019
11500	41650	0.0876	0.01283284	0.01924926	0.02566567
12000	43140	0.0882	0.01253342	0.01880012	0.02506683
12500	42960	0.0882	0.01271366	0.01907049	0.02542732
13000	43560	0.0882	0.01262256	0.01893384	0.02524512
13500	43420	0.0882	0.01273744	0.01910617	0.02547489
14000	43280	0.0882	0.01286681	0.01930021	0.02573362
14500	43180	0.0882	0.01291897	0.01937846	0.02583794
15000	42150	0.0882	0.01308466	0.019627	0.02616933
15500	42450	0.0882	0.01310519	0.01965778	0.02621038
16000	43000	0.0888	0.01305336	0.01958004	0.02610671
16500	44210	0.0888	0.01283293	0.0192494	0.02566586
17000	43750	0.0888	0.01301433	0.0195215	0.02602866
17500	43300	0.0888	0.01312779	0.01969168	0.02625557
18000	43810	0.0888	0.01306343	0.01959514	0.02612686
18500	44070	0.0888	0.01300883	0.01951325	0.02601767
19000	44620	0.0888	0.01290358	0.01935536	0.02580715
19500	44730	0.0888	0.01293676	0.01940514	0.02587351
20000	45010	0.0894	0.01285178	0.01927766	0.02570355

Table B35. PD Measured Data from Single-stage RTL Test for 50% Class 5 + 50% RAP TH 10 + 6% Fines at OMC% (σ_d = 17 psi)

No. of Cycles	Measured M_R (psi)	Measured PD (inches)	Pred. PD (inches)		
			H = 6 in.	H = 9 in.	H = 12 in.
1	26940	0.0012	0	0	0
10	30250	0.0042	2.4294E-33	3.6441E-33	4.8588E-33
20	29850	0.0048	7.2296E-18	1.0844E-17	1.4459E-17
50	30870	0.006	1.3571E-08	2.0356E-08	2.7141E-08
100	31540	0.0072	1.6696E-05	2.5044E-05	3.3392E-05
200	32370	0.009	0.0005779	0.00086684	0.00115579
300	33260	0.0096	0.00188906	0.0028336	0.00377813
400	33720	0.0096	0.00339716	0.00509575	0.00679433
500	33930	0.0102	0.00484664	0.00726995	0.00969327
600	34320	0.0102	0.0061249	0.00918735	0.0122498
700	34370	0.0108	0.00723824	0.01085736	0.01447648
800	35050	0.0108	0.00809237	0.01213855	0.01618473
900	35510	0.0108	0.00897382	0.01346072	0.01794763
1000	35370	0.0114	0.00970173	0.0145526	0.01940346
1250	36130	0.0114	0.01106123	0.01659185	0.02212246
1500	36760	0.012	0.01209621	0.01814432	0.02419242
1750	37050	0.012	0.01300859	0.01951289	0.02601718
2000	37430	0.0126	0.01372058	0.02058086	0.02744115
2250	38020	0.0126	0.01422268	0.02133401	0.02844535
2500	37970	0.0126	0.01447114	0.02170672	0.02894229
2750	37880	0.0126	0.01465808	0.02198711	0.02931615
3000	38230	0.0126	0.01513881	0.02270821	0.03027762
3500	38360	0.0132	0.01588289	0.02382434	0.03176579
4000	38570	0.0132	0.0163658	0.02454869	0.03273159
4500	39190	0.0132	0.01665035	0.02497553	0.0333007
5000	38890	0.0132	0.01694479	0.02541718	0.03388957
5500	38590	0.0132	0.01734195	0.02601292	0.0346839
6000	39400	0.0138	0.01740059	0.02610088	0.03480118
6500	39270	0.0138	0.01743225	0.02614838	0.03486451
7000	39370	0.0138	0.01765075	0.02647613	0.0353015
7500	39280	0.0138	0.01768541	0.02652811	0.03537081
8000	39150	0.0138	0.0178105	0.02671575	0.035621
8500	39190	0.0138	0.01808884	0.02713325	0.03617767
9000	38700	0.0144	0.01836478	0.02754718	0.03672957
9500	39430	0.0144	0.01800407	0.0270061	0.03600814
10000	39390	0.0144	0.01814379	0.02721569	0.03628759

Table B35. PD Measured Data from Single-stage RTL Test for 50% Class 5 + 50% RAP TH 10 + 6% Fines at OMC% (σ_d = 17 psi) (Continued)

No. of Cycles	Measured M_R (psi)	Measured PD (inches)	Pred. PD (inches)		
			H = 6 in.	H = 9 in.	H = 12 in.
11000	40940	0.0144	0.01794373	0.0269156	0.03588747
11500	40580	0.0144	0.01800412	0.02700618	0.03600824
12000	40520	0.0144	0.01806986	0.02710478	0.03613971
12500	41240	0.0144	0.01796619	0.02694929	0.03593239
13000	40910	0.0144	0.01807455	0.02711182	0.03614909
13500	41670	0.015	0.01798981	0.02698471	0.03597961
14000	41820	0.015	0.01794311	0.02691466	0.03588622
14500	41990	0.015	0.01803805	0.02705708	0.03607611
15000	42080	0.015	0.01798255	0.02697382	0.03596509
15500	42120	0.015	0.01789426	0.02684138	0.03578851
16000	42430	0.015	0.01795347	0.0269302	0.03590693
16500	42450	0.015	0.01790272	0.02685408	0.03580544
17000	42520	0.015	0.0179966	0.02699489	0.03599319
17500	43090	0.015	0.0178043	0.02670645	0.0356086
18000	42890	0.015	0.01787137	0.02680706	0.03574274
18500	43370	0.015	0.01780815	0.02671223	0.0356163
19000	42730	0.015	0.01802489	0.02703734	0.03604979
19500	43190	0.0156	0.01802138	0.02703207	0.03604275
20000	43080	0.0156	0.01795534	0.02693301	0.03591067

Table B36. PD Measured Data from Single-stage RTL Test for 50% Class 5 + 50% RAP TH 10 + 6% Fines at OMC% (σ_d = 24 psi)

No. of Cycles	Measured M_R (psi)	Measured PD (inches)	Pred. PD (inches)		
			H = 6 in.	H = 9 in.	H = 12 in.
1	23850	0.0024	0	0	0
10	25620	0.009	3.9614E-33	5.942E-33	7.9227E-33
20	26350	0.012	1.1636E-17	1.7454E-17	2.3273E-17
50	26710	0.018	2.2745E-08	3.4118E-08	4.5491E-08
100	28070	0.0228	2.8368E-05	4.2551E-05	5.6735E-05
200	29530	0.0288	0.00100743	0.00151115	0.00201487
300	30380	0.0318	0.00328786	0.00493179	0.00657572
400	31260	0.0342	0.00585743	0.00878615	0.01171487
500	31160	0.036	0.00845886	0.01268829	0.01691772
600	30890	0.0378	0.01087478	0.01631217	0.02174956
700	31270	0.039	0.01280856	0.01921284	0.02561712
800	31520	0.0396	0.01449527	0.02174291	0.02899055
900	32090	0.0408	0.01584623	0.02376935	0.03169246
1000	32670	0.0414	0.01698502	0.02547752	0.03397003
1250	33470	0.0426	0.01937446	0.02906169	0.03874892
1500	33770	0.0438	0.02121707	0.0318256	0.04243414
1750	33970	0.0444	0.02271821	0.03407732	0.04543642
2000	34140	0.045	0.02394416	0.03591624	0.04788832
2250	34310	0.0456	0.02485005	0.03727507	0.0497001
2500	34290	0.0456	0.02567207	0.03850811	0.05134415
2750	34330	0.0462	0.02629776	0.03944663	0.05259551
3000	34690	0.0462	0.02676883	0.04015324	0.05353766
3500	35040	0.0468	0.02755714	0.04133571	0.05511428
4000	35620	0.0474	0.02803301	0.04204952	0.05606602
4500	35860	0.0474	0.02847457	0.04271186	0.05694915
5000	35920	0.0474	0.02883967	0.0432595	0.05767934
5500	36570	0.048	0.0290094	0.0435141	0.0580188
6000	37170	0.048	0.02903624	0.04355436	0.05807247
6500	36920	0.048	0.02943664	0.04415495	0.05887327
7000	37400	0.0486	0.02931776	0.04397664	0.05863552
7500	37780	0.0486	0.02952348	0.04428523	0.05904697
8000	37520	0.0486	0.02978393	0.04467589	0.05956786
8500	38190	0.0492	0.02961827	0.04442741	0.05923655
9000	38340	0.0492	0.02977795	0.04466692	0.05955589
9500	38550	0.0492	0.0298227	0.04473405	0.05964541
10000	39030	0.0492	0.02962468	0.04443701	0.05924935

Table B36. PD Measured Data from Single-stage RTL Test for 50% Class 5 + 50% RAP TH 10 + 6% Fines at OMC% (σ_d = 24 psi) (Continued)

No. of Cycles	Measured M_R (psi)	Measured PD (inches)	Pred. PD (inches)		
			H = 6 in.	H = 9 in.	H = 12 in.
10500	38930	0.0492	0.02984813	0.0447722	0.05969627
11000	38780	0.0492	0.03010598	0.04515897	0.06021195
11500	39280	0.0498	0.02989621	0.04484432	0.05979242
12000	39720	0.0498	0.02985182	0.04477773	0.05970363
12500	39560	0.0498	0.02993	0.044895	0.05986001
13000	39440	0.0498	0.03015639	0.04523459	0.06031278
13500	39280	0.0498	0.03040217	0.04560325	0.06080434
14000	39980	0.0498	0.03012495	0.04518743	0.0602499
14500	40330	0.0498	0.02984134	0.04476201	0.05968268
15000	39720	0.0498	0.03031636	0.04547453	0.06063271
15500	40210	0.0504	0.03014826	0.04522239	0.06029652
16000	41310	0.0504	0.02946662	0.04419993	0.05893325
16500	40790	0.0504	0.02984203	0.04476305	0.05968406
17000	40820	0.0504	0.03002439	0.04503659	0.06004879
17500	42530	0.0504	0.02915555	0.04373333	0.05831111
18000	42350	0.0504	0.02923703	0.04385555	0.05847406
18500	41530	0.0504	0.02974381	0.04461571	0.05948762
19000	44250	0.051	0.02844842	0.04267263	0.05689685
19500	45840	0.051	0.027705	0.0415575	0.05541
20000	44770	0.051	0.02833509	0.04250264	0.05667019

Table B37. PD Measured Data from Single-stage RTL Test for 50% Class 5 + 50% RAP TH 10 + 6% Fines at OMC+2% (σ_d = 12 psi)

No. of Cycles	Measured M_R (psi)	Measured PD (inches)	Pred. PD (inches)		
			H = 6 in.	H = 9 in.	H = 12 in.
1	15450	0.0012	0	0	0
10	16420	0.0102	0	0	0
20	17020	0.0156	3.6162E-32	5.4242E-32	7.2323E-32
50	18060	0.0234	2.0721E-14	3.1082E-14	4.1442E-14
100	18940	0.03	1.7047E-08	2.557E-08	3.4094E-08
200	20120	0.0354	1.5501E-05	2.3252E-05	3.1002E-05
300	20520	0.0378	0.00015063	0.00022594	0.00030126
400	20330	0.0408	0.0004744	0.0007116	0.0009488
500	20740	0.0426	0.0009327	0.00139906	0.00186541
600	21420	0.0444	0.00145313	0.0021797	0.00290627
700	21260	0.0456	0.00202673	0.00304009	0.00405345
800	21830	0.0468	0.00253726	0.00380589	0.00507452
900	21900	0.048	0.0030844	0.0046266	0.0061688
1000	22220	0.0486	0.00356529	0.00534794	0.00713058
1250	22990	0.0504	0.00454035	0.00681052	0.00908069
1500	23390	0.0516	0.00542886	0.0081433	0.01085773
1750	24400	0.0528	0.00600094	0.00900141	0.01200188
2000	25350	0.0534	0.00641436	0.00962155	0.01282873
2250	25780	0.054	0.00688216	0.01032324	0.01376432
2500	26000	0.0546	0.00733663	0.01100495	0.01467326
2750	26600	0.0552	0.00753107	0.01129661	0.01506214
3000	26950	0.0552	0.00783859	0.01175789	0.01567718
3500	27310	0.0558	0.00825873	0.01238809	0.01651745
4000	27560	0.0564	0.00863893	0.0129584	0.01727787
4500	27920	0.057	0.00893656	0.01340483	0.01787311
5000	28020	0.057	0.00914203	0.01371304	0.01828405
5500	28380	0.0576	0.00927544	0.01391316	0.01855088
6000	28410	0.0576	0.00954032	0.01431048	0.01908064
6500	28760	0.0576	0.00960456	0.01440684	0.01920912
7000	28940	0.0582	0.00973681	0.01460522	0.01947363
7500	29850	0.0582	0.00971254	0.01456881	0.01942508
8000	29460	0.0582	0.00991759	0.01487639	0.01983518
8500	28890	0.0582	0.01010028	0.01515042	0.02020056
9000	28800	0.0582	0.01023497	0.01535245	0.02046994
9500	29320	0.0588	0.01027354	0.01541031	0.02054707
10000	29410	0.0588	0.01032221	0.01548331	0.02064442

Table B37. PD Measured Data from Single-stage RTL Test for 50% Class 5 + 50% RAP TH 10 + 6% Fines at OMC+2% (σ_d = 12 psi) (Continued)

No. of Cycles	Measured M_R (psi)	Measured PD (inches)	Pred. PD (inches)		
			H = 6 in.	H = 9 in.	H = 12 in.
10500	29350	0.0588	0.01035877	0.01553815	0.02071754
11000	29470	0.0588	0.01042434	0.01563651	0.02084868
11500	29620	0.0588	0.01046701	0.01570051	0.02093401
12000	29700	0.0594	0.0104101	0.01561515	0.02082021
12500	29830	0.0594	0.0105171	0.01577565	0.0210342
13000	29940	0.0594	0.01039616	0.01559424	0.02079232
13500	30200	0.0594	0.01044182	0.01566274	0.02088365
14000	30410	0.0594	0.01043181	0.01564772	0.02086362
14500	30790	0.0594	0.01043131	0.01564697	0.02086263
15000	30580	0.0594	0.01044403	0.01566604	0.02088806
15500	30910	0.06	0.01041504	0.01562257	0.02083009
16000	31170	0.06	0.01030884	0.01546326	0.02061768
16500	30870	0.06	0.01054843	0.01582264	0.02109686
17000	32140	0.06	0.01017126	0.01525689	0.02034253
17500	31630	0.06	0.01034141	0.01551211	0.02068282
18000	31420	0.06	0.01042745	0.01564118	0.02085491
18500	31910	0.06	0.01024791	0.01537187	0.02049582
19000	31180	0.06	0.01054179	0.01581269	0.02108358
19500	31720	0.06	0.01034422	0.01551632	0.02068843
20000	32090	0.06	0.01042941	0.01564411	0.02085881

Table B38. PD Measured Data from Single-stage RTL Test for 50% Class 5 + 50% RAP TH 10 + 6% Fines at OMC+2% (σ_d = 17 psi)

No. of Cycles	Measured M_R (psi)	Measured PD (inches)	Pred. PD (inches)		
			H = 6 in.	H = 9 in.	H = 12 in.
1	15060	0.0024	0	0	0
10	16310	0.0192	0	0	0
20	17480	0.0282	4.827E-32	7.2405E-32	9.654E-32
50	19470	0.042	2.7112E-14	4.0668E-14	5.4224E-14
100	21400	0.054	2.1822E-08	3.2733E-08	4.3644E-08
200	22020	0.0666	2.0332E-05	3.0498E-05	4.0664E-05
300	22570	0.075	0.00019637	0.00029456	0.00039274
400	22780	0.081	0.00061826	0.00092739	0.00123651
500	21790	0.0858	0.00129504	0.00194256	0.00259008
600	24230	0.09	0.00187743	0.00281614	0.00375486
700	24560	0.0924	0.00258263	0.00387395	0.00516527
800	26320	0.0954	0.00314283	0.00471424	0.00628566
900	25220	0.0972	0.0039472	0.00592079	0.00789439
1000	26070	0.099	0.00448148	0.00672221	0.00896295
1250	28640	0.1026	0.00551139	0.00826709	0.01102279
1500	29410	0.1056	0.00653931	0.00980896	0.01307861
1750	30130	0.1074	0.00736004	0.01104007	0.01472009
2000	29810	0.1092	0.00823839	0.01235758	0.01647677
2250	30520	0.111	0.0087766	0.0131649	0.01755321
2500	31710	0.1122	0.00909236	0.01363854	0.01818472
2750	31760	0.1134	0.00953578	0.01430366	0.01907155
3000	32430	0.1146	0.00987192	0.01480788	0.01974384
3500	33500	0.1164	0.0102376	0.0153564	0.0204752
4000	33650	0.1176	0.01078468	0.01617701	0.02156935
4500	33710	0.1188	0.01128455	0.01692682	0.0225691
5000	33400	0.1194	0.01169042	0.01753563	0.02338084
5500	32870	0.12	0.01223115	0.01834672	0.0244623
6000	32750	0.1206	0.01257224	0.01885837	0.02514449
6500	32480	0.1212	0.01290201	0.01935301	0.02580402
7000	32710	0.1218	0.01300772	0.01951157	0.02601543
7500	32460	0.1224	0.01332739	0.01999109	0.02665479
8000	32580	0.1224	0.01345901	0.02018852	0.02691802
8500	32670	0.123	0.01348399	0.02022598	0.02696798
9000	32140	0.123	0.01387091	0.02080637	0.02774183
9500	32660	0.123	0.01384563	0.02076845	0.02769126
10000	32300	0.1236	0.01400947	0.0210142	0.02801894

Table B38. PD Measured Data from Single-stage RTL Test for 50% Class 5 + 50% RAP TH 10 + 6% Fines at OMC+2% (σ_d = 17 psi) (Continued)

No. of Cycles	Measured M_R (psi)	Measured PD (inches)	Pred. PD (inches)		
			H = 6 in.	H = 9 in.	H = 12 in.
10500	31780	0.1236	0.01440413	0.0216062	0.02880827
11000	31680	0.1236	0.01449611	0.02174417	0.02899223
11500	31420	0.1242	0.01467836	0.02201754	0.02935672
12000	31670	0.1242	0.0146501	0.02197515	0.0293002
12500	31780	0.1242	0.01472577	0.02208866	0.02945155
13000	31720	0.1242	0.01481928	0.02222891	0.02963855
13500	319200	0.1248	0.01077018	0.01615526	0.02154035
14000	32880	0.1248	0.01450051	0.02175076	0.02900101
14500	33030	0.1248	0.01461367	0.0219205	0.02922734
15000	33030	0.1254	0.0145533	0.02182995	0.0291066
15500	33740	0.1254	0.01445435	0.02168153	0.02890871
16000	32950	0.1254	0.01482901	0.02224351	0.02965802
16500	32990	0.1254	0.01480462	0.02220692	0.02960923
17000	33120	0.1254	0.01479564	0.02219346	0.02959128
17500	33260	0.126	0.01482038	0.02223056	0.02964075
18000	33240	0.126	0.01484957	0.02227436	0.02969914
18500	32980	0.126	0.01498022	0.02247033	0.02996044
19000	32950	0.126	0.01503958	0.02255937	0.03007915
19500	33630	0.126	0.01482236	0.02223354	0.02964472
20000	33350	0.126	0.01497346	0.02246019	0.02994692

Table B39. PD Measured Data from Multi-stage RTL Test for Class 5 at OMC-2% (σ_d = 6 psi)

No. of Cycles	Measured M_R (psi)	Measured PD (inches)	Pred. PD (inches)		
			H = 6 in.	H = 9 in.	H = 12 in.
1	19220	0.0012	0	0	0
10	17980	0	4.72E-25	7.07E-25	9.43E-25
20	18340	0	6.63E-14	9.95E-14	1.33E-13
50	17390	0	3.34E-07	5.02E-07	6.69E-07
100	17260	0.0006	5.77E-05	8.65E-05	0.000115
200	17710	0.0006	0.000749	0.001123	0.001497
300	17250	0.0012	0.001806	0.002708	0.003611
400	17140	0.0012	0.002798	0.004196	0.005595
500	16920	0.0012	0.003674	0.005512	0.007349
600	16680	0.0018	0.004436	0.006654	0.008873
700	16780	0.0018	0.004986	0.007479	0.009972
800	16890	0.0018	0.005538	0.008307	0.011076
900	17090	0.0018	0.005927	0.008891	0.011854
1000	17120	0.0024	0.006265	0.009397	0.01253
1250	17160	0.0024	0.007058	0.010587	0.014116
1500	16840	0.0024	0.007577	0.011366	0.015155
1750	17080	0.0024	0.007969	0.011953	0.015937
2000	16800	0.003	0.008368	0.012552	0.016736
2250	16710	0.003	0.008651	0.012976	0.017302
2500	16930	0.003	0.00881	0.013214	0.017619
2750	16820	0.003	0.008986	0.013478	0.017971
3000	16810	0.003	0.009068	0.013601	0.018135
3500	17200	0.0036	0.009297	0.013945	0.018594
4000	17160	0.0036	0.009466	0.0142	0.018933
4500	17030	0.0036	0.009578	0.014367	0.019156
5000	16990	0.0036	0.00982	0.014731	0.019641

Table B40. PD Measured Data from Multi-stage RTL Test for Class 5 at OMC-2% (σ_d = 12 psi)

No. of Cycles	Measured M_R (psi)	Measured PD (inches)	Pred. PD (inches)		
			H = 6 in.	H = 9 in.	H = 12 in.
1	26330	0.0054	0	0	0
10	18830	0.0066	1.28E-24	1.92E-24	2.56E-24
20	17130	0.0078	1.82E-13	2.73E-13	3.64E-13
50	16170	0.0096	9.26E-07	1.39E-06	1.85E-06
100	12750	0.0126	7.32E-05	0.00011	0.000146
200	16580	0.0126	0.001984	0.002976	0.003968
300	16180	0.0168	0.004791	0.007187	0.009582
400	16100	0.0204	0.007456	0.011185	0.014913
500	16280	0.0228	0.009481	0.014221	0.018962
600	17400	0.0252	0.010707	0.01606	0.021414
700	17130	0.0276	0.012394	0.018591	0.024788
800	17320	0.0294	0.013675	0.020512	0.02735
900	16690	0.0306	0.014955	0.022433	0.02991
1000	16720	0.0324	0.015823	0.023735	0.031646
1250	17220	0.0354	0.017206	0.025809	0.034412
1500	17880	0.0372	0.017953	0.02693	0.035906
1750	18070	0.039	0.018621	0.027931	0.037241
2000	18910	0.0414	0.018546	0.027818	0.037091
2250	18810	0.0426	0.019209	0.028814	0.038418
2500	19110	0.0444	0.019384	0.029075	0.038767
2750	19800	0.0456	0.01921	0.028815	0.03842
3000	21190	0.0474	0.018558	0.027837	0.037115
3500	21870	0.0492	0.018587	0.027881	0.037174
4000	22190	0.0504	0.018945	0.028418	0.03789
4500	21530	0.0522	0.019657	0.029485	0.039313
5000	23600	0.054	0.018529	0.027793	0.037057

Table B41. PD Measured Data from Multi-stage RTL Test for Class 5 at OMC-2% (σ_d = 17 psi)

No. of Cycles	Measured M_R (psi)	Measured PD (inches)	Pred. PD (inches)		
			H = 6 in.	H = 9 in.	H = 12 in.
1	24530	0.0534	0	0	0
10	22860	0.054	1.64E-24	2.47E-24	3.29E-24
20	22190	0.054	2.29E-13	3.43E-13	4.57E-13
50	21850	0.0558	1.1E-06	1.66E-06	2.21E-06
100	21240	0.0576	0.00019	0.000285	0.00038
200	21280	0.0612	0.002463	0.003694	0.004926
300	20590	0.0642	0.005977	0.008966	0.011954
400	20370	0.0672	0.009249	0.013873	0.018497
500	20440	0.0702	0.01189	0.017835	0.023781
600	19960	0.0732	0.014377	0.021565	0.028754
700	20590	0.0762	0.015839	0.023758	0.031678
800	19940	0.0792	0.017883	0.026824	0.035766
900	20020	0.0822	0.019095	0.028642	0.038189
1000	20460	0.0846	0.019942	0.029913	0.039884
1250	20240	0.09	0.022335	0.033503	0.04467
1500	24320	0.0948	0.020608	0.030912	0.041215
1750	22730	0.0996	0.022883	0.034325	0.045766
2000	25630	0.105	0.021697	0.032545	0.043394
2250	24000	0.1086	0.023659	0.035488	0.047317
2500	23610	0.1122	0.024414	0.03662	0.048827
2750	23280	0.1152	0.025369	0.038054	0.050738
3000	23810	0.1188	0.025358	0.038037	0.050716
3500	25220	0.1236	0.02504	0.03756	0.05008
4000	25650	0.1278	0.02515	0.037725	0.050299
4500	26510	0.1326	0.025078	0.037617	0.050156
5000	27280	0.1356	0.024939	0.037408	0.049877

Table B42. PD Measured Data from Multi-stage RTL Test for Class 5 at OMC-2% (σ_d = 24 psi)

No. of Cycles	Measured M_R (psi)	Measured PD (inches)	Pred. PD (inches)		
			H = 6 in.	H = 9 in.	H = 12 in.
1	31640	0.1362	0	0	0
10	26110	0.138	2.24E-24	3.36E-24	4.48E-24
20	24710	0.141	3.16E-13	4.75E-13	6.33E-13
50	23290	0.1464	1.58E-06	2.37E-06	3.16E-06
100	21050	0.159	0.000288	0.000432	0.000576
200	20930	0.1722	0.003742	0.005612	0.007483
300	18380	0.1854	0.009819	0.014729	0.019638
400	19130	0.1998	0.014516	0.021774	0.029031
500	18650	0.2136	0.019074	0.028611	0.038148
600	18580	0.2292	0.022618	0.033927	0.045236
700	18530	0.2442	0.026019	0.039029	0.052039
800	17930	0.258	0.028938	0.043407	0.057876
900	17640	0.2724	0.031556	0.047334	0.063112
1000	17350	0.3096	0.033842	0.050763	0.067683
1250	17380	0.3492	0.037257	0.055886	0.074514

Table B43. PD Measured Data from Multi-stage RTL Test for Class 5 at OMC% (σ_d = 17 psi)

No. of Cycles	Measured M_R (psi)	Measured PD (inches)	Pred. PD (inches)		
			H = 6 in.	H = 9 in.	H = 12 in.
1	21590	0.0012	0	0	0
10	20380	0.0054	1.99E-43	2.99E-43	3.98E-43
20	19550	0.0078	6.93E-23	1.04E-22	1.39E-22
50	19040	0.0126	1.47E-10	2.21E-10	2.94E-10
100	19150	0.0186	1.87E-06	2.81E-06	3.75E-06
200	18290	0.0264	0.000222	0.000334	0.000445
300	18880	0.0324	0.001059	0.001589	0.002118
400	17880	0.0372	0.002519	0.003778	0.005038
500	19050	0.042	0.003872	0.005808	0.007744
600	17920	0.0462	0.005659	0.008489	0.011319
700	18550	0.0504	0.006907	0.010361	0.013814
800	18460	0.054	0.00826	0.01239	0.01652
900	18940	0.057	0.009251	0.013877	0.018502
1000	19600	0.06	0.010048	0.015071	0.020095
1250	19860	0.066	0.012123	0.018184	0.024246
1500	20530	0.0696	0.013576	0.020364	0.027151
1750	21550	0.0732	0.01418	0.021271	0.028361
2000	21240	0.0756	0.015348	0.023022	0.030696
2250	21380	0.0786	0.016166	0.024248	0.032331
2500	21420	0.081	0.016868	0.025302	0.033736
2750	21480	0.0834	0.017553	0.026329	0.035105
3000	21440	0.0858	0.018078	0.027118	0.036157
3500	22880	0.0894	0.018113	0.027169	0.036225
4000	22290	0.0924	0.019099	0.028648	0.038197
4500	22220	0.096	0.019797	0.029695	0.039593
5000	25390	0.0984	0.018223	0.027335	0.036446

Table B44. PD Measured Data from Multi-stage RTL Test for Class 5 at OMC% (σ_d = 24 psi)

No. of Cycles	Measured M_R (psi)	Measured PD (inches)	Pred. PD (inches)		
			H = 6 in.	H = 9 in.	H = 12 in.
1	29570	0	0	0	0
10	26760	0.0006	0	0	0
20	25460	0.0006	1.32E-43	1.98E-43	2.64E-43
50	24070	0.0012	3.06E-19	4.58E-19	6.11E-19
100	24330	0.0018	4.06E-11	6.1E-11	8.13E-11
200	22200	0.0018	4.63E-07	6.95E-07	9.27E-07
300	21830	0.0024	1.07E-05	1.61E-05	2.14E-05
400	21970	0.0024	5.13E-05	7.7E-05	0.000103
500	21400	0.0024	0.000133	0.000199	0.000265
600	23300	0.0024	0.000252	0.000378	0.000504
700	21050	0.003	0.000391	0.000586	0.000782
800	21210	0.003	0.000553	0.000829	0.001106
900	20820	0.003	0.000714	0.001072	0.001429
1000	21870	0.0036	0.000878	0.001317	0.001756
1250	22490	0.0036	0.001297	0.001945	0.002594
1500	22350	0.0036	0.001668	0.002502	0.003336
1750	21590	0.0036	0.001996	0.002994	0.003992
2000	20180	0.0042	0.002309	0.003464	0.004618
2250	20580	0.0042	0.002574	0.003861	0.005148
2500	20420	0.0042	0.002784	0.004176	0.005568
2750	20400	0.0042	0.002983	0.004475	0.005966
3000	18920	0.0042	0.003137	0.004705	0.006273
3500	21940	0.0048	0.00343	0.005145	0.006861
4000	21340	0.0048	0.003666	0.005499	0.007332
4500	21130	0.0048	0.003852	0.005778	0.007703
5000	21410	0.0048	0.00407	0.006105	0.00814

Table B45. PD Measured Data from Multi-stage RTL Test for Class 5 at OMC% (σ_d = 37 psi)

No. of Cycles	Measured M_R (psi)	Measured PD (inches)	Pred. PD (inches)		
			H = 6 in.	H = 9 in.	H = 12 in.
1	27485	0.3486	0	0	0
20	21832	0.357	1.77E-22	2.65E-22	3.53E-22
50	20259	0.3702	3.77E-10	5.65E-10	7.53E-10
100	18768	0.3972	4.98E-06	7.48E-06	9.97E-06

Table B46. PD Measured Data from Multi-stage RTL Test for Class 5 at OMC+2% (σ_d = 6 psi)

No. of Cycles	Measured M_R (psi)	Measured PD (inches)	Pred. PD (inches)		
			H = 6 in.	H = 9 in.	H = 12 in.
1	19220	0	0	0	0
10	17980	0.0006	0	0	0
20	18340	0.0006	1.32E-43	1.98E-43	2.64E-43
50	17390	0.0012	3.06E-19	4.58E-19	6.11E-19
100	17260	0.0018	4.06E-11	6.1E-11	8.13E-11
200	17710	0.0018	4.63E-07	6.95E-07	9.27E-07
300	17250	0.0024	1.07E-05	1.61E-05	2.14E-05
400	17140	0.0024	5.13E-05	7.7E-05	0.000103
500	16920	0.0024	0.000133	0.000199	0.000265
600	16680	0.0024	0.000252	0.000378	0.000504
700	16780	0.003	0.000391	0.000586	0.000782
800	16890	0.003	0.000553	0.000829	0.001106
900	17090	0.003	0.000714	0.001072	0.001429
1000	17120	0.0036	0.000878	0.001317	0.001756
1250	17160	0.0036	0.001297	0.001945	0.002594
1500	16840	0.0036	0.001668	0.002502	0.003336
1750	17080	0.0036	0.001996	0.002994	0.003992
2000	16800	0.0042	0.002309	0.003464	0.004618
2250	16710	0.0042	0.002574	0.003861	0.005148
2500	16930	0.0042	0.002784	0.004176	0.005568
2750	16820	0.0042	0.002983	0.004475	0.005966
3000	16810	0.0042	0.003137	0.004705	0.006273
3500	17200	0.0048	0.00343	0.005145	0.006861
4000	17160	0.0048	0.003666	0.005499	0.007332
4500	17030	0.0048	0.003852	0.005778	0.007703
5000	16990	0.0048	0.00407	0.006105	0.00814

Table B47. PD Measured Data from Multi-stage RTL Test for Class 5 at OMC+2% (σ_d = 12 psi)

No. of Cycles	Measured M_R (psi)	Measured PD (inches)	Pred. PD (inches)		
			H = 6 in.	H = 9 in.	H = 12 in.
1	26330	0.0054	0	0	0
10	18830	0.0066	0	0	0
20	17130	0.0078	3.63E-43	5.44E-43	7.26E-43
50	16170	0.0096	8.46E-19	1.27E-18	1.69E-18
100	12750	0.0126	5.16E-11	7.74E-11	1.03E-10
200	16580	0.0126	1.23E-06	1.84E-06	2.46E-06
300	16180	0.0168	2.84E-05	4.26E-05	5.68E-05
400	16100	0.0204	0.000137	0.000205	0.000274
500	16280	0.0228	0.000342	0.000514	0.000685
600	17400	0.0252	0.000608	0.000912	0.001215
700	17130	0.0276	0.000971	0.001457	0.001943
800	17320	0.0294	0.001365	0.002048	0.002731
900	16690	0.0306	0.001802	0.002704	0.003605
1000	16720	0.0324	0.002217	0.003326	0.004434
1250	17220	0.0354	0.003162	0.004742	0.006323
1500	17880	0.0372	0.003952	0.005929	0.007905
1750	18070	0.039	0.004664	0.006996	0.009329
2000	18910	0.0414	0.005118	0.007677	0.010236
2250	18810	0.0426	0.005716	0.008573	0.011431
2500	19110	0.0444	0.006126	0.009188	0.012251
2750	19800	0.0456	0.006378	0.009566	0.012755
3000	21190	0.0474	0.006419	0.009629	0.012839
3500	21870	0.0492	0.006858	0.010287	0.013716
4000	22190	0.0504	0.007337	0.011005	0.014674
4500	21530	0.0522	0.007905	0.011857	0.015809
5000	23600	0.054	0.007679	0.011518	0.015358

Table B48. PD Measured Data from Multi-stage RTL Test for Class 5 at OMC+2% (σ_d = 17 psi)

No. of Cycles	Measured M_R (psi)	Measured PD (inches)	Pred. PD (inches)		
			H = 6 in.	H = 9 in.	H = 12 in.
1	24530	0.0534	0	0	0
10	22860	0.054	0	0	0
20	22190	0.054	4.56E-43	6.83E-43	9.11E-43
50	21850	0.0558	1.01E-18	1.51E-18	2.02E-18
100	21240	0.0576	1.34E-10	2.01E-10	2.68E-10
200	21280	0.0612	1.52E-06	2.29E-06	3.05E-06
300	20590	0.0642	3.54E-05	5.31E-05	7.08E-05
400	20370	0.0672	0.00017	0.000254	0.000339
500	20440	0.0702	0.000429	0.000644	0.000859
600	19960	0.0732	0.000816	0.001224	0.001632
700	20590	0.0762	0.001241	0.001862	0.002483
800	19940	0.0792	0.001785	0.002678	0.003571
900	20020	0.0822	0.002301	0.003452	0.004603
1000	20460	0.0846	0.002794	0.004191	0.005588
1250	20240	0.09	0.004104	0.006156	0.008208
1500	24320	0.0948	0.004537	0.006805	0.009074
1750	22730	0.0996	0.005732	0.008598	0.011464
2000	25630	0.105	0.005987	0.008981	0.011975
2250	24000	0.1086	0.007039	0.010559	0.014079
2500	23610	0.1122	0.007715	0.011573	0.01543
2750	23280	0.1152	0.008422	0.012633	0.016844
3000	23810	0.1188	0.008772	0.013157	0.017543
3500	25220	0.1236	0.009239	0.013859	0.018478
4000	25650	0.1278	0.00974	0.01461	0.01948
4500	26510	0.1326	0.010085	0.015127	0.02017
5000	27280	0.1356	0.010335	0.015503	0.020671

Table B49. PD Measured Data from Multi-stage RTL Test for Class 5 at OMC+2% (σ_d = 24 psi)

No. of Cycles	Measured M_R (psi)	Measured PD (inches)	Pred. PD (inches)		
			H = 6 in.	H = 9 in.	H = 12 in.
1	31640	0.1362	0	0	0
10	27530	0.1368	0	0	0
20	26110	0.138	6.1E-43	9.14E-43	1.22E-42
50	24710	0.141	1.39E-18	2.08E-18	2.78E-18
100	23290	0.1464	1.88E-10	2.82E-10	3.76E-10
200	21050	0.159	2.31E-06	3.47E-06	4.63E-06
300	20930	0.1722	5.21E-05	7.82E-05	0.000104
400	18380	0.1854	0.000276	0.000414	0.000552
500	19130	0.1998	0.000678	0.001016	0.001355
600	18650	0.2136	0.001284	0.001927	0.002569
700	18580	0.2292	0.002003	0.003004	0.004006
800	18530	0.2442	0.002847	0.00427	0.005694
900	17930	0.258	0.003745	0.005618	0.00749
1000	17640	0.2724	0.004681	0.007021	0.009361
1250	17350	0.3096	0.00689	0.010335	0.01378
1500	17380	0.3492	0.008783	0.013174	0.017565

Table B50. PD Measured Data from Multi-stage RTL Test for 50% Class 5 + 50% RAP TH 10 at OMC-2% (σ_d = 17 psi)

No. of Cycles	Measured M_R (psi)	Measured PD (inches)	Pred. PD (inches)		
			H = 6 in.	H = 9 in.	H = 12 in.
1	54265	0.00078	0	0	0
10	55576	0.00162	2.66E-18	3.99E-18	5.32E-18
20	55145	0.0018	2.4E-10	3.6E-10	4.8E-10
50	56430	0.0021	1.41E-05	2.12E-05	2.83E-05
100	57135	0.0024	0.000551	0.000827	0.001103
200	58618	0.00276	0.003419	0.005128	0.006837
300	59051	0.00294	0.006307	0.009461	0.012615
400	60091	0.00306	0.00854	0.012809	0.017079
500	60322	0.00312	0.010275	0.015412	0.020549
600	60279	0.00318	0.011672	0.017508	0.023345
700	61105	0.00324	0.012595	0.018892	0.02519
800	60993	0.0033	0.013537	0.020305	0.027073
900	60283	0.0033	0.014277	0.021415	0.028554
1000	61205	0.00336	0.014782	0.022173	0.029563
1250	62120	0.00342	0.01593	0.023895	0.031861
1500	61260	0.00342	0.016811	0.025217	0.033622
1750	61048	0.00348	0.017482	0.026224	0.034965
2000	65940	0.00354	0.017149	0.025723	0.034298
2250	66536	0.00354	0.017566	0.02635	0.035133
2500	66282	0.0036	0.017707	0.026561	0.035415
2750	66773	0.00366	0.018031	0.027047	0.036063
3000	67271	0.00366	0.01811	0.027165	0.03622
3500	67524	0.00372	0.01841	0.027615	0.03682
4000	68689	0.00378	0.018495	0.027742	0.03699
4500	69923	0.00384	0.018616	0.027924	0.037232
5000	67063	0.00384	0.019077	0.028615	0.038153

Table B51. PD Measured Data from Multi-stage RTL Test for 50% Class 5 + 50% RAP TH 10 at OMC-2% (σ_d = 24 psi)

No. of Cycles	Measured M_R (psi)	Measured PD (inches)	Pred. PD (inches)		
			H = 6 in.	H = 9 in.	H = 12 in.
1	76263	0.00372	0	0	0
10	70324	0.00384	3.78E-18	5.67E-18	7.56E-18
20	69743	0.00384	3.4E-10	5.11E-10	6.81E-10
50	68288	0.00396	2.04E-05	3.06E-05	4.08E-05
100	67536	0.00408	0.000801	0.001202	0.001603
200	66992	0.0042	0.005036	0.007555	0.010073
300	65147	0.00432	0.00941	0.014115	0.01882
400	64832	0.00444	0.012762	0.019143	0.025524
500	64736	0.00456	0.015358	0.023037	0.030715
600	64864	0.00468	0.017392	0.026088	0.034783
700	65379	0.0048	0.018842	0.028263	0.037684
800	65619	0.00486	0.020208	0.030312	0.040416
900	65643	0.00498	0.021192	0.031788	0.042384
1000	65672	0.00516	0.022152	0.033228	0.044304
1250	66027	0.00552	0.023821	0.035732	0.047642
1500	66255	0.00576	0.024954	0.037431	0.049908
1750	66804	0.00594	0.025696	0.038544	0.051392
2000	67478	0.00618	0.026318	0.039476	0.052635
2250	68286	0.0063	0.026686	0.040029	0.053371
2500	70007	0.00642	0.026762	0.040144	0.053525
2750	69927	0.00654	0.027222	0.040833	0.054444
3000	70175	0.0066	0.02753	0.041295	0.05506
3500	71081	0.00678	0.02794	0.041911	0.055881
4000	71582	0.0069	0.028218	0.042327	0.056436
4500	71050	0.00714	0.028587	0.042881	0.057175
5000	70435	0.00732	0.029129	0.043694	0.058259

Table B52. PD Measured Data from Multi-stage RTL Test for 50% Class 5 + 50% RAP TH 10 at OMC-2% (σ_d = 37 psi)

No. of Cycles	Measured M_R (psi)	Measured PD (inches)	Pred. PD (inches)		
			H = 6 in.	H = 9 in.	H = 12 in.
1	81826	0.00738	0	0	0
10	74247	0.0075	6.09E-18	9.13E-18	1.22E-17
20	72662	0.00756	5.49E-10	8.23E-10	1.1E-09
50	69677	0.00786	3.33E-05	4.99E-05	6.65E-05
100	66740	0.00828	0.001318	0.001977	0.002636
200	64716	0.009	0.008361	0.012541	0.016722
300	65315	0.00954	0.015329	0.022993	0.030658
400	65826	0.0102	0.020734	0.031101	0.041468
500	64967	0.0105	0.025216	0.037825	0.050433
600	66214	0.01092	0.028225	0.042338	0.05645
700	67633	0.0114	0.030378	0.045568	0.060757
800	68950	0.0117	0.032359	0.048539	0.064719
900	70960	0.01188	0.033396	0.050095	0.066793
1000	68612	0.01194	0.0355	0.053249	0.070999
1250	68802	0.0123	0.038282	0.057423	0.076564
1500	69256	0.01254	0.040191	0.060286	0.080381
1750	69728	0.01278	0.041448	0.062172	0.082896
2000	70231	0.01296	0.042357	0.063536	0.084714
2250	69771	0.01314	0.043482	0.065223	0.086964
2500	68824	0.01326	0.044373	0.06656	0.088746
2750	69457	0.01338	0.044917	0.067375	0.089834
3000	69026	0.0135	0.04559	0.068384	0.091179
3500	67583	0.01362	0.047028	0.070542	0.094056
4000	70904	0.01392	0.046639	0.069958	0.093277
4500	71831	0.01416	0.046404	0.069606	0.092808
5000	72491	0.01434	0.046873	0.070309	0.093745

Table B53. PD Measured Data from Multi-stage RTL Test for 50% Class 5 + 50% RAP TH 10 at OMC-2% (σ_d = 53 psi)

No. of Cycles	Measured M_R (psi)	Measured PD (inches)	Pred. PD (inches)		
			H = 6 in.	H = 9 in.	H = 12 in.
1	79601	0.01422	0	0	0
10	76780	0.01434	8.71E-18	1.31E-17	1.74E-17
20	77879	0.01452	7.75E-10	1.16E-09	1.55E-09
50	74926	0.01464	4.65E-05	6.97E-05	9.29E-05
100	73052	0.01494	0.00183	0.002746	0.003661
200	75658	0.01584	0.011197	0.016796	0.022394
300	78652	0.01674	0.020222	0.030332	0.040443
400	75520	0.01758	0.027965	0.041947	0.055929
500	75950	0.01854	0.033471	0.050206	0.066941
600	74973	0.01926	0.037993	0.056989	0.075986
700	73954	0.0198	0.041879	0.062819	0.083758
800	72345	0.02034	0.045336	0.068004	0.090672
900	72007	0.0207	0.047664	0.071496	0.095327
1000	73004	0.02112	0.049338	0.074007	0.098676
1250	72286	0.02202	0.053472	0.080208	0.106944
1500	72191	0.02268	0.056282	0.084423	0.112565
1750	73989	0.02316	0.057677	0.086515	0.115354
2000	76077	0.02352	0.058603	0.087905	0.117206
2250	73389	0.02376	0.061051	0.091576	0.122102
2500	71607	0.02394	0.063023	0.094534	0.126046
2750	74731	0.02442	0.062416	0.093624	0.124833
3000	76326	0.02472	0.062541	0.093812	0.125082
3500	72122	0.02508	0.065532	0.098298	0.131064
4000	72899	0.0255	0.066384	0.099575	0.132767
4500	73164	0.02586	0.06709	0.100634	0.134179
5000	74618	0.02622	0.067142	0.100713	0.134284

Table B54. PD Measured Data from Multi-stage RTL Test for 50% Class 5 + 50% RAP TH 10 at OMC-2% (σ_d = 63 psi)

No. of Cycles	Measured M_R (psi)	Measured PD (inches)	Pred. PD (inches)		
			H = 6 in.	H = 9 in.	H = 12 in.
1	81984	0.02616	0	0	0
10	80780	0.02628	1.16E-17	1.73E-17	2.31E-17
20	81092	0.02634	1.04E-09	1.56E-09	2.07E-09
50	77488	0.0264	6.21E-05	9.32E-05	0.000124
100	76607	0.0267	0.002426	0.003639	0.004851
200	77729	0.02766	0.014982	0.022473	0.029965
300	76043	0.02898	0.027626	0.041439	0.055251
400	71078	0.02988	0.038715	0.058073	0.077431
500	70830	0.03102	0.046356	0.069534	0.092713
600	67222	0.0321	0.053894	0.080842	0.107789
700	65591	0.0333	0.059405	0.089107	0.118809
800	64824	0.03432	0.064461	0.096692	0.128923
900	64139	0.03516	0.067712	0.101568	0.135424
1000	68137	0.03606	0.068161	0.102241	0.136322
1250	66732	0.03798	0.074421	0.111632	0.148843
1500	63735	0.03936	0.080145	0.120217	0.160289
1750	61891	0.04062	0.084531	0.126797	0.169063
2000	59391	0.0417	0.088978	0.133467	0.177957
2250	61513	0.04296	0.089037	0.133555	0.178073
2500	67391	0.04446	0.086083	0.129124	0.172166
2750	70822	0.04602	0.085192	0.127788	0.170384
3000	71419	0.0471	0.085739	0.128608	0.171478
3500	74967	0.0492	0.085568	0.128352	0.171136
4000	76433	0.05016	0.086013	0.129019	0.172025
4500	77041	0.05082	0.086891	0.130336	0.173782
5000	75520	0.05148	0.088679	0.133018	0.177357

Table B55. PD Measured Data from Multi-stage RTL Test for 50% Class 5 + 50% RAP TH 10 at OMC-2% (σ_d = 73 psi)

No. of Cycles	Measured M_R (psi)	Measured PD (inches)	Pred. PD (inches)		
			H = 6 in.	H = 9 in.	H = 12 in.
1	80125	0.05142	0	0	0
10	80126	0.05148	1.39E-17	2.09E-17	2.78E-17
20	80922	0.0516	1.24E-09	1.86E-09	2.48E-09
50	80013	0.05172	7.4E-05	0.000111	0.000148
100	78583	0.05202	0.002896	0.004344	0.005792
200	76267	0.05262	0.018228	0.027342	0.036456
300	73275	0.0534	0.03412	0.05118	0.06824
400	69051	0.05448	0.047488	0.071232	0.094976
500	69234	0.05562	0.056721	0.085082	0.113443
600	67922	0.05694	0.064724	0.097086	0.129448
700	66083	0.05826	0.07151	0.107265	0.14302
800	65039	0.05976	0.077444	0.116165	0.154887
900	68502	0.06186	0.078587	0.117881	0.157175
1000	69936	0.06366	0.080946	0.121419	0.161892
1250	68309	0.0675	0.08816	0.13224	0.17632
1500	68523	0.07092	0.092558	0.138837	0.185116
1750	69860	0.0744	0.094628	0.141943	0.189257
2000	67620	0.07776	0.099149	0.148724	0.198299
2250	73262	0.08094	0.096942	0.145412	0.193883
2500	64956	0.08424	0.10467	0.157006	0.209341
2750	64005	0.0876	0.107254	0.160881	0.214508
3000	64960	0.09138	0.107571	0.161357	0.215142
3500	61544	0.10032	0.11256	0.16884	0.225121
4000	53080	0.1185	0.12218	0.183271	0.244361

Table B56. PD Measured Data from Multi-stage RTL Test for 50% Class 5 + 50% RAP TH 10 at OMC% (σ_d = 24 psi)

No. of Cycles	Measured M_R (psi)	Measured PD (inches)	Pred. PD (inches)		
			H = 6 in.	H = 9 in.	H = 12 in.
1	28980	0.0015	0	0	0
10	31200	0.00534	1.98E-30	2.97E-30	3.96E-30
20	31866	0.00684	2.56E-16	3.85E-16	5.13E-16
50	32873	0.00894	7.58E-08	1.14E-07	1.52E-07
100	34429	0.01074	5.01E-05	7.52E-05	0.0001
200	35327	0.01254	0.001292	0.001938	0.002584
300	36505	0.01374	0.003785	0.005678	0.00757
400	37492	0.01458	0.006448	0.009672	0.012896
500	37988	0.0153	0.008901	0.013352	0.017803
600	38328	0.01584	0.011138	0.016707	0.022276
700	39009	0.01632	0.01286	0.01929	0.02572
800	39420	0.0168	0.014474	0.02171	0.028947
900	40501	0.01722	0.01548	0.02322	0.030961
1000	40626	0.01758	0.016586	0.02488	0.033173
1250	40651	0.01824	0.019108	0.028662	0.038217
1500	41595	0.01884	0.020524	0.030786	0.041047
1750	42067	0.01926	0.021672	0.032508	0.043344
2000	42375	0.01956	0.022625	0.033938	0.045251
2250	43047	0.01986	0.023322	0.034983	0.046643
2500	42897	0.0201	0.02402	0.036029	0.048039
2750	43551	0.02034	0.02451	0.036764	0.049019
3000	44178	0.02058	0.024675	0.037012	0.04935
3500	44950	0.02094	0.025221	0.037832	0.050443
4000	46032	0.02136	0.025534	0.0383	0.051067
4500	46056	0.02166	0.026086	0.039128	0.052171
5000	46400	0.0219	0.02634	0.039509	0.052679

Table B57. PD Measured Data from Multi-stage RTL Test for 50% Class 5 + 50% RAP TH 10 at OMC% (σ_d = 37 psi)

No. of Cycles	Measured M_R (psi)	Measured PD (inches)	Pred. PD (inches)		
			H = 6 in.	H = 9 in.	H = 12 in.
1	59644	0.02226	0	0	0
10	52377	0.02232	2.68E-30	4.02E-30	5.36E-30
20	53576	0.02322	3.02E-16	4.54E-16	6.05E-16
50	45379	0.02334	1.1E-07	1.65E-07	2.2E-07
100	44402	0.02508	7.33E-05	0.00011	0.000147
200	43610	0.02856	0.001911	0.002867	0.003823
300	43831	0.03144	0.005636	0.008455	0.011273
400	44000	0.03396	0.009674	0.014511	0.019348
500	42999	0.03606	0.013657	0.020486	0.027315
600	42950	0.0378	0.01699	0.025486	0.033981
700	41527	0.03918	0.02039	0.030585	0.04078
800	45959	0.04074	0.021435	0.032152	0.042869
900	44446	0.04176	0.023991	0.035986	0.047982
1000	44219	0.04278	0.025854	0.038781	0.051708
1250	45415	0.04488	0.029041	0.043562	0.058082
1500	45665	0.04662	0.031701	0.047552	0.063403
1750	45092	0.04806	0.034114	0.05117	0.068227
2000	45873	0.04914	0.035454	0.053181	0.070909
2250	47467	0.05028	0.035971	0.053956	0.071942
2500	46573	0.05112	0.037701	0.056551	0.075402
2750	46598	0.05196	0.038668	0.058001	0.077335
3000	46953	0.05274	0.039328	0.058992	0.078656
3500	47933	0.05382	0.040158	0.060238	0.080317
4000	47190	0.05472	0.041569	0.062354	0.083138
4500	48284	0.0555	0.041859	0.062788	0.083717
5000	46973	0.05616	0.043446	0.065169	0.086891

Table B58. PD Measured Data from Multi-stage RTL Test for 50% Class 5 + 50% RAP TH 10 at OMC% (σ_d = 53 psi)

No. of Cycles	Measured M_R (psi)	Measured PD (inches)	Pred. PD (inches)		
			H = 6 in.	H = 9 in.	H = 12 in.
1	57467	0.0564	0	0	0
10	54759	0.05658	3.88E-30	5.82E-30	7.76E-30
20	53237	0.05676	4.99E-16	7.48E-16	9.97E-16
50	51756	0.05736	1.48E-07	2.22E-07	2.96E-07
100	49675	0.0588	9.99E-05	0.00015	0.0002
200	46002	0.0627	0.002685	0.004027	0.00537
300	45696	0.06732	0.007903	0.011854	0.015805
400	46459	0.072	0.013422	0.020132	0.026843
500	47529	0.07602	0.018244	0.027366	0.036488
600	47235	0.08064	0.022749	0.034123	0.045497
700	46377	0.08472	0.02686	0.04029	0.05372
800	44681	0.08856	0.031208	0.046812	0.062416
900	43726	0.09216	0.034432	0.051649	0.068865
1000	42818	0.09636	0.037572	0.056357	0.075143
1250	50447	0.10536	0.038293	0.05744	0.076586
1500	48214	0.11352	0.043091	0.064637	0.086183
1750	47156	0.12018	0.046595	0.069892	0.09319
2000	49253	0.1257	0.047475	0.071213	0.09495
2250	49487	0.13032	0.049146	0.073719	0.098292
2500	51465	0.13506	0.049425	0.074138	0.09885
2750	55594	0.13926	0.048241	0.072361	0.096481
3000	60985	0.1431	0.046719	0.070079	0.093439
3500	59707	0.1503	0.048784	0.073175	0.097567
4000	60889	0.15714	0.049236	0.073853	0.098471
4500	60117	0.1626	0.050692	0.076038	0.101384
5000	55370	0.16824	0.053743	0.080615	0.107486

Table B59. PD Measured Data from Multi-stage RTL Test for 50% Class 5 + 50% RAP TH 10 at OMC% (σ_d = 63 psi)

No. of Cycles	Measured M_R (psi)	Measured PD (inches)	Pred. PD (inches)		
			H = 6 in.	H = 9 in.	H = 12 in.
1	67920	0.16872	0	0	0
10	64009	0.1692	4.5E-30	6.74E-30	8.99E-30
20	60931	0.16986	5.88E-16	8.83E-16	1.18E-15
50	56352	0.17214	1.75E-07	2.63E-07	3.51E-07
100	56262	0.1722	0.000117	0.000175	0.000234
200	52789	0.17814	0.003	0.0045	0.005999
300	46372	0.19818	0.009146	0.013719	0.018292
400	28984	0.28584	0.015354	0.023031	0.030708

Table B60. PD Measured Data from Multi-stage RTL Test for 50% Class 5 + 50% RAP TH 10 at OMC+2% (σ_d = 6 psi)

No. of Cycles	Measured M_R (psi)	Measured PD (inches)	Pred. PD (inches)		
			H = 6 in.	H = 9 in.	H = 12 in.
1	19825	0	0	0	0
10	20111	0.00072	2.32E-56	3.47E-56	4.63E-56
20	19844	0.00102	1.21E-29	1.82E-29	2.43E-29
50	19945	0.00162	1.29E-13	1.93E-13	2.58E-13
100	20423	0.00216	2.84E-08	4.25E-08	5.67E-08
200	21523	0.0027	1.3E-05	1.94E-05	2.59E-05
300	22174	0.003	9.91E-05	0.000149	0.000198
400	22741	0.00318	0.000271	0.000407	0.000542
500	23391	0.00336	0.000505	0.000758	0.00101
600	23323	0.00348	0.000747	0.00112	0.001494
700	23646	0.0036	0.000992	0.001488	0.001984
800	24431	0.0036	0.001242	0.001863	0.002485
900	24199	0.00372	0.001479	0.002218	0.002958
1000	24222	0.00372	0.00169	0.002535	0.00338
1250	24329	0.00384	0.002147	0.003221	0.004294
1500	24724	0.00396	0.002518	0.003777	0.005036
1750	25195	0.00402	0.002773	0.00416	0.005547
2000	24875	0.00408	0.003067	0.004601	0.006135
2250	24536	0.0042	0.003278	0.004916	0.006555
2500	25786	0.00432	0.003407	0.00511	0.006813
2750	25612	0.00432	0.003541	0.005312	0.007082
3000	25257	0.00432	0.00369	0.005534	0.007379
3500	25534	0.00444	0.003978	0.005967	0.007956
4000	25650	0.0045	0.004116	0.006174	0.008231
4500	25651	0.00456	0.00425	0.006375	0.0085
5000	26194	0.00468	0.004298	0.006448	0.008597

Table B61. PD Measured Data from Multi-stage RTL Test for 50% Class 5 + 50% RAP TH 10 at OMC+2% (σ_d = 12 psi)

No. of Cycles	Measured M_R (psi)	Measured PD (inches)	Pred. PD (inches)		
			H = 6 in.	H = 9 in.	H = 12 in.
1	30658	0.00474	0	0	0
10	26213	0.00552	4.87E-56	7.31E-56	9.74E-56
20	25035	0.00612	2.56E-29	3.85E-29	5.13E-29
50	23936	0.00726	2.86E-13	4.29E-13	5.73E-13
100	24298	0.0087	6.27E-08	9.41E-08	1.25E-07
200	24903	0.01044	2.91E-05	4.36E-05	5.82E-05
300	25491	0.01152	0.000224	0.000336	0.000448
400	25853	0.01236	0.000614	0.000922	0.001229
500	26201	0.0129	0.00114	0.001709	0.002279
600	26288	0.01338	0.001714	0.00257	0.003427
700	26557	0.0138	0.002283	0.003424	0.004566
800	26578	0.0141	0.00287	0.004305	0.00574
900	26516	0.0144	0.003406	0.005109	0.006812
1000	26780	0.0147	0.003911	0.005867	0.007822
1250	27154	0.01524	0.004903	0.007355	0.009806
1500	27495	0.0156	0.005796	0.008694	0.011592
1750	28093	0.01596	0.006412	0.009618	0.012824
2000	28386	0.01626	0.007004	0.010507	0.014009
2250	28676	0.01656	0.007443	0.011165	0.014886
2500	29391	0.0168	0.007666	0.0115	0.015333
2750	29469	0.01692	0.00809	0.012135	0.01618
3000	29370	0.01704	0.008386	0.012579	0.016772
3500	29344	0.01734	0.008913	0.013369	0.017825
4000	30638	0.01758	0.009108	0.013662	0.018216
4500	30468	0.01782	0.009419	0.014129	0.018838
5000	31174	0.01788	0.009558	0.014337	0.019116

Table B62. PD Measured Data from Multi-stage RTL Test for 50% Class 5 + 50% RAP TH 10 at OMC+2% (σ_d = 17 psi)

No. of Cycles	Measured M_R (psi)	Measured PD (inches)	Pred. PD (inches)		
			H = 6 in.	H = 9 in.	H = 12 in.
1	36404	0.01788	0	0	0
10	35031	0.01794	6.23E-56	9.34E-56	1.25E-55
20	33652	0.018	3.26E-29	4.89E-29	6.52E-29
50	32400	0.01824	3.56E-13	5.35E-13	7.13E-13
100	31388	0.0186	8.02E-08	1.2E-07	1.6E-07
200	30210	0.01938	3.88E-05	5.82E-05	7.76E-05
300	29762	0.02022	0.000303	0.000454	0.000605
400	29611	0.02088	0.000852	0.001277	0.001703
500	29744	0.02166	0.001572	0.002358	0.003144
600	29665	0.02226	0.002371	0.003557	0.004742
700	29677	0.0228	0.003172	0.004758	0.006344
800	29942	0.02328	0.003949	0.005923	0.007897
900	29956	0.02376	0.00469	0.007035	0.009379
1000	30050	0.02418	0.005342	0.008014	0.010685
1250	30322	0.02508	0.006824	0.010237	0.013649
1500	30501	0.0258	0.008017	0.012026	0.016034
1750	30957	0.0264	0.008963	0.013445	0.017927
2000	31569	0.02688	0.00966	0.014489	0.019319
2250	31385	0.02724	0.010377	0.015565	0.020754
2500	31647	0.02748	0.010984	0.016476	0.021968
2750	31392	0.02778	0.011535	0.017303	0.02307
3000	31621	0.02802	0.011918	0.017877	0.023837
3500	31713	0.0285	0.012633	0.018949	0.025266
4000	32335	0.02886	0.013023	0.019535	0.026046
4500	32722	0.02922	0.013462	0.020194	0.026925
5000	32803	0.02946	0.013779	0.020669	0.027559

Table B63. PD Measured Data from Multi-stage RTL Test for 50% Class 5 + 50% RAP TH 10 at OMC+2% (σ_d = 24 psi)

No. of Cycles	Measured M_R (psi)	Measured PD (inches)	Pred. PD (inches)		
			H = 6 in.	H = 9 in.	H = 12 in.
1	39883	0.02946	0	0	0
10	37514	0.0297	9.07E-56	1.36E-55	1.81E-55
20	36531	0.02988	4.72E-29	7.07E-29	9.43E-29
50	34766	0.03042	5.19E-13	7.78E-13	1.04E-12
100	33245	0.0315	1.16E-07	1.75E-07	2.33E-07
200	32515	0.0339	5.53E-05	8.3E-05	0.000111
300	32368	0.03618	0.000432	0.000648	0.000864
400	32178	0.03816	0.00121	0.001816	0.002421
500	32121	0.03996	0.002245	0.003367	0.00449
600	32111	0.04152	0.00339	0.005084	0.006779
700	32022	0.04284	0.004583	0.006874	0.009165
800	32289	0.04398	0.005692	0.008538	0.011384
900	32200	0.04506	0.006749	0.010123	0.013498
1000	32153	0.04596	0.007768	0.011653	0.015537
1250	32331	0.04794	0.009946	0.014919	0.019892
1500	32671	0.0495	0.011697	0.017545	0.023393
1750	32993	0.05088	0.013116	0.019674	0.026232
2000	33227	0.05202	0.014236	0.021355	0.028473
2250	32865	0.05298	0.015453	0.02318	0.030907
2500	33020	0.05394	0.016243	0.024364	0.032486
2750	32889	0.05466	0.017128	0.025692	0.034256
3000	32975	0.05538	0.01776	0.02664	0.03552
3500	33472	0.05658	0.018671	0.028006	0.037342
4000	34269	0.05742	0.019282	0.028923	0.038563
4500	34876	0.05814	0.019769	0.029653	0.039538
5000	35114	0.0588	0.020273	0.03041	0.040547

Table B64. PD Measured Data from Multi-stage RTL Test for 50% Class 5 + 50% RAP TH 10 at OMC+2% (σ_d = 37 psi)

No. of Cycles	Measured M_R (psi)	Measured PD (inches)	Pred. PD (inches)		
			H = 6 in.	H = 9 in.	H = 12 in.
1	44054	0.05898	0	0	0
10	38572	0.05952	1.43E-55	2.14E-55	2.85E-55
20	36293	0.06036	7.6E-29	1.14E-28	1.52E-28
50	32463	0.06384	8.65E-13	1.3E-12	1.73E-12
100	30235	0.07134	1.99E-07	2.98E-07	3.97E-07
200	29786	0.0858	9.42E-05	0.000141	0.000188
300	30467	0.0981	0.000722	0.001083	0.001444
400	32288	0.10854	0.001933	0.002899	0.003866
500	31933	0.11778	0.003627	0.005441	0.007254
600	33246	0.1257	0.005326	0.00799	0.010653
700	29990	0.13314	0.007776	0.011664	0.015552
800	30544	0.14016	0.009643	0.014465	0.019286
900	30321	0.14592	0.011461	0.017192	0.022923
1000	29853	0.15126	0.013305	0.019957	0.02661
1250	30645	0.16254	0.016743	0.025115	0.033487
1500	30530	0.17208	0.019928	0.029891	0.039855
1750	31310	0.18012	0.022135	0.033202	0.044269
2000	31622	0.1872	0.024076	0.036114	0.048151
2250	32324	0.19272	0.025523	0.038284	0.051045
2500	32216	0.19698	0.027094	0.040641	0.054188
2750	32400	0.201	0.028307	0.04246	0.056614
3000	32826	0.2046	0.029108	0.043661	0.058215
3500	32929	0.21102	0.031046	0.04657	0.062093
4000	33242	0.21672	0.032317	0.048476	0.064635
4500	32043	0.22116	0.034372	0.051558	0.068743
5000	31712	0.2256	0.035818	0.053728	0.071637

Table B65. PD Measured Data from Multi-stage RTL Test for 50% Class 5 + 50% RAP TH 10 at OMC+2% (σ_d = 53 psi)

No. of Cycles	Measured M_R (psi)	Measured PD (inches)	Pred. PD (inches)		
			H = 6 in.	H = 9 in.	H = 12 in.
1	36984	0.2256	0	0	0
10	34995	0.22656	2.23E-55	3.35E-55	4.46E-55
20	33319	0.22788	1.18E-28	1.77E-28	2.36E-28
50	30314	0.23364	1.32E-12	1.98E-12	2.64E-12
100	28187	0.24876	2.97E-07	4.45E-07	5.94E-07
200	24611	0.29496	0.000149	0.000224	0.000299
300	23669	0.35976	0.001163	0.001745	0.002326
400	31101	0.43758	0.002525	0.003787	0.005049

Table B66. PD Measured Data from Multi-stage RTL Test for 50% Class 5 + 50% RAP TH 10 + 3.5% Plastic Fines at OMC-2% (σ_d = 17 psi)

No. of Cycles	Measured M_R (psi)	Measured PD (inches)	Pred. PD (inches)		
			H = 6 in.	H = 9 in.	H = 12 in.
1	61180	0.0036	0	0	0
10	57690	0.0096	2.8E-16	4.21E-16	5.61E-16
20	64500	0.0108	2.39E-09	3.59E-09	4.79E-09
50	69660	0.012	3.52E-05	5.28E-05	7.04E-05
100	74500	0.0132	0.00085	0.001276	0.001701
200	80000	0.0138	0.004157	0.006235	0.008313
300	80860	0.0144	0.007083	0.010624	0.014165
400	82980	0.015	0.009068	0.013602	0.018135
500	84420	0.015	0.010612	0.015918	0.021224
600	84990	0.015	0.011768	0.017652	0.023536
700	85670	0.015	0.012667	0.019	0.025334
800	87250	0.0156	0.013496	0.020244	0.026992
900	87710	0.0156	0.01396	0.02094	0.02792
1000	87350	0.0156	0.01449	0.021734	0.028979
1250	90040	0.0156	0.015315	0.022973	0.03063
1500	96010	0.0162	0.015592	0.023388	0.031184
1750	93620	0.0162	0.016215	0.024323	0.032431
2000	97580	0.0162	0.0165	0.02475	0.033
2250	97150	0.0162	0.016708	0.025061	0.033415
2500	98200	0.0162	0.016961	0.025441	0.033922
2750	97750	0.0162	0.017185	0.025778	0.03437
3000	96160	0.0162	0.017554	0.026331	0.035108
3500	97530	0.0168	0.017795	0.026692	0.03559
4000	99870	0.0168	0.017886	0.026829	0.035772
4500	102970	0.0168	0.017827	0.026741	0.035654
5000	99640	0.0168	0.018122	0.027182	0.036243

Table B67. PD Measured Data from Multi-stage RTL Test for 50% Class 5 + 50% RAP TH 10 + 3.5% Plastic Fines at OMC-2% (σ_d = 24 psi)

No. of Cycles	Measured M_R (psi)	Measured PD (inches)	Pred. PD (inches)		
			H = 6 in.	H = 9 in.	H = 12 in.
1	102620	0.0168	0	0	0
10	88150	0.0168	3.72E-16	5.58E-16	7.44E-16
20	86450	0.0168	3.43E-09	5.14E-09	6.85E-09
50	80480	0.0174	5.22E-05	7.83E-05	0.000104
100	78050	0.018	0.001301	0.001951	0.002602
200	74370	0.0186	0.006604	0.009906	0.013209
300	75400	0.0192	0.01123	0.016846	0.022461
400	76030	0.0198	0.014616	0.021923	0.029231
500	80130	0.0198	0.016812	0.025218	0.033624
600	84340	0.0204	0.01833	0.027495	0.036661
700	86300	0.0204	0.019589	0.029383	0.039178
800	91870	0.0204	0.020231	0.030346	0.040462
900	91720	0.021	0.02123	0.031845	0.04246
1000	94190	0.021	0.021869	0.032803	0.043738
1250	97700	0.021	0.022958	0.034438	0.045917
1500	98080	0.0216	0.024069	0.036103	0.048138
1750	98350	0.0216	0.024716	0.037074	0.049432
2000	98600	0.0222	0.02529	0.037935	0.05058
2250	99840	0.0222	0.025746	0.038618	0.051491
2500	99690	0.0222	0.026115	0.039173	0.052231
2750	106810	0.0222	0.025984	0.038976	0.051968
3000	103940	0.0222	0.026374	0.039561	0.052748
3500	105240	0.0228	0.02651	0.039765	0.05302
4000	106150	0.0228	0.026991	0.040487	0.053983
4500	106330	0.0228	0.027136	0.040704	0.054272
5000	107750	0.0228	0.02732	0.04098	0.054641

Table B68. PD Measured Data from Multi-stage RTL Test for 50% Class 5 + 50% RAP TH 10 + 3.5% Plastic Fines at OMC-2% (σ_d = 37 psi)

No. of Cycles	Measured M_R (psi)	Measured PD (inches)	Pred. PD (inches)		
			H = 6 in.	H = 9 in.	H = 12 in.
1	114290	0.0228	0	0	0
10	97380	0.0234	5.95E-16	8.93E-16	1.19E-15
20	94920	0.0234	5.41E-09	8.12E-09	1.08E-08
50	91160	0.024	8.13E-05	0.000122	0.000163
100	93780	0.0252	0.001992	0.002987	0.003983
200	89610	0.0258	0.010127	0.01519	0.020253
300	89040	0.0264	0.017276	0.025914	0.034552
400	91070	0.027	0.022429	0.033644	0.044858
500	95150	0.0276	0.025851	0.038776	0.051701
600	95380	0.0276	0.028694	0.043041	0.057388
700	99200	0.0276	0.030356	0.045534	0.060712
800	98040	0.0282	0.032379	0.048568	0.064758
900	100600	0.0282	0.033677	0.050515	0.067354
1000	101950	0.0282	0.034825	0.052238	0.06965
1250	104770	0.0288	0.036983	0.055475	0.073966
1500	106820	0.0294	0.038433	0.05765	0.076867
1750	110410	0.0294	0.039462	0.059193	0.078925
2000	111180	0.0294	0.040246	0.060368	0.080491
2250	109010	0.03	0.041334	0.062	0.082667
2500	112150	0.03	0.041819	0.062729	0.083639
2750	100350	0.03	0.0435	0.06525	0.087
3000	103950	0.0306	0.043512	0.065268	0.087025
3500	108540	0.0312	0.043704	0.065556	0.087408
4000	109330	0.0318	0.044226	0.066339	0.088452
4500	113430	0.0318	0.044103	0.066155	0.088206
5000	121010	0.0324	0.043916	0.065874	0.087832

Table B69. PD Measured Data from Multi-stage RTL Test for 50% Class 5 + 50% RAP TH 10 + 3.5% Plastic Fines at OMC-2% (σ_d = 53 psi)

No. of Cycles	Measured M_R (psi)	Measured PD (inches)	Pred. PD (inches)		
			H = 6 in.	H = 9 in.	H = 12 in.
1	125210	0.0318	0	0	0
10	118770	0.0324	8.18E-16	1.23E-15	1.64E-15
20	116460	0.0324	7.43E-09	1.11E-08	1.49E-08
50	111390	0.0324	0.000111	0.000166	0.000222
100	112150	0.0324	0.002741	0.004112	0.005482
200	100760	0.0324	0.013943	0.020915	0.027886
300	95190	0.033	0.024249	0.036374	0.048499
400	96730	0.0336	0.031466	0.047199	0.062932
500	96770	0.0342	0.036986	0.055479	0.073972
600	94870	0.0342	0.041409	0.062114	0.082819
700	100720	0.0348	0.043901	0.065851	0.087801
800	101970	0.0348	0.046338	0.069507	0.092676
900	101830	0.0354	0.048479	0.072718	0.096958
1000	101860	0.0354	0.050323	0.075485	0.100646
1250	102830	0.0354	0.053476	0.080215	0.106953
1500	105190	0.036	0.055542	0.083313	0.111084
1750	108110	0.036	0.056866	0.085299	0.113732
2000	111240	0.0366	0.057856	0.086785	0.115713
2250	110070	0.0366	0.059073	0.08861	0.118146
2500	110940	0.0366	0.059856	0.089783	0.119711
2750	110070	0.0366	0.060701	0.091052	0.121403
3000	113330	0.0372	0.060886	0.091329	0.121773
3500	113770	0.0372	0.061835	0.092752	0.12367
4000	114520	0.0372	0.062639	0.093958	0.125277
4500	116690	0.0378	0.063304	0.094956	0.126608
5000	115880	0.0378	0.063678	0.095518	0.127357

Table B70. PD Measured Data from Multi-stage RTL Test for 50% Class 5 + 50% RAP TH 10 + 3.5% Plastic Fines at OMC-2% (σ_d = 63 psi)

No. of Cycles	Measured M_R (psi)	Measured PD (inches)	Pred. PD (inches)		
			H = 6 in.	H = 9 in.	H = 12 in.
1	117520	0.0378	0	0	0
10	110280	0.0378	1.12E-15	1.67E-15	2.23E-15
20	108630	0.0378	1.02E-08	1.52E-08	2.03E-08
50	107590	0.0378	0.000152	0.000228	0.000304
100	104170	0.0384	0.003766	0.005649	0.007532
200	96650	0.0384	0.019012	0.028518	0.038025
300	93230	0.039	0.032878	0.049317	0.065756
400	88290	0.0396	0.043761	0.065642	0.087522
500	88080	0.0396	0.051412	0.077118	0.102823
600	87670	0.0402	0.057324	0.085986	0.114648
700	84850	0.0408	0.062662	0.093994	0.125325
800	86010	0.0408	0.066311	0.099467	0.132623
900	86200	0.0414	0.069033	0.10355	0.138066
1000	85410	0.0414	0.071884	0.107827	0.143769
1250	86490	0.042	0.076457	0.114686	0.152914
1500	86900	0.0426	0.079553	0.11933	0.159106
1750	94260	0.0438	0.07979	0.119686	0.159581
2000	97390	0.0444	0.080741	0.121111	0.161481
2250	96530	0.045	0.082524	0.123787	0.165049
2500	98510	0.0456	0.083118	0.124676	0.166235
2750	99360	0.0462	0.083694	0.125541	0.167387
3000	100900	0.0468	0.08466	0.12699	0.16932
3500	106880	0.0474	0.084498	0.126748	0.168997
4000	109140	0.048	0.085285	0.127928	0.17057
4500	110880	0.0486	0.085779	0.128668	0.171558
5000	113940	0.0486	0.085964	0.128946	0.171928

Table B71. PD Measured Data from Multi-stage RTL Test for 50% Class 5 + 50% RAP TH 10 + 3.5% Plastic Fines at OMC-2% (σ_d = 73 psi)

No. of Cycles	Measured M_R (psi)	Measured PD (inches)	Pred. PD (inches)		
			H = 6 in.	H = 9 in.	H = 12 in.
1	114820	0.0486	0	0	0
10	110390	0.0486	1.37E-15	2.06E-15	2.74E-15
20	111700	0.0486	1.24E-08	1.86E-08	2.48E-08
50	112380	0.0486	0.000184	0.000276	0.000369
100	110180	0.0492	0.004538	0.006807	0.009076
200	109220	0.0492	0.022595	0.033893	0.04519
300	103720	0.0492	0.038959	0.058438	0.077917
400	104510	0.0498	0.050699	0.076049	0.101398
500	103110	0.0498	0.059808	0.089713	0.119617
600	104660	0.0504	0.06616	0.09924	0.13232
700	100530	0.0504	0.072128	0.108192	0.144256
800	97560	0.051	0.077388	0.116082	0.154776
900	97220	0.051	0.080835	0.121253	0.16167
1000	99110	0.0516	0.083213	0.124819	0.166425
1250	98880	0.0528	0.088638	0.132957	0.177276
1500	99040	0.0534	0.092554	0.138832	0.185109
1750	97110	0.054	0.09597	0.143956	0.191941
2000	94980	0.0546	0.098785	0.148177	0.19757
2250	96570	0.0552	0.10016	0.150241	0.200321
2500	95720	0.0558	0.10192	0.15288	0.20384
2750	96990	0.0564	0.10264	0.153959	0.205279
3000	102020	0.0564	0.102246	0.153369	0.204492
3500	98690	0.057	0.10501	0.157515	0.21002
4000	109340	0.0582	0.10317	0.154755	0.20634
4500	109710	0.0588	0.104199	0.156299	0.208399
5000	111210	0.0594	0.104843	0.157265	0.209687

Table B72. PD Measured Data from Multi-stage RTL Test for 50% Class 5 + 50% RAP TH 10 + 3.5% Plastic Fines at OMC% (σ_d = 17 psi)

No. of Cycles	Measured M_R (psi)	Measured PD (inches)	Pred. PD (inches)		
			H = 6 in.	H = 9 in.	H = 12 in.
1	46870	0.0012	0	0	0
10	45440	0.0018	9.33E-27	1.4E-26	1.87E-26
20	44890	0.0024	1.35E-14	2.03E-14	2.7E-14
50	44920	0.003	2.67E-07	4.01E-07	5.34E-07
100	45980	0.0036	7.14E-05	0.000107	0.000143
200	48640	0.0042	0.001138	0.001706	0.002275
300	49030	0.0042	0.002889	0.004334	0.005779
400	50650	0.0042	0.00453	0.006795	0.00906
500	51250	0.0042	0.005971	0.008956	0.011941
600	51400	0.0042	0.007177	0.010766	0.014354
700	51810	0.0042	0.008195	0.012293	0.016391
800	51520	0.0042	0.009054	0.013582	0.018109
900	51640	0.0048	0.009797	0.014696	0.019594
1000	52090	0.0048	0.010368	0.015552	0.020736
1250	52350	0.0048	0.011649	0.017474	0.023298
1500	52480	0.0048	0.012451	0.018677	0.024902
1750	53290	0.0048	0.01309	0.019635	0.026181
2000	54230	0.0048	0.013345	0.020018	0.02669
2250	53340	0.0048	0.01411	0.021164	0.028219
2500	54350	0.0048	0.014277	0.021416	0.028555
2750	54130	0.0048	0.014627	0.02194	0.029253
3000	54160	0.0048	0.014767	0.02215	0.029533
3500	55340	0.0048	0.015128	0.022692	0.030256
4000	56540	0.0054	0.015251	0.022877	0.030503
4500	56610	0.0054	0.015449	0.023173	0.030898
5000	56810	0.0054	0.015679	0.023518	0.031358

Table B73. PD Measured Data from Multi-stage RTL Test for 50% Class 5 + 50% RAP TH 10 + 3.5% Plastic Fines at OMC% (σ_d = 24 psi)

No. of Cycles	Measured M_R (psi)	Measured PD (inches)	Pred. PD (inches)		
			H = 6 in.	H = 9 in.	H = 12 in.
1	63630	0.0048	0	0	0
10	59790	0.0054	1.27E-26	1.91E-26	2.55E-26
20	59820	0.0054	1.81E-14	2.72E-14	3.63E-14
50	57960	0.0054	3.6E-07	5.4E-07	7.2E-07
100	57930	0.0054	9.81E-05	0.000147	0.000196
200	56780	0.0054	0.001624	0.002435	0.003247
300	56730	0.006	0.004112	0.006168	0.008224
400	55630	0.006	0.006665	0.009998	0.013331
500	55850	0.006	0.00878	0.01317	0.017561
600	56580	0.006	0.010615	0.015923	0.02123
700	55870	0.006	0.012126	0.01819	0.024253
800	56570	0.006	0.013355	0.020033	0.02671
900	56910	0.006	0.014336	0.021503	0.028671
1000	56620	0.0066	0.015331	0.022997	0.030663
1250	56750	0.0066	0.017147	0.025721	0.034295
1500	56820	0.0066	0.018419	0.027629	0.036839
1750	56900	0.0066	0.019447	0.029171	0.038895
2000	56840	0.0066	0.020338	0.030507	0.040676
2250	56920	0.0066	0.020914	0.031371	0.041828
2500	57570	0.0072	0.021225	0.031838	0.042451
2750	57760	0.0072	0.021759	0.032639	0.043519
3000	57950	0.0072	0.022098	0.033147	0.044197
3500	58300	0.0072	0.022603	0.033905	0.045206
4000	60970	0.0072	0.022533	0.033799	0.045066
4500	61850	0.0072	0.022719	0.034078	0.045437
5000	62220	0.0078	0.022946	0.034419	0.045892

Table B74. PD Measured Data from Multi-stage RTL Test for 50% Class 5 + 50% RAP TH 10 + 3.5% Plastic Fines at OMC% (σ_d = 37 psi)

No. of Cycles	Measured M_R (psi)	Measured PD (inches)	Pred. PD (inches)		
			H = 6 in.	H = 9 in.	H = 12 in.
1	70970	0.0078	0	0	0
10	65680	0.0078	1.99E-26	2.98E-26	3.98E-26
20	63520	0.0078	2.88E-14	4.31E-14	5.75E-14
50	60540	0.0078	5.79E-07	8.69E-07	1.16E-06
100	58420	0.0084	0.00016	0.00024	0.00032
200	57000	0.009	0.002661	0.003992	0.005323
300	56480	0.0096	0.006823	0.010235	0.013646
400	56200	0.0102	0.010944	0.016416	0.021888
500	56220	0.0102	0.014494	0.021741	0.028989
600	56130	0.0108	0.01756	0.02634	0.03512
700	56020	0.0108	0.020074	0.030111	0.040148
800	55800	0.0108	0.022289	0.033434	0.044579
900	55850	0.0114	0.024102	0.036153	0.048204
1000	56080	0.0114	0.025618	0.038427	0.051235
1250	56120	0.0114	0.028763	0.043144	0.057526
1500	55670	0.012	0.031166	0.046748	0.062331
1750	56120	0.012	0.032872	0.049308	0.065743
2000	56010	0.0126	0.034479	0.051718	0.068958
2250	56420	0.0126	0.035375	0.053062	0.07075
2500	56900	0.0126	0.036221	0.054332	0.072443
2750	56690	0.0132	0.036904	0.055356	0.073808
3000	57240	0.0132	0.037402	0.056103	0.074804
3500	57670	0.0132	0.038227	0.05734	0.076453
4000	58250	0.0138	0.038943	0.058414	0.077885
4500	58510	0.0138	0.039332	0.058998	0.078665
5000	58690	0.0138	0.039908	0.059862	0.079815

Table B75. PD Measured Data from Multi-stage RTL Test for 50% Class 5 + 50% RAP TH 10 + 3.5% Plastic Fines at OMC% (σ_d = 53 psi)

No. of Cycles	Measured M_R (psi)	Measured PD (inches)	Pred. PD (inches)		
			H = 6 in.	H = 9 in.	H = 12 in.
1	65840	0.0138	0	0	0
10	63680	0.0138	2.98E-26	4.47E-26	5.96E-26
20	63240	0.0138	4.26E-14	6.39E-14	8.52E-14
50	62180	0.0144	8.41E-07	1.26E-06	1.68E-06
100	61090	0.0144	0.000229	0.000343	0.000458
200	59970	0.0156	0.003788	0.005683	0.007577
300	59740	0.0162	0.009636	0.014453	0.019271
400	59520	0.0168	0.015399	0.023099	0.030799
500	58830	0.0174	0.020535	0.030803	0.041071
600	58890	0.018	0.024785	0.037178	0.049571
700	58940	0.0186	0.028267	0.0424	0.056534
800	59700	0.0186	0.031185	0.046778	0.06237
900	59600	0.0192	0.033677	0.050515	0.067353
1000	59630	0.0198	0.035827	0.05374	0.071654
1250	60280	0.0204	0.039944	0.059916	0.079888
1500	60850	0.021	0.04277	0.064155	0.08554
1750	61170	0.0216	0.045107	0.067661	0.090214
2000	61630	0.0216	0.046869	0.070304	0.093738
2250	64030	0.0222	0.047504	0.071256	0.095007
2500	64470	0.0228	0.048425	0.072638	0.09685
2750	64370	0.0228	0.04966	0.074491	0.099321
3000	65060	0.0234	0.0502	0.075299	0.100399
3500	61850	0.0234	0.053182	0.079774	0.106365
4000	62150	0.024	0.054264	0.081396	0.108527
4500	62530	0.024	0.054865	0.082298	0.10973
5000	62770	0.0246	0.055519	0.083278	0.111038

Table B76. PD Measured Data from Multi-stage RTL Test for 50% Class 5 + 50% RAP TH 10 + 3.5% Plastic Fines at OMC% (σ_d = 63 psi)

No. of Cycles	Measured M_R (psi)	Measured PD (inches)	Pred. PD (inches)		
			H = 6 in.	H = 9 in.	H = 12 in.
1	69020	0.0246	0	0	0
10	69980	0.0246	3.82E-26	5.73E-26	7.64E-26
20	70860	0.0246	5.42E-14	8.14E-14	1.08E-13
50	68800	0.0252	1.07E-06	1.61E-06	2.14E-06
100	67620	0.0252	0.000291	0.000437	0.000582
200	65780	0.0264	0.004827	0.007241	0.009655
300	63650	0.0282	0.012446	0.01867	0.024893
400	62400	0.0294	0.020021	0.030031	0.040041
500	61270	0.0312	0.026747	0.04012	0.053493
600	61490	0.033	0.032144	0.048216	0.064288
700	61370	0.0348	0.036785	0.055177	0.073569
800	60060	0.036	0.041382	0.062074	0.082765
900	60080	0.0372	0.044606	0.066909	0.089212
1000	60040	0.0384	0.047323	0.070984	0.094645
1250	60440	0.0408	0.052894	0.079341	0.105787
1500	60000	0.0426	0.057341	0.086012	0.114683
1750	61260	0.0444	0.059961	0.089942	0.119923
2000	60620	0.0456	0.063048	0.094572	0.126096
2250	60700	0.0468	0.065124	0.097686	0.130247
2500	59620	0.048	0.067437	0.101156	0.134875
2750	60170	0.0486	0.068721	0.103082	0.137443
3000	59690	0.0492	0.070274	0.105411	0.140548
3500	59820	0.0504	0.072311	0.108467	0.144622
4000	60260	0.0516	0.073573	0.110359	0.147146
4500	60810	0.0528	0.074383	0.111574	0.148765
5000	61010	0.0534	0.075256	0.112884	0.150513

Table B77. PD Measured Data from Multi-stage RTL Test for 50% Class 5 + 50% RAP TH 10 + 3.5% Plastic Fines at OMC% (σ_d = 73 psi)

No. of Cycles	Measured M_R (psi)	Measured PD (inches)	Pred. PD (inches)		
			H = 6 in.	H = 9 in.	H = 12 in.
1	65810	0.0534	0	0	0
10	65100	0.0534	4.85E-26	7.27E-26	9.7E-26
20	64590	0.0534	6.92E-14	1.04E-13	1.38E-13
50	63570	0.054	1.36E-06	2.04E-06	2.72E-06
100	62470	0.054	0.00037	0.000555	0.00074
200	60220	0.0552	0.00617	0.009254	0.012339
300	58870	0.057	0.015803	0.023704	0.031605
400	57570	0.0588	0.02542	0.03813	0.05084
500	56530	0.0618	0.033916	0.050875	0.067833
600	54660	0.0654	0.041544	0.062316	0.083088
700	53160	0.0702	0.048068	0.072101	0.096135
800	52190	0.0762	0.05386	0.08079	0.107721
900	48890	0.0828	0.060101	0.090152	0.120202
1000	50180	0.09	0.062858	0.094287	0.125716
1250	46630	0.1104	0.073493	0.110239	0.146986
1500	47660	0.1362	0.076951	0.115426	0.153902
1750	46400	0.1794	0.080093	0.12014	0.160187

Table B78. PD Measured Data from Multi-stage RTL Test for 50% Class 5 + 50% RAP TH 10 + 3.5% Plastic Fines at OMC+2% (σ_d = 6 psi)

No. of Cycles	Measured M_R (psi)	Measured PD (inches)	Pred. PD (inches)		
			H = 6 in.	H = 9 in.	H = 12 in.
1	22940	0	0	0	0
10	21840	0.003	2.44E-48	3.65E-48	4.87E-48
20	21580	0.0042	1.13E-25	1.69E-25	2.25E-25
50	21840	0.0054	4.38E-12	6.58E-12	8.77E-12
100	22030	0.0066	1.54E-07	2.3E-07	3.07E-07
200	23490	0.0078	2.8E-05	4.2E-05	5.6E-05
300	23530	0.0084	0.000159	0.000239	0.000318
400	23270	0.009	0.000391	0.000586	0.000781
500	23940	0.009	0.000653	0.00098	0.001307
600	24150	0.0096	0.000936	0.001404	0.001872
700	24110	0.0096	0.001201	0.001802	0.002403
800	24180	0.0096	0.001458	0.002187	0.002915
900	24300	0.0096	0.001686	0.002529	0.003372
1000	23960	0.0096	0.00191	0.002866	0.003821
1250	24650	0.0102	0.002364	0.003547	0.004729
1500	25120	0.0102	0.002637	0.003956	0.005274
1750	26180	0.0108	0.002815	0.004222	0.00563
2000	25700	0.0108	0.003144	0.004717	0.006289
2250	26140	0.0108	0.003286	0.004929	0.006571
2500	25640	0.0108	0.00348	0.00522	0.00696
2750	26130	0.0114	0.003542	0.005313	0.007085
3000	26690	0.0114	0.003618	0.005427	0.007237
3500	26860	0.0114	0.003783	0.005674	0.007565
4000	27660	0.0114	0.003869	0.005804	0.007739
4500	28220	0.012	0.00391	0.005865	0.00782
5000	28440	0.012	0.004023	0.006034	0.008046

Table B79. PD Measured Data from Multi-stage RTL Test for 50% Class 5 + 50% RAP TH 10 + 3.5% Plastic Fines at OMC+2% (σ_d = 12 psi)

No. of Cycles	Measured M_R (psi)	Measured PD (inches)	Pred. PD (inches)		
			H = 6 in.	H = 9 in.	H = 12 in.
1	30400	0.012	0	0	0
10	24190	0.0132	7.12E-48	1.07E-47	1.42E-47
20	23350	0.0144	3.1E-25	4.66E-25	6.21E-25
50	22540	0.0174	1.25E-11	1.87E-11	2.49E-11
100	24400	0.0198	4.03E-07	6.04E-07	8.06E-07
200	27810	0.0228	6.77E-05	0.000101	0.000135
300	28600	0.024	0.000376	0.000564	0.000752
400	28790	0.0246	0.000907	0.001361	0.001814
500	28850	0.0252	0.001536	0.002303	0.003071
600	29500	0.0258	0.002139	0.003209	0.004278
700	29850	0.0264	0.002732	0.004098	0.005464
800	30450	0.027	0.003261	0.004892	0.006523
900	30700	0.027	0.003741	0.005612	0.007482
1000	31380	0.0276	0.004149	0.006223	0.008298
1250	32390	0.0282	0.005039	0.007559	0.010078
1500	33400	0.0288	0.00566	0.00849	0.01132
1750	33710	0.0288	0.006266	0.009399	0.012532
2000	34130	0.0294	0.006674	0.01001	0.013347
2250	35040	0.0294	0.006951	0.010427	0.013902
2500	35460	0.03	0.007263	0.010895	0.014527
2750	35440	0.03	0.007605	0.011407	0.015209
3000	34980	0.03	0.007889	0.011834	0.015778
3500	36020	0.0306	0.008155	0.012233	0.016311
4000	36680	0.0306	0.008358	0.012537	0.016716
4500	37170	0.0306	0.008527	0.01279	0.017054
5000	37560	0.0306	0.008749	0.013124	0.017499

Table B80. PD Measured Data from Multi-stage RTL Test for 50% Class 5 + 50% RAP TH 10 + 3.5% Plastic Fines at OMC+2% (σ_d = 17 psi)

No. of Cycles	Measured M_R (psi)	Measured PD (inches)	Pred. PD (inches)		
			H = 6 in.	H = 9 in.	H = 12 in.
1	40000	0.0306	0	0	0
10	36450	0.0312	9.06E-48	1.36E-47	1.81E-47
20	35540	0.0312	3.84E-25	5.76E-25	7.68E-25
50	34170	0.0318	1.47E-11	2.21E-11	2.95E-11
100	33250	0.0324	4.99E-07	7.48E-07	9.97E-07
200	32530	0.0342	9.24E-05	0.000139	0.000185
300	33880	0.036	0.000511	0.000766	0.001022
400	34260	0.0372	0.001207	0.001811	0.002414
500	34150	0.0384	0.002046	0.003069	0.004092
600	33900	0.039	0.002898	0.004346	0.005795
700	33770	0.0396	0.00375	0.005626	0.007501
800	34010	0.0402	0.004546	0.006819	0.009093
900	34070	0.0408	0.005193	0.007789	0.010386
1000	34340	0.0414	0.005848	0.008771	0.011695
1250	35450	0.0426	0.007035	0.010553	0.014071
1500	35820	0.0432	0.008065	0.012098	0.01613
1750	36670	0.0438	0.008788	0.013181	0.017575
2000	37320	0.0444	0.009414	0.014121	0.018828
2250	37920	0.045	0.009878	0.014817	0.019756
2500	38560	0.0456	0.01022	0.015329	0.020439
2750	38770	0.0456	0.010644	0.015966	0.021288
3000	39170	0.0462	0.010896	0.016344	0.021792
3500	39690	0.0462	0.011302	0.016954	0.022605
4000	40430	0.0468	0.011725	0.017587	0.02345
4500	40070	0.0474	0.012172	0.018258	0.024344
5000	40020	0.0474	0.012485	0.018727	0.02497

Table B81. PD Measured Data from Multi-stage RTL Test for 50% Class 5 + 50% RAP TH 10 + 3.5% Plastic Fines at OMC+2% (σ_d = 24 psi)

No. of Cycles	Measured M_R (psi)	Measured PD (inches)	Pred. PD (inches)		
			H = 6 in.	H = 9 in.	H = 12 in.
1	46570	0.0474	0	0	0
10	41890	0.048	1.25E-47	1.87E-47	2.49E-47
20	39720	0.048	5.37E-25	8.05E-25	1.07E-24
50	35490	0.0498	2.15E-11	3.22E-11	4.29E-11
100	32370	0.0534	7.62E-07	1.14E-06	1.52E-06
200	30870	0.06	0.000145	0.000217	0.000289
300	30360	0.0654	0.000833	0.00125	0.001667
400	29490	0.0702	0.00205	0.003075	0.004099
500	30980	0.0744	0.003332	0.004999	0.006665
600	29800	0.078	0.004861	0.007291	0.009721
700	30260	0.081	0.006182	0.009273	0.012364
800	30150	0.084	0.007528	0.011292	0.015057
900	30860	0.087	0.008551	0.012826	0.017101
1000	30640	0.09	0.009708	0.014562	0.019416
1250	31020	0.0966	0.011824	0.017736	0.023647
1500	31080	0.1032	0.013606	0.020409	0.027212
1750	29710	0.1086	0.015578	0.023367	0.031156
2000	29330	0.1146	0.016971	0.025457	0.033943
2250	28700	0.12	0.018288	0.027433	0.036577
2500	29270	0.1254	0.018856	0.028284	0.037713
2750	29460	0.1308	0.019474	0.029211	0.038948
3000	29340	0.1362	0.020225	0.030337	0.040449
3500	28060	0.1464	0.022071	0.033107	0.044142
4000	27950	0.1578	0.022889	0.034334	0.045778
4500	27170	0.1692	0.024011	0.036017	0.048022
5000	25870	0.1824	0.025424	0.038136	0.050848

Table B82. PD Measured Data from Multi-stage RTL Test for 50% Class 5 + 50% RAP TH 10 + 3.5% Plastic Fines at OMC+2% (σ_d = 37 psi)

No. of Cycles	Measured M_R (psi)	Measured PD (inches)	Pred. PD (inches)		
			H = 6 in.	H = 9 in.	H = 12 in.
1	29470	0.2286	0	0	0
10	24760	0.2352	2.69E-47	4.04E-47	5.38E-47
20	27390	0.2424	9.49E-25	1.42E-24	1.9E-24
50	23040	0.2568	4.54E-11	6.81E-11	9.08E-11
100	22290	0.2796	1.59E-06	2.39E-06	3.18E-06
200	21230	0.3138	0.000305	0.000457	0.000609
300	19940	0.354	0.001821	0.002732	0.003643

APPENDIX C. CORRELATION DATA OF M_R AND PD

Table C1. PD Data Collected from M_R test at Different Confining Pressure Levels

W.C Condition	Conf. Pressure (psi)	% RAP				Extracted RAP
		0	50	75	100	
OMC-2%	3	0.2	0.12	0.13	0.23	NA
	6	0.23	0.13	0.15	0.24	
	10	0.25	0.12	0.14	0.26	
	15	0.28	0.14	0.18	0.28	
	20	0.35	0.19	0.23	0.34	
OMC%	3	1.28	1.69	1.04	0.42	0.52
	6	1.3	1.64	1.07	0.5	0.5
	10	1.4	1.58	1.14	0.53	0.55
	15	1.2	1.67	0.77	0.55	0.62
	20	1.83	1.75	1.96	0.71	0.52
OMC+2%	3	3.74	2.71	4.07	3.49	NA
	6	3.64	2.9	4.06	2.89	
	10	3.82	3.07	4.13	3.52	
	15	4.22	3.48	4.32	3.67	
	20	3.61	2.77	4.07	3.46	

Table C2. M_R Measured Data from M_R test at Different Confining Pressure Levels

W.C Condition	Conf. Pressure (psi)	% RAP				Extracted RAP
		0	50	75	100	
OMC-2%	3	27430	64518	95632	92423	NA
	6	44221	81140	105397	106154	
	10	62241	100735	132855	127910	
	15	75629	113612	153277	153506	
	20	90294	139198	169715	171716	
OMC%	3	19368	35583	27842	41797	27484
	6	26077	46843	37765	56438	42561
	10	34532	62623	49528	79637	58046
	15	41882	75744	62364	96318	73444
	20	53440	87539	70755	119049	90718
OMC+2%	3	16331	23364	27107	37177	NA
	6	19457	29974	31936	43819	
	10	26454	38749	37652	50506	
	15	35903	53257	45156	60967	
	20	46943	59392	54832	65292	

Table C3. M_R Versus PD data for 50% RAP Blends at Different Confining Pressure Levels

RAP Source	Confining Pressure (psi)	WC = OMC-2%		WC = OMC%		WC = OMC+2%	
		PD%	M_R (psi)	PD%	M_R (psi)	PD%	M_R (psi)
TH 10	3	0.12	64518	1.69	35583	2.71	23364
	6	0.13	81140	1.64	46843	2.9	29974
	10	0.12	100735	1.58	62623	3.07	38749
	15	0.14	113612	1.67	75744	3.48	53257
	20	0.19	139198	1.75	87539	2.77	59392
TH 19-101	3	0.209	55504	0.201	63091	1.024	26296
	6	0.219	57904	0.211	67677	0.804	29794
	10	0.228	70791	0.233	76702	1.098	35838
	15	0.267	84405	0.265	85272	1.314	45063
	20	0.323	95967	0.326	94869	1.176	54350
TH 19-104	3	0.287	57599	0.828	33438	3.61	22733
	6	0.273	65503	0.814	38330	3.678	24761
	10	0.227	79788	0.829	47107	2.592	31966
	15	0.249	103404	0.969	60355	3.142	38476
	20	0.301	112119	0.871	70543	3.623	44964
TH 22	3	0.204	67020	0.638	31355	1.79	34517
	6	0.215	82634	0.676	41690	1.827	40988
	10	0.235	106100	0.67	60361	1.963	49160
	15	0.249	130707	0.735	77372	2.385	58207
	20	0.309	141339	0.899	91118	1.864	68442

Table C4. M_R Versus PD data for 100% RAP Blends at Different Confining Pressure Levels

RAP Source	Confining Pressure (psi)	WC = OMC-2%		WC = OMC%		WC = OMC+2%	
		PD%	M_R (psi)	PD%	M_R (psi)	PD%	M_R (psi)
TH 10	3	0.23	92423	0.42	41797	3.49	37177
	6	0.24	106154	0.5	56438	2.89	43819
	10	0.26	127910	0.53	79637	3.52	50506
	15	0.28	153506	0.55	96318	3.67	60967
	20	0.34	171716	0.71	119049	3.46	65292
Cell 18	3	0.286	67097	0.41	53386	0.354	40284
	6	0.278	86588	0.4	75749	0.372	57065
	10	0.314	108636	0.425	104289	0.406	75472
	15	0.275	132675	0.458	127616	0.531	89213
	20	0.303	151828	0.553	146235	0.397	107423

APPENDIX D. POISSON'S RATIO MEASURED DATA

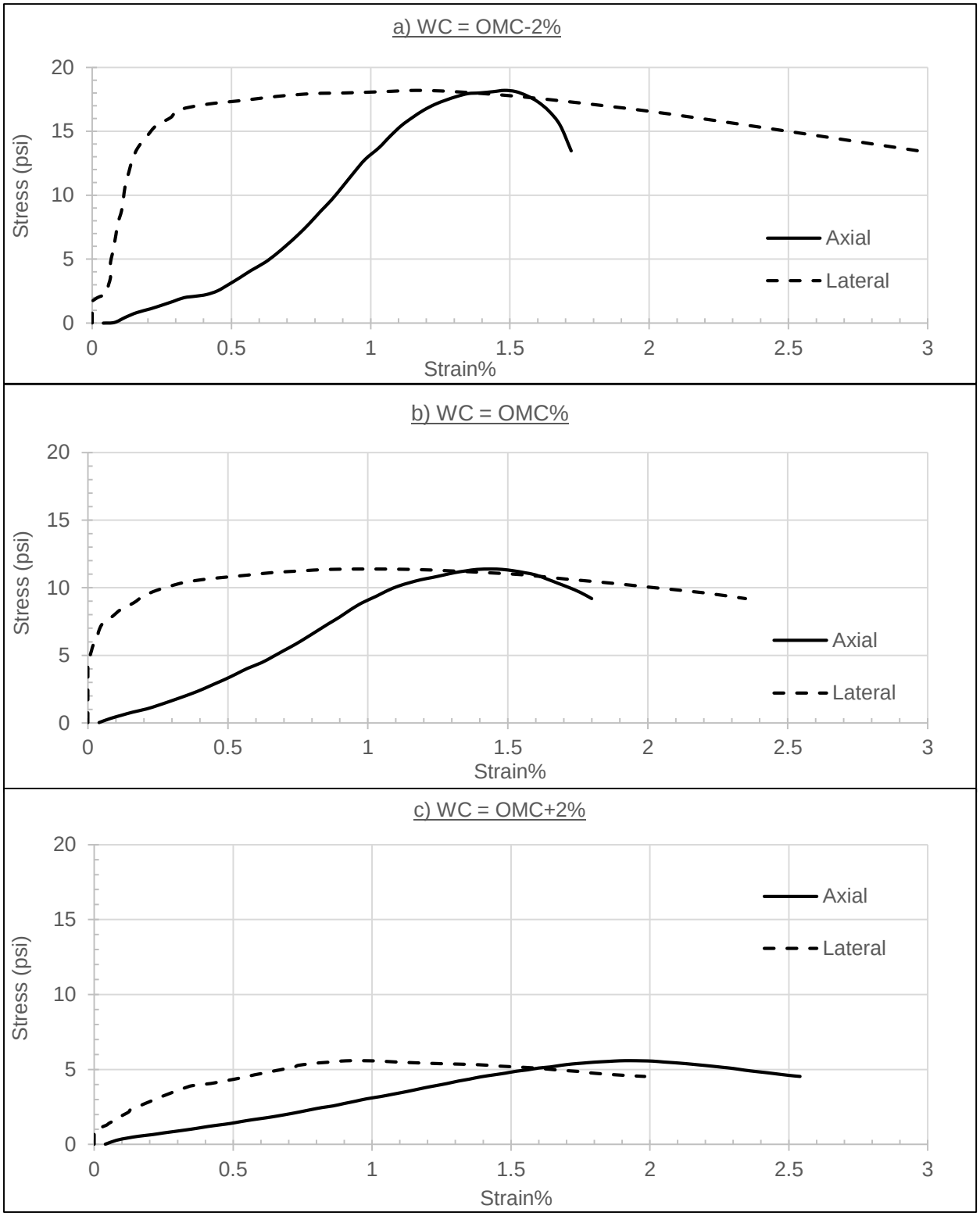

Figure D1. Stress- Strain Biaxial Relationship for New Class 5

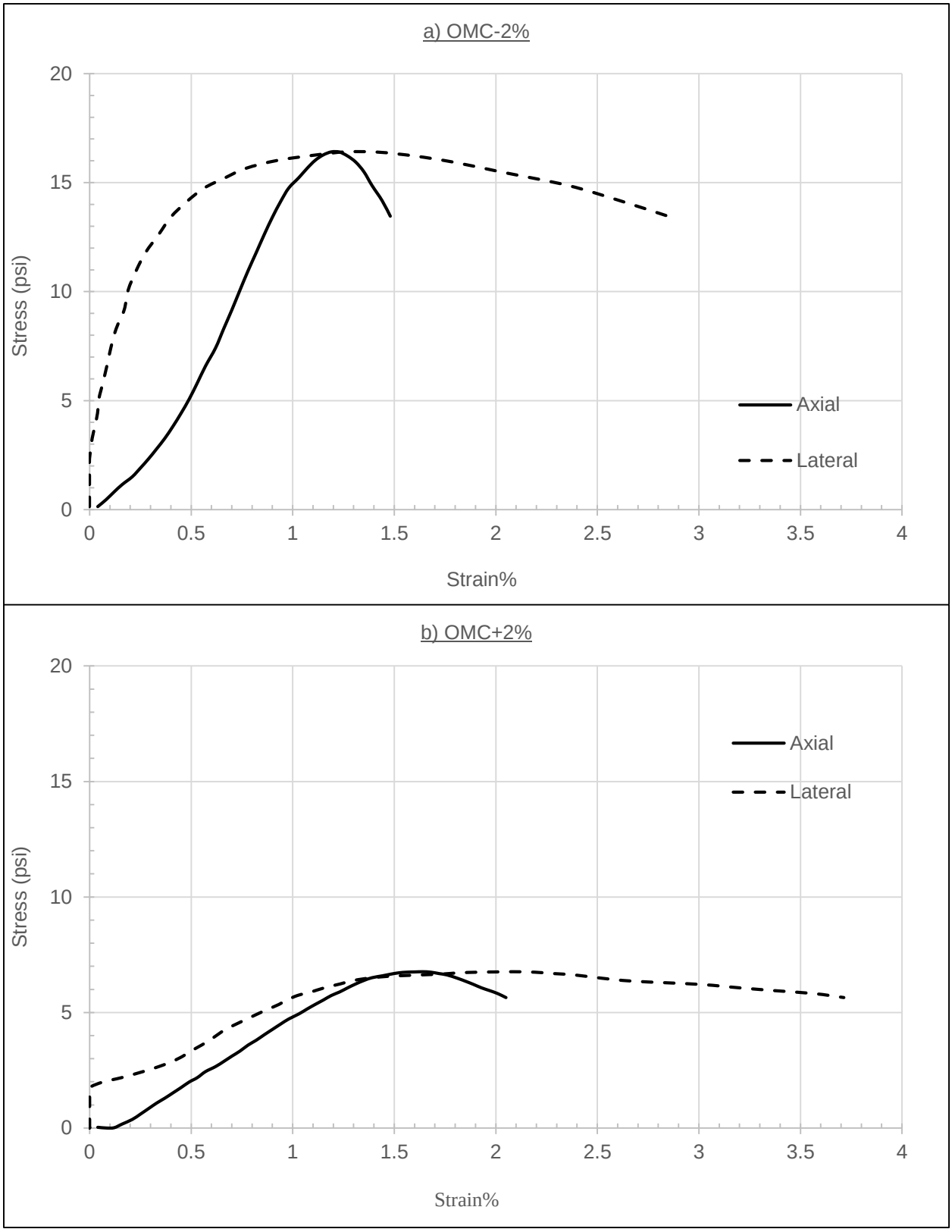

Figure D2. Stress- Strain Biaxial Relationship for New Class 5 (Replicate)

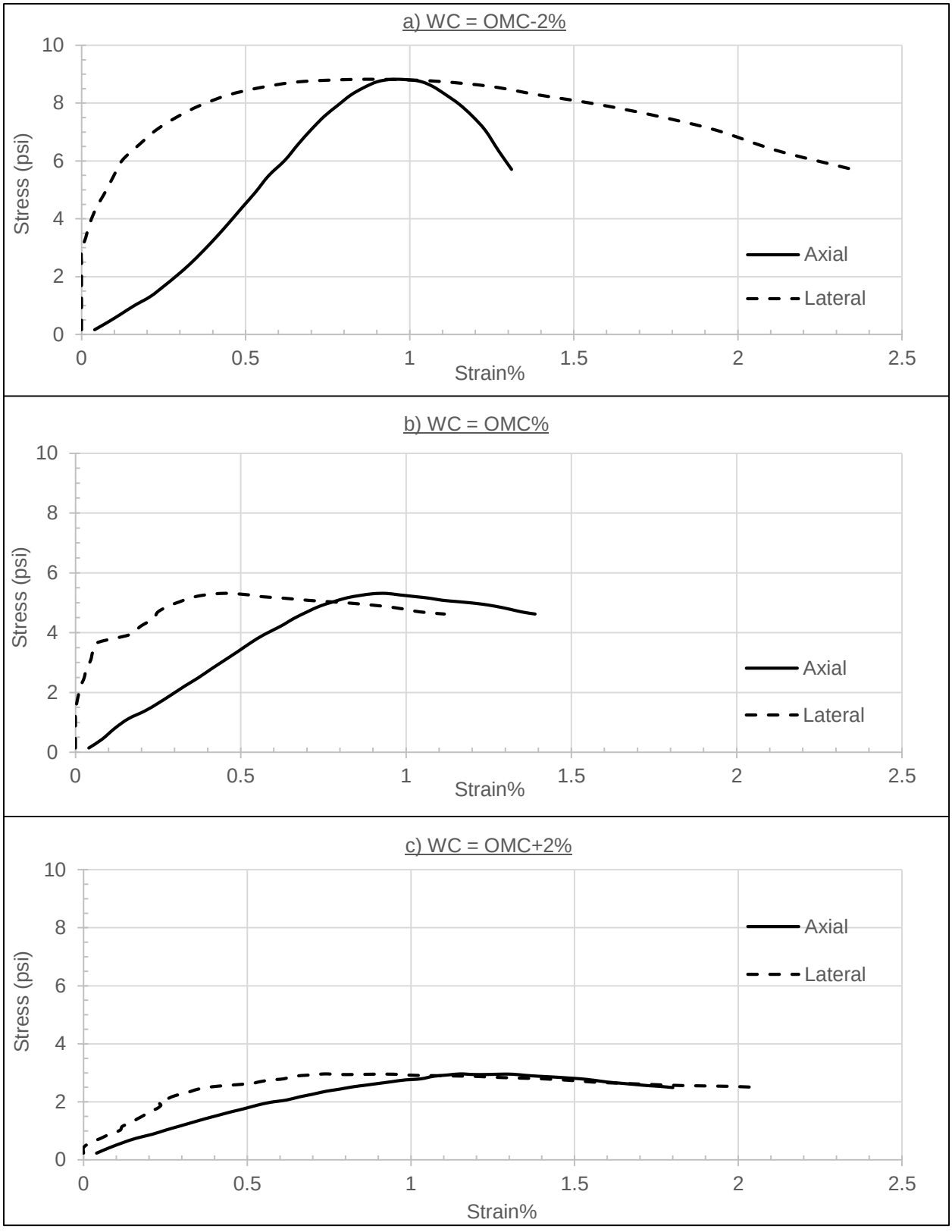

Figure D3. Stress- Strain Biaxial Relationship for Old Class 5

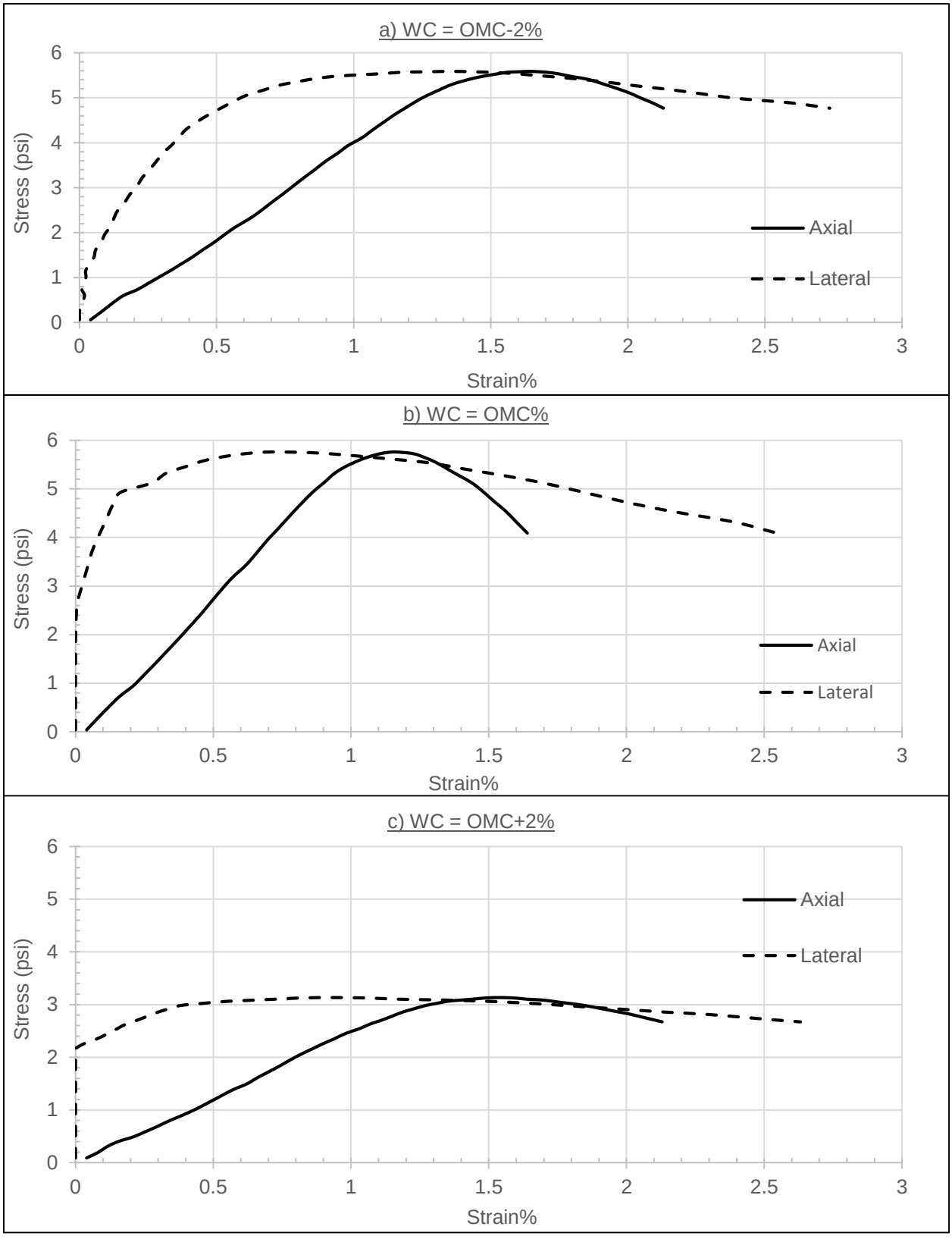

Figure D4. Stress- Strain Biaxial Relationship for 50% New Class 5 + 50% RAP TH 29

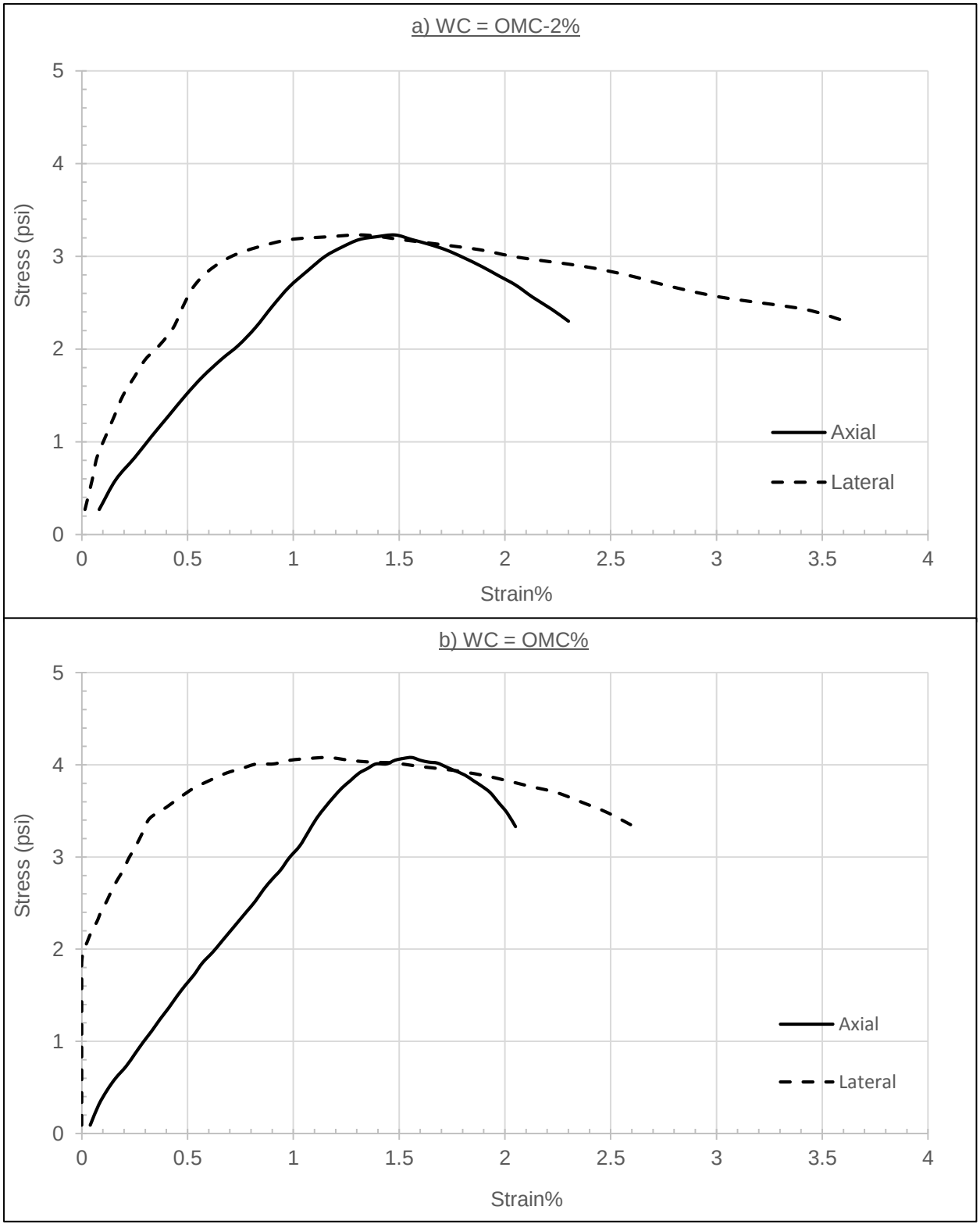

Figure D5. Stress- Strain Biaxial Relationship for 50% New Class 5 + 50% RAP TH 29 (Replicate)

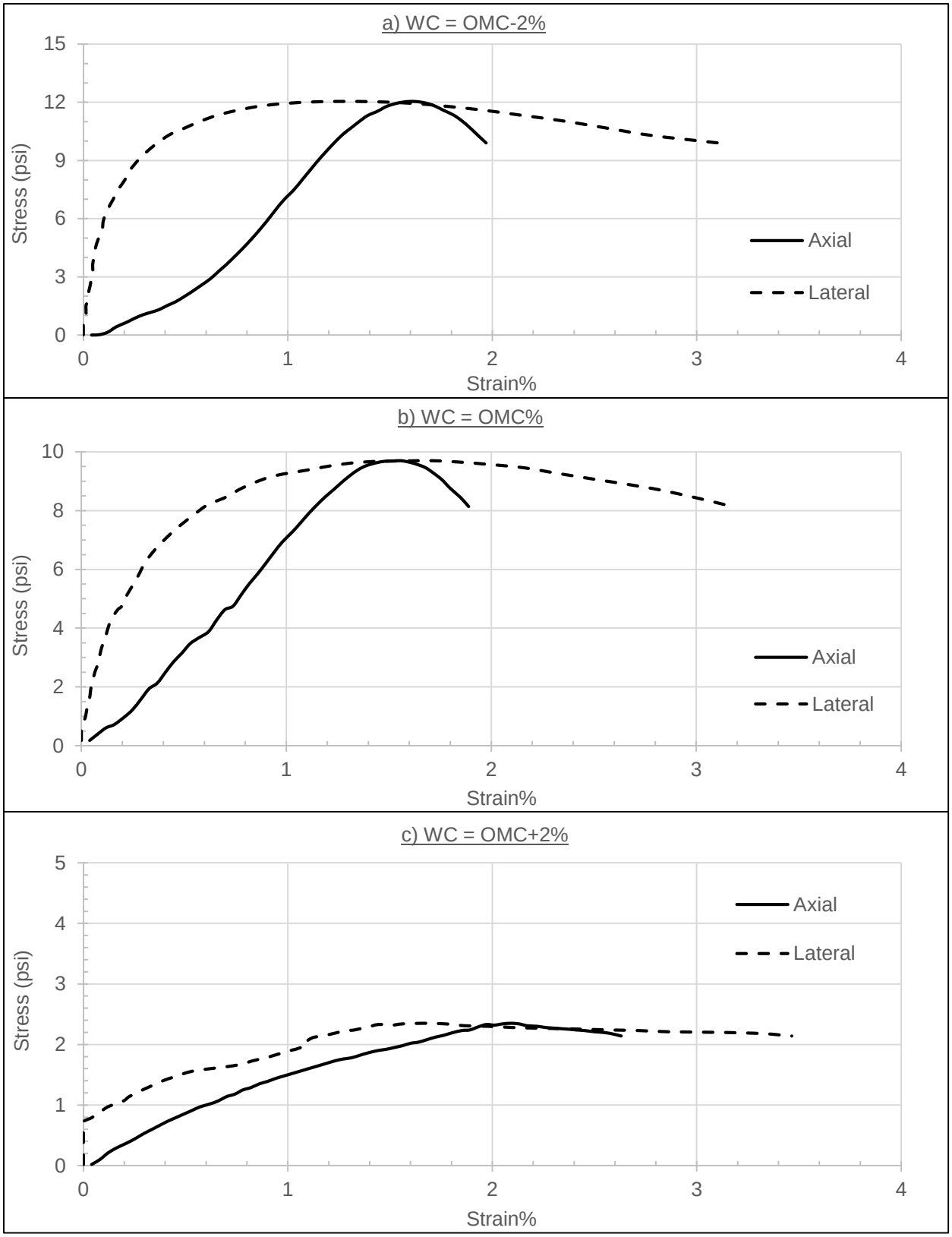

Figure D6. Stress- Strain Biaxial Relationship for 50% Old Class 5 + 50% RAP TH 10

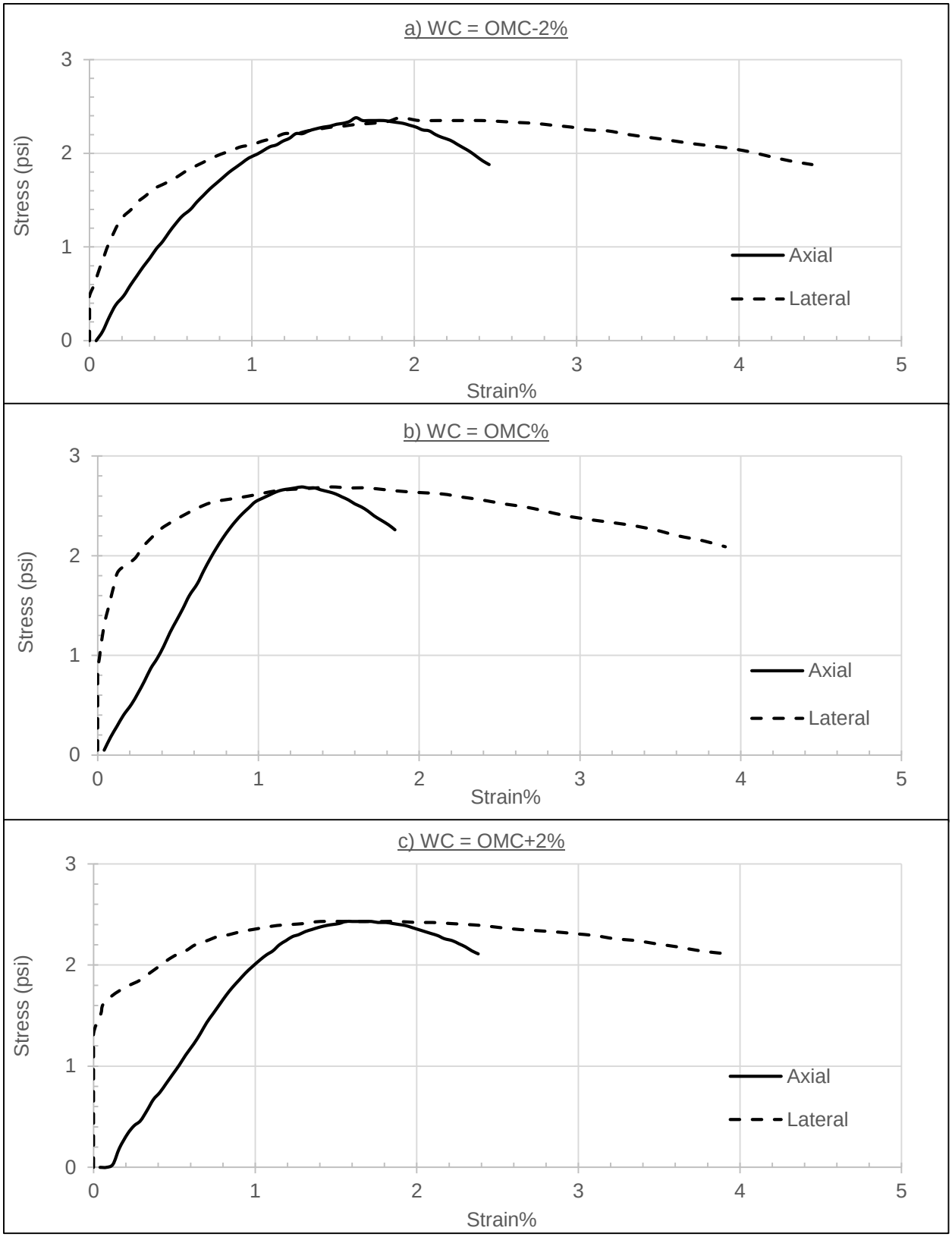

Figure D7. Stress- Strain Biaxial Relationship for 100% RAP TH 29

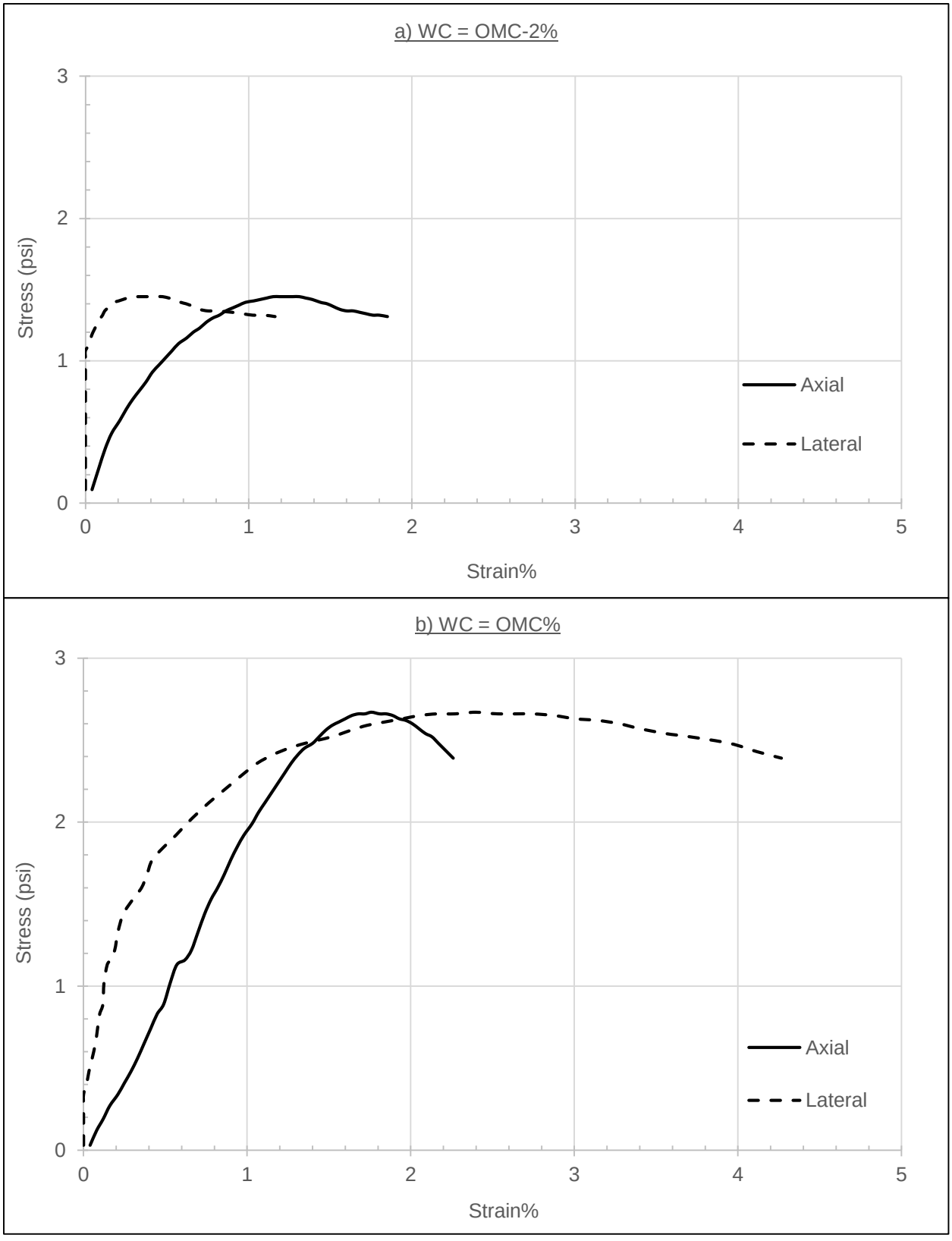

Figure D8. Stress- Strain Biaxial Relationship for 100% RAP TH 29 (Replicate)

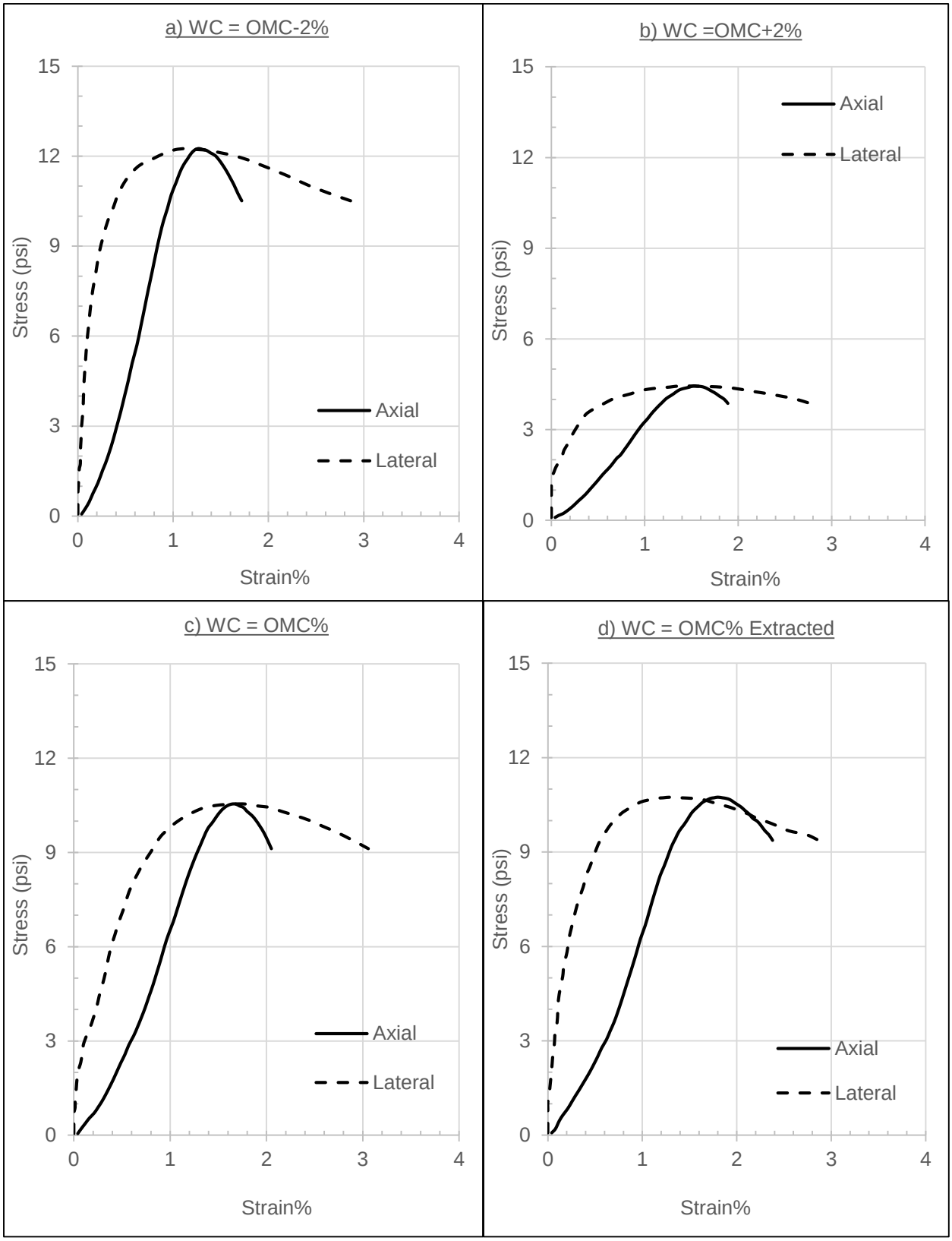

Figure D9. Stress- Strain Biaxial Relationship for 100% RAP TH 10

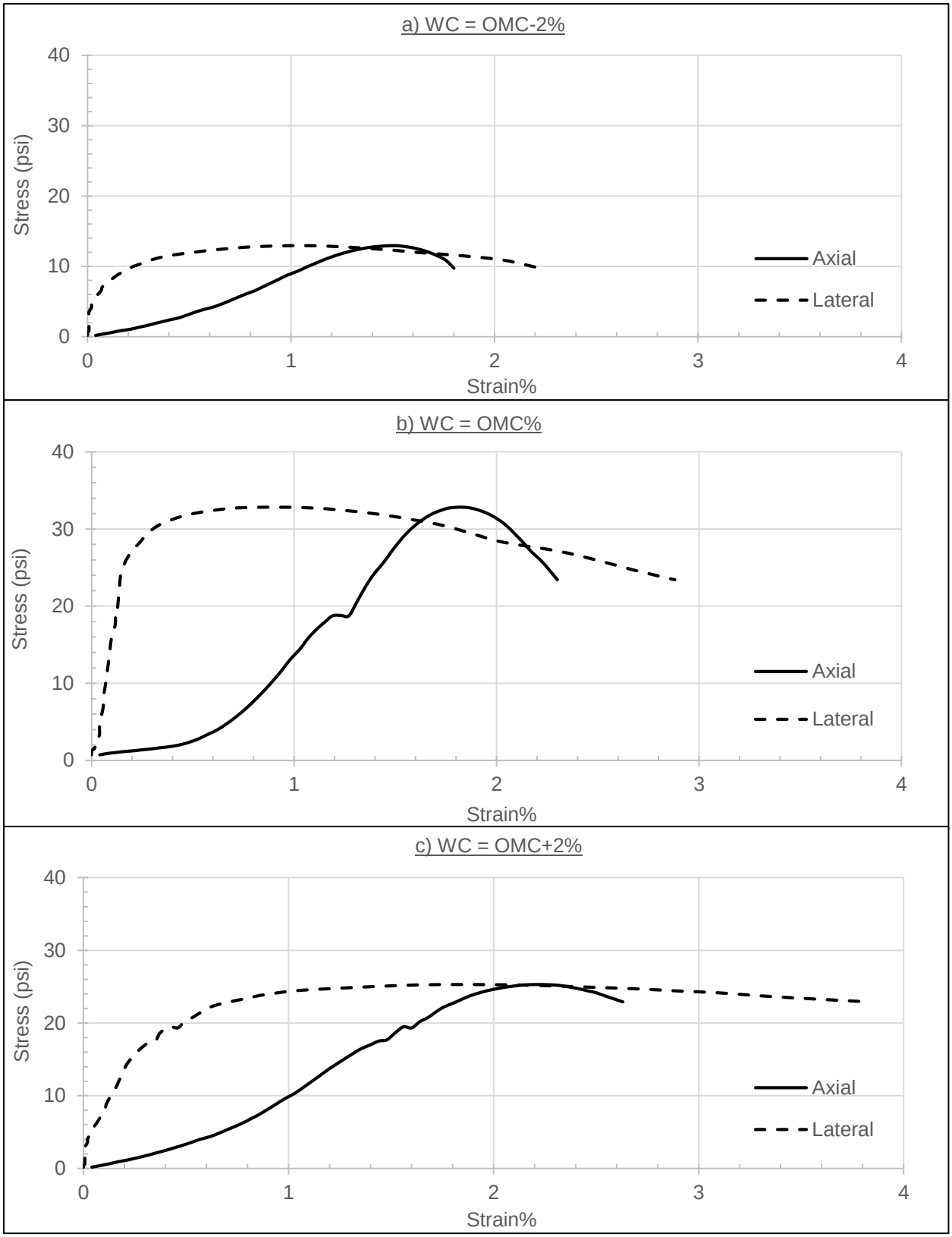

Figure D10. Stress- Strain Biaxial Relationship for RAP TH 19-101

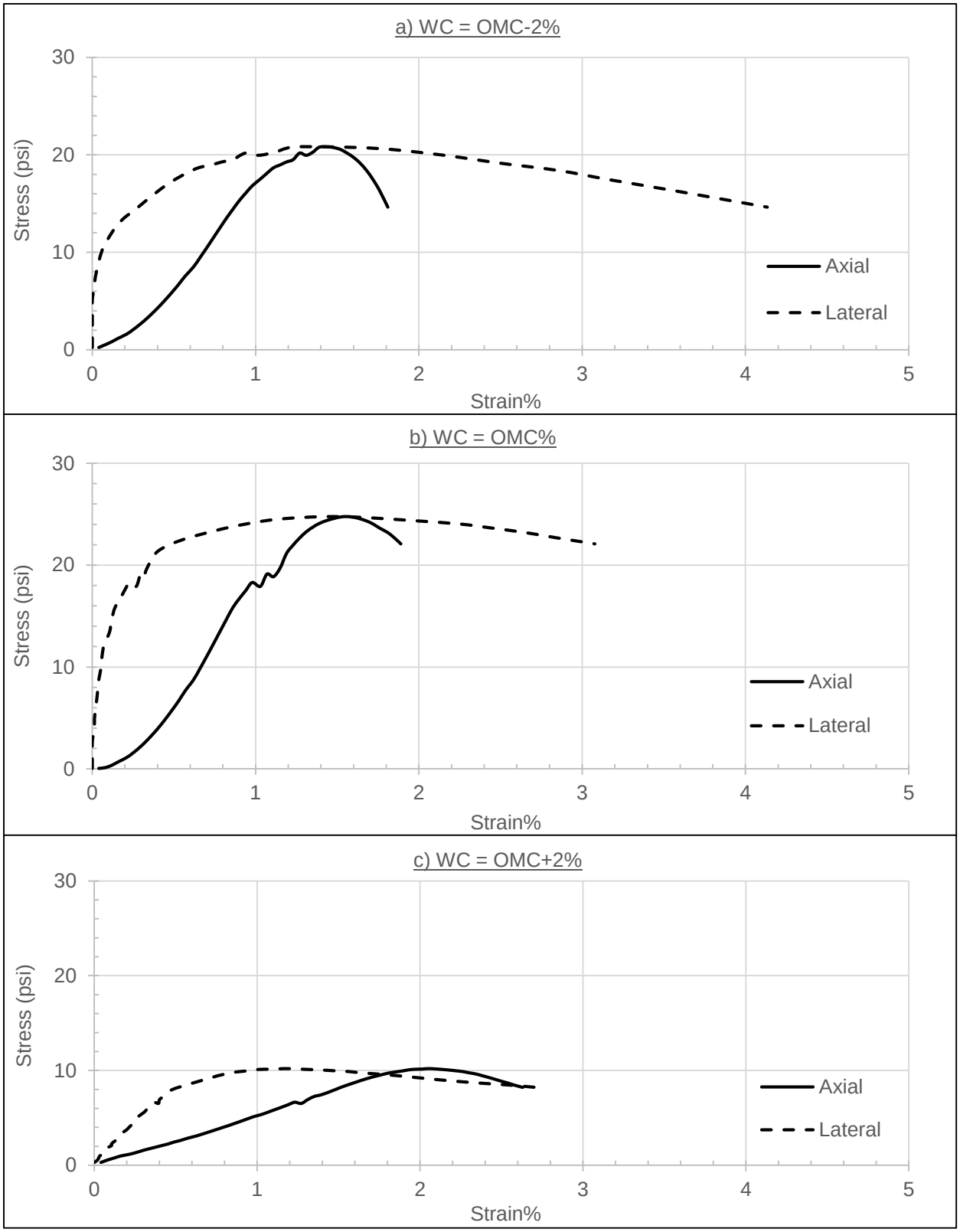

Figure D11. Stress- Strain Biaxial Relationship for RAP TH 19-104

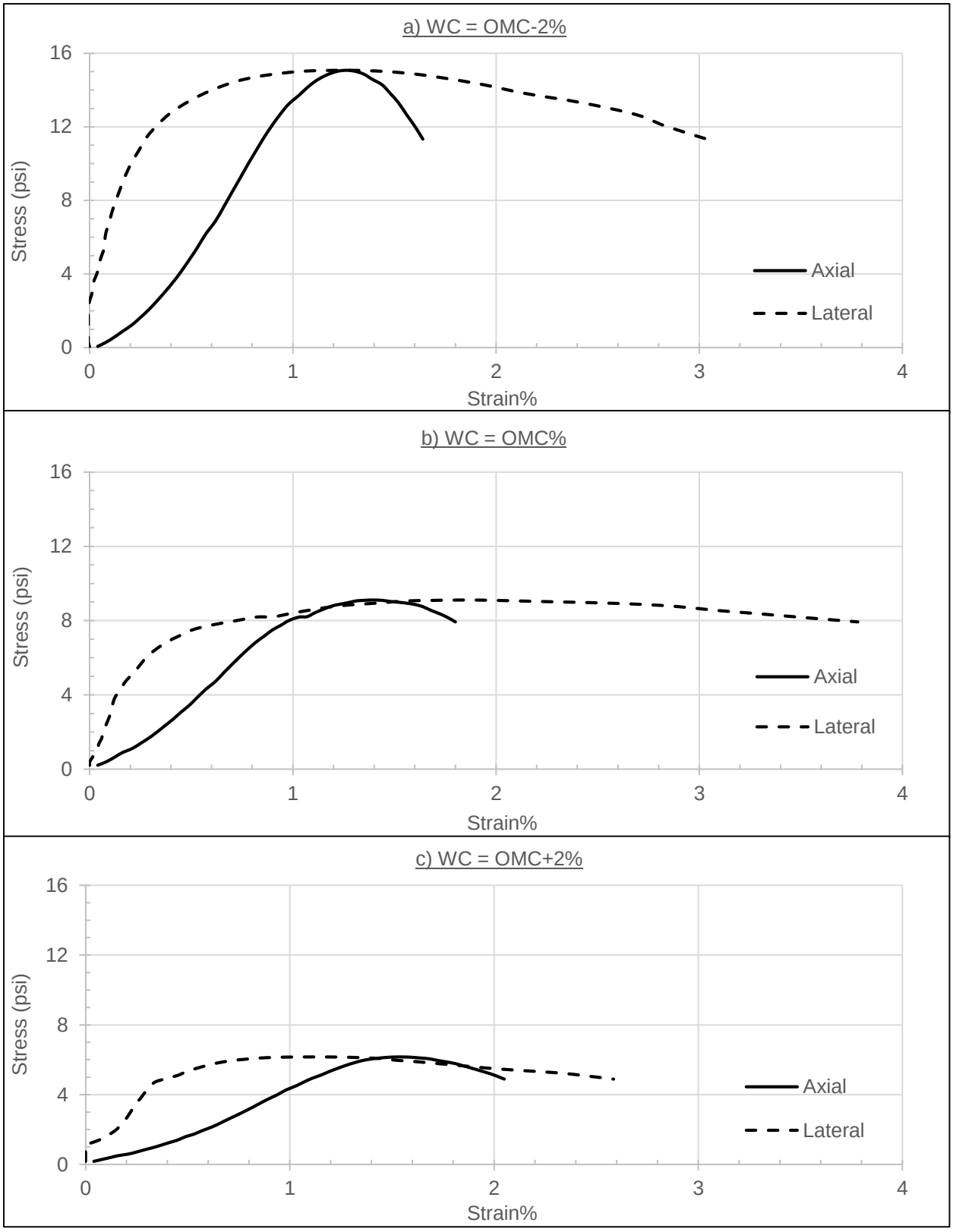

Figure D12. Stress- Strain Biaxial Relationship for RAP TH 22

Table D1. Summary of Poisson's Ratio Results for All RAP/Aggregate Tested Samples

Material	WC Condition	Ultimate Compressive Strength (psi)	Linear Relation Stress Range Levels		Poisson's Ratio	
			From	To	Value	Stress Level
New Class 5	OMC-2%	17.31	32%	88%	0.25	60%
	OMC%	11.39	40%	88%	0.13	64%
	OMC+2%	6.18	15%	85%	0.36	50%
50% RAP TH 29	OMC-2%	4.41	32%	87%	0.3	60%
	OMC%	4.92	20%	89%	0.31	55%
	OMC+2%	3.13	19%	80%	0.07	50%
100% RAP TH 29	OMC-2%	1.92	32%	68%	0.24	50%
	OMC%	2.68	19%	79%	0.29	49%
	OMC+2%	2.43	17%	79%	0.19	48%
Old Class 5	OMC-2%	8.82	34%	87%	0.21	61%
	OMC%	5.31	30%	77%	0.16	54%
	OMC+2%	2.96	41%	68%	0.41	55%
50% RAP TH 10	OMC-2%	12.04	38%	83%	0.19	61%
	OMC%	9.7	10%	88%	0.35	49%
	OMC+2%	2.35	32%	75%	0.34	54%
100% RAP TH 10	OMC-2%	12.25	42%	82%	0.26	62%
	OMC%	10.54	33%	90%	0.45	62%
	OMC+2%	4.45	38%	84%	0.25	61%
Extracted RAP TH 10	OMC%	10.74	33%	79%	0.28	56%
RAP TH 19-101	OMC-2%	12.95	31%	89%	0.18	60%
	OMC%	32.83	18%	85%	0.11	52%
	OMC+2%	25.3	20%	79%	0.17	50%
RAP TH 19-104	OMC-2%	20.83	29%	82%	0.25	56%
	OMC%	24.76	16%	77%	0.15	47%
	OMC+2%	10.19	25%	93%	0.35	59%
RAP TH 22	OMC-2%	15.07	20%	86%	0.25	53%
	OMC%	9.11	17%	88%	0.47	53%
	OMC+2%	6.16	32%	81%	0.31	57%